UNIVERSITY *of the*
WESTERN CAPE

Voice and rural wireless mesh community networks: a framework to quantify scalability and manage end-user smartphone battery consumption

by
Shree Om

A thesis submitted in fulfilment of the requirements for the degree of

Doctor of Philosophy

in

Computer Science

Faculty of Science
Department of Computer Science

Supervisor: Prof. William D. Tucker

April 2021

Declaration of authorship

I, Shree Om, declare that this thesis entitled “Voice and rural wireless mesh community networks: a framework to quantify scalability and manage end-user smartphone battery consumption” is my own work, that it has not been submitted for any degree or assessment at any other University, and that all the sources I have used or quoted have been indicated and acknowledged by means of complete references.

Signed__  **_____**

Shree Om

Date_01 April 2021_____

Abstract

Community wireless mesh initiatives are a pioneering option to cheap 'last-mile' access to network services for rural low-income regions primarily located in Sub-Saharan Africa and Developing Asia. However, researchers have criticized wireless mesh networks for their poor scalability; and scalability quantification research has mostly consisted of modularization of per-node throughput capacity behaviour. A scalability quantification model to design wireless mesh networks to provide adequate quality of service is lacking. However, scalability quantification of community mesh networks alone is inadequate because rural users need affordable devices for access; and they need to know how best to use them. Low-cost low-end smartphones offer handset affordability solutions but require smart management of their small capacity battery. Related work supports the usage of Wi-Fi for communication because it is shown to consume less battery than 2G, 3G or Bluetooth. However, a model to compare Wi-Fi battery consumption amongst different low-end smartphones is missing, as is a comparison of different over-the-top communication applications. This thesis presents a scalability framework consisting of two components that address scalability quantification and battery management gaps. Both components use indoor multi-hop testbeds using dual-radio and dual-band mesh routers. The scalability quantification is addressed via measurement of throughput during transmission control traffic transmission; and latency, jitter, and packet loss during synthetic voice traffic transmission over two dual-band and dual-radio clustered wireless mesh network testbeds. Voice traffic is prioritized to measure latency, jitter, and packet loss because of its strict quality of service requirements. The data have been converted into equations to predict maximum hop-limit from mesh router to gateway under a worst-case scenario while maintaining recommended quality of service. The scalability quantification model can be used by network engineers to design, deploy, and re-design any type of wireless mesh community network. The battery management component consists of two sets of voice call experiments over two testbeds. Voice calls are prioritized for the battery management component following survey results from Zenzeleni that highlighted usage of mobile devices primarily for voice calls. The battery management component can be applied towards any type of smartphone and communication application. Therefore, the overall scalability framework successfully addresses scalability quantification and low-end smartphone battery consumption management gaps to aid in the deployment of wireless mesh community networks in rural areas.

Acknowledgements

First and foremost, I thank the Almighty God for blessing me with the knowledge, perseverance, and good health to reach this level of success.

My heartfelt thanks and appreciations are conveyed to my supervisor, Prof. William D. Tucker. I feel fortunate and privileged to have been guided by such a remarkable academic. I value his insights, unparalleled knowledge, and the valuable time he spent guiding me in my research. Without his constructive critiques and advice, this thesis would not have been the same.

Many thanks to the National Research Foundation (NRF) – The World Academy of Science (TWAS); and the Telkom/Cisco/Aria Technologies Centre-of-Excellence at the Department of Computer Science at the University of the Western Cape for their financial support throughout the duration of my studies. Without their support, it would not have been possible to do this research.

Many thanks to the Department of Computer Science Department staff, especially, Mrs. Jacobs-Samsodien, Ms. Abbott, and Mr. Leenderts for their selfless assistance in seeing to my (at times urgent) needs.

One of the joys of completing my thesis is looking back at the long journey and remembering all the people that I met along the road and ended up forming close bonds with them. My heartiest thanks Mr. Ghirish Chibba, Mrs. Saira-Banu Chibba; and the Chibba and Adams family for their unconditional support and concerns in my well-being during this long but fulfilling road. Special thanks to Mr. Andre Henney (and family) and Ms. Prangnat Chininthorn for their concerns in my well-being; and constantly supporting and motivating me to finish.

To my friends – Mr Waleed Deaney, Mr Zenville Erasmus, Ms Prangnath Chininthorn, Ms Semande Tovide, Mr Taha Abdalla, Mr Frank Kassongo, and Mr Freedwell Shingange – Thank you for all your support.

Lastly, to the three pillars of my life – Prof. Girija S. Singh (Pa), Mrs. Geeta K. Singh (Ma), and Miss. Surabhi Singh (Sis) – this PhD would not have been possible without you. You guys kept me sane through the uphill-battles and the many frustrations that I faced during this PhD journey. I am thankful to my parents who instilled in me the values of hard work and dedication. It is a blessing to be born in to this family.

Publications

Om, S., & Tucker, W. D. (2018). Battery and Data Drain of Over-The-Top Applications on Low-end Smartphones. 2018 IST-Africa Week Conference (IST-Africa), 1–12. Retrieved from: https://ieeexplore.ieee.org/document/8417297

Om, S., & Tucker, W. D. (2018). Investigation of a Dual-band Dual-radio Indoor Mesh Testbed. *Southern Africa Telecommunication Networks and Applications Conference (SATNAC 2018)*, 330–335. Retrieved from: http://hdl.handle.net/10566/5251

Om, S., Rey-Moreno, C., & Tucker, W. (2017). Investigating battery consumption in low-end smartphones: Preliminary results. *2017 IST-Africa Week Conference (IST-Africa)*, 1–11. Retrieved from: https://doi.org/10.23919/ISTAFRICA.2017.8102309

Om, S., Erasmus, Z., Rey-Moreno C., & Tucker, W. D. (2015). Evaluating energy consumption on low-end smartphones. *Southern Africa Telecommunication Networks and Applications Conference (SATNAC 2015)*, 2:29–30. Retrieved from: http://hdl.handle.net/10566/5253

Om, S., Rey-Moreno C., & Tucker, W. D. (2015). Towards a Scalability Model for Wireless Mesh Networks. *Southern Africa Telecommunication Networks and Applications Conference (SATNAC 2015)*, 2:49–50. Retrieved from: http://hdl.handle.net/10566/1947

Contents

List of tables

List of figures

Glossary

3G	Voice calls using 3G data with Wi-Fi radio OFF
3G-X	Voice calls using 3G data with Wi-Fi radio ON but not connected to any AP
ABC	Average Battery Consumption
ACWN	Akwapim Community Wireless Network
ADSL	Asynchronous Digital Subscriber Line
AODV	Ad-hoc On-demand Distance Vector
AODV-UU	Ad-hoc On-demand Distance Vector – Uppsala University
AOMDV	Ad-hoc On-demand Multipath Distance Vector
AP	Access Point
ASORCOM	Alternative Solutions for Rural Communities
ATA	Analog Telephone Adaptor
BATMAN	Better Approach to Mobile Ad-hoc Networking
BATMAN-adv	Better Approach to Mobile Ad-hoc Networking - advanced
BT	Bluetooth
CBLit	Community-Based Libraries and Information Technology
CBR	Constant Bit Ratio
CG	Cluster Gateway
CSIP	CSipSimple
CTS	Clear-to-send
CWMN	Community wireless Mesh Network. CWMNs is used for plural cases.
DBM	Difference Between Means
DCWMN	Dharamsala Community Wireless Mesh Network
DHCP	Dynamic Host Configuration Protocol
D-ITG	Distributed-Internet Traffic Generator
DIY	Do It Yourself
DRC	Democratic Republic of Congo
DSDV	Destination Sequence Distance Vector
DSR	Dynamic Source Routing
DSR-MP	Dynamic Source Routing - Multipath
DTR	Data Transmission Rate
ETT	Expected Transmission Time
ETX	Expected Transmission Count
FTP	File Transfer Protocol
GB	Gigabyte
GHz	Gigahertz
GMR	Gateway Mesh Router
GSM	Global Systems for Mobile communications
GSMA	Global Systems for Mobile communications Association
HS	Hole Size
HSD	Honest Significance Difference
HT	High Throughput
HWMP	Hybrid Wireless Mesh Protocol
ICASA	Independent Communications Authority of South Africa
ICT	Information Communication and Technology
IEEE	Institute of Electrical and Electronics Engineers
IH-AODV	Improved Hierarchical Ad-hoc On-demand Distance Vector

IM	Instant Messenger
IMAP	Internet Message Access Protocol
InteRLab	Internet Education and Research Laboratory
IP	Internet Protocol
I-PEX	I-PEX Company Limited.
ISM	Industrial, Scientific, and Medical
ISP	Internet Service Provider. ISPs is used for plural cases.
ITU	International Telecommunication Union
ITU-T	International Telecommunications Union – Telecommunication Standardization Sector
Kbps	Kilobits per second
KBps	Kilobytes persecond
Km	Kilometre
KPMs	Key Performance Metrics – throughput, latency, jitter, and packet loss.
LB	Litebeam
LeS	Low-end Smartphone. LeSs is used for plural cases.
LQSR	Link Quality State Routing
MAC	Multiple Access Control
MANET	Mobile Ad-hoc Network
MB	Megabytes
Mbps	Megabits per-second
MIAM	Malaria Institute at Macha
MIMO	Multiple Input Multiple Output
MP	Mesh Potato. MPs is used for plural cases.
MPP	Mesh Portal Point
MPv2	Mesh Potato – "all wheel drive"
MR-LQSR	Multi-Radio Link Quality Source Routing
Ms	millisecond
mW	milliwatts
NMS	Node-mobility scenario
NPC	Not-for-Profit Company
NS-2	Network Simulator version 2
NSS	Node-static scenario
OLSR	Optimal Link State Routing Protocol
OTS	Off-the-shelf
OWJ	One-way jitter
OWL	One-way latency
PBX	Private Branch Exchange
PDR	Packer deliver rate
PL	Packet loss
PL%	Packe loss percentage
Pps	packets per second
PRR	Packet reception rate
PtMp	Pont-to-Multipoint
PtP	Point-to-Point
PWAN	Portable Multi-hop Ad hoc Nodes
PWRP	Predictive Wireless Routing Protocol
QoS	Quality of Service
RANN	Route Announcement

RPi2	Raspberry Pi 2
RREQ	Route Request
RTL	Round-trip latency
RTP	Real-time protocol
RTS	Request-to-send
RUDE/CRUDE	Real-time UDP Data Emitter/ Collector for RUDE
Rx	Received signal strength
SAMBA	Samba comes from SMB (Server Message Block)
SAP	Systems Applications and Products in Data Processing
SCYNO	Siyin-Chin Youth Network Organization
SIP	Session Initiation Protocol
SMTP	Simple Mail Transfer Protocol
SoC	System-on-Chip
SQL	Structured Query Language
Srcr	Roofnet routing protocol based on DSR
TA	Tribal Authority
TCP	Transmission Control Protocol
TH	Throughput round-trip
TQ	Transmission Quality
Tx	Transmitting signal strength
UDP	User Datagram Protocol
UniFi	Ubiquiti UniFi AC
USD	United States Dollars
UWC	University of the Western Cape
V	Volt
VLC	Video LAN client
VLE	Village Level Entrepreneur. VLEs is used for plural cases.
VoIP	Voice over Internet Protocol
VSAT	Very Small Aperture Terminal
W-2G	Wi-Fi calls with cellular radio in GSM network mode
W-3G	Wi-Fi calls with cellular radio in 3G network mode
W-AUTO	Wi-Fi calls with cellular radio in 2G/3G network mode
WCETT	Weighted Cumulative Expected Transmission Time
Wi-Fi	Wireless Fidelity
WMN	Wireless Mesh Network. WMNs is used for plural cases.
W-PLAIN	Wi-Fi calls with cellular radios turned off, hence achieving partial-airplane mode
WWAN	Wireless wide area network

1 Introduction

Community telecommunication initiatives are paving the way to closing the digital divide by opening doors to cheap 'last-mile' access to Information Communication and Technology (ICT) services for rural areas of the world that have a scarce supply of electricity and a low per-capita income to cellular network usage cost ratio. In coverage area and size, some rural community networks service just a few dozen households in a settlement, while others provide connectivity for thousands of users spread across a dozen or more villages (Bidwell & Jensen, 2019a). The community telecommunication projects are developed on an *inverse infrastructure* strategy whereby they are built, owned, operated, and used by citizens in a participatory and open manner; this is in contrast to the centralized approach adopted by established telecommunication operators and by government (Egyedi et al., 2007; Song et al., 2018). Therefore, community networks present themselves as opportunities for end-users, especially in rural low-income communities, to setup their own Internet infrastructure with mobile data tariffs decided by the community that could be based around their incomes. The world's largest community network, *guifi.net*[1] is evidence that community networks can be successful and carry socio-economic benefits. The creation of *guifi.net* began in 2004 in the Osona county of Catalonia, and now has more than 35000 working nodes with approximately 39000 links spanning over 66000 Kilometre (Km) across Catalonia, the Valencian Community, the Balearic Islands, Madrid, Andalusia, Asturias, and the Basque country, as of August 2019.

The scope of the research, presented via this thesis, focuses on the deployment of mesh community networks, widely known as Community Wireless Mesh Networks (CWMNs) geared toward sub-Saharan Africa and developing Asia. The rural low-income regions of sub-Saharan Africa and developing Asia are reported as the contributors of the most population with the least Internet penetration by Bahia (2018). Wireless Mesh Networks (WMNs) are dynamically self-organized and self-configured, with the routers in the network automatically establishing and maintaining mesh connectivity amongst themselves; creating, in effect, an ad hoc network (Akyildiz et al., 2005; Akyildiz & Wang, 2009). The automatic self-organization and self-configuration features bring advantages to WMNs over the traditional Wireless-Fidelity (Wi-Fi)

[1] http://guifi.net

infrastructures such as: low up-front cost, easy network maintenance, robustness, and reliable service coverage. Mesh routers, like common Wi-Fi routers, operate on the license-exempt Industrial, Scientific and Medical (ISM) spectrum which is an advantage for regions with strict wireless spectrum usage rules. Several research studies have revealed CWMN deployments in the rural low-income regions of: (a) Democratic Republic of Congo (Carlos Rey-Moreno, 2017; Zikomangane, 2018), Ghana (Agbenonwossi, 2018; Ebenezer et al., 2006), Zambia (Backens et al., 2010; Mweetwa & van Stam, 2018), and South Africa (Johnson, 2007b; Luca de Tena & Rey-Moreno, 2018; Tucker, 2018) in Sub-Saharan Africa; and (b) India (Belur, 2018; Buttrich, 2006; HimVani, 2006; Surana et al., 2008), Thailand (Kanchanasut et al., 2018; Sathiaseelan, 2017), and Myanmar (Suantak, 2018) in developing Asia; all deployed with the objective to provide affordable network services[2].

Equally important as providing cheap network services to low-income earning end-users through CWMNs, is the capability of the end-user to be able to regularly access the network. Smartphones, in recent years, have become the primary go-to device for making voice calls and accessing online services. Whereas smartphones provide easy mobile solutions to Wi-Fi access, their purchase prices and batteries present challenges to users earning low income; and to those who reside in rural areas with scarce electricity supply. Mobile phone users in rural areas often prefer to use basic feature phones due to their low cost and long battery life that can last over a week before requiring a recharge (Heimerl et al., 2015). Failure to integrate smartphones due to handset affordability and recharging issues can be deemed as a major drawback for CWMN projects. In addition WMNs have been criticized over the years by researchers for their scalability issues with increase in traffic, and distance between source and destination. However, the CWMN deployments in rural low-income regions imply that network performance issues of WMN have a lower priority than establishing a cheap ICT infrastructure for closing the digital gap.

Before presenting the research problems, the thesis presents details of a CWMN, Zenzeleni, which forms the basis to the research work presented via this thesis.

[2] Chapter 2, Section 2.2.1 and 2.2.2 are dedicated to the review of CWMN deployments in sub-Saharan Africa and developing Asia, respectively.

1.1 Background - Zenzeleni

1.1.1 Region demographics and context

Despite being the industrial and political stronghold of sub-Saharan Africa, South Africa has around 55.5% of its population living in poverty, with the percentage rising to 80% in the rural areas (Luca de Tena & Rey-Moreno, 2018). Belonging to such a rural demography is the Mankosi community located on the coast of the Eastern Cape Province of South Africa. The governance of the community, which consists of 12 villages, falls under a local Tribal Authority (TA) led by a Headman overseeing Sub-headmen from each village of the community. The Mankosi community has approximately 580 thatched roof or tin-roofed dwellings scattered over a 30 square kilometre (Km^2) area. A typical community household, which consist of families of up to 5 adults and 7 children, survive on monthly income of approximately 163-United Stated Dollars (USD) and an individual monthly income of 27USD that includes government grants and payments from family members that temporarily migrate for work (Carlos Rey-Moreno et al., 2016, 2014, 2013). A feasibility study of the community, that included the investigation of the English language reading and writing abilities, showed that only 46.7% of the members could read, and 35.6% could write English (Carlos Rey-Moreno et al., 2013). Further findings of Rey-Moreno et al. (2013) with regards to the inquiry into the level of schooling, revealed that only 13% of the population had completed secondary schooling or a higher level of education. An investigation of the ICT ecosystem of the 12 villages of Mankosi by Rey-Moreno et al. (2016) revealed that: (a) the mobile phone presence in households was 97.7% with individual ownership at 81.2%; (b) community members spent a fair share of their disposable income (21.97%) on mobile phone services (especially older people) which forced them to sacrifice basic food and household necessities; and (c) the average expenditure on communications enabled the users to fund approximately 18 cellular voice calls, 7 text messages, and 25-30 Megabytes (MB) data bundles. The statistics revealed constrained usage of mobile services, especially mobile data, due to high communication costs in relation to the community income. This digital gap has revealed a socioeconomic crisis that threatens the future development of people and communities in general that are facing a lack of affordable connectivity; and hence, people are deprived of digital opportunities such as job search, e-commerce, education, and other resources.

1.1.2 The Zenzeleni mesh

The Zenzeleni[3] (from isiXhosa meaning "do it yourselves") mesh initiative, through a partnership between dedicated community residents, researchers from the University of the Western Cape (UWC), and some grant funding, started off in 2012 with the objective to deploy a low-cost telecommunications network to provide free intra-network voice calls to members of the community with the idea of later charging a small fee for breakout calls (decided by the TA) and using the excess capacity of (mostly) solar powered 12-V deep cycle batteries to recharge phone batteries. The collection of the fees was intended to be used for network maintenance and finance other community improvement projects. The principle element of the network during this time was a low-cost low-powered off-the-shelf (OTS) outdoor mesh router called Mesh Potato (MP) (VillageTelco, 2011). The MP was built using open-source routing software with the principal feature being Asterisk[4] software-based private branch exchange (PBX) system that supported Session Initiation Protocol (SIP) and Voice over Internet Protocol (VoIP) calls. The PBX system was utilized with a standard on-board Analog Telephone Adapter (ATA) that took a normal analog phone handset and allowed for the provision of telephony without adding an extra device that would increase the power consumption. The first network consisted of 12 MPs placed on top of the thatched roof houses selected by the TA; in effect, the TA designed the network by choosing safe spots that had the necessary line of sight to form the mesh network. The single-radio single-band property of the MPs allowed the mesh backbone and access point (AP) to operate on the 802.11b/g wireless standard utilizing the 2.4 GigaHertz (GHz) frequency spectrum. The infrastructure was powered using 12 Volt (V) solar-charged batteries due to an absence of electricity in the community at the time. The mesh network empowered community members to make free intra-community calls and, also offered breakout voice calls, by subscribing to a cheap VoIP provider, at half the cost of charges by South African telecommunication operators (again, with cost decided by the community cooperative). Additionally, the power generated by the solar-charged batteries was used to provide mobile phone recharge facilities to community residents and generated revenue for covering network maintenance costs. The recharge service in Mankosi was offered at approximately 0.20USD per charge, half the cost charged by the privately-owned mobile

[3] www.zenzeleni.net
[4] Asterisk link: https:// www.asterisk.org

recharging kiosks in the area. Figure 1 shows the original 12 MP architecture in Mankosi as of about 2014. The operative maintenance plan of the MP-powered Zenzeleni was divided into three-levels consisting of: (1) local users to carry out basic maintenance tasks; (2) trained local technicians and more skilled technicians from the nearest city who possessed the confidence necessary to address problems by themselves; and (3) higher level support from research activities for improving services (Carlos Rey-Moreno et al., 2013).

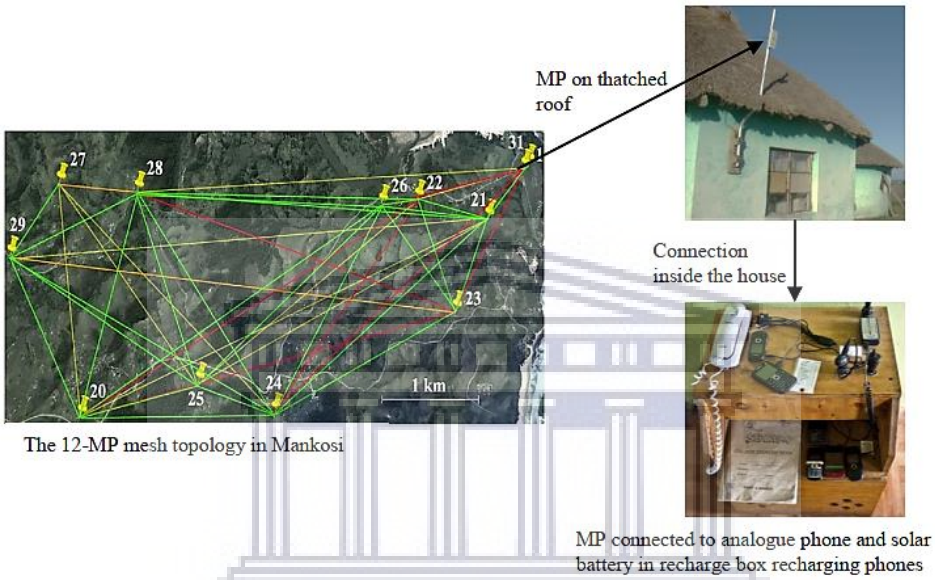

Figure 1: A 12 MP mesh architecture in Mankosi.
The figure above shows the location points of the MP units located on top of thatched roof houses, and connected to the solar batteries placed inside the recharge box via power-over-Ethernet.

In 2014, Zenzeleni established a local cooperative with full license exemptions to operate as an Internet Service Provider (ISP) and offer communication services given by the telecommunication regulating body of South Africa, Independent Communications Authority of South Africa (ICASA) (Luca de Tena & Rey-Moreno, 2018; C. Rey-Moreno et al., 2015). The operation of Zenzeleni has also led to the formation of a not-for-profit company (NPC), also called Zenzeleni that acts as a support mechanism for the cooperative (there are currently two) and as a bridge between the local community and the established telecommunications sector. The goals of Zenzeleni NPC and the Zenzeleni cooperatives are to reduce the cost of communications for the community members, maintain the network infrastructure, and manage billing and selling of data services.

With the progression of time, the Zenzeleni NPC and community members expressed interest in exploring cost-effective and power-efficient ways to broaden the use of Zenzeleni so

that residents, in addition to voice calls, could also access Internet services such as Facebook and WhatsApp. Therefore, in 2015, the Zenzeleni project commenced the upgrade of the 12 MP nodes to their newer version with better hardware specifications, Mesh Potato – 'all-wheel-drive' (MPv2) (VillageTelco, 2016); began working towards a data gateway; and considered introduction of smartphones in the community. Anticipating an increase in network traffic due to an increase in the number of network nodes, motivated the replacement of single-radio single-band MP devices with dual-band and dual-radio multiple-input multiple-output (MIMO) capable MPv2 routers. Both radio modules in the MPv2 unit used the 802.11n wireless standard as compared to the 802.11b/g of the MP, and therefore were capable of transmitting at much higher capacities. To provide higher throughput capacity, the mesh backbone was set to use the MIMO capable 5GHz radio module and the second radio was for the AP services set to use the 2.4GHz frequency spectrum.

1.1.3 Smartphones in the community

Upgrades that considered the introduction of smartphones in the Mankosi community raised challenges in terms of affordability. A report by Global Systems for Mobile communications Association (GSMA) Intelligence showed that the average smartphone selling price of smartphones was above 100USD at the time (GSMA Intelligence, 2015). The use of over-the-top social communication applications such as Messenger, WhatsApp, Skype, and IMO, which are only available on smartphones, have uprooted the traditional voice calling methods and texting (Farooq & Raju, 2019; Stork et al., 2017; Sujata et al., 2015).

Table 1: Three of the lowest once-off data bundle prices offered by South African operators
The once-off data bundle prices are presented to show the disparity between them and the monthly individual income of Mankosi.

	Deal 1	Deal 2	Deal 3
MTN	20MB for 0.66USD	50MB for 1.32USD	100MB for 1.91USD
Vodacom	15MB for 0.66USD	30MB for 0.79USD	55MB for 1.65USD
Telkom	27MB for 0.48USD	50MB for 0.97USD	100MB for 1.93USD
Cell C	40MB for 0.79USD	65MB for 1.32USD	200MB for 1.91USD

However data bundles required for use of the social communication applications are questionably affordable for low-income residents of Mankosi. To present evidence of high costs of communication in South Africa, Table 1 shows examples of three of the lowest priced monthly

once-off data deals[5] offered by the four major mobile network operators in South Africa, amongst whom Cell C has the best offer at approximately 1.9USD per month for 200MB of data.

In addition to the purchase cost of the device, and secondly, the network usage cost, a third cost of recharging batteries has regularly played an important role in the reluctance to adopt smartphones. It is commonly observed that smartphone batteries barely make it through the 24-hours of the day. Taking such into perspective, if a Mankosi resident owned a smartphone, an expenditure of approximately 6USD per month would be needed for recharging[6]. Further, recharging mobile devices is a micro-business opportunity in sub-Saharan African regions with scarce electricity supplies, therefore recharge costs are similar to those of the Mankosi cooperative; the monthly revenues of the top recharging businesses are in the range of 100–250USD (Collings, 2011).

1.1.4 The Zenzeleni migration and expansion

Zenzeleni began a major network topology overhaul towards the end of year 2017, including a backhaul data connection to fibre in a 'nearby' city. The transformation was driven by Zenzeleni's goal of supporting approximately 20 to 30 communities surrounding Mankosi and sustainably connecting about 300,000 people including schools, clinics, hospitals and homes, to cheaper voice, data and phone battery charging (Tucker, 2018). In order to accomplish these goals, commercial Ubiquiti Litebeam *5AC Gen2* Point-to-Point (PtP) devices were utilized for long distance backbone links; and the MPv2 routers were replaced by commercial Ubiquiti UniFi AC (UniFi) mesh devices. In addition, approximately 100 other UniFi APs were deployed which included the neighbouring Zithulele community. The Zithulele network is overseen locally by the Zithulele cooperative that was formed in 2018, and is also supported by the Zenzeleni NPC. The amalgamation of mesh and PtP supports AP connections of up to 10 Megabits per second (Mbps) with the network usage averaging around 40Mbps, but peaking to about 350Mbps. The Zenzeleni upgrade to a mesh+ infrastructure has connected more than 11,000 people and 10 institutions (including three schools, two small businesses, a rural branch of a major South African bank and

[5] The deals were acquired from the mobile network operator websites in the first quarter of 2018. The prices are volatile and change frequently.
[6] The total recharge cost is calculated by multiplying the 0.20 USD recharge cost offered by Zenzeleni with 30 days.

two hotels), offering prices as much as 20 times lower than those offered by existing operators, with substantially better quality.

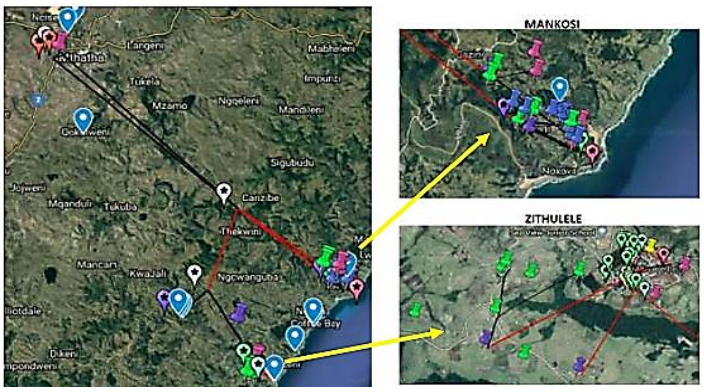

Figure 2: Architecture of Mankosi and Zithulele community networks
Figure shows a condensed topology of the two connected communities of Mankosi and Zithulele, and a backhaul to Mthatha.

Figure 2 shows the inter-connected architecture of Mankosi and Zithulele community networks. The Mankosi and Zithulele networks average about 500 users a day collectively with the concurrent devices peaking at 60 in Mankosi, and 150 in Zithulele. The latest Zenzeleni network features mesh networks at the leaves of the networks, in the villages. One of the major mesh network challenges, scalability, is left unexplored; and the challenge of relaying to end users how the use of Wi-Fi services affects their phone battery use becomes a priority in order to help them make more informed choices.

1.2 Research problems

1.2.1 Scalability quantification of wireless mesh networks

Scalability is the characteristic of a network that ensures quality of service (QoS) with change in network topology such as increase in traffic and network growth. A scalable network can provide QoS because it will keep maintaining the recommended targets for throughput, latency, jitter, and packet loss recommended in G.1010 recommendations (ITU-T, 2001b). A CWMN is bound to see growth in the number of users and thus experience increase in network traffic and network resource contention. However, it is often reported in related work[7] that the QoS of a WMN is affected negatively, exhibited by drop in throughput, latency and jitter, and increase in packet loss, due to the addition of new nodes and new users. Throughput scaling models (Gupta et al., 2001; Gupta & Kumar, 2000; Jiandong Li et al., 2002; Johnson, 2007b), have been devised over the years to

[7] A detailed review of related work investigating performance of WMNs is presented in Section 2.2.2.

predict throughput degradation with an increase in the number of nodes (hop-count) between source and destination. The models serve as a foundation for predicting throughput scalability limits of WMNs with an increase in hop count[8]. However, research work at developing network scalability quantification models using performance results of all four key performance metrics (throughput, latency, jitter and packet loss) with increasing hop count and traffic load is lacking. Such scalability quantification model(s) can be used to predict the maximum hop limit between source and destination and maximum end-users per mesh node, for WMNs while maintaining acceptable QoS limits. Therefore, this scalability quantification research attempts to answer the following research question:

Given the baseline (first hop) throughput, latency, jitter, and packet loss, what is the maximum hop length limit between mesh nodes and the gateway in a given wireless mesh network, while maintaining acceptable quality of service limits?

1.2.2 Smartphone battery consumption

Faced with high costs of smartphone handsets and data tariffs along with high recharge costs in rural areas without electricity, it is only natural that mobile phone owners residing in such areas would refrain from using smartphones and stick with feature phones. In order to bridge the device ownership gap, GSMA recommended 25-50USD low-end smartphones (LeSs) in their mobile economy report (GSMA Intelligence, 2015). However, the low-end smartphones are resource constricted devices, especially when it comes to battery capacity. Small-size battery capacity in the low-end smartphones is a problem in areas with little or no electricity. Social communication applications consume a significant share of smartphone battery with their frequency of usage being directly proportional to smartphone batteries depletion rate. In the case of low-end smartphones, frequent communication using such applications would mean quicker battery depletion and frequent recharging; thereby, increasing dependence on a constant supply of electricity in rural areas with scarce electricity supply. Further, if the case of regions with little or no electricity where mobile users pay recharging micro-businesses to recharge their handsets, is considered, frequent visits to these recharging stations can be a financial burden if users switched to low-end smartphones. Whereas Zenzeleni provides a battery-friendly and inexpensive communication

[8] The phrase ‘hop count’ and ‘hop length’ are used interchangeably throughout the remaining part of the thesis.

model, usage of low-end smartphones still requires careful management to get the maximum out of both limited battery capacity and airtime in a single recharge. It is well established that Wi-Fi consumes less battery than wireless technologies such as 2G, 3G, and Bluetooth (BT) commonly found in mobile phones (Carroll & Heiser, 2010; Friedman et al., 2011; Kalic et al., 2012; Nurminen & Noyranen, 2008; Om et al., 2017; Perrucci et al., 2011; Subramanian et al., 2006; Xiao et al., 2008). The smartphone battery consumption research is driven by the hypothesis that given the presence of a CWMN in a low-income rural community, smartphone usage can be promoted via the usage of LeSs and their efficient battery management, by using Wi-Fi as the primary mode of communication, together with the least battery consuming social communication application. However, during usage of Wi-Fi, the cellular radios are always active in the background consuming battery; and a hierarchy of social communication applications based on their battery consumption is lacking. Therefore, the smartphone battery consumption research attempts to answer the following research question:

What is the most efficient Wi-Fi and network mode combination; and social communication application, in terms of battery and data consumption, for low-income off-grid users residing in rural areas, given the presence of community wireless mesh networks?

1.3 Thesis outline

The rest of the thesis is organized as follows:

Chapter 2: Related work. The chapter begins with notable examples of CWMN deployments in developing Asia and sub-Saharan Africa, emphasizing the challenges they are tackling and the services being provided. The chapter then delves into scalability in WMNs and presents a review of multimedia quality of service requirements, quality of service in WMNs, and scalability quantification in WMNs. Afterwards the chapter presents a review of smartphone penetration in sub-Saharan African and developing Asia along with related work on battery consumption by different wireless technologies in mobile phones and battery consumption by commonly used social communication applications. The chapter concludes by pointing out the research gaps in the field of scalability quantification in wireless mesh networks and smartphone battery consumption.

Chapter 3: Methodology. This chapter discusses the methodology entailed in the research and description of the experimental design addressing the network scalability quantification in WMNs and smartphone battery consumption. The experimental design consists of the details of: type of

tests, physical topology, experimental technique, testbed design, data collection methods, and data analysis techniques; used for wireless mesh network scalability quantification and smartphone battery consumption experiments.

Chapter 4: Results. The chapter is divided into two sections. The first section presents the performance results of throughput, latency, jitter, and packet loss obtained from the network scalability quantification experimentation over MPv2 and UniFi testbeds, respectively; and the application of regression analysis and mathematical techniques to convert the results into performance trend equations. The second section presents the results of smartphone battery consumption experiments, this consists of a) wireless technology evaluation which compares battery drain in three LeSs during VoIP calls over Wi-Fi with different cellular radio combinations and 3G with Wi-Fi combinations; and b) mobile applications evaluation which compares battery and (additionally) data drain by most common instant messenger (IM) and SIP applications.

Chapter 5: Discussion. The chapter is also divided in two sections. The first section discusses the motivation, methods, and results of the network scalability quantification research. The second section discusses the same aspects of the smartphone battery consumption research.

Chapter 6: Conclusion. The chapter concludes the thesis with a presentation of the contribution of the overall research along with the limitations and future work.

2 Literature review

This chapter begins with an overview of CWMNs in sub-Saharan Africa and developing Asia; and their impact on the socio-economic challenges faced by the regions. The chapter then presents related work on scalability in WMNs covering the topics of QoS requirements; performance behaviour of key performance metrics (KPMs) in WMNs; and scalability/capacity models. End-users and their devices are key players in the scalability of CWMNs, and smartphones are leading the mobile Internet connectivity race due to applications such as Facebook, Messenger and WhatsApp. However, the developing regions of the world are facing a digital gap due to low mobile Internet penetration. Even if a CWMN is deployed in an area with absence of, or unaffordable, telecommunications infrastructure, the residents still require a smartphone to access the network. The socio-economic benefits related to CWMNs can only be realized fully if everyone in the community has access to affordable devices and network services. Thus, following the literature review on scalability of WMNs, related work is presented including an examination smartphone Internet connectivity factors such as handset price, mobile prepaid tariffs, and electricity access (to recharge) in developing regions of sub-Saharan Africa and Asia. Smartphones require frequent recharging, and even if they are available in the developing regions at low-cost, along with a CWMN to offer low mobile Internet tariffs, careful management of the aforementioned devices is required to reduce battery consumption. Therefore, related work investigating battery consumption in smartphones is presented next. The penultimate section of this chapter presents the research gaps in work related to both scalability in WMNs and battery consumption in smartphones. The chapter closes with a brief summary of the whole chapter.

2.1 Community wireless mesh networks in developing regions

According to the 2019 year-end Internet usage report by International Telecommunication Union (ITU): (a) about 46 percent of the world population were not using the Internet; (b) about 13 percent of the population of developed countries are not using the Internet; (c) approximately 53 percent of developing countries' population are not using Internet; and (d) about 88 percent of least developed countries' population are not using Internet (ITU, 2019). Sub-Saharan Africa and developing Asia comprise almost all the least-developed countries; and it was reported in 2018 that out of the global rural population of approximately 3.4 billion, the two above mentioned regions contributed nearly 90% of the total (UN, 2018, 2019). A rather large percentage of the

unconnected is borne by sub-Saharan and developing Asia due to lack of infrastructure, affordability, consumer readiness, and availability of relevant online content and services (Bahia, 2018). Huge costs associated with rolling out wired infrastructure, in addition to the lack of commercial viability due to a low user base, have in many instances deterred governments and the private sector from prioritizing rural connectivity (Noll, 1999). In many cases, Internet regulation bodies also present a hurdle in setting up alternative communication infrastructures because they discourage competition in the provision of backhaul services (Wallsten, 2003).

However, the technological progress in key areas of wireless communication and cost reduction in core equipment components over the past decade has led to the emergence of distributed and decentralized wireless community networks as a form of communication technology to bridge the connectivity gap in remote areas (FGV Direito Rio, 2016). Community wireless networks are built, owned, operated and used by citizens in an open and participatory manner to meet different societal objectives at an affordable price (Song et al., 2018). This section presents a review of such notable CWMN deployments in sub-Saharan Africa and developing Asia which are addressing the issues of network infrastructure, and providing affordable networking services by offering relevant content.

2.1.1 CWMN deployments in sub-Saharan Africa

Presented below are notable deployments that have changed the face of connectivity in sub-Saharan Africa outside of Zenzeleni, including the Democratic Republic of Congo (DRC), Ghana, Zambia and another network in South Africa.

2.1.1.1 Mesh Bukavu, DRC

As mentioned in the report by Zikomangane (2018), Bukavu is a city of more than 870000 inhabitants in a space of 45Km^2; and like everywhere else in the DRC, suffers from frequent electricity outages, with several areas having no electricity at all. The cost of the Internet offered by the main telecommunication operators in DRC remains high, which makes it difficult for the majority of the DRC population that survives on less than 1USD per day to access Internet services. The Internet packages offered by the three main mobile phone operators cost 100USD and 62USD to purchase a 4 Gigabytes (GB) monthly data bundle for Vodacom and Orange subscribers, respectively; and 100USD to purchase a 25GB monthly data bundle for Airtel users (Zikomangane, 2018). In order to tackle the high costs of connectivity, Mesh Bukavu, a CWMN

project was set up in 2015 by a group of journalists, bloggers, and computer scientists that allows people in the city of Bukavu with low incomes, and especially those living in poor neighbourhoods, to have free access to a Wi-Fi intranet network (Carlos Rey-Moreno, 2017; Zikomangane, 2018).

According to Zikomangane (2018), the Mesh Bukavu project utilizes mesh routers (Ubiquiti and TP-Link) setup on the rooftops of houses for long-distance coverage; and a central server setup at a local community radio station with a generator to counter the severe shortage of electricity. The mesh project was received with such optimism by community members that the homeowners enthusiastically approved of network equipment installation on the rooftops of their houses, and volunteered to setup and take care of the equipment without asking for compensation (Zikomangane, 2018). The Mesh Bukavu project is an internet-intranet ecosystem whereby people access cached Internet resources such as: Wikipedia; a digital library consisting of more than 360,000 e-books; course material for online Computer Science and English courses; and an intranet chat application, Chat Secure; all of which are setup by a technical team (Zikomangane, 2018).

2.1.1.2 Wireless Ghana, Akwapim, Ghana

As reported by Agbenonwossi (2018), Wireless Ghana is a rural project implemented by a non-government organization called Community-Based Libraries and Information Technology (CBLit). The project was initially deployed by CBLit in 2005 as Akwapim Community Wireless Network (ACWN) at the Apirede Resource Centre, Akwapim, at the request of the local community to find ways to break their shackles of digital isolation and progress their children and the community closer to the 21st century (Agbenonwossi, 2018; Ebenezer et al., 2006). The ACWN has over 20 nodes, and has a range of between 10-15 Km providing connectivity to Koforidua Technical University, secondary schools, churches, non-profit organizations, businesses and community activity centres across six towns in the mountainous region of Akwapim. The report by Agbenonwossi (2018), also mentions that the Wireless Ghana project has gone through a striking expansion over the years with projects such as Campus Wi-Fi at the University of Cape Coast in the western region for students and lecturers to share resources and data among themselves; and another network launched at Sakumono in the Tema Metropolitan District in the Greater Accra region of Ghana.

Wireless Ghana is based on mesh architecture using low-cost Wi-Fi hardware which consists of a mix of Ubiquiti brand devices that include NanoStation *NSM2* (2.4GHz), Bullet *M2* and PicoStation *M2*. The Internet backhaul for the nodes on the Akwapim network is provided via a shared 128/32 Kbps Very Small Aperture Terminal (VSAT) connection (Agbenonwossi, 2018). Agbenonwossi (2018) further reports that network nodes are installed by the volunteers working on Wireless Ghana and the total cost of a typical node installation comes to approximately 500USD which covers both equipment and installation costs. Due to the uneven dispersal of electrical grid and an unreliable supply of electricity in the region, the volunteer mesh team innovates alternative power supply systems to power the network, such as using car batteries capable of powering a wireless network node for up to 24-hours during a power outage, (Agbenonwossi, 2018). Since its introduction in the community, the initiative has built local digital libraries that have become hubs for free and open access to information and documentation for students and teachers. The initiative not only provides Internet access to community libraries to allow students to browse and do their research, but also trains the students (through volunteers) on computer literacy, Internet use, and coding (Agbenonwossi, 2018).

2.1.1.3 The Macha Network, Zambia

Macha is a semi-arid flat farming area situated in the Choma District of Southern Zambia populated by some 135,000 villagers residing in homesteads scattered over a circular area with a 35Km radius and surviving on an average per villager income of approximately 1USD a day (Backens et al., 2010; Mweetwa & van Stam, 2018). According to Backens et al. (2010), the motivation for the Macha Network project was fuelled by (a) the unreliability of the deployed Global System for Mobile Communications (GSM), or commonly known as 2G, that experienced constant service outages; and (b) the expensive cost of unreliable Internet (marred by weather and power fluctuations) provided in the area, through VSAT, Enhanced Data rates for GSM Evolution (EDGE) and Short Wave technologies. Therefore, in 2006, the LinkNet[9] organization laid the foundation of an inspiring and powerful ICT infrastructure, The Macha Network, with the vision of empowering isolated rural communities in Zambia with community-built, maintained and managed Internet infrastructures while providing ICT training to locals (Backens et al., 2010; Mweetwa & van Stam, 2018).

[9] http://www.machaworks.org/en/linknet.html

With the deployment of 52 mesh nodes and 99 APs, the Macha Network, at the time it was deployed, was one of the largest community-run rural WMNs in Africa (Backens et al., 2010). The most common router used in the network was the Linksys WRT54GL[10] flashed with custom open-source firmware used in Freifunk[11] community networks in Germany for mesh connectivity; and default Linksys firmware based on DD-WRT[12] router operating system for AP mode (Backens et al., 2010). A central tower within the Malaria Institute at Macha (MIAM) complex served as the Internet gateway and connected using C-Band VSAT with bursty committed information rate between 128Kbps to 1Mbps and a Ku-Band VSAT with bursty rate between 32Kbps and 256Kbps (Backens et al., 2010). As reported by Backens et al. (2010), the Macha Network provided Internet services to approximately 150 users per day scattered between the MIAM campus, the Macha Mission Hospital residences, and the Macha community centre. The community centre was used as an Internet cafe for e-learning via a massive open online course platform, where courses ran on acquiring farming knowledge on crop diversification (Backens et al., 2010).

2.1.1.4 The Peebles Valley Mesh, South Africa

Peebles Valley is located in a hilly area of the north-eastern region South Africa and is home to the Masoyi tribal community (Johnson, 2013). As reported by Johnson (2013), the Masoyi community is a low-income, under-serviced community with untarred roads, houses lacking running water, and irregular electricity supply. Further, the community is gravely impacted by acquired immune deficiency syndrome (AIDS) affecting the lives of many salaried members of households (Johnson, 2013).

According to Johnson (2013, 2007b), the Peebles Valley Mesh network was deployed to provide Internet services to a non-governmental AIDS Care Training and Support clinic in the community. A 9 node WMN spanning 15Km^2 was deployed in the mountainous rural valley using router and firmware similar to the ones used in the Macha Network (Backens et al., 2010) with added modifications such as (a) placing router-boards in aluminium boxes for outdoor usage; and (b) usage of either commercial directional antennas or hand-made 'cantennas' on high poles to overcome line-of-sight challenges (Johnson, 2007b). The Internet backhaul was provided via a

[10] https://www.linksys.com/nz/p/P-WRT54GL/
[11] https://freifunk.net/en/what-is-it-about/
[12] https://dd-wrt.com/

VSAT link which provided a 2GB data usage limit per month at 256Kbps download and 64Kbps upload rates, respectively (Johnson, 2013, 2007b). Johnson (Johnson, 2013, 2007b) further reports that since the acquired data-limit was always underutilized due to an idle network (the link remained idle 40% of the time in a month), the left over data was distributed to surrounding schools, homes, farms and other clinics connected via the mesh network free-of-charge through an expertly configured firewall such that the free usage did not affect the AIDS clinic's Internet availability. Several network services were provided through the mesh with the key features being the localization of traffic of services such as VoIP, file/print server, and Wikipedia in order to save bandwidth and data (Johnson, 2007b).

2.1.2 CWMN Deployments in developing Asia

Presented here are notable CWMN deployments that have changed the face of connectivity in developing Asia, including India, Thailand and Burma.

2.1.2.1 Palghar Project by Gram Marg, India

As reported by Belur (2018), Gram Marg[13] is a rural broadband project initiated by the Electrical Engineering Department of the Indian Institute of Technology, Bombay in 2012 with the objective to provide affordable broadband solutions, especially Internet, to rural India. Since the initiation, the Gram Marg project has enabled wireless connectivity via community networks in 25 villages in the Palghar district of Maharashtra, India, covering an area of approximately 300Km^2 (Belur, 2018).

As further reported by Belur (2018), mesh networks have been set up in 10 out of the 25 villages for the following reasons: (1) the villages are remote and hilly; and (2) there is an absence of mobile coverage in the villages. In each of the 10 villages, mesh APs are placed at the Gram Panchayat (self-governing body at village level) office; the primary health care centres; at least one school; and one community centre; and are powered by 48-hour battery backups charged using solar power to the infrastructure so that it is less dependent on unreliable grid electricity (Belur, 2018). The network in each of the 10 villages is maintained by its own Village Level Entrepreneur (VLE) who is a nominated village youth that undergoes training and skills development to maintain and operate the network in the village (Belur, 2018). It is further reported by Belur (2018)

[13] https://www.grammarg.in

that the 10 villages have a VLE-based revenue model whereby an ISP license holder (only) called Wi-Fi Choupal acquires bandwidth from local ISPs and sells bandwidth inside the villages via VLEs. In these 10 villages, the VLEs sell Internet coupons in value such as 0.14USD for 500MB data with 10 day validity, and 1.28USD for 12GB data valid for 28 days (Belur, 2018). It is reported that the number of broadband subscribers is increasing gradually leading to a steady growth in revenue generation by the VLEs (Belur, 2018).

2.1.2.2 Dharamsala Community Wireless Mesh Network by AirJaldi, India

The Dharamsala CWMN (DCWMN) project was initiated in 2005 by an ex-Silicon Valley techie and members of a security group with the objective to provide cheap, and reliable data and telephony services in the harsh mountainous terrain of the Dharamsala region (Buttrich, 2006; HimVani, 2006). The mesh networking infrastructure was preferred over point to multi-point (PtMp) links because (a) the PtMp links were unable to overcome the line-of-sight problem presented by the mountainous terrain of the region; and (b) the self-healing characteristic of WMNs proved to be crucial since the region faced scarce electricity supply (Buttrich, 2006). It was reported that in the later months of 2005 that the DCWMN operated from a single room in the Tibetan Children's Village that included a mesh backbone of 30 nodes and connected more than 3,000 computers (Buttrich, 2006; HimVani, 2006). The mesh backbone consisted of solar-powered in-house developed mesh routers called Himalayan-Mesh-Routers (built from recycled hardware and open-source software) installed at different locations; and the shapes of the router antennas varied between omnidirectional, directional, and occasionally high-gain (and cost) sectorial types along with their respective transmission strengths (HimVani, 2006). Along with Internet access, the mesh network was utilized for file-sharing, off-site backups, playback of high-quality video from remote archives and extensive VoIP telephony to network members (HimVani, 2006).

The growth of DCWMN led to the establishment of a class-A ISP in 2009 called Rural Broadband Privately Limited, with the objective to implement technically and economically viable Internet connectivity solutions for rural areas such as Dharamsala (AirJaldi, 2018). The abovementioned class-A ISP under the brand name *AirjJaldi*[14] has expanded WMN coverage around Dharamsala by combining multiple existing open-source hardware and software; and in

[14] AirJaldi link: https://airjaldi.com

the process managed to build one of Asia's largest CWMNs, owning approximately 17 operational networks in 6 Indian states with overall network coverage of approximately 30000 Km^2 and more than 250000 customers (AirJaldi, 2018). *AirjJaldi* networks provide Internet connectivity to end-users via Wi-Fi hotspots called *JaldiFi*[15] at subscription rates such as[16] single-day validity pack costing 0.27USD, 0.34USD and 0.41USD for 200MB, 300MB, and 500MB data limits, respectively; 7 day validity packs costing 0.68USD and 1.08USD for 1GB and 3GB data limit, respectively; and 30 day validity packs costing 1.35USD and 3.38USD for 6GB and 20GB data limit, respectively (AirJaldi, 2018).

2.1.2.3 TakNet Community Wireless Mesh Networks, Thailand

The creation of TakNet was motivated by the lack of cheap broadband connectivity, teachers, ICT literacy, and job opportunities in the low-density rural agricultural areas around the Mae-Sot city of Tak province in Thailand (Bidwell & Jensen, 2019b). The first TakNet CWMN started off as an academic project in 2013 and was deployed in the rural Thai Samakhee village with the assistance of the Internet Education and Research Laboratory (intERLab) at the Asia Institute of Technology in Bangkok, and financial support from the Thai Network Information Centre Foundation (Bidwell & Jensen, 2019b; Kanchanasut et al., 2018; Sathiaseelan, 2017). The early phases of TakNet deployment were assisted on a voluntary basis by university students and recent graduates, which included convincing the village residents to permit installation of the mesh routers outside on their home walls; and training the villagers to use and maintain the network at the completion of network setup to a local technical support team (Bidwell & Jensen, 2019b; Kanchanasut et al., 2018). The first TakNet (TakNet1) had a single Asynchronous Digital Subscriber Line (ADSL) backhaul that cost 28USD at the time and therefore to ensure sustainability, the cost of the backhaul was repaid equally by the households that were connected; this reduced the cost to approximately 2USD per month per household (Sathiaseelan, 2017). The success of the first TakNet led to several other TakNet CWMN deployments in the surrounding rural villages with the aim of providing educational content for schools and Internet services for the community members. By the end of 2017, TakNet had been deployed over 10 rural

[15] https://www.jaldifi.net
[16] The prices are converted from Indian Rupees to USD and is based on the conversion rate provided www.xe.com on March 14, 2020.

communities[17]. As reported by Sathiaseelan (2017), the intERLab team started a social enterprise in late 2016 called Net2Home, a team made up of a wireless ISP and a community network operators. Since the establishment of Net2Home, the TakNet infrastructure has moved from ADSL to fibre backhaul which costs approximately 7USD per month per household to cover the fibre, network installation, maintenance, monitoring, and support costs (Sathiaseelan, 2017).

2.1.2.4 Alternative Solutions for Rural Communities, Myanmar

As reported by Suantak (2018), a group called Siyin-Chin Youth Network Organization (SCYNO) deployed the Alternative Solutions for Rural Communities (ASORCOM) CWMN to overcome the absence of mobile network coverage in villages spanning the mountainous Siyin Valley in the Chin state of Myanmar. With the objective to deploy a low-cost CWMN, the SCYNO group acquired low-cost TP-Link long-range AP devices to initiate the project in 2013; and later redesigned the network infrastructure by replacing the TP-link devices with Ubiquiti devices to utilize 5GHz for the backhaul mesh connection between the villages, and 2.4GHz for AP mode (Suantak, 2018). Suantak (2018) further reported that the network infrastructure was powered using privately-built hydropower and solar power due to the absence of an electricity grid in the area; and the community members assisted the technical team with physical work, sharing houses for accommodation, and making food donations.

The SCYNO group provided basic computer and mobile literacy skills to the community members to enable them to use the services provided by the network (Suantak, 2018). According to Suantak (2018), the services provided by the ASORCOM network were utilized by different sections of the community as follows: (a) farmers gained knowledge on techniques and methods for agriculture cultivation, checked the weather forecast, and communicated with buyers from cities to negotiate vegetable prices; (b) school teachers and students gained access to educational content via locally cached educational content from Khan Academy[18], World Possible[19] and the Internet; and (c) users watch locally hosted entertainment videos on smartphones and laptops.

The examples presented in Section 2.1.1 and Section 2.1.2 show CWMNs' ability to: overcome environmental challenges such as mountainous terrain and to provide coverage over

[17] The TakNet deployment details including locations can be found on: https://interlab.ait.ac.th/cwmn/index.php
[18] https://www.khanacademy.org
[19] https://worldpossible.org

large surface areas; use unlicensed 2.4/5GHz frequency spectrum; and deploy low-power devices; all of which appear to show the advantages of WMNs over traditional Wi-Fi. Once the networks are set up, numerous innovative ideas to provide network services such as local content caching, VoIP, and chat can be implemented (and in some cases provided free of charge). A summary of all the examples presented in Section 2.1.1 and Section 2.1.2 is presented in Table A1.1 in Appendix A1. When CWMNs keep growing in coverage along with the number of users, network engineers are challenged by the scalability issue. The next section presents a review on scalability in WMNs.

2.2 Scalability in wireless mesh networks

Network scalability is the property of a network to guarantee end-user delivery of information and communication services without significant degradation of network performance regardless of increasing network size (Sampaio & Vasques, 2014a, 2014b). According to the International Telecommunication Union - Telecommunication (ITU-T) Standardization Sector recommendation G.1000, network performance contributes to QoS as experienced by the user (ITU-T, 2001a). Network performance is determined by the performance of network elements one by one, or the collective performance of all single elements as a whole; and pertains to the planning, development, operations, and maintenance of the network (Janevski et al., 2017). Quality of service is defined as the totality of characteristics of a telecommunications service that bear on its ability to satisfy stated and implied needs of the user of the service (ITU-T, 2008).

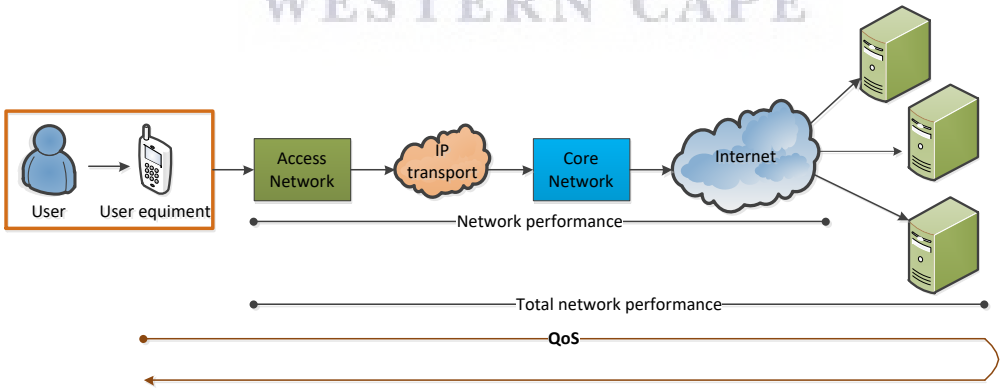

Figure 3: Elements affecting QoS in a network
Figure shows the different components that contribute towards QoS. It has been adapted from the Quality of Service regulation manual (Janevski et al., 2017).

As shown in Figure 3, end-to-end QoS depends on the successful synergy of components that include: the user and user equipment; the access network; Internet Protocol (IP) transport; the

core network; and the rest of the path end-to-end (e.g. through the Internet). The next section presents QoS requirements for multimedia traffic.

2.2.1 Quality of service requirements for multimedia traffic

For either wired or wireless network infrastructure, certain QoS requirements must be met depending on the type of network traffic. The ITU-T recommendation G.1010 identified that applications generating traffic can be categorized into eight groups shown in Table 2 (ITU-T, 2001b).

Table 2: Groups of application traffic

Traffic generated by application are classified in these groups by ITU-T G.1010 (ITU-T, 2001b). Colour coding is used to identify traffic types in further discussions.

Application Groups			
Interactive	**Responsive**	**Timely**	**Non-critical**
Conversational voice and video	Voice/video messaging	Streaming audio and video	Fax
Command/control	Transactional	Messaging, downloads	Background

Table 3: Data applications by class

The eight groups of application traffic mentioned in G.1010 can be aggregated into four classes, presented here along with properties and examples (Szigeti & Hattingh, 2004). The colour coding from Table 2 is followed to show the link between the four classes and the eight groups

Application class	Application/Traffic properties	Example applications
Interactive	Conversational voice and video. Highly-interactive applications with tight user feedback requirements.	Instant messenger audio/video calls, Telnet, Citrix, and Oracle Thin Clients.
Transactional	Transactional applications typically use a client-server protocol model. User initiated client-based queries followed by server response. Query response may consist of many messages between client and server. Query response may consist of many TCP and FTP sessions running simultaneously (for example, HTTP based applications)	SAP, PeopleSoft (Vantive) Oracle - financials, Internet procurement, buisness2business services, supply chain management, and application server, Oracle 8i Database, Ariba Buyer, Siebel, Epiphany Broadvision, Microsoft SQL,
Bulk	Long file transfers. Always invokes TCP congestion management	Database synchronizations, Network-based backups, Lotus Notes, Microsoft Outlook, E-mail download (SMTP, POP3, IMAP, Exchange), video content distribution, Large ftp file transfers
Best-effort		All non-critical traffic, HTTP Web browsing, and other miscellaneous traffic

Szigeti and Hattingh (2004) have reduced the eight groups of application traffic presented in Table 2 to four application classes along with their respective traffic characteristics and

examples of applications. The application class based traffic classification by Szigeti and Hattingh (2004) is presented in Table 3.

The recommended QoS requirements for KPMs throughput, latency, jitter, and packet loss of important day-to-day end-user network application classes presented in Table 3 compiled using G.1010 (2001b), G.114 (2003), and Szigeti and Hattingh (2004) is presented in Table 4 below.

Table 4: Performance targets for end-user application examples

It is very important to know the performance targets of general end-user application usage types in order to deliver QoS for those specific applications. The colour coding is again matched to application class and application/traffic properties in Table 3. The VoIP recommendations are those recommended by Szigeti and Hattingh (2004).

Medium	Application	KPM target values			
		Typical data rates (see Note 1)	Average one-way		PL%
			Latency	Jitter	
VoIP	Conversational voice (bearer traffic)	21-320 Kbps per call	Preferred < 150ms; Limit < 400ms limit	< 30ms	< 1 %
Video	Interactive video	>= 384 Kbit/s	Preferred < 150ms; Limit < 400ms	< 30ms	< 1%
	Streaming video	Varying	< 4-5s	none	< 5%
Data (see Note 2)	Best-effort data		Preferred < 2s per page Acceptable; < 4s per page	NA	NONE
	Bulk data		Preferred < 15; Acceptable < 60s	NA	NONE
	Transaction/Interactive Data		Preferred < 2s; Acceptable < 4s	NA	NONE
Note 1	Bandwidth requirements per call of several commonly used codecs can be found in Section A1.3.				
Note 2	In some cases, it may be more appropriate to consider these values as response times.				

However, maintaining scalability is challenging in multi-hop WMNs due to deteriorating QoS exhibited by drop in network performance of throughput, delay, jitter, and packet loss when increasing the number of users, and of hops between source and destination. The next section presents evidence of declining QoS in WMNs with increased network size and/or traffic in the form of a review of notable scholarly publications that have investigated network performance of the KPMs in WMNs for different application classes when changing network traffic and/or topology.

2.2.2 Quality of service in wireless mesh networks

The investigations of Draves et al. (2004) have explored efficiency of a routing metric called Weighted Cumulative Expected Transmission Time (WCETT) for improving routing in multi-radio and multi-hop WMNs by choosing a high-throughput path between a source and a destination. The WCETT metric was implemented in the Link Quality State Routing (LQSR) protocol developed by the same researchers; and the modified routing protocol was called Multi-Radio Link Quality Source Routing (MR-LQSR). To evaluate the efficiency of the WCETT metric, the change in throughput performance with an increase in the numbers hops between source and destination was measured, and the results were compared with results Expected Transmission Count (ETX), a routing metric developed by De Couto et al. (2003). Network emulation experiments were conducted over an indoor mesh testbed consisting of 23 desktops fitted with two 802.11-a/b/g compliant wireless cards per desktop as mesh nodes; and the traffic application class used for experimentation was transactional TCP data type. Results of experiments using single radio mesh backbone operating in 802.11-a mode, and dual-radio mesh backbone operating in combination of 802.11a and 802.11g modes, showed that throughput dropped with an increase in hops for both WCETT and ETX routing metrics. However, they found WCETT performed better than ETX. Notably, the achieved throughput per-hop in the dual-radio experiments was higher than that of single-radio for both WCETT and ETX metrics, and indicated that dual-radio WMN setups have better performance than single-radio WMNs.

Dilmaghani et al. (2005) evaluated performance of a hybrid WMN called RescueMesh with the aim of providing an easily reconfigurable alternative for first responders handling emergency response. Briefly, RescueMesh consisted of a three-tier architecture where AP clients formed the first tier; the WMN infrastructure formed the second tier; and the third tier included a long haul wireless wide area network (WWAN) backbone composed of PtP and PtMp wireless links operating at 5.2GHz and 5.7GHz respectively. The performance of RescueMesh was evaluated on the basis of change in throughput and one-way latency (OWL), with increasing hop length between client and gateway nodes. The change was measured using network emulation experiments over a testbed setup in a building; and used 802.11a/b/g OTS mesh node routers implementing a

proprietary Predictive Wireless Routing Protocol[20] (PWRP). The mesh node locations in the building were fixed and configured to operate in 802.11b mode; and the client nodes were regular laptops of people working in the building (and followed their mobility). The application class of the experimental data traffic consisted of transactional TCP and best-effort UDP types. The RescueMesh evaluation results showed that the throughput achieved by clients nodes for both TCP and UDP types of traffic decreased; and the OWL increased with an increase in the number of hops between client and gateway. Further results from Dilmaghani et al. (2005) showed that the transmitted data load decreased with an increase in distance from the gateway to the mesh nodes; which was indication of the emergency response packets being dropped with an increase in hops. It is also shown in results by Dilmaghani et al. (2005) that if a bottleneck was caused by a mesh node due to incoming traffic from several nodes or a weak signal, the packets were discarded and never made it to the Internet.

Tao et al. (2005) investigated optimization of WMNs implementing shortest path first-based routing protocols by proposing a traffic balancing system to solve the uneven traffic load problem appearing with such routing protocols. The proposed traffic balancing system was implemented with Dynamic Source Routing[21] (DSR) and compared against the default shortest-path routing approach of DSR. As reported by Tao et al. (2005), in a WMN with multiple gateway APs, it was highly likely that during the route establishment process, mesh nodes using shortest-path approach would converge their routes to a common AP, and avoid building routes to other APs because of longer paths. Traffic load from multiple source nodes flowing through the common AP would increase its processing complexity, and induce high congestion and collision rates leading to high packet loss and delay, respectively (Tao et al., 2005). In order to avoid traffic flow via a busy AP, the traffic balancing system proposed by Tao et al. (2005) built secondary routes via less busy paths to other gateway APs, and avoided the busy AP altogether. The experiments to evaluate the efficiency of the traffic balancing system was conducted in a simulated environment using network simulator–2[22] (NS-2); and the network performance metric measured to decide the efficiency of the traffic balancing system was packet delivery rate (PDR). The simulation

[20] PWRP information link: https://new.abb.com/communication-networks/communication-networks/products/wireless-networks/technology/Scalability
[21] DSR RFC link: https://tools.ietf.org/html/rfc4728
[22] NS-2 link: https://www.isi.edu/nsnam/ns/

parameters consisted of 100 nodes randomly distributed in a 2X2 Km^2 area with two APs located at coordinates x = 500m and y = 1000m; and x = 1500m and y = 1000m. Every sender generated best-effort UDP application class traffic at a 5.3Kbps constant-bit rate (CBR) between a wired node through one of the two APs. Scenarios with different node client node mobility (20, 5, and 0 metres per second maximum node speed) were simulated. The results showed that the DSR implemented with the proposed traffic balancing system was more effective at packet delivery than the default DSR; in fact, by 50% when there was high mobility of client nodes. However, as the number of communicating pairs increased in the area, the PDR of DSR with the traffic balancing system kept declining at a rate of 1.32%; and higher in case of DSR at 7.32%. Even though the traffic balancing system improved the PDR, the results still declined with an increase in traffic load and client mobility.

Experiments of Bicket et al. (2005) investigated performance of throughput and round-trip latency (RTL) in an outdoor WMN, Roofnet, with an increasing number of nodes between source and destination. The multi-hop Roofnet consisted of static 37 in-house developed mesh nodes operating in 802.11b mode deployed over an area of approximately $4Km^2$ in Cambridge, Massachusetts. The mesh nodes implemented an in-house mesh routing protocol called Srcr[23]. The experiments evaluated performance by transmitting TCP traffic, representative of transactional data application class, between hop pairs using *ping*. A similar experiment method to Bicket et al. (2005) was adopted by Johnson (2007b) to evaluate performance of the Peebles Valley mesh (reviewed in Section 2.1.1.4). The mesh nodes used in the Peebles Valley mesh network implemented Optimal Link State Routing[24] (OLSR) protocol. Experiments of Bicket et al. (2005) and Johnson (2007b) were conducted between hop pairs for a single flow of traffic which can be considered representative of a single user using the network at a time; and the results showed decline in throughput and an increase in RTL with an increase in number of hops between source and destination. The results of Bicket et al. (2005) showed that as the number of hops increased from 1 to 10, (a) throughput dropped from 2451Kbps to 182Kbs; and (b) RTL increased from 14ms to 218ms. The results of Johnson (2007b) showed that as the number of hops increased from

[23] Only the abbreviation of the routing protocol was given in the article. A Google search gave many full-names of SRCR that could not be tracked to the routing protocol used in Roofnet.

[24] OLSR RFC link: https://tools.ietf.org/html/rfc3626

1 to 5, (a) throughput dropped from 4867Kbps to 336Kbs; and (b) RTL increased from 4.69ms to 7.3ms.

Pirzada et al. (2006) investigated the performance of multi-path ad-hoc routing protocols to select the best multi-path routing protocol for WMNs. Multi-path variants of Ad-hoc On-demand Distance Vector[25] (AODV) routing protocol called Ad-hoc On-demand Multi-path Distance Vector Routing Protocol (AOMDV) (Marina & Das, 2006); and a DSR routing protocol called DSR-Multi-path (DSR-MP) (Nasipuri & Das, 1999) were compared against each other. The main idea behind multi-path routing protocols is to compute multiple disjoint routes/paths from source to destination to avoid route discoveries during link failures and path breaks (Pirzada et al., 2006). Most traditional ad-hoc routing protocols establish a single path from a source to a destination and new router discovery is performed only when the single path becomes unavailable. Thus by having multiple paths ready from a source to one particular destination, multi-path ad-hoc routing protocols overcome the shortcomings of the traditional single-path variants such as high routing overhead and limited scalability. The efficiency of AOMDV over AODV has been shown by Marina and Das (2001); and DSR-MP over DSR has been shown by Nasipuri and Das (1999). The KPM measured in the experiments of Pirzada et al. (2006) to evaluate performance of AOMDV and DSR-MP were goodput (application-level throughput), OWL, packet loss, and packet loss percentage (PL%). The selected experiment type was simulation in NS-2 configured with simulation parameters such as (a) 16 mesh routers deployed in a 4x4 grid topology spanning across 1Km^2 which assisted in establishing 20 simultaneous connections between the mobile mesh clients; (b) a total of 50 mesh clients in the simulation area; (c) application class of best-effort UDP data packets of 512B sent at CBR of 4 packets per-second (pps). The results showed that even though AOMDV performed better than MP-DSR, the packet loss increased and the goodput dropped for both protocols as the mobility of mesh clients increased, even though the transmission rate was kept constant. The OWL of the network was primarily determined by the route establishment time. A source node executing DSR-MP makes use of the cached routing information and is therefore able to quickly find routes. Results showed that with the increase in node mobility, the cached routes became stale causing more route discoveries to be initiated, which increased the OWL in the network. In the case of AOMDV, path selection had to be made at the

[25] AODV RFC link: https://tools.ietf.org/html/rfc3561

destination as well as at each forwarding node; which in turn increased the OWL of the network. The comparison experiment of Pirzada et al. (2006) showcased the scalability issue with change in network topology and traffic patterns.

Niculescu et al. (2006) carried out investigations to improve VoIP performance in WMNs using various traffic optimizations. The performance metric used to determine the call quality was R-score, a worst case and best case scale from 0 to 100 with 100 being best quality of voice rating; it was developed by Cole and Rosenbluth (2001). The R-score of Cole and Rosenbluth (2001) was a modified version of a similar scale evaluated during E-model development in ITU-T recommendation G.107 (ITU-T, 1998). The R-score combined performances of: the total ear to mouth delay comprising the vocoder delay; delay in the de-jitter buffer; network delay; and network and jitter losses. The VoIP calls in the experiments were encoded using G.729 codec, and the selected R-score threshold was 70 for a voice call to be considered successful. The experimentation consisted of testbed emulation and simulation. The testbed consisted of 15 dual-radio mesh nodes built using Click modular router architecture (Kohler et al., 2000); and used a Destination Sequence Distance Vector[26] (DSDV) routing protocol for mesh backhaul. The testbed was deployed in a 70X55 metre (m) area divided into two subsections such that one section had 11 nodes, and the other had 4 nodes (it was not disclosed if the subsections were halves). G.729 voice traffic was generated using RUDE/CRUDE[27] UDP traffic generator software. VoIP performance was tested for optimizations such as: (a) a dedicated interface and channel for sending and receiving to increase capacity; (b) use of separate channels to reduce self-interference; (c) a label-based traffic forwarding algorithm that separated the signalling and other types of best-effort traffic from voice traffic based on labels assigned to headers of the IP packets; (d) a pre-computed paths algorithm for voice traffic to create a list of 5 lowest OWL paths used by mesh at different times and therefore, send voice traffic over a pre-established path; and (e) an aggregation mechanism implemented at the outgoing mesh interface to encapsulate multiple small sized VoIP packets into larger packets to reduce the Medium Access Control (MAC) and physical layer overheads. Performance of VoIP call support for (a), (b) and single channel (default case) wireless interface configurations was evaluated over six hops in the testbed. The results showed that with

[26] DSDV link: https://www.cse.iitb.ac.in/~mythili/teaching/cs653_spring2014/references/dsdv.pdf
[27] RUDE/CRUDE link: http://rude.sourceforge.net/

increasing hop length between source and destination, (a) and (b) configurations supported more calls per hop length than the single channel configuration; configuration (a) supported more calls than (b) over short 1-hop length; configuration (b) supported more calls than (a) from hop length of 2 up to 5; and call support equalized for (a) and (b) at hop length of 6. Overall, there was marked improvement in the number of voice calls supported per hop length under (a) and (b) configurations than the default single channel configuration, but the number of supported calls per hop length showed a declining trend with increased distance. The (c) and (d) configurations worked in cohesion, and their overall performance was evaluated for one voice call over a pair of nodes at maximum physical distance in the testbed. The maximum physical distance between the two nodes allowed the possibility of maximum hop length paths, and path variety. Results of (c) showed that path lengths from 4 to 5 hops were formed between the two pairs of nodes; and that label-based forwarding is able to route the voice traffic around pre-computed alternate paths with less interference and congestion, yielding an average R-score of 71.2 for 86% of the time. Performance of (e) was compared against voice traffic sent with no-aggregation over a distance of six hops using testbed and simulation. For simulation, a WMN similar to the physical testbed was set up in NS-2. The results implementing (e) in the testbed and simulation setups showed that even though voice call support performance for every hop length was always higher with aggregation than no-aggregation, the overall number of voice calls supported per hop length declined with an increase in distance. Results of (e) further showed that with aggregation implemented, the testbed results were slightly lower than those simulation results; and similar to the simulation results with no-aggregation. Niculescu et al. (2006) mentioned the inability of the testbed nodes to maintain the set hop capacity (bandwidth) between pairs of nodes as the reason for the results of (e) being lower than simulation. A header compression mechanism was further combined with aggregation to further improve call support. Results of experiments carried out over the simulation network used for (e) showed that voice call capacity at each hop length (1 up to 6) with nodes implementing aggregation with header compression, was twice the number under a network implementing plain aggregation. In the final phase of evaluations, (b) was implemented with (e), and compared against results of no-aggregation and 'single channel with aggregation'. Simulation experiment results showed that the network implementing 'single channel with aggregation' mechanism on nodes supported approximately 4 times more voice calls per hop length than the network with no-aggregation implemented on nodes; and a network implementing configuration (e) with (b) on

nodes, supported approximately 1.7 times more voice calls per hop length from hop length 3 onwards than the network implementing 'single channel with aggregation' on nodes. However, even under (e) with (b) implementation, there was a gradual decline in the number of voice calls with increase in hop length. In addition, the difference between results of testbed and simulation experiments during evaluation of (e) highlighted the fact that simulations yield optimal performance results whereas the real-word performance would always be lower than optimal.

The experiments of Castro et al. (2007) evaluated the effectiveness of a packet aggregation mechanism at improving VoIP performance in WMNs. Performances of three KPMs, OWL, one-way jitter (OWJ) and packet loss ratio (PLR), were measured for VoIP traffic sent using no aggregation and compared against the proposed aggregation algorithm. The experimental topology was a tiered architecture that consisted of a VoIP gateway server connected over Ethernet to an Internet router; a gateway mesh router (GMR) linked via Ethernet to the Internet router; and mesh routers connected to the GMR in 802.11b mode. The VoIP traffic was modelled to represent a G.729a voice codec profile and the mesh routing protocol utilized was AODV-UU[28], a version of AODV developed by Erik Nordstrom at Uppsala University, Sweden. The experimentation, conducted in NS-2 simulation, consisted of VoIP traffic being sent from two separate mesh routers connected to the GMR over 2 hops. The results showed that the number of injected VoIP flows could be increased up to a certain threshold, above which the values of OWL, OWJ, and PLR increased immediately. With no aggregation the threshold was about 40 flows, and with aggregation it was about 60 flows; leading to capacity increase of 50%.

Abolhasan et al. (2009) compared the performance of three different routing protocols: Babel[29]; Better Approach to Mobile Ad-hoc Networking (BATMAN) and OLSR, to propose an optimal mesh routing protocol for WMNs. The experiments were conducted over a 5-hop indoor dual-band multi-hop testbed deployed using custom made routers by the same researchers called Portable Multi-hop Ad hoc Nodes (PWANs) (Abolhasan et al., 2007). The mesh backbone of the testbed was configured to use 802.11a; and the performance results of throughput, RTL, and PL% of Babel, BATMAN, and OLSR, respectively, were compared. The obtained throughput results showed that with an increase in the number of hops from 1 up to 5, the throughput of Babel dropped

[28] AOD-UU link - https://github.com/erimatnor/aodv-uu
[29] Babel RFC link: https://tools.ietf.org/html/rfc6126

from 32.8Mbps to 3.9Mbps; BATMAN dropped from 26.1Mbps to 2.9Mbps; and OLSR dropped from 28.6Mbps to 0Mbps (performance diminished after 2-hops in the case of OLSR). The obtained RTL results showed that with an increase in the number of hops from 1 up to 5, RTL of Babel increased from 0.93ms to 3.85ms; BATMAN increased from 0.97ms to 3.55ms; and OLSR increased from 0.99ms to 16.68ms. The overall PL% results showed that with an increase in the number of hops from 1 up to 5, PL% of Babel increased from 0% to 1 %; BATMAN stayed at 0%; and OLSR increased from 0% to 71%. The results of Abolhasan et al. (2009) showed that even though performance of a given WMN can be optimized by selecting a scalable routing protocol based on its performance in the given WMN, the overall performance of the WMN will still decline with an increase in the number of hops.

In order to optimize routing performance in WMNs, an improved hierarchical AODV (IH-AODV) routing protocol was proposed by Pei et al. (2009). IH-AODV was an improvement over traditional AODV and combined concepts of Clusterhead-Gateway Switch Routing (Chiang et al., 1997) and Way Point Routing (Bai & Singhal, 2006) with AODV. The performance results of OWL and PDR were compared for WMNs using IH-AODV and AODV. The experiments were conducted in NS-2 for two sets of scenarios with similar best-effort UDP traffic sent at CBR amongst the nodes. In scenario 1, while the CBR flow of 512B UDP packets was kept constant at 20pps, the nodes in the network were increased gradually from 100 to 1000. The node size and the area were selected as 100 nodes in 1400X1400 square metre (m^2); 200 nodes in 2000X2000m^2; 400 nodes in 2800X2800m^2; 600 modes in 3500X3500m^2; 800 nodes in 4000X400m^2; and 1000 nodes in 4500X4500m^2, to properly reflect the scalability of the routing protocols. The results of scenario 1 exhibited the following (a) both IH-AODV and AODV showed high (number not disclosed by researchers) PDR, even for networks with 1000 nodes; (b) IH-AODV consistently delivered about 1-2 percent more data packets than AODV; (c) with fewer than 400 nodes, IH-AODV registered slightly higher OWL than AODV; and (d) with growth in network size, IH-AODV showed a smaller OWL than AODV. In scenario 2, the performance of the routing protocols was measured for increase in packet rate from 20 to 60 in networks of 400 nodes. Results of scenario 2 showed that (a) IH-AODV registered higher PDR than AODV; and (b) IH-AODV had better OWL than AODV. However, if the overall results of IH-AODV for scenario 2 are considered, the performance of PDR and OWL dropped with an increase in the number of flows.

Though IH-AODV showed an improvement over traditional AODV, performance results still declined with an increase in traffic.

Investigations by Nassereddine et al. (2009) evaluated the performance of Hybrid Wireless Mesh Protocol[30] (HWMP) under varying network sizes and traffic loads. The QoS indicators used to evaluate mesh performance were throughput, OWL, and PDR. Square grid topologies with network size of 9, 16, 25, 32, 64, 100, and 225 nodes were configured in NS-2 for experimentation. The configured distance between two nodes was 175m; and the entire simulation area was calculated using the formula: 175X(Z-1)X175X(Z-1), where Z was the number of nodes. Simulations were conducted for three sets of measurements whereby set 1 consisted of a network with no gateway mesh portal point (MPP); set 2 comprised a network with one node playing the gateway role called mesh portal point (MPP) using the HWMP proactive Route Request (RREQ) packet; and set 3 consisted of a network with MPP using the HWMP Route Announcement (RANN) packet. For every set of experiments, the application class was best-effort UDP packets of 512B size transmitted at CBR; the network size was scaled from 9 to 225; and each network size was evaluated for traffic load from 10pps to 100pps. Results for experiment set 1 showed that (a) OWL increased with an increase in the number of nodes for the same traffic load, and increase in traffic load for the same number of nodes; (b) PDR pattern is the same for all traffic loads, however the loss increased significantly with an increase in network size especially past 64 nodes; and (c) the network throughput was very low for larger networks regardless of the load. The results of experiment set 2 showed that (a) OWL increased with network size and traffic load; (b) the packet rate decreased linearly and reached a very low rate when the size went over 64 nodes; and (c) throughput behaviour was similar to that of set 1 and was seriously affected by network size especially for networks larger than 64 nodes. Results of experiment set 3 showed that (a) OWL increased with network size and the gap kept getting larger with the traffic load getting bigger; (b) the packet delivery rate was also very low for networks with size larger than 64 nodes and even with small size, the delivery rate decreased with heavy traffic; and (c) the network throughput showed a declining trend with increasing traffic load and network size, and was very similar to the set 2 and set 1 experiment results. The results of Nassereddine et al. (2009) are further evidence of the scalability issues in WMNs with increasing network size and traffic.

[30] For HWMP specification: https://mentor.ieee.org/802.11/public/06/11-06-1778-01-000s-hwmp-specification.doc

The factual capability of WMN technology in supporting multimedia applications was investigated by Hamidian et al. (2009). The experiments were conducted over an indoor WMN testbed setup that used laptops as mesh nodes with Wi-Fi cards functioning in 802.11b/g mode; and LQSR mesh routing protocol. The network performance was evaluated using results of packet reception rate (PRR), and download time. PRR is considered as the goodput in packets successfully received at the destination per second. The application class consisted of bulk data in form of File Transfer Protocol (FTP) and video streaming; and conversational voice in the form of G.711 VoIP packets. The voice codec streams were generated using Distribute Internet Traffic Generator (D-ITG) (Avallone et al., 2005); the video streaming tests used Real Time Protocol (RTP) and VideoLAN Client[31] (VLC) media player; and the FTP tests was performed using Filezilla[32] client. The first experiment consisted of a single FTP/TCP download session of a 17.3MB file over the WMN, varying the number of hops that packets have to traverse from the source (the FTP server) to the destination (the FTP client). The client was connected to one mesh AP whereas the position of the FTP server varied. Results showed that the time to download the file increased linearly with the number of hops the flow had to traverse. The second experiment considered several users simultaneously engaging in voice chat with each other; and one background FTP session between two nodes at distance of 2 hops from each other. Results of 10 simultaneous VoIP streams and 1 background FTP session showed decrease in the average PRR with increase in number of hops. In a third experiment, the number of VoIP flows was varied from 1 to 10, and each set of flows traversed all 5 hops. The background traffic was either represented by an FTP flow or by a video stream traversing between the FTP/video streaming server and a mesh node 2 hops away. The results showed that the average PRR for the VoIP streams deteriorated more than that of the second experiment with an increasing number of simultaneous VoIP flows. The researchers claimed interference from the various flows and background traffic as the cause of decrease in average PRR with an increase in the number of hop and VoIP streams. The experiments of Hamidian et al. (2009) employed real-world network usage scenarios that consisted of VoIP, file transfer, and media streaming traffic types flowing across networks simultaneously. Whereas the experiments of Hamidian et al. (2009) proved that WMNs are capable of supporting multimedia, the results of

[31] VLC link: https://www.videolan.org/index.html

[32] Filezilla link: https://filezilla-project.org/

these experiments also showed that WMN performance declines with an increase in network size and traffic.

Kulla et al. (2012) investigated two scenarios to test performance of linear topology mobile-ad hoc networks (MANETs) under routing protocols BATMAN and OLSR. The performance was evaluated using results of throughput, OWL, and packet loss per second. Best-effort UDP packets of size 256B were transmitted at CBR of 200pps. Thus, a Data Transmission Rate (DTR) of (200ppsX256BX8 bit = 409600bps) 409.6Kbps was expected overall. The first scenario investigated a nodes-static scenario (NSS) where all nodes are stationary and the second scenario explored a node-mobility scenario (NMS). During the NMS scenario experiment: the final destination node was stationary; the source node started at maximum distance number of hops from the destination; the source node moved by 1 hop at a time to the position of its closest intermediary node; the intermediary node moved by 1 hop to the position of its next intermediary neighbour; and so on, to shorten the physical link distances and test mobility. The results of NSS scenario showed that for link distances of 3 or 4 hops from source, the throughput lessened by 50% of DTR. In the case of the NMS scenario, if the destination was node 3 or 4, the throughput decreased by 60% of DTR. The OWL in NSS scenario increased from 4.5ms to 1640ms; and in NMS scenario increased from 21ms to 3542ms, with increase in hop-length from 1 to 4; and PL% showed significant increase after 3 hops in NSS scenario, and after 2 hops for NMS scenario.

Chissungo et al. (2012) evaluated performance of throughput, OWL, OWJ, and PL% during conversational voice and best-effort data transmission, with increasing number of hops between source and destination in an indoor WMN testbed. The testbed used MP routers running BATMAN. VoIP packets were emulated using 73B UDP packets for conversational voice, and Ethernet packets were emulated via 1500B UDP packets in the experiments. A UNIX-based desktop emulating caller (source) was linked to one MP, and another desktop emulating receiver (destination) jumped connections from one MP to another to get the desired hop length. The overall results of throughput, OWL, jitter, and PL% showed a steep downward trend with an increase in hop lengths. The VoIP results showed intolerable drops with measurements going far beyond the recommended tolerance level of <1% as shown in Table 4. In the case of Ethernet data packets, the PL increased to 74.29% at the second hop and even though there is no standardized packet loss performance target for best-effort data, such a high number of packets lost from source to destination is undesirable in a network.

Rao et al. (2013) studied the performance of WMNs under proactive and reactive routing protocols to select the optimal one. The reactive routing protocols evaluated were DSR and AODV, and the proactive routing protocol evaluated was DSDV. The evaluation was based on performance of throughput, PDR, and PLR. The experiments were conducted using simulation in NS-2. Number of nodes varied from 10-1000. Simulation was conducted for two types of topologies: (1) fixed topology where node position was similar on every simulation run; and (2) random topology in which all the nodes were placed randomly for different simulation runs. The application class consisted of transactional TCP data. Results of throughput showed that in a fixed topology, even though throughput dropped with increase in hop count, AODV achieved higher throughput values than DSR and DSDV. In fact, as the network size increased, the data rates of DSR and DSDV dropped to below 50Kbps. In the case of random topology, AODV again had better throughput values when compared to DSR and DSDV, even though throughput showed a declining trend for all three protocols, and drops to zero in the case of DSR and DSDV. This result indicates DSR and DSDV are not efficient routing protocols for large networks. Results of PDR with increasing numbers of hops showed that even though PDR decreased in both random and fixed topologies using AODV with an increase in hop count, AODV outperformed DSR and DSDV. In fact, the performance of DSR and DSDV deteriorated so heavily that the researchers deemed the two routing protocols unsuitable for large WMNs. Results of PLR for fixed topology displayed increasing PLR with increase in hop count, with AODV showing lower PLR than DSR and DSDV. The random topology experiment started at 50 nodes in the network with similar performance from each routing protocol. When network size of the random topology was increased, the PLR was inclined for all routing protocols with AODV exhibiting lower PLR values than DSR and DSDV. The experiments identified AODV as a suitable routing protocol for optimal performance of WMNs. However, even with usage of AODV, the scalability issue is evident in WMNs as proven by decreasing values of throughput, PLR and PDR.

Investigation of WMN performance under different routing protocols using different routing metrics with the objective to find the optimal routing metric was conducted by Ahmeda and Farhan (2014). Routing metrics, Hop count and ETX were implemented in OLSR, and Expected Transmission Time (ETT), developed by Draves et al. (2004), was implemented in AODV. It is important to mention that hop count and ETX can also be implemented in AODV. However, it is shown by Hatti and Kamakshi (2013) that the ETT metric exhibited better

throughput, OWL, and packet loss rate with AODV than ETX and Hop count metrics, with increasing traffic and number of nodes. Ahmeda and Farhan (2014) measured the performance of throughput and OWL, with increasing number of nodes; traffic flow; and normalized routing load, to propose the most optimal routing metric. The selected experiment type was simulation using Objective Modular Network Testbed in C++[33] (OMNeT++) and the application class consisted of best-effort data of UDP type. In the first experiment scenario, the impact of changing network size from 25 to 200 on the performance of routing metrics was evaluated. The results showed that (a) the throughput for all the routing metrics dropped with ETX exhibiting the lowest drop, with hop count in second place, and ETT showing the largest drops; (b) OWL dropped for all the routing metrics with hop count performing marginally better than ETX, that in turn outperformed ETT; and (c) the normalized routing load for all the three routing metrics increased, with ETT experiencing the highest increase, hop count in second place and ETX the least growth. The second scenario of the experiments investigated the impact of network load by progressively increasing the number of traffic flows from 10 to 40 for a network composed of 40 nodes. The results exhibited that (a) throughput measurements were highest under ETX followed by ETT and Hop count, respectively; (b) OWL increased for all three routing metrics with ETX yielding the best results followed by hop count for up to 30 flows, past which ETT showed lowest delays, followed by ETX, and hop count with the largest delay; and (c) the normalized routing load for ETX and hop count remained almost similar with marginal growth as flows increased and were better than ETT that registered higher readings and kept increasing with growth in the number of flows. The experiments of Ahmeda and Farhan (2014) assisted in identifying a suitable routing metric in the form of ETX in OLSR for WMNs. However, the drop in performance with increasing traffic and nodes cannot be discarded. In addition, the scaling of the routing metric in terms of distance between source and destination is not evaluated/disclosed.

The work of Oe et al. (2015) proposed a multicast routing protocol to efficiently manage large amounts of different types of traffic in WMNs. The proposed protocol is compared against an existing multicast routing protocol called Multicast AODV[34] (MAODV). The comparison was based on performances of throughput, OWL, and PDR. The experiment type chosen was

[33] OMNET++ link: https://omnetpp.org/
[34] MAODV IETF link: https://tools.ietf.org/id/draft-ietf-manet-maodv-00.txt

simulation in NS-2. The application class was best-effort data comprising of UDP packets of size 1000B each. The network topology consisted of a grid of 7X7 APs. The topology was divided into 3 multicast groups in which 2 out of 3 or 4 randomly selected nodes generated background traffic to add load to the network. The change in throughput, OWL and PDR was observed for traffic loads of 5, 10, 15, 20, 25, and 30pps under two scenarios. Scenario 1 consisted of one source node in each of the three multicast groups. The results of scenario 1 showed that the throughput between nodes under usage of the proposed protocol is higher than the MAODV at all traffic loads; OWL of the proposed protocol fared better than MAODV at low traffic loads of 5-10pps; OWL of the proposed protocol was similar to MAODV at traffic load of 15-20pps; OWL of the proposed protocol deteriorated more than MAODV at traffic load of 25 and 30pps; and the PDR of the proposed and MAODV protocols dropped with increase in traffic, with PDR performance for proposed protocol higher than MAODV at all traffic loads. Scenario 2 consisted of two source nodes per multicast group and thus had higher traffic load than scenario 1. The results of scenario 2 showed that the throughput between nodes under usage of the proposed protocol is much higher than MAODV; OWL dropped for both protocols with increasing traffic load, with the values of the proposed protocol being lower than MAODV at all traffic loads; and PDR decreased for both protocols with increasing traffic load, but the proposed protocol performed consistently better than MAODV. The usage of the proposed multicast routing protocol showed improved network performance over MAODV in terms of throughput. However, the drops in OWL and PDR with an increase in traffic load cannot be ignored. In experiments such as that of Oe et al. (2015), revelation of throughput, OWL, and PDR performance in relation to hop count between source and destination could have shed more light on the network scalability.

This section presented a review of related work that observed the performance of KPMs in WMNs as evidence to show that the performance of KPMs declines with increasing traffic load and/or increasing hop count. Knowing the results of network performance metrics can be considered a precursor to scalability quantification of a WMN because the performance results of KPMs can be modularized to predict the scalability limits of WMNs. The next section presents related work that has investigated scalability quantification in WMNs.

2.2.3 Scalability quantification in wireless mesh networks

This section presents related work that has addressed network scalability quantification of WMNs using throughput, latency, jitter, and packet loss performance parameters. The objective of the literature review is to find articles which, instead of starting off with a theoretical framework and then applying it to a simulation or testbed scenario, rather set up a simulation or testbed WMN, collect data for various shapes of traffic and establish the maximum scalability for that network. That process mostly yields related work on per-node throughput capacity scaling for ad-hoc networks and WMNs. Study of throughput capacity scaling can provide an understanding of the behaviour of per-node throughput capacity for asymptotically large wireless networks, and could likely be applied to predict network performance that can provide theoretical guidance on network design and deployment (Goldsmith et al., 2011; Li et al., 2012; Lu & Shen, 2014).

The line of throughput capacity scaling investigations can be traced as far back as the theoretical analysis by Gupta et al. (2000) of wireless ad-hoc networks. The authors scale space and suppose X numbers of nodes are located in an area of $1m^2$; and each X is capable of transmitting at W bits per second (bps) over a common wireless channel. Arbitrary and random types of ad-hoc networks were considered, and a theoretical quantification model was devised for the throughput capacity per-node for both type of networks from a routing protocol layer point-of-view. In the case of arbitrary networks, the node locations, destination of sources, and traffic demands, were all arbitrary. For this setting, it was assumed that each of the X nodes are arbitrarily located in a disk of unit area in the plane; each X has arbitrarily chosen destinations to send traffic at an arbitrary rate; and each node can choose an arbitrary power range or power level for each transmission. The throughput capacity per-node is a result of analysis of the transport capacity in this setting. The transport capacity of an arbitrary network is the sum of products of bits and the distances over which they are carried. Therefore, if the nodes are placed optimally, the traffic pattern is chosen optimally, and if the range of each transmission is chosen optimally, then the transport capacity, $T_{CAP} = W*\sqrt{X}$ bit-metre per second. Now, if the T_{CAP} were equally divided between all the N nodes present in the transmission path, and if each source had its next-hop neighbour (which can also be the destination) about 1m away, then each node would obtain a throughput capacity, $T(X) = W/\sqrt{X}$. In the case of random networks, the location of the nodes was independent and identically distributed on the surface of a sphere or on a disk, both 1 m^2 in area, and operating under a multi-hop fashion of information transfer. All transmissions employ the

same range or power, and wish to transmit at a common rate. The throughput capacity per node $T(X) = W/\sqrt{(X \log X)}$. The throughput capacity model for a random network in Gupta et al. (2000) was further investigated using experiments by Gupta et al. (2001). Experiments were conducted for 2 up to 12 nodes that were laptops with external Wi-Fi cards. Each node in the network generated packets of size 1KB at a periodic rate and sent each to random destination independently and uniformly from the list of reachable nodes in the routing table. The sending node then established a UDP socket with the chosen destination and delivered the packet to the operating system kernel. In the experimental setup, the average number of correctly received packets per second was used as a measure of the received throughput at a node. For each network, the traffic generating rate for each node varied from 1Kbps to 1000Kbps to evaluate the variation in received throughput at each node. The maximum value of the received throughput averaged over all nodes in the network was used as a measure of the throughput capacity of the network. The experimental results showed that the average received throughput decayed at the rate of $2.583/X^{1.68}$ Mbps, where X is the number of nodes in the network. The results concluded that the network scaled much worse than the theoretical throughput capacity model obtained for random networks by Gupta et al. (2000). Hence, work of Gupta et al. (2001) showed that WMN scalability quantification models developed using theoretical modelling technique are not a good option for throughput scalability prediction of WMNs because they yield best-case results; and do not consider the unpredictable behaviour of mesh hardware and software evident in real-world WMNs.

The capacity performance of multi-channel multi-hop ad-hoc networks was further analysed using simulation by Li et al. (2002). The single-channel and multi-channel ad-hoc network model capacity performance was evaluated for grid, and linear topologies consisting of different number of nodes equipped with a half-duplex radio transceivers. Results of extensive simulations for the different topologies with different number of nodes were transformed into scaling laws to discover guaranteed throughput per node as a function of number of nodes. In addition, since the traditional 802.11 Wi-Fi uses Request-to-send (RTS) and Clear-to-send (CTS) to tackle the wireless hidden-node problem, single-channel ad-hoc network simulations were conducted for topologies with and without RTS/CTS. The throughput capacity per-node, $T(X)$, obtained for the guaranteed throughput per node, W, for the different single-channel multi-hop ad-hoc networks with X number of nodes were as follows: (1) for grid topology with RTS/CTS; $T(X) = W / X^{0.988}$ Mbps; (2) for grid topology without RTS/CTS; $T(X) = W / X^{1.744}$ Mbps; (3) for linear

topology with RTS/CTS; $T(X) = W / X^{4.98}$ Mbps; and (4) for linear topology without RTS/CTS; $T(X) = W / X^{3.43}$ Mbps. The results of Li et al. (2002) revealed that throughput capacity per-node can have different scaling behaviour depending on the configuration of the network.

Johnson (2007b) compared the results of Gupta et al. (2001) against throughput capacity per-node results obtained from the outdoor Peebles Valley mesh network. A detailed description of Peebles Valley mesh setup is presented under Section 2.1.1.4. The results of throughput experimentation consisted of sending one-way bulk TCP traffic of 100 packets of 8192B each, sent between each pair of nodes in the mesh. Hop count was recorded by examining the routing tables generated by OLSR on each node in the network. All radios were set to auto-select 802.11b or 802.11g mode as well as the data rate being used. A linear regression on the log of the number of hops and throughput measured at each hop was carried out using a least mean squares fit that revealed a slope of 1.62 which is close to the 1.68 discovered by Gupta et al. (2001). Based on the value of the slope, the throughput capacity per node was determined to be; $T(X) = W/X^{1.62}$ by Johnson (2007b).

The objective of this section was to present related work on network scalability quantification models using network performance results of throughput, latency, jitter, and packet loss. It is logical to have a baseline pre-deployment scalability prediction of a given WMN to avoid post-deployment network performance issues likely due to very long mesh links and high traffic. A comprehensive baseline pre-deployment scalability prediction of a given WMN must consider performance of throughput, latency, jitter *and* packet loss (and not just one or two). However, the literature review revealed related work on only throughput scalability modelling with increasing hop lengths between source and destination nodes, thus revealing a research gap. The next section presents a review of the factors affecting smartphone adoption in sub-Saharan Africa and developing Asia. It was the existence of these factors which initiated the smartphone battery consumption investigations.

2.3 Smartphones in developing regions

For the least developed regions of sub-Saharan Africa and developing Asia, mobile Internet connectivity is established as a key enabler of social and economic development, providing a platform for reducing poverty, improving healthcare and education, and driving economic growth; and yet the highest percentage of the *unconnected* reside in these two regions (Bahia, 2018). This

section presents a review of mobile handset affordability and electricity access in sub-Saharan and developing Asia, (in Section 2.3.1,) in order to understand the reasons behind the low mobile Internet penetration in the aforementioned regions. Secondly, in Section 2.3.2, a review of related work investigating smartphone battery consumption is presented in order to show that Wi-Fi is the least battery consuming wireless technology for smartphones.

2.3.1 Mobile handset affordability and electricity access

In order to understand the possible reasons for such low mobile Internet penetration, this part of the literature review investigates mobile handset pricing and tariffs, and electricity access across sub-Saharan Africa and developing Asia. The investigation relies on the assumption that besides network coverage, affordability of Internet-ready handsets, mobile data tariffs and device charging difficulties due to inconsistent supply of electricity, are key hindrances towards successful penetration of mobile Internet in sub-Saharan African and developing Asia. Since it was near impossible to track handset prices and mobile tariffs of all the countries, scores of the GSMA Mobile Connectivity Index[35] (MCI) were used. The MCI is an analytical tool that measures the performance of 134 countries, representing more than 95% of the world's population, against the four key enablers of mobile Internet adoption: infrastructure, affordability, consumer readiness and content (GSM Alliance, 2016). Handset pricing and mobile tariffs are dimensions of the affordability enabler and their descriptions are as follows (GSM Alliance, 2016): (a) handset price is the cost of the cheapest Internet-enabled feature phone or smartphone calculated as a proportion of GNI per capita; and (b) mobile tariffs are the cost of a 100MB prepaid mobile broadband plan calculated as a proportion of GNI per capita. A detailed breakdown of the enablers, along with their dimensions comprising the individual indicators, is presented in Appendix 0, Table A1.2.

As for electricity access in sub-Saharan Africa and developing Asia, according to the Energy Access Outlook 2017 report (2017), out of the estimated 1.1 billion people, approximately 14% of the global population, that do not have access to electricity, around 84% reside in rural areas, and more than 95% are in countries in sub-Saharan Africa and developing Asia. In addition, many more suffered from poor supply quality. Using the Energy Access Outlook 2017 report (2017), the review has tallied up the electricity access percentages out of the total population for countries in Sub-Saharan Africa and developing Asia. It is worth mentioning that the electrification

[35] MCI link: http://www.mobileconnectivityindex.com

percentage in the datasets only shows that there is a power grid in the region, but it does not show the percentage of continuous electricity supply.

2.3.1.1 Mobile affordability and electricity access in sub-Saharan Africa

Adapted from the MCI and IEA datasets, respectively, Table 5 presents handset price, mobile tariffs, and electricity access data for sub-Saharan Africa. With reference to Table 5, the low scores for mobile tariffs and Internet-ready mobile handsets by all countries is evidence that the sub-Saharan population is struggling with mobile Internet penetration.

Table 5: Mobile affordability and electrification in sub-Saharan Africa

Table shows data for mobile affordability indicators, adapted from MCI tool, and electricity supply percentage in urban and rural areas, adapted from IEA database, for sub-Saharan countries to discover interdependencies between the indicators. In the table, the heading 'Mobile affordability' shows the mobile tariff and handset price indicators; and table heading 'Grid%' shows the electricity supply percentage in urban and rural areas.

	Mobile affordability		Grid %			Mobile affordability		Grid %	
Country	**Tariffs**	**Handsets**	**Urban**	**Rural**	**Country**	**Tariffs**	**Handsets**	**Urban**	**Rural**
Angola	45.86	27.42	69	6	Lesotho	27.80	18.97	63	24
Benin	26.52	10.12	56	11	Liberia	21.32	13.35	16	3
Botswana	44.60	58.00	69	32	Madagascar	7.38	23.44	52	7
Burkina Faso	28.06	15.19	58	2	Malawi	7.97	4.08	49	3
Burundi	21.99	0.00	35	7	Mali	18.32	7.44	83	6
Cabo Verde	52.61	34.21	100	89	Mauritius	59.04	47.36	100	100
Cameroon	38.29	41.56	94	21	Mozambique	33.68	11.63	57	15
CAR	0.42	3.95	5	1	Namibia	47.88	46.70	78	34
Chad	8.16	1.62	32	1	Niger	11.12	0.82	54	0
Congo*	54.94	50.83	56	16	Nigeria	50.32	19.92	86	34
DRC**	0.00	20.17	35	0	Rwanda	32.06	2.88	72	12
Cote d'Ivoire	46.54	32.23	88	32	Senegal	44.97	27.60	90	44
Eswatini	36.90	17.15	90	71	Sierra Leone	10.85	12.90	12	6
Ethiopia	23.58	2.67	85	29	South Africa	62.40	54.89	87	83
Gabon	54.49	45.64	97	38	Tanzania	34.94	25.99	65	17
Gambia	29.35	13.71	66	13	Togo	9.17	8.68	74	5
Ghana	63.28	38.84	95	71	Uganda	27.77	21.43	23	19
Guinea	48.22	28.69	46	1	Zambia	34.10	29.18	67	7
Guinea-Bissau	9.38	10.92	23	1	Zimbabwe	19.80	0.00	81	11
Kenya	47.75	32.98	78	60	*CAR = Central African Republic **DRC = Congo, Democratic Republic				

In addition, ownership of a smartphone can be regarded as the first step towards increasing mobile Internet penetration and the MCI of handset prices is lower than that of mobile tariffs in

almost all of the sub-Saharan countries leading to the conclusion that the GNI per-capita is insufficient to afford even the lowest cost Internet-ready mobile phones in this region of the world. As for electricity access, the rural communities of most countries have low electrification percentage. This population is going to struggle with keeping handheld devices recharged and will opt for longer battery lasting feature phones as compared to smartphones, which require daily recharging.

2.3.1.2 Mobile affordability and electricity access in developing Asia

Adapted from the MCI and IEA datasets, respectively, Table 6 below presents handset price, mobile tariffs, and electricity access data for developing Asia and the discussion following pertains to the data in this table.

Table 6: Mobile affordability and electrification rate in developing Asia

Table shows data for mobile affordability indicators, adapted from MCI tool, and electricity supply percentage in urban and rural areas, adapted from IEA database, for developing Asia, to discover interdependencies between the indicators. In the table, the heading 'Mobile affordability' shows the mobile tariff and handset price indicators; and table heading 'Grid%' shows the electricity supply percentage in urban and rural areas.

	Mobile affordability		Grid %			Mobile affordability		Grid %	
Country	**Tariff**	**Handset**	**Urban**	**Rural**	**Country**	**Tariff**	**Handset**	**Urban**	**Rural**
Brunei Darussalam	75.19	66.92	100	100	Timor-Leste	34.05	20.73	100	72
Cambodia	48.32	28.93	97	50	Vietnam	67.11	38.65	100	98
China	77.30	46.50	100	100	Afghanistan	37.07	0.00	100	100
Indonesia	61.58	41.85	99	82	Bangladesh	67.36	46.73	90	67
Laos	49.73	23.03	99	85	Bhutan	73.99	35.84	99	97
Malaysia	66.25	43.33	100	97	India	71.79	49.43	97	74
Mongolia	48.92	30.46	98	73	Nepal	47.90	21.11	97	72
Myanmar	60.07	35.43	79	44	Pakistan	59.39	29.48	90	63
Philippines	37.38	36.25	98	83	Sri Lanka	80.55	36.61	100	100
Thailand	58.64	52.73	100	100					

The high mobile tariff scores, with few exceptions, are conclusive that the cheapest 100MB prepaid data bundle is affordable by most in developing Asia. However, the mobile handset scores show that the cost of the lowest priced smartphone, when compared to GNI per capita, is high. As for electricity access, Table 6 shows that much of developing Asia has grid power which indicates smartphone penetration issues, besides high cost of handsets, are likely due to constant availability of recharging facilities due to poor supply of electricity, especially in rural areas. Thus, based on

the data presented in Table 6, the high handset prices and poor supply of electricity are considered causes of low mobile Internet penetration in developing Asia.

In order to bridge the handset affordability issue, GSMA intelligence (GSMA Intelligence, 2015) recommends 25-50USD entry-level LeS devices that provide all the functionality of a mid-range to high-end smartphone but with limited hardware specifications, one being battery capacity. Lack of power infrastructure or regular supply of electricity, however, means that regular recharging of the smartphone batteries will be a key obstacle limiting the benefits of ICT innovations available through smartphones, that are not available on feature phones (Heimerl et al., 2015). Therefore, battery management techniques focused at making LeS phone batteries last as long as possible need to be made available to end-users. In order to understand the consumption of battery in smartphones, the next section reviews experiments that have targeted such investigations.

2.3.2 Smartphone battery consumption

The advancement of mobile phones from simple devices offering only voice services into smartphones that are essentially multi-purpose computers follows Moore's law, yet the technological advancement of the batteries powering the devices contradicts that law. Moore's law states that the computational complexity exhibited by the increase in the number of transistors in an integrated circuit is doubled every two years; however battery capacities are doubling only every decade (Kosky et al., 2013; Perrucci et al., 2011). Thus, usage of smartphones and their recharging goes hand-in-hand with smart management of battery consumption by phone owners. There are several elements in a smartphone that contribute towards battery consumption such as backlight, CPU, memory, storing data, applications, and wireless radios. The scope of this current study focuses on battery consumption in smartphones during communication using wireless technologies and mobile applications. The scope surrounds the idea that given the presence of a CWMN in a low-income rural community, smartphone usage can be promoted via usage of LeSs and efficient battery management by using Wi-Fi as the primary mode of communication alongside the least battery consuming social communication applications. This section presents notable related work that has investigated battery consumption by different wireless technologies present in a smartphone, to show that Wi-Fi is the least battery draining wireless technology for communication.

Xiao et al. (2008) investigated energy consumption between 3G and Wi-Fi communication technologies during video streaming via YouTube with the Nokia N95[36] smartphone. The experiments used applications such as emTube for viewing videos online (as there was no mobile application for YouTube at the time), downloading videos, and playing local FLV files; and YMobile for uploading videos to YouTube servers. Energy consumed during progressive download and download-and-play phases during usage of 3G and Wi-Fi, respectively, were compared. The progressive download process was separated into three-phases. The first phase included video download from the YouTube server to the mobile device. When there was enough data in the cache, the mobile device started playback signalling the beginning of the second phase and consisted of both download, and playback until the download completed. The energy consumption results of progressive download had three traffic bursts between the starting point of playback, the ending point of download, and the ending point of playback. The download completion marked the beginning of the third phase that continued until the end of video playback. The three phases can be separated by the starting point of playback and the ending point of download. The results showed that the total energy consumption during progressive download and playback of a 9284KB video using 3G was around 1.45 times larger than Wi-Fi. Comparisons of phases showed that power consumption for 3G was higher than Wi-Fi in second and third phases; and lower in first phase. The download-and-play process was also separated into two phases. The first phase involved downloading and storing the video in the phone memory and the second phase involved playback of the video from the phone memory after completion of the first phase. Results showed that energy consumption using 3G was approximately double that of Wi-Fi from the first phase. Since, the second playback phase did not involve usage of 3G or Wi-Fi, the energy consumption for both wireless technologies was similar. Energy consumption during 3494KB video upload experiments showed that 3G consumed approximately 1.5 times more energy than Wi-Fi.

Balasubramanian et al. (2009) compared the energy consumption characteristics of 2G, 3G and Wi-Fi for four Nokia N95 smartphones. Experiments were conducted for data transfers of varying sizes (1 to 1000KB) with fluctuating intervals (1 to 20 seconds) between successive

[36] Nokia N95 details link: https://www.gsmarena.com/nokia_n95-1716.php

transfers. The 2G and 3G experiments evaluated the ramp[37] energy, transmission energy and tail[38] energy. Wi-Fi energy consumption was measured separately for the processes of scanning and associating to an AP and data transfer. Wi-Fi measurements were divided into two sets of measurements. In the first set, Wi-Fi APs were scanned and associated with an available AP using the smartphones for each variable size data transfer; and energy consumed during each data transfer was measure. In the second set, only one scan and association process was conducted (more suited to a real world scenario) for the entire set of data transfers in order to isolate the transfer energies. In addition, 3G, GSM and Wi-Fi incurred a maintenance energy, which is the energy used to keep the interface up; calculated by measuring the total energy consumed to keep the interface up for a given time period. The results showed that 3G consumed significantly more energy to download data of all sizes (12-20 Joules) compared to GSM and Wi-Fi. The results of GSM when compared with 3G showed that GSM consumed 40% to 70% less energy than 3G mainly due to lower power requirements of the 2G radio than 3G radio; and lower tail energy settings from 2G than 3G. Wi-Fi exhibited the best efficiency of the three wireless technologies once it was associated with an AP, with the transfer energy growing with the size of data transfer almost three times slower than with the cellular networks. In fact, Wi-Fi consumed one-sixth of the energy consumed by 3G and one-third of the energy consumed by GSM for a download size of 10KB. Whereas the energy efficiency of Wi-Fi grew with increasing data size, when the cost of scan and transfer was included, Wi-Fi consumed more energy than GSM, but still remained more energy efficient than 3G.

Experiments by Perrucci et al. (2011, 2009) evaluated energy consumption by BT, Wi-Fi, 2G and 3G wireless technologies in smartphones. The smartphone used for the measurements was a Nokia N95 fitted with BT version 2, 802.11b/g, 2G, and 3G wireless radios. The measurements were taken using the in-built energy profiler on the Nokia N95 smartphone in milliwatts (mW). The results of 500KB data download tests showed that: (a) BT consumed 685mW and transferred data at the rate of 650–850Kbps thus took approximately 6.15–4.70 seconds to complete transfer; (b) 2G consumed 500mW and downloaded data at the rate of 44Kbps, and thus, took approximately 91 seconds to complete the download; (c) 3G consumed 1400mW and downloaded

[37] Ramp energy is the energy required to switch to the high-power state.
[38] Tail energy is the energy spent in high-power state after the completion of the transfer.

data at the rate of 1Mbps, and thus, took approximately 4 seconds to complete download; and (d) Wi-Fi consumed 1450mW and downloaded at the rate of 4.5Mbps, and thus, took approximately 0.9 seconds to complete the download. The results showed that Wi-Fi offered the highest download rate even though it consumed the most power. However, this is an indication that for longer data downloads, Wi-Fi will be very efficient in terms of battery consumption because downloads will finish faster as compared to other wireless technologies. In addition, their cellular voice call test results showed that during a 5 minute voice call between two phones: (a) 3G consumed 1265.7mW during making, and 1224.3mW during receiving a voice call, respectively; and (b) 2G consumed 683.6mW during making, and 612.7mW during receiving a voice call, respectively. Therefore, the voice call test results clearly showed that 2G was much better option in terms of battery consumption than 3G for cellular voice calls. Overall, the work of Perrucci et al. (2011, 2009) has shown that Wi-Fi consumes less battery during data transfer, and 2G drains less battery during cellular voice calls.

A power and throughput study of Wi-Fi and BT on modern smartphones was done by Friedman et al. (2011) to examine the connection between obtained throughput and power consumption in the various usage states of these wireless interfaces. The experiments were conducted with Samsung Galaxy (Galaxy), Samsung Omnia i900 (Omnia), HTC Diamond 2 (Diamond), and Samsung Spica (Spica) smartphones. Instead of using energy profilers installed on the smartphones, a circuit was designed to evaluate power consumption. A constant voltage was supplied to the circuit using a DC power supply, and the current in the circuit was determined by measuring the voltage across a resistor that was connected serially to the phones. The phones were connected through pin contacts normally used to connect a battery. A digital oscilloscope was used to acquire and integrate the signal across the resistor. In the first type of communication experiments, throughput achieved and energy consumed in mW was measured during data transmission over Wi-Fi in AP and ad-hoc modes; and BT. Since, Spica and Galaxy phone did not support ad-hoc mode, the experimentation was conducted using Omnia and Diamond smartphones only. Data over Wi-Fi was transmitted using TCP and UDP protocols whereas BT used Radio Frequency Communication (RFCOMM) protocol for data transfer. Network management tool *Iperf* was modified to work with the Omnia and Diamond mobile phones to generate traffic. In case of transmission of UDP traffic over Wi-Fi, *Iperf* was configured to send traffic at 54Mbps which is the theoretical limit for 802.11g standard. In case of TCP and RFCOMM, *Iperf* sent at

the highest possible rate, which was ultimately controlled by the internal congestion and flow control mechanisms of the protocols. The results for BT showed that data rates between 128-137 Kilobytes per second (KBps) with energy consumption of 456-520mW was achieved with Omnia whereas data rates of 115-135KBps with energy consumption of 708-748mW was achieved in Diamond. The results of Wi-Fi in AP mode showed that using TCP, data rates of 1186-1201KBps were achieved at the cost 1504-1568mW of energy in Omnia and data rates of 1041-1345KBps were achieved at the cost of 1484-1530mW of energy in Diamond. The results of Wi-Fi in AP mode using UDP showed achieved data rates of 627-1137KBps at the consumption of 1496-1544mW of energy in Omnia and achieved data rates of 969-1446KBps at the cost of 1468-1524mW energy in Diamond. The results of Wi-Fi in ad-hoc mode using TCP showed achieved data rates of 1232-1336KBps costing 1496-1600mW of energy in Omnia and achieved data rates of 1034-1294KBps consuming 1512-1548mW of energy in Diamond. The results of Wi-Fi in ad-hoc mode using UDP showed achieved data rates of 618-1075KBps at the cost of 1448-1560mW of energy in Omnia and achieved data rates between 978-1223KBps at cost of 1460-1548mW of energy in Diamond. The second type of communication experiment by Friedman et al. (2011) investigated throughput and power trade-off during actual file transfers using FTP that utilizes TCP as the underlying transport protocol. The energy consumption and throughput during file transfer for BT was measured for Omnia, Diamond, and Spica phones using the file transfer features built into the corresponding operating systems of the three phones. Galaxy phones were not tested for BT evaluations because the phone did not have BT FTP functionality. The performance results of Wi-Fi were obtained for all the phones. The phones were installed with an FTP server and a laptop installed with an FTP client was used for transfers. Results for BT showed that data rates of approximately 113-116KBps was achieved at the cost of 376-584mW of energy in Spica; data rates of approximately 67-85KBps were achieved at the cost of 489-511mW of energy in Omnia; and data rate between approximately 64-104KBps was achieved at the cost of 696-724mW of energy with Diamond. Results for Wi-Fi in AP mode showed that: (a) data rate of approximately 752-1100KBps at the cost of 704-992mW of energy was achieved in Galaxy; (b) data rates of approximately 742-898KBps was achieved at the cost of 936-992mW of energy in Spica; (b) data rate of approximately 243-888KBps was achieved at the cost of 1120-1572mW of energy in Omnia; and (c) data rate of approximately 491-756KBps was achieved at the cost of 1516-1532mW in Diamond. Results for Wi-Fi in ad-hoc mode (Omnia and Diamond tests only)

showed that: (a) data rate of approximately 300-888KBps was achieved at the cost of 1144-1608mW of energy in Omnia; and (b) data rate of approximately 468-811KBps was achieved at the cost of 1516-1556mW in Diamond. Though the overall results showed Wi-Fi to consume more battery than BT in both testing scenarios of Friedman et al. (2011), the researchers concluded that the higher the throughput achieved by the interface, the higher the power consumed; and that BT would become more power consuming than Wi-Fi if it were to achieve the throughput levels of Wi-Fi. In addition, the work of Friedman et al. (2011) further revealed that smartphones with similar Wi-Fi radio can achieve different data rates and consume different amounts of energy.

Experiments of Kalic et al. (2012) evaluated relationships between energy consumption and elapsed time, as well as between energy consumption and the amount of transferred data when using BT, Wi-Fi and 3G wireless technologies. All measurements were performed on the HTC Desire HD[39] phone running Android version 2.3. The data was collected using an in-house developed Android application that sent or received data continuously, and monitored the battery percentage status (i.e. percentage of available battery). The application also recorded the elapsed time and the amount of transferred data. The measurements started with a battery at full capacity of 100 and ended with the percentage dropping all the way to 0. The measurements for data transfer using BT, Wi-Fi and 3G were collected for continuous data download from a server and for continuous data upload to the server. The results for energy consumption during data transfer showed that: (a) BT consumed significantly less energy than Wi-Fi or 3G; (b) the battery lasted approximately 4 hours longer during usage of BT than Wi-Fi or 3G; and (c) the battery lasted approximately equally for Wi-Fi and 3G, but Wi-Fi transferred twice more data than 3G. The comparison of results of energy consumption with amount of transferred data showed that: (a) the smallest amount of data is transferred when using 3G (3.04GB data in download and 1.42GB in upload); (b) Wi-Fi transferred 5.91GB in download and 5.66GB in upload; (c) BT transferred 4.04GB in download and 5.54GB in upload. It was observed that though the amount of data transferred during usage of Wi-Fi and BT were data transfer over BT lasted twice as long as Wi-Fi. The results of Kalic et al. (2012) showed that 3G communication technology was the largest consumer of energy during data download and upload, followed by Wi-Fi and Bluetooth communication technologies. However, BT transferred at lower speeds as compared to Wi-Fi, and

[39] HTC Desire HD link: https://www.gsmarena.com/htc_desire_hd-3468.php

if BT were to achieve the same throughput rate as Wi-Fi, then BT will end up consuming more energy. The energy consumption model as a function of amount of data transferred developed by Kalic et al. (2012) showed that for same amount of data download, the energy consumption will be highest during usage of 3G followed by BT and least during usage of Wi-Fi. Thus, the related work of Kalic et al. (2012) also showed Wi-Fi as the least battery draining technology for data transfer.

The analyses and measurement of battery consumption by wireless technologies showed that data transfer over Wi-Fi uses the least energy when compared to both cellular and BT technologies. This is encouraging for areas with the presence of Wi-Fi Aps, such as communities relying on WMNs for low cost access to mobile Internet; as they could likely use Wi-Fi for communication and keep the other technologies disabled to save battery power. However, by default, during (usage of) Wi-Fi usage, cellular radios are constantly active in the background consuming battery. The literature review on smartphone battery consumption was unable to find related work that evaluated the least battery draining cellular technology to keep active in the background, during the usage of Wi-Fi, as a primary mode of communication. In addition, usage of social communication applications such as IMs have become a norm and it is commonly noticed that end-users have multiple social communication applications installed on their smartphone devices (for example both Facebook and WhatsApp installed on a smartphone). However, the literature review on smartphone battery consumption was unable to find related work evaluating battery consumption based on comparing the use of different social communication applications.

2.4 Chapter summary (research gaps)

Even though mesh devices have evolved over the years, the performance decay in throughput, latency, jitter, and packet loss with increase in hop count and network traffic is still a persistent issue, as shown by virtually all of the related work presented in Section 2.2.2. Investigation of related work on a scalability quantification model for WMNs mostly yielded throughput capacity scaling models developed to predict per-node throughput degradation in ad-hoc networks and WMNs. Notable throughput capacity models proposed by Gupta et al. (2001), Li et al (2002), and Johnson (2007b) were included because their throughput scalability models were developed using data collected from simulation or real-world experiments. Gupta et al. (2001) showed that models-based theoretical analysis, which often assume real-world anomalies, can actually mislead

predictions. The simulation results in Gupta et al. (2001) showed that throughput decay per-node was much higher than what was evaluated theoretically in Gupta et al. (2000). In order to deliver multimedia QoS, minimum requirements of throughput, latency, and jitter and packet loss must be met. However, the literature review was unable to find related work that developed a WMN scalability quantification model/framework considering all four KPMs in predicting optimal hop limit between source and destination mesh nodes while meeting the recommended QoS requirements.

The smartphone battery consumption related work presented in Section 2.3.2 showed that Wi-Fi is the least battery draining wireless technology in a smartphone. Given the presence of CWMNs in low-income rural areas with scarce electricity, usage of Wi-Fi as a primary means of communication is an encouraging option with LeSs. However, the cellular radios inside a smartphone are by default active in the background, constantly draining the battery. In the case of LeSs, usage of least battery draining Wi-Fi and cellular radio mode combination (active in background) would further extend the battery life of the resource-constricted devices and decrease the recharge frequency. The literature review of smartphone battery consumption was unable to reveal any related work that evaluated usage of Wi-Fi with different cellular mode combinations to reveal the least draining combination. In addition, social communication applications such as IM applications e.g. Messenger, WhatsApp, Skype, and IMO have dethroned traditional voice calling and texting due to their attractive features and presumably cheaper cost of data (Farooq & Raju, 2019; Stork et al., 2017; Sujata et al., 2015). However to provide users with continual presence, IM applications constantly contact the network, alerting the phone whenever a message arrives thus repeatedly waking the device, especially its screen, from a dormant state (Chmielewski, 2014). Alcatel-Lucent (2014) reported such behaviour as “chattiness” of an application and defined it as a measure of how often an IM application connects to the network to send or receive data. Also, voice and video communication using IM applications utilize codecs to compress/decompress media (Koehncke, 2017). Codecs differ in their algorithmic complexity, and combined with the chattiness factor of IM applications, have a strong influence on battery consumption in smartphones. In order to get the maximum charge life out of an LeS, it is also necessary to investigate the usage of the least battery draining social communication application. However, the literature review was unable to find published articles with evidence of rankings of IM applications based on battery consumption in smartphones.

3 Methodology

This chapter begins with a presentation of the research methodology adopted to answer the two research questions presented in Section 1.2 and also presented as follows:

Question 1: *Given the baseline (first hop) throughput, latency, jitter, and packet loss, what is the maximum hop length limit between mesh nodes and the gateway in a given wireless mesh network, while maintaining acceptable quality of service limits?*

Question 2: *What is the most efficient Wi-Fi and network mode combination; and social communication application, in terms of battery and data consumption, for low-income off-grid users residing in rural areas given the presence of community wireless mesh networks?*

The description of research methodology (in Section 3.1) is followed by presentation of the experimental design adopted to answer the two abovementioned research questions.

3.1 Research methodology

Empirical analysis using testbeds was adopted for the investigation of both network scalability quantification of WMNs and smartphone battery consumption because the investigation required numerical data to make conclusions. Empirical analysis, which is confined within a quantitative research approach, employs strategies such as experimentation to collect numerical data, using predetermined tools, that can be analysed using statistical methods for testing objective theories (Creswell, 2014). For both network scalability quantification of WMNs and smartphone battery consumption investigations, the numerical data was obtained from experimental methods over an actual WMN setup using hardware/software in a controlled environment. Empirical analysis tends to have a general set of steps that are followed sequentially, and at certain stages of the research, one step is completed before the next stage can commence; for example, data collection is followed by data analysis and interpretation (Mertler, 2018). Methodological approaches in WMN-related PhD dissertations (Chaudhry, 2015; Johnson, 2013; Lee, 2010; Raluca, 2010) and smartphone battery consumption (Palit, 2011), were reviewed and showed a similar set of steps being adopted toward research as those listed by Mertler (2018). The empirical analysis steps applied in the network scalability quantification and the smartphone battery consumption investigations consisting of three interconnected stages, is illustrated in Figure 4.

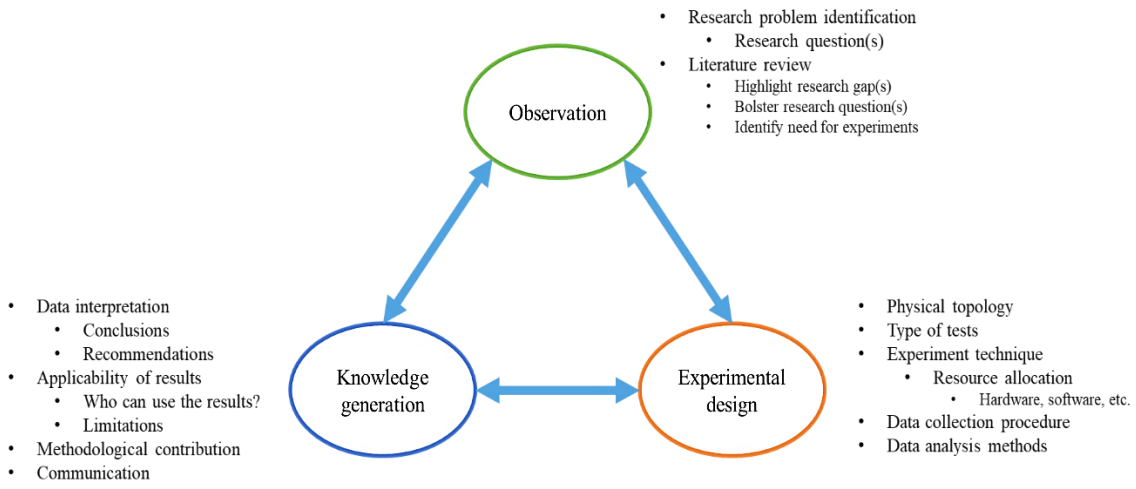

Figure 4: The adopted empirical analysis methodology

The research methodology is adapted from a general set of steps in a quantitative research study in Mertler (2018).

The observation stage shown in Figure 4 is presented via Chapters 1 and 2 in this thesis. The remainder of this chapter is dedicated to the description of experimental design adopted to answer the two research questions mentioned at the start of this chapter. As shown in Figure 4, the high-level blueprint of the experiment design, to pursue both research questions consisted of physical topology, type of tests, experimental technique, testbed design, data collection and data analysis phases. The physical topology plan consisted of schematics of the network to visualize the experiment setup. The type of test consisted of planned traffic types to be transmitted over the experiment setup. The experiment technique phase consisted of selecting the appropriate experiment environment. The testbed setup phase consisted of the experiment setup that is based on the choice of experiment technique. The data collection phase consisted of laying out the plan to collect the relevant data for the type of tests from experiments over the testbed. The data analysis method consisted of the mathematical and/or statistical methods adopted to analyse the raw collected data. The analysed data was interpreted to answer the research questions.

The experiment design for scalability quantification is laid out in Section 3.2; and the experiment design of smartphone battery consumption is laid out in Section 3.3.

3.2 Scalability quantification experiment design

This section reveals the details of the scalability quantification experiment design in line with the high-level blueprint components presented in Figure 4.

3.2.1 Physical topology

Two types of topologies are common in WMN: flat and clustered-hierarchical (Akyildiz & Wang, 2009; Zhao & Raychaudhuri, 2009). Researcher(s) should opt for a physical topology shown to be most efficient in terms of network performance for WMNs in the 'real world'. The scalability quantification study used a clustered-hierarchical WMN topology that is shown by Zhao and Raychaudhuri (2009) to have better throughput capacity scaling and performance in comparison to flat WMN topology approaches. A clustered-hierarchical WMN topology consists of small mesh networks connected to each other over a common link via Internet gateway or intranet link. A cluster-hierarchical topology is depicted in Figure A3.1, Section A3.1, Appendix A3.

3.2.2 Type of tests

In order to conduct experiments to quantify scalability, results of KPMs, namely throughput, latency, jitter, and packet loss were required. Maximum achievable throughput using TCP traffic was considered to measure throughput between nodes. VoIP traffic was considered for evaluating latency, jitter, and packet loss performance over the WMN. The end-user multimedia QoS requirements for VoIP (conversational voice) are very strict as compared to data (ITU-T, 2001b). VoIP traffic is effectively a type of data traffic which is packed/compressed in fixed sized packets sent at a constant rate. The rate of voice packets sent per second burdens a network, and therefore voice call traffic can be considered a benchmark type of traffic for testing network performance of WMNs. Therefore, the scalability quantification study assumed that a WMN ready to support VoIP traffic while maintaining the recommended conversational voice QoS requirements, presented in Table 4, is also ready to offer QoS to other types of network traffic within their respective requirements. In addition, when this study commenced in 2015, there was an emphasis on voice calls by Mankosi community members as reported by Rey-Moreno et al. (2016). The mobile communication hierarchy reported by Rey-Moreno et al. (2016) showed mobile phone users conducted approximately 18 cellular voice calls and 7 text messages; and purchased 25-30MB data bundles (not for VoIP) per month. In fact, community members had asked the UWC research team to explore cost-effective and power-efficient ways to expand the use of the Zenzeleni mesh such that members could make voice calls, as well as access other data services using their personal mobile handsets (Om et al., 2017). The emphasis on voice calls by Mankosi at the time coincided with the scalability quantification experiments prioritizing voice call tests. Therefore, the type of

tests for scalability quantification experiments can be summarized as: (1) throughput testing with TCP traffic; and (2) latency, jitter and packet loss testing with VoIP (voice) traffic. With the type of tests identified, the best suitable experiment technique was looked for and this search is presented in the next section.

3.2.3 Experiment technique

The literature review of QoS in WMNs presented in Section 2.2.2 and scalability quantification in WMNs presented in Section 2.2.3 showed usage of techniques such as analytical modelling, simulation, network emulation and real-world testing. During selection of an experimental technique, the realism of experiments was considered a must to yield valid numerical data. Network emulation and analytical modelling were chosen as the experiment techniques for the scalability quantification experiments. Network emulation contains usage of real network hardware and tests real-world scenarios that are modelled virtually through networking software. Analytical modelling encompasses the application of rigorous mathematical techniques to predict the behaviour of network systems, applications and protocols (Beuran, 2012). Therefore, analytical modelling was selected to be applied to the results obtained from emulation experiments.

The conundrum was the choice of experimental technique to obtain the results. Real-world testing was not viable for the experiments in this study. Real-world testing procedure involves placing the real system, application, or protocol under test in a real environment (both physically and from a network point of view); and results of these experiments are often generated by human users of the network (Beuran, 2012). Setting up a real-world experimentation network was complicated due to the ethical issues underlying usage of humans to use the network and capture their traffic results for further analysis. Therefore, real-world testing was not considered for experiments in this study. In the experiments pertaining to scalability, synthetic TCP and VoIP traffic were to be used in experiments to yield results. Left with the choice between simulation and network emulation, the later was chosen for experiments. Simulation is an experiment technique whereby computer software is used to virtually model real-world networks based on specifications of the network type such as wired or wireless, the geographical region; and network elements such as routers, switches, and routing protocols (Beuran, 2012). However, conclusions made from simulations challenge the practicality and credibility for making decisions about a real network or system because assumptions are made from experimental results from virtualized network models

consisting of limited real-world (or real-hardware) physical layer modelling capabilities (Beuran, 2012; Pawlikowski et al., 2002). In the related work of Niculescu et al. (2006), the difference between results of testbed and simulation experiments during evaluation of packet aggregation mechanism to increase VoIP capacity highlighted the fact that simulations yield optimal performance results whereas the real-word performance would always be lower than optimal. Thus, the inclusion of real equipment makes network emulation more reliable in terms of results than simulation for scenarios in which performance of real equipment and/or applications/protocols must be tested; and from this point of view it is only slightly inferior to real-world testing.

On the other hand, network emulation requires resources to setup the experiment, in the form of intermediary and end-user devices; and software to generate traffic and collect data. The next section presents the resource acquisition process.

3.2.3.1 Hardware requirements

Starting off with the intermediary devices for network topology, it was deemed necessary that the testbed be built using OTS mesh equipment; either available in the local market or functional in a real-world WMN deployment. Since the study uses Zenzeleni as the background, the mesh equipment used in Zenzeleni mesh infrastructure was considered for the testbed setup. In order to emulate end-user devices, Raspberry Pi 2 (RPi2) System-on-chip (SoC) devices were selected. The RPi2 can be installed with open-source Linux based operating system (OS) which opens doors to numerous traffic emulation scenarios.

3.2.3.2 Software requirements

The key software requirement of the scalability experiments was software for traffic emulation by injecting synthetic network traffic. In the field of network engineering, a traffic generator is utilized to create and transmit synthetic TCP/UDP traffic with various parameters to evaluate the efficiency of the network for optimization purposes. The first criterion set for selection of the traffic generator(s) was that it must be able to measure the network performance of KPMs: throughput, latency, jitter and packet loss. The second criterion set for selecting a traffic generator for the scalability quantification experiments was that the software must support TCP and VoIP traffic generation. Kolahi et al. (2011) and Mishra et al. (2015) compared performance of traffic generation tools by measuring TCP throughput performance in experimental network. Kolahi et

al. (2011) used IP Traffic[40], Netperf[41], *iPerf*, and D-ITG; and Mishra et al. (2015) used PackETH[42], Ostinato[43], D-ITG, Netperf, and *iPerf*. The results of Kolahi et al. (2011) and Mishra et al. (2015) showed high TCP throughput values while using *iPerf*. Therefore, in order to measure maximum achievable throughput between links, *iPerf* network traffic generator was selected. Usage of *iPerf* for measurement of throughput in WMN performance experiments can also be found in Johnson (2007a, 2013) and ElRakabawy (2008). However, *iPerf* cannot generate particular types of application layer traffic profiles. Therefore, another traffic generator with the capability of generating VoIP traffic specifically had to be selected. In order to generate VoIP traffic specifically, D-ITG tool was chosen because it is capable of generating specific types of application layer traffic (Avallone et al., 2005; Botta et al., 2012, 2013). Usage of D-ITG to study WMN performance can be seen in Hamidian et al. (2009) and Kulla et al. (2012); and to send VoIP traffic over WMNs in Tiemeni (2015). In addition to *iPerf* and D-ITG, the network connection verification utility, Packet Internet Groper[44] (*PING*), was used to check connectivity between the mesh routers.

3.2.4 Testbed setup

This study began in 2015 when Zenzeleni was migrating to MPv2 routers. Therefore, an experimental testbed setup procedure began using MPv2 units towards end of 2015. While experiments were in process over the MPv2 testbed, Zenzeleni went through another device migration towards the end of 2017 from MPv2 to Ubuiqiti UniFi devices for mesh. Thus, around late-2018 another experimental testbed setup procedure commenced using UniFi devices. Therefore, the experiment process to quantify scalability used results from two indoor testbeds: one built using MPv2 units and a second built using UniFi units. This section presents the final steps of the MPv2 and UniFi testbeds, respectively. It is noteworthy to mention that the MPv2 testbed setup was communicated via Om and Tucker (2018b).

[40] IP Traffic tool link: https://www.zti-communications.com/iptraffic/
[41] Netperf link: https://hewlettpackard.github.io/netperf/
[42] PackETH tool link: http://packeth.sourceforge.net/packeth/Home.html
[43] Ostinato tool link: https://ostinato.org/
[44] PING description link: https://docs.microsoft.com/en-us/windows-server/administration/windows-commands/ping

3.2.4.1 MPv2 testbed setup

This section presents a stepwise description of the MPv2 testbed setup that used 6 MPv2 mesh routers with 5GHz for the mesh backbone and 2.4GHz for the APs. The device specifications of MPv2 routers are presented in Section A2.3, Appendix A2. A pre-setup procedure consisted of: selection of the number of devices; understanding the routing process; and addressing of hardware device shortcomings. This was completed for the MPv2 testbed setup and is presented in Section A3.2, Appendix A3. A room measuring 9.5m by 4.24m, with the presence of two 14 centimetre (cm) thick concrete walls partitioning the room was used for the setup of the MPv2 testbed. For the MPv2 testbed setup, an unplanned layout process was adopted for the placement of the MPv2 units to achieve the planned multi-hop clustered topology. The unplanned layout process was considered representative of WMN setup process in the real-world, and work of Bicket et al. (2005) served as an example of experiments over unplanned mesh. However, modifications and configurations were required to achieve the multi-hop clustered topology in the given space. Related work of Sanghani et al. (2003), Clancy and Walker (2007), Johnson and Lysko (2007), and ElRakabawy et al. (2008) had applied methods such as reduction in radio transmit power and usage of shielding and attenuators to obtain indoor multi-hop WMN testbed setup. The usage of the methods in the aforementioned related work were considered to inform the setup of the MPv2 testbed. However, expenditure on additional experiment accessories such as shielding cages and attenuators were kept for a stage when modifications and configurations to the MPv2 unit proved unsuccessful at obtaining a multi-hop topology as planned. It was understood from the route establishment process of the Better Approach to Mobile Ad-hoc Networking – advanced (BATMAN-adv)[45] implemented in MPv2 units, that in order to create a multi-hop route between two routes, the total transmission quality (TQ) of a single-hop route between two nodes had to be less than 15 than the overall TQ of a multi-hop route between the same nodes for BATMAN-adv to select the multi-hop route option. Two examples of the mesh-link formation scenarios are presented in Figure 5 for a single-hop route (a) and a multi-hop route (b). The first trials at manipulating TQ explored placement of the MPv2 units at different angles, heights and distances proved unsuccessful due to strong Transmission power (Tx) and Receiving power (Rx) strengths. The second trials considered reducing Tx of the 5GHz radio to the lowest setting of 1dBm (the

[45] Route establishment process of BATMAN-adv is presented in Appendix A3, Section A3.1, Index 2.

default setting was 29dBm) in combination with the different placement options used in the first trials; and this also proved to be unsuccessful. The preliminary controls proved unsuccessful due to the small size of the experimental space causing near placement of MPv2 units. Thus, additional extreme controls such as shielding and disabling MIMO functionality were considered. The MIMO functionality was disabled by turning off the High Throughput (HT) mode on the MPv2 units and to keep the mesh backbone on 5GHz, the radio was configured to operate on legacy 802.11a mode (with one radio transmitting and receiving).

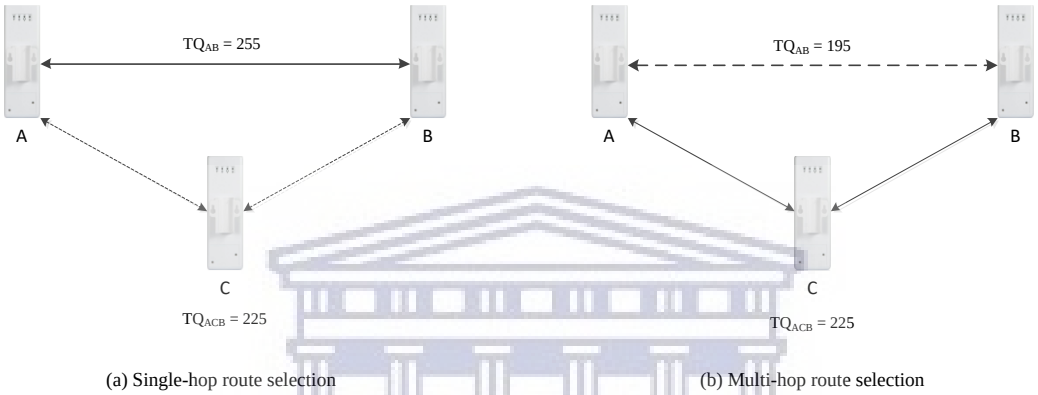

Figure 5: Scenario of single-hop and multi-hop route selection
In (a), Node A forms a single-hop route with Node B because $TQ_{AB} > TQ_{ABC}$; in (b), Node A forms a multi-hop route with Node B via Node C because $TQ_{ABC} > TQ_{AB}$.

Even with MIMO disabled and signal Tx set at 1dBM, the Tx/Rx strengths were still strong enough to form direct single-hop links between MPv2 units. Thus, the next modification explored shielding of the MPv2 units. This study adopted a do-it-yourself (DIY) approach to keep the shielding expenditure cost[46] as low as possible, and in the process proposed a low-cost DIY shielding solution for future network emulation researches over an indoor multi-hop WMN testbed. Faraday cages were built in-house using readily available and cheap aluminium mesh wire from a local hardware vendor. In order to shield the mesh frequency with short wavelengths, mesh wire with holes less than approximately 3X3 millimetre (mm) was chosen. The hole-size (*HS*) was calculated using Equation 3.1, where *C* is speed of light, and *F* is Frequency. The computation of HS was based on the assumption that to effectively shield a given frequency, *HS* for a mesh wire

[46] Attenuator price check: A quick browse on the globally trusted and reasonably priced online vendor-based website www.amazon.com showed that a 30dB attenuator used in Clancy and Walker (2007), Johnson and Lysko (2007) and ElRakabawy et al (2008) cost approximately 28USD per unit (plus shipping).
30dB attenuator link: https://www.amazon.com/SMA-Attenuator-30dB/dp/B00IFCLTY6

should be less than the wavelength of that particular frequency. For the cage assembly, cardboard boxes of size 25X8X8cm were shielded with the mesh wire.

$$HS = {}^{20 \cdot C}/_{F} \qquad 3.1$$

Two preliminary 'before-after' type experiments were conducted to measure the isolation levels from shielding. As depicted in Figure 6, two MPv2 units, mounted on the camera tripod stands were placed 3m apart facing each other, firstly without, and secondly inside the hand-made Faraday cages. Using wireless scan command, *iwlist scan* via the command line on the MPv2 units, the Rx at each node was measured. The difference between Rx of shielded and unshielded was approximately 20dB.

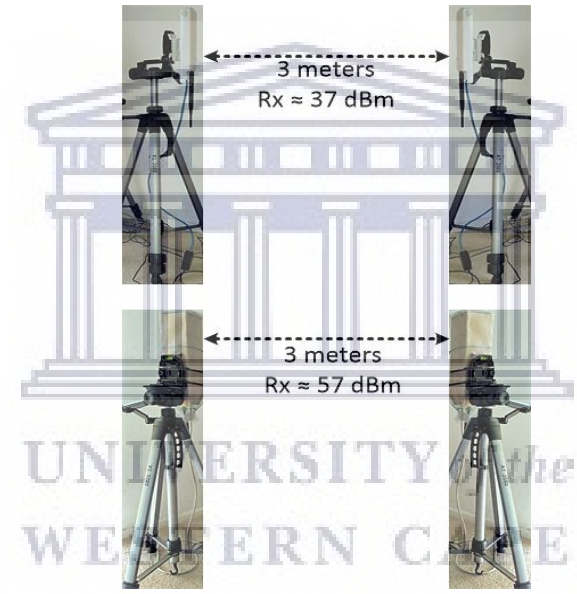

Figure 6: Setup to measure received signal strength with and without Faraday cages
Figure shows the MPv2 setup with and without homemade Faraday cages. One mesh node was linked via Wi-Fi to a laptop and the second mesh node was accessed through it remotely. There were no walls or objects in-between the nodes.

For the final phase of MPv2 testbed setup, the combination of different physical placements and angles reduced Tx level of the 5GHz radio, disabled MIMO; and hand-made Faraday cages were applied to build a clustered multi-hop WMN testbed. The final setup began with modifications to all the internal 2.4GHz AP antenna in the MPv2 units. These antennas were detached from the radio chipset I-PEX connector because of the extreme signal shielding from the caging. As a replacement, 2dBi omni-directional external antennae were attached to the RP-SMA connectors on each MPv2, which were further connected to the I-PEX connector of the 2.4GHz AP radio chipset. Afterwards, work began on setting up two clusters of three MPv2 units, as shown

in Figure 7. The two clusters were placed at diagonal corners in the rectangular experiment room for maximum distance between clusters (in the room) and to eliminate any chance of single-hop links formation except for the designated MPv2 units from each cluster. Using Figure 7 for clarification, the MPv2s numbered 252 and 25 were assigned cluster gateway (CG) role which meant that the MPv2 nodes in the two clusters connected to each other via a single link between the two CG MPv2 units numbered 252 and 25 only, and no single-hop links between 23 and 25, 23 and 22, 23 and 20, 252 and 22, and 252 and 20, existed.

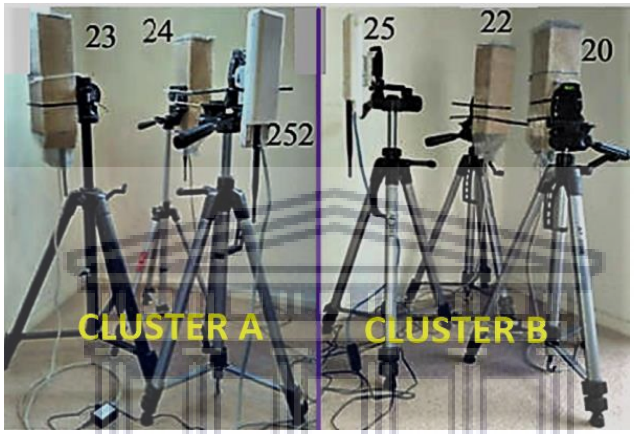

Figure 7: Two clusters made of three MPv2 nodes per cluster

Figure shows two clusters mounted on camera tripod stands. The two MPv2 units numbered 252 and 25 did not have Faraday cages on them because they played the gateway role for the cluster; and 252 was gateway for the entire mesh network.

The angles and the distance between the MPv2 units in each cluster were adjusted such that the two clusters connected to each other over one single-hop link formed between the CG units. In the initial setup, all MPv2s were shielded with Faraday cages, and the Tx power setting of all the 5GHz radios was set to 1dBm. However, the Rx between CG nodes was -85dBm whereas, -67dBm is considered the ideal Rx for reliable and timely delivery of VoIP packets (Metageek, 2019; Sonicwall, 2019). Therefore, the Tx of both[47] CG MPv2 units was incremented by 1dBm to find the optimal setting such that the units did not form single hop links with the caged MPv2 units in the opposite clusters. The Tx of CG nodes reached a threshold at 3dBm. However, the Rx was still less than -67dBm. Therefore, keeping the Tx settings at 3dBm, the cages were removed from the CG MPv2 units in an attempt to improve Rx strength. The testbed was able to hold the topology with cages removed from the gateway MPv2 nodes with Rx improving to approximately -68dBm.

[47] 'both' means that the dBm values were incremented first on both CG MPv2 units before every test; and not increase on one then test, and then increase the other and then test and so on.

The Rx fluctuations at each MPv2 unit for each single-hop link were observed for 30 minutes; and the results showed that the Rx values fluctuated to a different value for no more than five occurrences for each pair with average Rx staying close to -67dBm. The recorded Rx strengths are presented in Table A3.3 Section A3.4, Appendix A3. Therefore, the final testbed setup consisted of four MPv2 units placed inside the cages, and two without cages (CG nodes). The final MPv2 physical topology is presented in Figure 8.

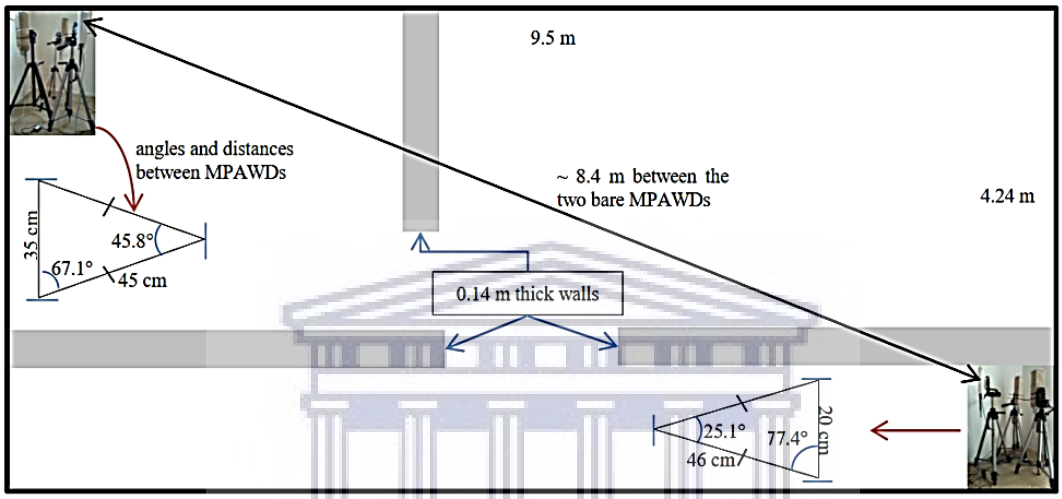

Figure 8: The final physical topology of MPv2 testbed.
The topology shows the angles and the distances between each MPv2 in each cluster. The figure shows the diagonal placement of the clusters in a rectangular room at maximum possible distance.

The completed MPv2 testbed had primary mesh multi-hop connections of lengths of up to 3 hops and the different number of mesh hop links are shown in Table 7. To generate traffic, one RPi2 installed with iPerf and D-ITG was linked to each MPv2 in AP mode.

Table 7: Pairs of multi-hop connections in the MPv2 testbed
The table shows the number of pairs of different hop-count lengths between MPv2 nodes. The hop count between RPi2 and the MPv2 units is not considered.

Hop length	Connections	Total pairs
1	23–24; 23–252; 24–252; 252–25; 25–22; 25–20, 20–22	7
2	24 - 252 - 25; 23 - 252 - 25; 22 - 25 - 252; 20 - 25 – 252-	4
3	24–252–25–22; 24–252–25–20; 23–252–25–22; 23–252–25–2	4

3.2.4.2 UniFi testbed setup

This section presents the UniFi testbed setup using 9 UniFi and 2 Litebeam AC-*Gen2* (LB) PtMP units. The device specifications of UniFi and LB are presented in Sections A2.4 and A2.5, respectively, of Appendix A2. The UniFi scalability experiments were added to the scope in the third quarter of 2018 because the MPv2 units had gone out of production, and also because

Zenzeleni had moved to Ubiquiti equipment. Similar to the MPv2 testbed setup, the UniFi testbed setup consisted of a pre-setup procedure consisting of the selection of the number of devices, understanding the routing process and addressing hardware device shortcomings. Each of these is presented in Section A3.1, Appendix A3. The UniFi and LB devices were placed on the false roofing of the lab approximately 2.5m from the floor; and with surface dimension of approximately 9X9m. Additionally, a desktop (specifications presented Section A2.3, Appendix A2) was used to implement the Dynamic Configuration Host Configuration Protocol (DHCP) server, UniFi controller, and act as an Internet gateway (however, Internet was not used). During initial setup tests, it was discovered that any type of modification to the UniFi firmware using the command line utility tool was blocked by the manufacturer. The UniFi testbed followed the adopted physical topology design mentioned in Section 3.2.1. Unlike the MPv2 units, the UniFi devices allowed manual path configuration so that the desired UniFi uplink could be manually set from the settings to form the desired mesh topology. Manual configuration of uplink paths enabled fixed placement of the UniFi nodes in the given space. Therefore, adopting the grid layout idea of Johnson and Lysko (2007), a 3X3 square grid pattern was used for placement of the UniFi units, and all units were placed 4m apart from one another (see Figure 9).

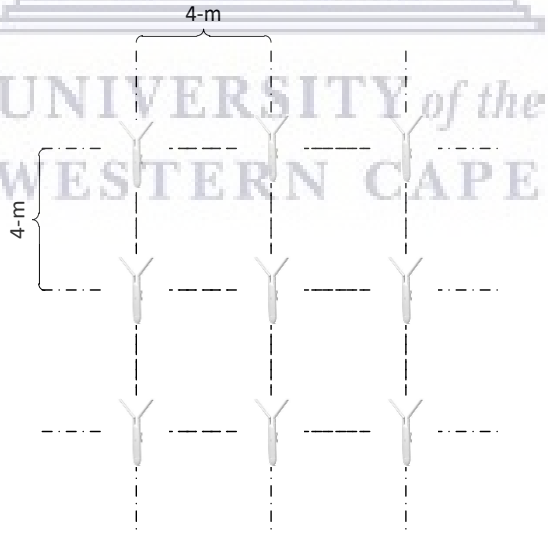

Figure 9: Unifi node grid layout
The figure shows the grid pattern used for UniFi testbed setup. It is a square grid pattern because the distance between vertices in both directions are same.

The UniFi testbed topology consisted of (a) two clusters of 4 UniFi units each; (b) a base UniFi unit functioning as a cluster gateway (CG); (c) an LB configured in station mode to act as

gateway for the CG; (d) a second LB unit configured as AP to act as PtP gateway for the station-mode LB; and (e) a desktop with wired connection to the AP-mode LB. The logical topology of UniFi testbed is shown in Figure 10.

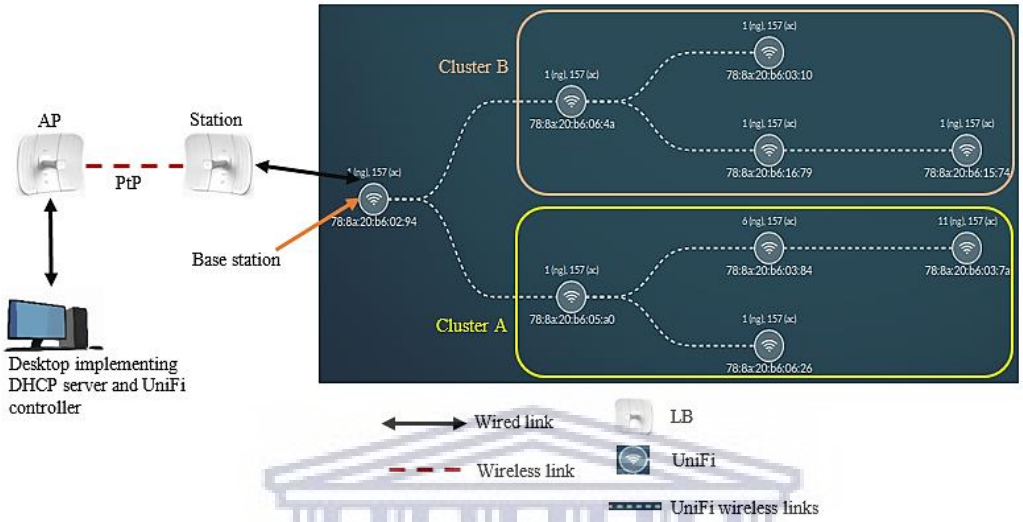

Figure 10: The UniFi testbed logical topology

The figure shows the logical connections of the nodes in the UniFi testbed.

The mesh uplink of each UniFi unit was manually configured from the UniFi controller running on the desktop. The mesh backhaul and the PtP link utilized 5GHz; and the AP utilized 2.4Ghz. The antenna gain in each LB was pre-set to 23dBi by the manufacturer and could not be changed. The Tx power in the LB units was reduced to the lowest setting possible of 4dBm. The MIMO feature could not be disabled in the UniFi units (locked by manufacturer), and the Tx and the antenna gain levels could only be minimized down to 4dBm and 4dBi, respectively.

Similar to MPv2 testbed, Rx for each single-hop link in every UniFi unit was observed and the different fluctuations were recorded for a timeframe of 30 minutes. The Rx fluctuated for different values on no more than two occurrences with the average well within the -67-Bm considered suitable for VoIP calls (Metageek, 2019; Sonicwall, 2019). The Rx values (in dBm) are presented in Table A3.4 in Section A3.5, Appendix A3. At the completion of the UniFi testbed setup, mesh multi-hop connections of length up to 6 hops were possible, as shown in Table 8. In order to commence the final phase of UniFi emulation, an RPi2 installed with *iPerf* and D-ITG were linked to each of the UniFi units in AP mode.

Table 8: Pairs of multi-hop connections in the UniFi testbed

The table shows the numbered pairs of different hop lengths between UniFi nodes. The hop count between RPi2 and the UniFi units is not considered.

Route length (hops)	Connections	Total Pairs
1	94–a0; 94 - 4a; a0 - 84; 84 - 7a; a0 - 26; 4a - 79; 79 - 74; 4a - 10	8
2	94 - a0 - 26; 94 - a0 - 84; 94 - 4a - 10; 94 - 4a - 79; a0 – 94 - 4a; a0 – 84 - 7a; 26 - a0 - 84; 4a – 79 - 74; 10 - 4a - 79	9
3	94 - a0 - 84 - 7a; 94 - 4a - 79 - 74; 26 - a0 - 84 - 7a; 10 - 4a - 79 - 74; a0 - 94 - 4a - 79; a0 - 94 - 4a - 10; 4a - a0 - 94 - 84; 4a - a0 - 94 - 26	8
4	a0 - 94 - 4a - 79 - 74; 84 - a0 - 94 - 4a - 79; 84 - a0 - 94 - 4a - 10; 26 - a0 - 94 - 4a - 10; 26 - a0 – 94 - 4a - 79; 4a – 94 - a0 – 84 - 7a	6
5	84 - a0 – 94 - 4a – 79 - 74; 26 - a0 - 94 - 4a - 79 - 74; 7a – 84 - a0 – 94 - 4a - 79; 7a - 84 - a0 - 94 - 4a - 79	4
6	7a – 84 - a0 – 94 - 4a – 79 - 74	1

3.2.5 Data collection

This section presents the procedure underlying the collection of the data types required for analysis. Results of maximum achievable throughput (TH); round-trip latency (RTL); round-trip jitter (RTJ); and packet loss percentage (PL%) during round trip transmission were collected from the experiments over both MPv2 and UniFi testbeds. The next section presents the data collection procedure for MPv2 testbed, and the follow section for the UniFi testbed.

3.2.5.1 MPv2 data collection

iPerf version-2.0.5 was used to measure maximum achievable TCP round-trip throughput (TH) between links of every hop count in the MPv2. Built on a client and server model, *iPerf* can generate unidirectional or bi-directional IPv4/IPv6 TCP/UDP traffic to measure network performance between selected end points of the specified network (Dugan et al., 2016). To yield TH results, TCP traffic for 1 minute duration was sent for 20 iterations in intervals of 5 seconds between each iteration from an *iPerf* client instance running on an RPi2 linked to a MPv2 to an *iPerf* server instance running on a destination RPi2 linked to another MPv2. The TCP window size was kept at default 85.3KB. After completion of 20 iterations in one direction, the tests were repeated in the backward direction with the RPi2 units changing roles of client and server. Therefore, a total of 40 iterations (20 forth and 20 back) were conducted for one link. The tests were carried for each hop-length pair in the MPv2 testbed node as shown in Table 7. The testbed was not saturated with other tests or traffic types during a test in progress. A sample implementation of *iPerf* for one iteration of ten seconds (the parameter *-t10* in *iPerf* client

command refers to the duration of 10 seconds) is shown in Figure 11. The output shown on the *iPerf* server side was saved at end of every iteration to a spreadsheet for statistical analysis.

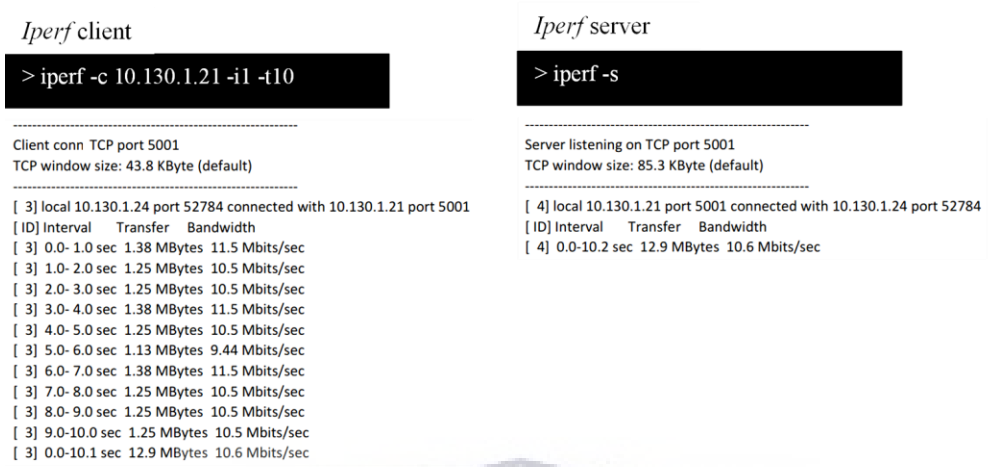

Figure 11: Sample output from iPerf usage

These are screen captures from actual usage of iPerf. The results are displayed on the server side and was recorded for every iteration of the TH tests.

Data for RTL, RTJ, and PL% were collected using emulated voice traffic with D-ITG version-2.8.1-r1023. D-ITG is able to generate particular application layer traffic profiles, including VoIP, under several encoding schemes (Botta et al., 2010, 2012, 2013). The core features of D-ITG used in the experiments were ITGSend, ITGRecv, and ITGDec (Botta et al., 2013). The ITGSend module generated traffic towards ITGRecv module, and produced log files containing information of every sent and received packet that was captured using ITGLog. The ITGDec component decoded the log files in order to extract performance metrics related to the traffic flows. The G.711 VoIP encoding scheme was selected for the voice traffic in D-ITG to be in line with the G.711 encoded SIP voice calls supported by the MPv2 units. In the experiments, 20 iterations of single 5 minute G.711 encoded VoIP flow were transmitted over each hop length pair in the MPv2 testbed as shown in Table 7. The 20 iterations of ITGSend instances were executed at 5 second interval by a bash script executed on an RPi2 linked to an MPv2; and the traffic was received by ITGRecv running on another RPi2 linked to another MPv2. The MPv2 testbed network was not saturated with other tests or traffic types during transmission of voice traffic over a given hop pair. The configuration details of (a) the ITGSend script file for the G.711 codec profile VoIP flow; (b) the ITGSend command to execute the ITGSend script file and save log; (c) the bash script used to execute 20 iterations of the ITGSend command at 5 minute intervals; and (d) the bash script used to execute the ITGDec command to decode all the saved log files, are presented in

Section A3.6 of Appendix A3. The information of RTL, RTJ, and PL% from the decoded text files were transferred to a spreadsheet for further analysis.

3.2.5.2 UniFi data collection

The throughput and VoIP data collection procedure adopted for MPv2 testbed experiments provided a framework for UniFi testbed experiments. However, the UniFi devices do not have intra-network VoIP call capabilities due to absence of in-built PBX system, and much like a traditional Wi-Fi AP, require access to Internet via a base station to route voice traffic. Therefore, UniFi testbed experiments were conducted to measure network performance of TH, RTL, RTJ, and PL% across the two clusters in the UniFi testbed to emulate breakout network traffic. The inter-cluster network performance experimentation was considered an extension of scalability quantification investigations because, even though the UniFi testbed represented one network, traffic had to breakout from one local mesh network to get into another local mesh network. In the inter-cluster UniFi experiments, the TH, RTL, RTJ and PL% metrics were measured for inter-cluster hop lengths between UniFi APs. In the UniFi testbed, inter-cluster hop length ranged from minimum hop length of 2 hops up to a maximum hop length of 6 hops. With reference to Figure 10 showing the UniFi testbed, Table 9 is presented to show the inter-cluster UniFi AP mesh links and the hop lengths considered for data collections.

Table 9: Inter-cluster connections in UniFi testbed

The table shows the inter-cluster links between UniFi APs in cluster A and cluster B in UniFi testbed as shown in Figure 10. The hexadecimal numbers used to represent each UniFi AP is taken from its last block of MAC address.

Hop length	UniFi AP Links between Cluster A and Cluster B						Number of links
2-hops	a0-to-4a						1
3-hops	a0-to-10	a0-to-79	84-to-4a	26-to-4a			4
4-hops	a0-to-74	84-to-10	84-to-79	26-to-10	26-to-79	7a-to-4a	6
5-hops	84-to-74	26-to-74	7a-to-79	7a-to-10			4
6-hops	7a-to-74						1

For TH data collection, testing was conducted using *iPerf* to measure the maximum achievable TCP TH between each pair of inter-cluster hop length shown in Table 9. To measure TH, TCP packets were transmitted for 1 minute from an *iPerf* client instance running on an RPi2 linked to a UniFi AP in one cluster to an *iPerf* server instance running on another RPi2 linked to a UniFi AP in another cluster. Similarly to the MPv2 testbed, the default *iPerf* TCP window size of 85.3KB was used in the TH experiments. After completion of 20 iterations in one direction, the

tests were repeated in the backward direction of each inter-cluster connection. During a running test, the testbed was not saturated with other tests or traffic types. The output shown on the *iPerf* server side, already depicted in Figure 11, was saved at end of every iteration to a spreadsheet for statistical analysis.

Data for network performance of RTL, RTJ, and PL% was measured and using D-ITG which synthesized the G.711 encoded VoIP traffic. However, unlike the MPv2 testbed, the voice call flows in UniFi testbed were scaled for every inter-cluster hop length. D-ITG has a multithreaded design where the ITGSend can send multiple parallel traffic flows toward multiple ITGRecv instances; and ITGRecv can receive multiple parallel traffic flows from multiple ITGSend instances (Botta et al., 2013). Therefore, the ITGSend scripts of D-ITG being were configured to send and receive multiple VoIP flows to emulate multiple callers. Usage of linear increment in VoIP flows over WMN testbed can observed in Niculescu et al. (2006) and Castro et al. (2007). For VoIP experiments in the UniFi testbed, an intermittent growth trend in the number of VoIP flows was considered in an attempt to match the sporadic Wi-Fi client connections often observed in the real world. The number of VoIP flows were scaled from 2 up to 41 flows in increments of prime numbers. The scaling approach can be considered selective; and the upper limit of 41 flows was based under the assumption that with so many concurrent flows, there will likely be a case where one or all of the KPMs have surpassed the recommended QoS requirements for interactive voice shown in Table 4. To measure network performance of RTL, RTJ, and PL%, 20 iterations of 5 minute G.711 encoded VoIP traffic were transmitted for each flow over each inter-cluster hop length as shown in Table 9. The 20 iterations of ITGSend instances were executed at 5 second intervals from an RPi2 linked to a UniFi AP in one cluster to ITGRecv instance running on another RPi2 linked to a UniFi AP in another cluster. An example of an ITGSend script file configured to send 5 flows is presented in Section A3.6, Appendix A3. The configuration details of other scripts were similar to that used in MPv2 experiments, and are presented in Section A3.6 of Appendix A3. The final data collected from MPv2 and UniFi testbed experiments are presented in Section A3.7, Appendix A3. The next section presents the data analysis methods adopted to interpret the results obtained from MPv2 and UniFi testbed experiments, respectively.

3.2.6 Data analysis

The TH, RTL, RTJ, and PL% data from MPv2 and UniFi testbed experiments were analysed to interpret trends in performance behaviour over increasing number of hops. Firstly, the mean of total iterations of TH, RTL, RTJ, and PL% results obtained for each hop length pair in MPv2 and UniFi testbed were evaluated. Further, the RTL, RTJ, and PL% analysis of UniFi testbed data consisted of evaluating means of iterations for each flow count (from 2 up to 41). Secondly, the performance behaviour of the evaluated means of TH, RTL, RTJ, and PL% for MPv2 and UniFi testbeds were analysed for increasing hop length using power and exponential regression analysis techniques. The regression analysis tool built into the Microsoft Excel version 2013 (Excel) was used to carry out the regression analysis. In the case of performance behaviour of RTL, RTJ, and PL% with increasing hop length for the UniFi testbed, the regression analysis was conducted for every prime number flow from 2 up to 41. In order to select between the power and exponential regression trend to represent the performance behaviour of a given performance metric with an increasing number of hops, the R^2 (R-squared) coefficient, also known as coefficient of determination, was evaluated using Excel for the power and exponential regression trends. The regression trend yielding the higher R^2 value was chosen as best fit to represent the performance behaviour of a given KPM with an increasing number of hops; and an equation for the respective regression trend was formulated using Excel to represent the performance behaviour.

The equations obtained from regression analysis of each performance metric of MPv2 and UniFi testbed results were used for scalability quantification modelling. Techniques were brainstormed to generalize and/or combine equations so that they could be applied to predict performance of WMNs. The TH equations from MPv2 and UniFi; and RTL, RTJ, and PL% equations for MPv2 were generalized, because there was one equation for each performance metric. For the RTL, RTJ, and PL% equations of UniFi: firstly, each equation of every flow was generalized; and secondly the generalized flows equations were combined to yield a single general overall equation to represent the performance trend of RTL, RTJ, and PL%, respectively, with increasing hop length. The regression analysis results, and generalization and combination processes are described in detail in Chapter 4. The next section presents the experimental design of smartphone battery consumption experiments.

3.3 Smartphone battery consumption experiment design

The smartphone battery consumption experiments consisted of investigations of: 1) least battery consuming Wi-Fi and cellular radio combination; and 2) least battery consuming IM and SIP application. For the remainder of the thesis, the investigation of least battery consuming Wi-Fi and cellular radio combination is referred to as wireless technologies evaluation; and the investigations of least battery consuming IM and SIP application is referred to as mobile applications evaluation. This section presents the details of the wireless technology evaluation and the mobile applications evaluation in line with the high-level experimental design components presented in Figure 4. The ICT ecosystem of the Mankosi community published by Rey-Moreno et al. (2016) informed the smartphone battery consumption experiments. It is noteworthy to mention that although the battery consumption study commenced in 2015 along with MPv2 testbed setup, the data published by Rey-Moreno et al. (2016) was collected between years of 2012-2014.

3.3.1 Physical topology

Battery consumption is a characteristic of an end-user device that uses the network services using the wireless technologies installed. Therefore the presence of a physical network that provides network services is a requirement to evaluate battery consumption while a set network topology design is not a requirement to carry out the experiments. This can be observed in battery consumption experiments of Xiao et al. (2008), Balasubramanian et al. (2009), Carroll and Heiser (2010), Perrucci et al. (2011), and Friedman et al (2011); there is no emphasis on adopting a pre-set network topology design for evaluation of battery consumption.

3.3.2 Type of tests

As presented in Rey-Moreno et al. (2016), there was an emphasis on voice calls by the Mankosi community members and therefore VoIP calls were prioritized for battery consumption experiments. The following two experiment types were considered to evaluate battery consumption: (1) evaluate battery consumption during VoIP calls over Wi-Fi with LeSs in different cellular network mode combinations; and (2) evaluate both battery and data consumption by commonly used over-the-top IM and SIP applications used for VoIP calls. The related work of Nurminen, and Noyranen (2008), Xiao et al. (2008), Balasubramanian et al. (2009), Carroll and Heiser (2010), Perrucci et al. (2011), Kalic et al. (2012)and Friedman et al (2011) have shown Wi-Fi to be the best wireless technology for communication in terms of battery consumption. In light

of this related work, this study investigated the most efficient way to conduct VoIP calls over Wi-Fi in terms of battery consumption in the presence of cellular technologies such as 2G and 3G being active and consuming battery in the background.

3.3.3 Experiment technique

Since actual hardware is required for battery consumption experiments, the choice of experimental technique is narrowed to network emulation and real-world testing. Network emulation was chosen so that the experimental technique for this study would be in line with the technique in the related work of Nurminen, and Noyranen (2008), Xiao et al. (2008), Balasubramanian et al. (2009), Carroll and Heiser (2010), Perrucci et al. (2011), and Friedman et al (2011); all of which have shown usage of network emulation to yield results. In addition, battery consumption experiments required several controls to yield data specific to the type of tests. In real-world testing the behaviour of potential human users participating in the experiment cannot be completely controlled and hence consistency of results may be low (Beuran, 2012). In addition, setting up a real-world experimentation scenario involves complications related to ethical issues underlying the usage of humans for experiments. Therefore, real-world testing was not considered for experiments in this study. Network emulation experiments required hardware and software to generate VoIP traffic and collect data. The next two sections present the type of hardware and software identified for the smartphone battery consumption experiments.

3.3.3.1 Hardware requirements

The study considered low-end low-cost variants of smartphones in the sub-50USD for smartphone battery consumption as proposed in the report by GSMA Intelligence (2015). Three different LeSs within the price range of approximately 37USD to 52USD, available locally, were selected for experiments: Samsung Galaxy Pocket Neo[48] (Brand 1), Vodafone SmartKicka[49] (Brand 2), and Vodacom Smart4Mini[50] (Brand 3)[51]. Table 10 shows the out-of-box specifications of the LeSs used for experiments; and shows that hardware and OS specifications differed amongst the brands.

[48] Samsun Galaxy Pocket Neo link: https://www.gsmarena.com/samsung_galaxy_pocket_neo_s5310-5391.php
[49] Vodacom SmartKicka link: https://techcentral.co.za/vodacom-smart-kicka-review/50181/
[50] Vodacom Smar4Mini link: https://www.gsmarena.com/vodafone_smart_4_mini-6295.php
[51] Funding provided by the Center of Excellence at the Department of Computer Science, UWC

Table 10: Specifications of the three brands of low end smartphones

The table presents the specifications of the LeSs highlighting the limited and different hardware profiles of the phones.

	Brand 1	Brand 2	Brand 3
Battery (mAh)	1200	1400	1400
Wireless technologies	GSM, 3G, Wi-Fi 802.11 b/g/n	GSM, 3G, Wi-Fi 802.11 b/g/n	GSM, 3G, Wi-Fi 802.11 b/g/n
Claimed talk time	6 hours	8.5 hours	8 hours
Claimed stand-by time	600 hours	403 hours	600 hours
Android OS	4.4.2	4.4.2	4.2.2
Memory (MB)	512	512	512
Processor	850 MHz single-core	1 GHz dual-core	1.3 GHz dual-core
Display/ Resolution	3.0 inches, 240X320 pixels	3.5 inches, 320X480 pixels	4.0 inches, 480X800 pixels
Cost (USD)	44.47	37.62	51.32

Selection of more than one type of LeSs was deemed appropriate by the study because it can be observed in the related work of Friedman et al. (2011), which used multiple smartphones with similar wireless technology specifications, that the overall build of the smartphone, including overall hardware and software specifications, are critical factors in deciding energy consumption in smartphones. Therefore, multiple brands of smartphones with different specifications in different price ranges were selected for these experiments. It is worth mentioning that Android LeSs were chosen because Android smartphones have the biggest application store, Google Play (Master of Code Global, 2017), therefore, enabling the vast selection of preference of applications that might be required during experimentation.

During acquisition of the LeSs, initial testing was done to ensure that the batteries were not defective at the time of unboxing. Therefore, 20 units of each LeS were acquired, totalling 60 LeSs for the experiments. The wireless technology evaluation assumed that with 20 units per LeS, inconsistency in battery consumption between units of similar brand for similar experiments would indicate the presence of an LeS unit(s) with defective battery, given similar experimental conditions. Usage of such a large number of smartphones for battery consumption experiments is absent in the related work presented in Section 2.3.2. However, the related work of Nurminen, and Noyranen (2008), Balasubramanian et al. (2009), Friedman et al (2011) and Kalic et al. (2012) considered usage of multiple brand of smartphones.

3.3.3.2 Software requirements

Software was required, firstly, to initiate the VoIP calls, and secondly to measure battery consumption during the VoIP calls. For evaluation of battery consumption during VoIP calls over Wi-Fi with different cellular radio technologies, CSIPSimple (CSIP) and Viber mobile applications were used. CSIP is a SIP client that was shown to work with MPv2 units, being installed in the Zenzeleni mesh at the time of experiments, by the manufacturers of the devices, Village Telco (Gillet, 2017). The MPv2 units allowed free inter-network SIP voice calls because of the built-in PBX system (VillageTelco, 2016), and thus experimentation using CSIP application emulated inter-network voice calls. Breakout voice calling using CSIP could also be configured through subscription to a VoIP service provider. However, in order to minimize experiment costs, usage of an IM with calling feature was considered. Therefore Viber was selected as the application for breakout calls because of a recent report at the time of the experiments by Alcatel-Lucent (2014) which showed that Viber had the least impact on battery and data consumption as compared to other widely used IM applications such as WhatsApp, Facebook Messenger, Blackberry Messenger, and Skype.

The default battery profiling application was used to measure battery consumption during VoIP calls over Wi-Fi with different cellular mode combinations. Usage of a default battery profiling application can also be observed in the work of Balasubramanian et al. (2009), Perrucci et al. (2011) and Kalic et al. (Kalic et al., 2012). Adding further, at the time of experimentation, the LeSs were still under warranty, and therefore, use of a multimeter was avoided to measure battery consumption, as shown in the work of Friedman et al. (2011), since that required physical tampering with the phones in order to take voltage and current readings. Any physical modifications to so many devices, and considering the likelihood of devices malfunctioning due to modifications, would have led to a breach of warranty terms, and extra unplanned expenses to get the devices repaired (or buy new ones).

The evaluation of battery consumption by different social communication applications followed the evaluation of battery consumption during VoIP calls over Wi-Fi with different cellular radio technologies. Therefore, the selection process of social communication applications, consisting of IM applications and SIP clients, was conducted at the full completion of wireless technologies evaluation to consider recent usage trends. The 2017 first quarter report from Avast

Software (2017) which analysed the performance and trends of the top fifty most-installed Android applications was used to make the selections. Due to the large number of IM applications in the list of 50 applications, a rank-based selective sampling approach was applied to the list to select the IMs. The sampling approach applied to the list of most commonly installed Android applications considered: (a) use of IM applications in the top 30 ranking; and (b) the top two most installed IM applications in rankings; 1 to 10; 11 to 20; and 21 one to 30. The top thirty Android applications in first quarter report from Avast Software (2017) are shown in Figure 12. The sampling approach applied to the top 30 ranking list to select IMs yielded WhatsApp Messenger (WhatsApp), Messenger, Viber messenger (Viber), and IMO free video calls and chat applications for experiments.

Figure 12: Top 30 most installed Android applications in the Avast Software report

The figure lists the top 30 most installed Android based applications. It can be seen that; in top 10, the top two IMs are WhatsApp and Messenger; in rankings 11 to 20, there is only Viber; and in rankings 21-30 there only IMO.

It can be observed in Figure 12 that there are no SIP clients in the list. Further investigations were unable to find reports/articles ranking SIP clients based on most installations, or battery consumption. Therefore, a selective sampling approach was applied for the choice of SIP clients. The SIP clients were selected from the Google Play store based on their user review rating. In order to compare a similar number of SIP clients as IM applications, four SIP clients were selected from the search results. The search process, shown in Figure 13, consisted of (a) opening Google play on the LeS; (b) searching for SIP clients using the phrase “Sip Clients”; and (c) select the top 4 SIP clients from the search results. The selected SIP clients consisted of Zoiper, CSIP, Mizudroid, and SipDroid. Though the SIP client Media5-fone was third on the list of search results as shown in Figure 13, it was discarded due to in-app advertisements. Evidence showed that

advertisements that pop-up in applications during usage gobble up more energy, and increase processing time and data consumption (Konrad, 2015; Perkins, 2015).

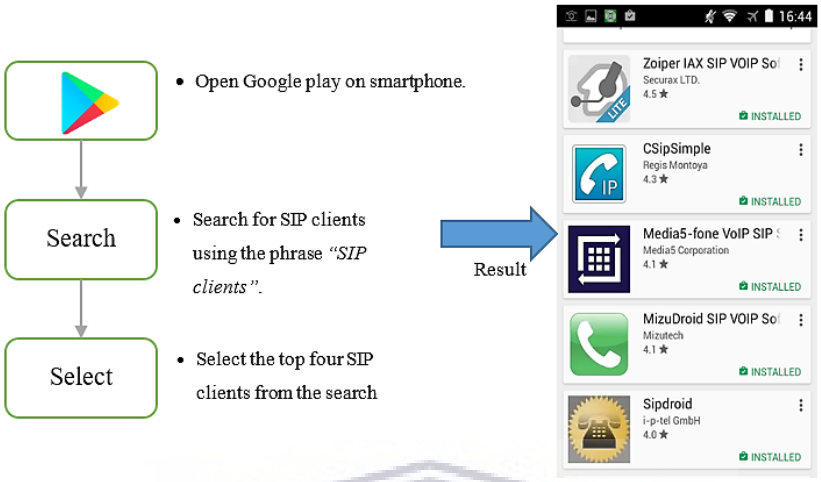

Figure 13: SIP clients search and results using an LeS

Figure shows the steps taken to create SIP client rankings. The user review rating can be observed in search results.

In addition, applications were required to measure battery and data consumption during VoIP calls. For battery profiling, a third-party software was used to measure consumption during VoIP call by a given mobile communication application only. Usage of a third-party application to measure battery consumption is considered an extension of the battery consumption measurement technique applied during wireless technology evaluations. A power estimation tool developed by Zhang et al (2010), PowerTutor (PTut) version 1.4, was used to measure average power consumption by the IM applications and SIP clients in mW units. The selection is based on the energy profiler comparison results of Bakker (2014) which showed PTut as the best choice for measuring energy consumption by applications. Bakker (2014) compared Intel Performance Viewer, PTut, eDoctor, Trepn, GSam Battery Monitor and CPU Monitor third-party battery profilers. In PTut, users can switch off power usage by the wireless radios, e.g. Wi-Fi or 3G, from the display because they are summed with the total battery consumption by applications. By doing so, the battery consumption by application specifically, due to CPU utilization, can be recorded.

To measure data consumption by IM and SIP applications during a VoIP call, the default data profiling application provided with the Android OS was selected. The mobile application evaluation literature review was unable to find related work that evaluated and compared data consumption of applications using a third-party tool. The reports of Alcatel-Lucent (2014) and Avast Software (2017) have reported ranking of several Android applications based on their data consumption. However, the tool or the method used to measure the data consumption was not

revealed in the reports. Therefore, the default data usage application provided with Android OS was considered for measuring data consumption.

3.3.4 Testbed setup

This section reports on the testbeds used for the wireless technology evaluation and mobile applications evaluation, respectively. The wireless technology evaluation was communicated via Om et al. (2017) and the mobile applications evaluation testbed was communicated via Om and Tucker (2018a).

3.3.4.1 Wireless technology evaluation

An improved version of the MP, Mesh Potato-2.0[52] (MP2) was used in the setup. The specifications of MP2 are presented in Section A2.2, AppendixA2. SIP call support was possible by simply enabling SIP settings in the MP2 firmware settings. For Viber to register and function, the MP2 was configured for Internet access. The MP2 AP mode was left in default 802.11b/g/n mode. The testbed setup for wireless technology evaluation is shown in Figure 14.

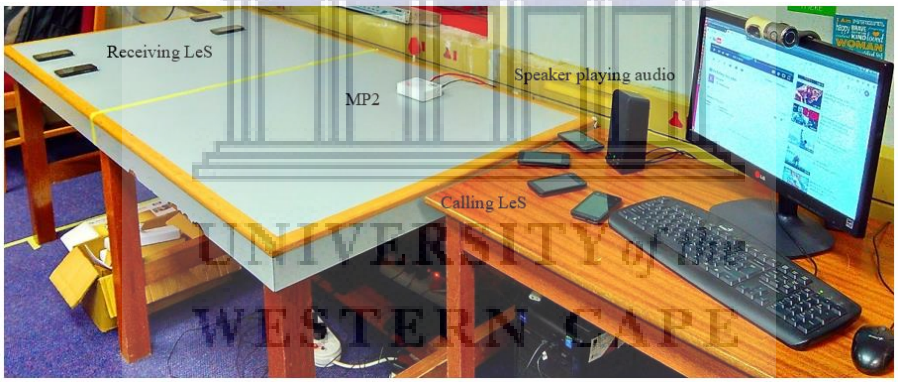

Figure 14: Testbed setup for wireless technologies evaluation
Figure shows the setup used to evaluate battery consumption by different wireless technologies using VoIP calls.

3.3.4.2 Mobile applications evaluation

The testbed from the wireless technology evaluation was expanded to include the mesh backbone aspect in-line with WMNs. As shown in Figure 15, a 3 node testbed using MPv2 units was set up in a lab in a space of 230X200cm. The MPv2 units were placed in a straight line distanced equally from one another along the 230cm length. The middle MPv2 unit set up as SIP master and Internet gateway with its AP feature disabled. The remaining two MPv2 units were placed on the right and

[52] Mesh Potato-2.0 link: https://store.villagetelco.com/mesh-potatoes/mesh-potato-2-basic.html

left side of master MPv2, and each was configured for AP functionality along with its own DHCP server. Two MPv2 units with AP mode enabled functioned in dual-radio dual-band mode and connected to master MPv2 over 5GHz. The mesh and the AP radios were left to operate in their default 802.11n and 802.11b/g/n modes, respectively. The phones connected to the two MPv2 units with AP mode enabled the researcher to authenticate the SIP settings; and use Internet via the master MPv2. Two desktops with external speakers were used for voice playback; and placed in-line with the AP MPv2 units at a maximum distance of 200cm.

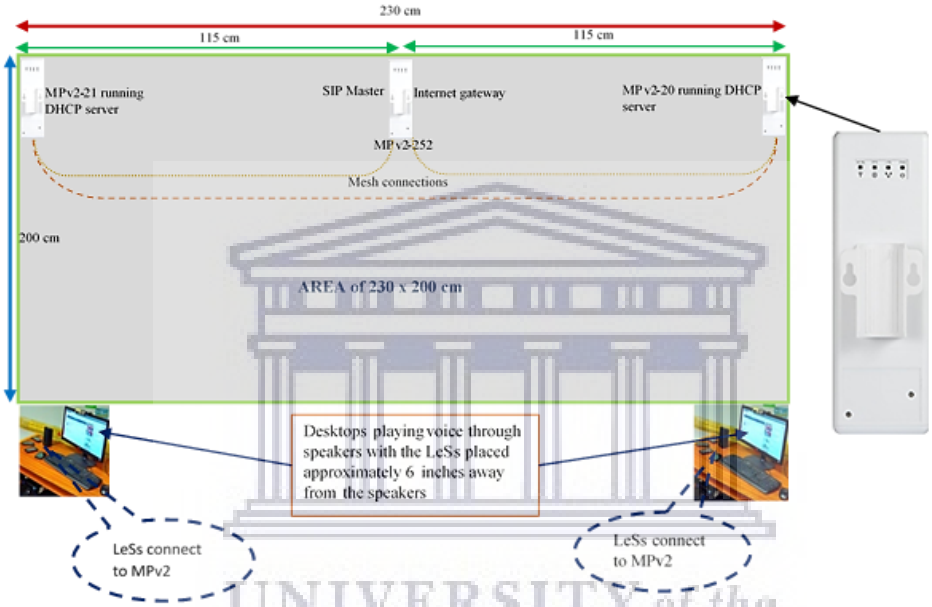

Figure 15: Testbed setup for mobile applications evaluation.
The figure shows the testbed setup for evaluation battery and data drain by IM and SIP applications. It was made sure that no physical interference was present between the MPv2 nodes; or the smartphones and the speaker.

3.3.5 Data collection

This section presents the data collection process for wireless technologies evaluation; and mobile applications evaluation, respectively.

3.3.5.1 Wireless technology evaluation

The battery percentages displayed on the notification bar of the Android OS were recorded at the beginning and at the end of VoIP call (the data collected) to evaluate battery consumption. As shown in Figure 16, the battery percentage notification feature in Android setting was enabled in order to display the battery percentage on the notification bar of the LeSs. The battery drain (in percentage) during a VoIP call was evaluated as the difference between battery percentages displayed on the notification bar at the beginning and at the end of VoIP call. Recording battery

percentage by manually accessing the settings menu of the LeSs, before and after every call, was considered an unreliable option because of extra battery consumption, not representative of the consumption during VoIP call, being added to the overall data while accessing the settings menu.

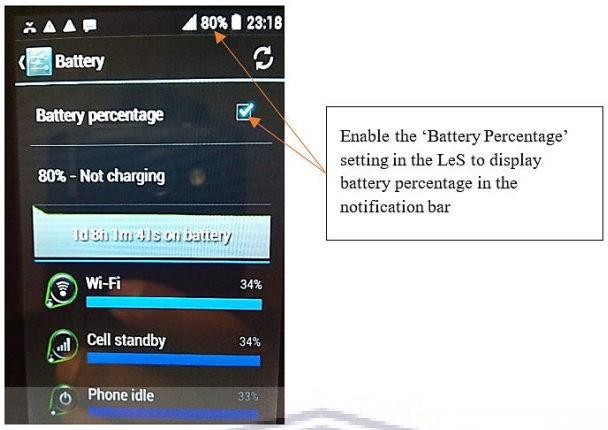

Figure 16: Battery percentage display in the notification bar of the smartphones.
Figure shows the configuration applied to display the battery percentage in the notification bar of the LeSs to record battery consumption during VoIP calls,

Further experiment controls were applied to ensure reliability of battery percentage data and to be representative of wireless technologies evaluation, using VoIP calls. The type and description of the experiment control measures applied in advance of the experiments for wireless technology evaluation are shown in Table 11.

Table 11: Control measures applied to the low-end smartphones in advance of experiments
The table shows the control measure applied to the LeSs to increase battery percentage result reliability..

Control	Description
Firmware update	Updates bring along bug fixes and driver updates aimed at improving overall performance of device. The availability of recent firmware was checked advance of experiments. However, none were available for any of the LeSs brand.
Disable auto-execution	Applications can auto-update or auto-sync in the background when a smartphone is connected to Internet, hence adding to the overall battery consumption Therefore auto-update and auto-sync functions were turned off to stop background execution of network processes during tests.
App versions	Make sure same version of CSIP; and Viber is installed across all smartphones for the entire duration of experiments
Volume	System volume and app volume are two different settings. Make sure they are same across all phones.
Brightness	Make sure brightness setting are same across all the LeSs.

Wireless technology evaluation data was collected for two of the best wireless technology options for VoIP calls present in the LeSs acquired, Wi-Fi and 3G, because in the absence of a Wi-Fi hotspot, 3G data is the next best option . VoIP calls using 2G were not considered because Perrucci et al. (2009) have shown that when a data connection is needed, 3G networks offer higher

data rates with lower battery consumption as compared to 2G. In addition, related work of Nurminen, and Noyranen (2008), Xiao et al. (2008), Balasubramanian et al. (2009), Carroll and Heiser (2010), Perrucci et al. (2011), Friedman et al (2011), and Kalic et al. (2012) has already shown Wi-Fi to consume less battery than 3G during data transmission.

In order to identify the least battery consuming Wi-Fi and cellular technology combination, data was collected for VoIP calls, conducted using CSIP and Viber, over Wi-Fi with 4 different cellular network mode combinations possible with the LeSs. In order to assess the impact of Wi-Fi radio being active in the background during a 3G call, data was collected with VoIP calls conducted using Viber over 3G with 2 different states of Wi-Fi. The wireless network mode combinations for VoIP calls using CSIP and Viber are presented in Table 12.

Table 12: Types of battery consumption data collected for analysis
The table shows all the different data collected for each LeS. Data was collected for VoIP calls in each network mode combination. The description of the acronyms is provided in the last row.

	Battery Consumption Data					
	Brand 1		**Brand 2**		**Brand 3**	
	CSIP	VIBER	CSIB	VIBER	CSIP	VIBER
Network Mode Combinations	W-AUTO	W-AUTO	W-AUTO	W-AUTO	W-AUTO	W-AUTO
	W-2G	W-2G	W-2G	W-2G	W-2G	W-2G
	W-3G	W-3G	W-3G	W-3G	W-3G	W-3G
	W-PLAIN	W-PLAIN	W-PLAIN	W-PLAIN	W-PLAIN	W-PLAIN
		3G		3G		3G
		3G-X		3G-X		3G-X

W-AUTO - Wi-Fi calls with cellular radio in 2G/3G network mode
W-2G - Wi-Fi calls with cellular radio in GSM network mode
W-3G - Wi-Fi calls with cellular radio in 3G network mode
W-PLAIN - Wi-Fi calls with cellular radios turned off , hence achieving partial-airplane mode
3G-X - Voice calls using 3G data with Wi-Fi radio ON but not connected to any AP
3G - Voice calls using 3G data with Wi-Fi radio OFF

Battery percentage difference was collected for a single cycle of 1 hour voice calls between a pair of LeSs. Therefore the battery percentage in an LeS was recorded at the beginning of a VoIP call; and then at the end of the VoIP call from the battery percentage indicator on the notification bar.

The calls were conducted for both ON and OFF screen states to highlight the impact of screen state on battery consumption during a voice call. A common brightness setting was applied

across all the LeSs. The Android OS installed on the smartphones had a brightness bar that could be accessed from the device settings, as shown in Figure 17, to set the brightness levels.

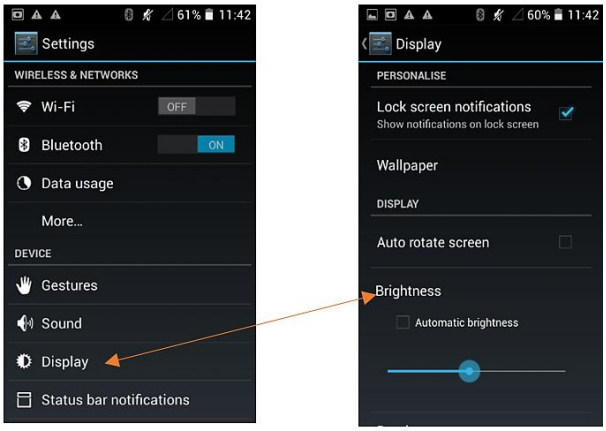

Figure 17: Brightness setting in the low-end smartphones
Figure shows how the display settings were accessed and the brightness was modified in the LeSs.

In order to set brightness at 75% brightness, the indicator was first moved to the mid-point of the brightness bar representing approximately 50%, and then moved towards right to the mid-point of the 50% and 100% marks.

All the VoIP calls were conducted and observed manually. To emulate voice, media containing varying audio tone of length more than 1 hour was streamed using YouTube via speakers as shown in Figure 14. It can be further noticed in Figure 14 that in order to conduct a VoIP call: the LeSs were linked to an MPv2; audio via YouTube was played via the PC speakers; a call was placed using one LeS to another LeS; the calling LeS was placed facing upwards next to the speaker playing audio; the call was received on the ringing LeS; and the receiving LeS was placed approximately 2 metres away from the calling LeSs to avoid interference. Therefore, in the wireless technologies evaluation, voice was transmitted in one direction. For the calls, the PC speaker volume was set manually to approximately 50%, whereas PC internal hardware audio and YouTube player volume settings were kept at 100%. The volume setting of LeSs were turned to full for experiments for coherence in volume setting across all 60 units. If a call dropped during an ongoing experiment, then that call was repeated in order to provide 1 hour of undisrupted voice call data. The number of LeS units to be linked to the MP2 AP unit during experiments was evaluated through a network load test. During the network load test, an LeS pair was linked to an MPv2 AP unit, and test VoIP call was placed. The number of calling pairs were incremented gradually in single pair progression, and the call reception between LeS pairs was observed

manually. The audio of the receiving LeSs was very audible due to the maximum volume setting of the LeS speakers. The number of total pairs over which the VoIP calls started breaking was decided as the threshold of LeS pairs that could be linked to the MP2 units in a single cycle of an experiment. For screen OFF tests, each phone screen was manually turned off by pressing respective power buttons after 5 seconds of reception of a call because the screens would not turn OFF automatically. Smartphones use proximity sensors to turn-off screens automatically. The proximity sensor in smartphones uses an infrared light-emitting diode to emit a beam of light and a light detector to detect the reflection of the light beam, to judge the closeness of the phone to the ear (Nield, 2017). There was no surface to reflect the light beam in the experiments because the LeSs were placed with their screens facing upwards during a VoIP call.

VoIP calls were conducted for each network mode combination shown in Table 12 in both screen ON and OFF states. The battery percentage at the beginning and end of each call was recorded manually (pen and paper); and the data was transferred to a spreadsheet for analysis.

3.3.5.2 Mobile applications evaluation

Mobile application evaluations were conducted after the evaluation of wireless technologies. The experiments were conducted to evaluate the battery consumption and data usage by IMs and SIP clients during VoIP calls while using the best LeS and wireless technology and network mode combination. Power requirements (in mW) by IM and SIP applications during VoIP calling were measured using PTut to evaluate battery consumption. Overall data usage by IM and SIP applications during VoIP calling was measured using the default Android data consumption app. The versions of the IM and SIP applications used in the experiments are listed in Table A3.8, Section A3.10, Appendix A3. The mobile application evaluations refined version of the experimental setup of the wireless technologies evaluation. The testbed was expanded to use the MPv2 units and conduct VoIP calls over mesh links using 5GHz as shown in Figure 15. The VoIP call procedure was refined to include real voice call characteristics such as voice playback at intervals from both caller and receiver ends. The audio for the voice call sample was prepared using an episode from a television show interview called *"Inside the actor's studio with Robin Williams"*. The extracted audio consisted of the following characteristics:

a. Back and forth talking – the interview had a host questioning and the guest answering.

b. Different tones – the guest answered questions in different tones and included laughter, screaming, and mimicry.
c. Background noise – presence of clapping, laughing, and screaming (of audience, and guest), while the guest or the host were in conversation. The background music is also considered background noise.
d. Simultaneous silence/talking – there were instances in the interview whereby the guest began answering a question while the question was still being asked, hence simultaneous talking, or took a moment to answer after certain questions, hence simultaneous silence.

Since the file was in video format, the audio was extracted from the file using an open-source audio editing and recording software, Audacity[53]. The extracted audio sample was further split into two chunks, A and B, respectively, as shown in Figure 18. Chunk B was a cut-paste of audio clips at random times and intervals from the extracted audio. The modified original audio became chunk A. Silence was inserted at every empty audio section in the two chunks. Therefore, if both chunks were played simultaneously, chunk A will start with the audio while chunk B will be silent, and vice versa. In addition, the two chunks were overlapped at random to insert simultaneous talking.

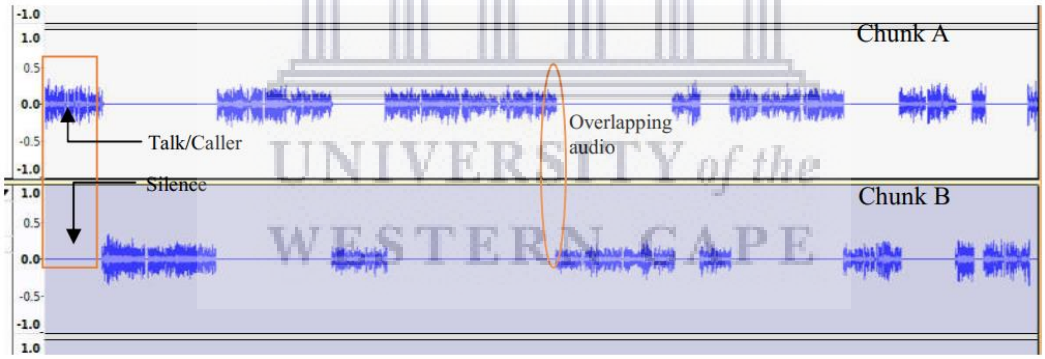

Figure 18: Audio chunk used for voice calls.
The figure shows the two audio chunks used for the voice call experiments compared against each other. The chunks are created from one audio file. The figure is screenshot from Audacity.

The procedure for VoIP calls consisted of manually conducting 30 minute calls for each application, to be installed on the LeS one at a time. For example, the voice call procedure of WhatsApp consisted of: installing and activating WhatsApp on all 20 LeS units obtained from wireless technologies evaluation; complete the 30 minute WhatsApp VoIP call tests; and uninstall WhatsApp from all the LeSs. This procedure was repeated for all the IM and SIP applications.

[53] Audacity link: https://www.audacityteam.org/

Since calls terminating precisely at the end of 30 minutes was next to impossible with so many phones calling each other concurrently, calls were terminated manually after durations over 30 minutes was completed. Dropped calls were observed manually and were repeated from beginning to ensure continuous 30 minutes of battery and data consumption. For playback synchronization, the PCs were to be accessed remotely so that audio chunks A and B could be played simultaneously from one point. The number of LeS units paired to an AP, and the volume settings were kept the same as those in the wireless technologies evaluation. For a call in a test: (1) the audio was played on a desktop; (2) PTut was started on the LeS pair and configured to record consumption by IMs and SIP clients excluding the power usages by Wi-Fi radio and LCD screen; (3) PTut was minimized to run in the background; (3) the call was placed using an LeS from the pair and placed in front of the PC speaker playing audio; and (4) the call was received on the ringing LeS unit from the pair and was placed in front of the silent speaker (see mobile application evaluation testbed setup in Figure 15). The battery profiler, PTut, automatically logs the power consumption by different entities in a smartphone. Therefore, at the completion of each call, PTut was accessed in the corresponding LeS pairs. The power consumption log of PTut was saved locally on each LeS, and later transferred to a desktop for further analysis. To collect data usage, the default data profiling application provided with Android OS was accessed manually at the end of each VoIP call to record the data used by an IM or SIP application. Figure 19 shows the method to access data consumption using WhatsApp as an example.

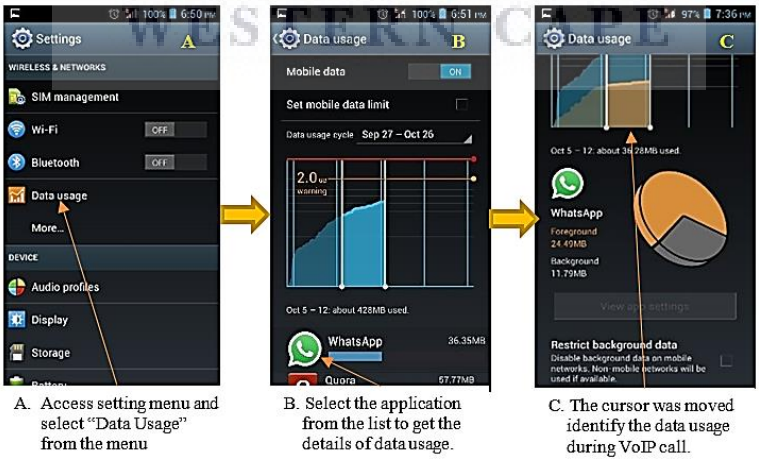

A. Access setting menu and select "Data Usage" from the menu

B. Select the application from the list to get the details of data usage.

C. The cursor was moved identify the data usage during VoIP call.

Figure 19: The process to collect data usage by mobile communication applications

Figure shows the process of collecting data usage by the IMs and SIP applications after a VoIP call. It can be observed that during usage of the applications the data usage graph spiked.

It can be observed in Figure 19 part C that during usage of the WhatsApp, the data usage graph spiked. Since the IM and SIP applications were installed and evaluated one by one (every

application was uninstalled after completion of its evaluation), and Internet access was enabled during experiments only, the spike represented the data usage during VoIP calls by the specific IM or SIP application under evaluation. The data usage cursor was moved between the range of highest spike states and data usage displayed under "Foreground" in Figure 19, which represents the data consumed during active usage of the application; and was recorded manually.

3.3.6 Data analysis

This section presents the data analysis processes adopted for experimentation for wireless technology and mobile applications evaluation, respectively.

3.3.6.1 Wireless technology evaluation

The battery consumption data collected from wireless technologies evaluation was for 60 LeSs comprising 20 units of three different brands. Table 12 showed the different network mode combination data collected (in battery percentage form) for each LeS. Data analysis consisted of: (a) comparing the difference between means of each network mode combination data between the three brand of LeS for each application, and for both screen ON and OFF states, to identify the most suitable LeS in terms of battery consumption during VoIP calls; (b) the least battery draining Wi-Fi and cellular radio network combination mode within each LeS; and (c) comparing means of screen ON and OFF states data of each network combination type within each brand of LeS. The Department of Statistics and Population Studies at the UWC was consulted for a suitable statistical method to compare the battery consumption data of the 60 LeSs. Their recommendation was to use Analysis of Variance (ANOVA), and Tukey's Honest Significance Difference (HSD) post-hoc analysis methods; to analyse and compare the difference between means of different types of data collected from experiments. The one-way ANOVA determines whether there are any statistically significant differences amongst means of several independent groups (Laerd Statistics, 2018; Leedy & Ormrod, 2015; SAS, 2013). The wireless technology evaluation consisted of three independent groups of LeSs with different data types within each group. One-way ANOVA determined whether there was significant difference between means of data collected for each data network mode combination, as shown in Table 12, across the three LeSs. The following four steps describe the one-way ANOVA steps used to analyse the data collected and draw conclusions on the significance of the difference between means (Sullivan, 2016):

1. Setup hypothesis and determine level of significance, alpha (α). The null and alternative hypotheses that are generally used in ANOVA are:

   H_0: $\mu_1 = \mu_1 = \mu_2 = \ldots = \mu_n$; *all means, μ, are equal, where n = number of groups*

   H_1: *not all μ are equal*

   The chosen significance level, alpha (α), which is the probability of rejecting the null hypothesis when it is true, was 0.05. Significance levels are related confidence levels such that, to get α, the confidence level is subtracted from 1. Therefore, an α of 0.05 represents 95% confidence level in data.

2. One-way ANOVA uses the F-statistic to find out if the means between two populations are significantly different.
3. A P-value associated with the F-statistic is evaluated by one-way ANOVA; and if $p \leq \alpha$, the null hypothesis is rejected and H_1 is true.
4. Based on results from step (3), a conclusion such as H_1 or H_0 is made by one-way ANOVA.

However, the one-way ANOVA does not distinguish which specific means are significantly different from each other. A *post-hoc* analysis is usually conducted to determine which means are significantly different. Therefore, one-way ANOVA was followed by Tukey's HSD test for *post-hoc* analysis (Minitab, 2016) which consisted of pairwise comparison between means of similar network mode combination results shown in Table 12. Tukey's HSD test created confidence intervals for all pairwise comparisons while controlling the family error rate to α level. The post-hoc analysis was also conducted between screen ON and OFF results, of CSIP and Viber, respectively. For example, with reference to Table 12, the mean of W-AUTO for CSIP from Brand 1 was compared with Brand 2; Brand 2 was compared with Brand 3; and Brand 1 was compared with Brand 3. The outcome of Tukey's HSD post-hoc analysis was interpreted to decide the least battery draining LeS. The least battery draining Wi-Fi and cellular radio combination mode within each LeS was identified by comparing the mean battery consumption results of least battery draining screen OFF. Further, the difference between means of battery consumption results of screen ON and OFF states for each network mode combination for each application in Table 12 were analysed for each brand of LeS with a 95% confidence interval. The analysis was conducted to show the extra percentage of battery that could be saved by keeping screen OFF during VoIP calls and to promote awareness amongst users of LeSs that could accidentally turn (or keep) screen

ON during VoIP call. The work of Perrucci et al. (2011) investigated the effect of different brightness settings on power consumption in one smartphone (and one sample size) and showed that with reduction in brightness, the power consumption by the display was also lowered. In this way, the comparison of screen ON and OFF conducted by this study extends the work of Perrucci et al. (2011) by the usage of newer models of different types of smartphones.

3.3.6.2 Mobile applications evaluation

The log file generated by PTut contained power consumption data of all running applications on the LeSs during a VoIP call. Therefore, a Python script was used to extract the relevant battery data from the log file, using the CPUID of the IM and SIP applications, and exported to a comma separated value (CSV) file for further analysis. The details of the Python script are presented in Section A3.9, Appendix A3. Equation 3.2 was then used to calculate average battery consumption (ABC_x) for each application using the data in the CSV file. The ABC_x values were used to analyse and contrast the battery consumption by IM and SIP applications.

$$\boldsymbol{ABC_x = {\sum_{\mathbf{n \geq 30}}^{\mathbf{n+1799}} (\mathbf{PU_n})} / {\mathbf{1800}}} \quad 3.2$$

whereby ABC_x is Average Battery Consumption in mW by application x, and PU_n is power usage in mW at time $n \geq 30$ seconds.

The data consumption results were normalized for 30 minutes (1800 seconds) for each IM and SIP application because each call was conducted for a duration of longer than 30 minutes. For normalization, it was assumed that if *X* MB of data were used during *Y* seconds of VoIP call, then, for $Y > 1800$ seconds, the amount of data used in 1800 seconds, D_{X30}, is given by Equation 3.3.

$$D_{X30} = {(1800 \cdot X)} / {Y} \quad 3.3$$

Equation 3.3 yielded the data usage by each IM and SIP application over 30 minutes of VoIP call. The data usage values were used to analyse and contrast data consumption by IM and SIP applications.

3.4 Chapter summary

This chapter began with a presentation of empirical analysis as the selected research methodology to answer the research questions that required empirical data from experiments. Since the experiments required testbed setup, the chapter presented the experiment designs consisting of steps such as; physical topology; type of test; experiment technique; data collection; and data

analysis for the two types of experiments to answer the two research questions - scalability quantification and smartphone battery consumption. The scalability quantification experiment design presented in Section 3.2 (a) selected clustered topology as the physical topology for the experiment testbeds, TCP tests to measure performance of TH and voice tests to evaluate performance of RTL, RTJ, and PL%, and network emulation as the experimental technique along with the accompanying hardware and software requirements; (b)showed the testbed setup processes of the MPv2 and UniFi testbed; and (c) showed the data collection methods consisting of the TCP packet size, the VoIP codec profile, and the number of flows and iterations details for TCP and VoIP tests, and data analysis techniques consisting of power and exponential regression and R^2. The smartphone battery consumption experiment design presented in Section 3.3 showed that a set network topology was not a requirement to evaluate battery consumption; voice calls as the suitable type of tests because of their strict QoS requirements; network emulation as the experiment technique along with selection of 3 types of LeSs fulfilling the hardware requirements and selection of mobile applications satisfying software requirements; the testbed setup processes for wireless technology and mobile applications evaluations, respectively; the data collection techniques to measure change in battery percentage during VoIP calls in different network mode combinations using default LeS battery profiler for wireless technology evaluation and usage of PTut to measure energy consumption and default data profiler of LeSs to measure data consumption by IM and SIP applications during VoIP calls during mobile applications evaluation; and data analysis techniques ANOVA and Tukey post-hoc methods to analyse wireless technology evaluation data, and mean of power and data consumption data by the IM and SIP applications to analyse the mobile applications. The results of scalability quantification and smartphone battery consumptions are presented in Chapter 4.

4 Results

This chapter reports on the empirical findings of the scalability quantification and smartphone battery consumption experiments. The scalability quantification findings in Section 4.1 are comprised of the MPv2 testbed scalability quantification in Section 4.1.1; and UniFi testbed scalability quantification in Section 4.1.2. The MPv2 scalability quantification consists of the average results of the TH, RTL, RTJ, and PL% performance with increasing hop length for MPv2 testbed followed by regression modelling of the respective results. The UniFi testbed scalability quantification consists of the TH, RTL, RTJ, and PL% performance with increasing inter-cluster hop length for UniFi testbed followed by regression modelling of the respective results.

The smartphone battery consumption findings in Section 4.2 consist of the results of wireless technology evaluation in Section 4.2.1 and mobile applications evaluation in Section 4.2.2. The wireless technology evaluation results consist of significant Tukey post-hoc data obtained after pairwise comparison of the battery percentage data of the 3 LeSs. In addition the average difference in battery consumption between VoIP calls in screen ON and OFF modes; and average battery drop during a VoIP call in screen OFF mode for each network combination mode presented in Table 12 are also presented under wireless technology evaluation. The mobile applications evaluation results consist of average battery and data consumption figures after Equation 3.2 and 3.3 were applied to battery and data consumption data, respectively, of IM and SIP applications obtained using VoIP calls over Wi-Fi in screen OFF mode.

4.1 Scalability quantification

This section presents the scalability quantification modelling using the data collected from experiments over MPv2 and UniFi testbed setups. The nomenclature used in the equations is presented under Section A5.1. As a reminder, the acronym TH represents the overall round-trip throughput; RTL represents round-trip latency; RTJ represents jitter during RTL; and PL% represents packet loss percentage during round-trip traffic.

4.1.1 MPv2 testbed scalability quantification

The MPv2 testbed setup was presented in Section 3.2.4.1 and the data collection method was presented in Section 3.2.5.1. It is noteworthy to mention that the MPv2 testbed and preliminary results to show that the testbed was ready for further experiments, were communicated via Om and Tucker (2018b). This section presents the details of the scalability quantification modelling

using the results of TH, RTL, RTJ, and PL% obtained from experimentation over the MPv2 testbed. This section is divided into two further subsections. Subsection 4.1.1.1 presents the average results of the performance metrics and the R^2 coefficient of exponential and power regression of the average results. Subsection 4.1.1.2 presents the equations formed for the best-fit regression for each performance metric.

4.1.1.1 Performance metric results

The MPv2 testbed consisted of: 7 mesh links of 1 hop; 4 mesh links of 2 hops and 3 hops, respectively (see Table 7). The throughput experiments collected results of maximum achievable TH with increasing hop length between MPv2 nodes. In order to do so, TCP packets of size 85.3KB each were sent over each hop-length (or mesh link) in the MPv2 testbed using *iPerf* running on RPi2 devices linked to each mesh device. Since 40 iterations of 1 minute *iPerf* tests were performed for each mesh link (20 iterations in each direction of a link), the results consisted of: 280 iterations for 1 hop; and 160 iterations for 2 and 3 hops, respectively. The average of number of iterations were evaluated for each hop length, and exponential and power regression analyses were conducted for the trend in average throughout values with increasing hop length. The latency experiments collected results of round-trip latency, RTL, performance for G.711 encoded voice traffic with increasing hop length between MPv2 units; and therefore, the RTJ and PL% that were included in the overall results were also representative of the round-trip performance. In order to collect RTL, RTJ, and PL% results, 20 iterations of single G.711 encoded VoIP flows of 5 minute duration were transmitted over each hop length (or mesh link). Therefore, the overall results consisted of: 140 iterations for 1 hop; and 80 iterations each for 2 and 3 hops. Similarly to TH, the average of number of iterations were evaluated for each hop length, and exponential and power regression analyses were conducted for the trend in average RTL, RTJ, and PL% values with increasing hop length. Table 13 shows the average values of the iterations for each metric with increasing hop length along with the R^2 coefficients of the exponential and power regression analyses of the result trend. The results in Table 13 show a declining trend for TH; and inclining trend for RTL, RTJ, and PL% with increasing hop-length, emphasizing the expectation that performance would drop below the recommended QoS requirements past a certain number of hops and become unreliable for VoIP traffic. In Appendix A4, plots showing the declining trend along with exponential and regression trend lines for TH, RTL, RTJ and PL% results are presented via Figures A4.1, A4.2, A4.3, and A4.4, respectively.

Table 13: Key performance metrics and R^2 values for MPv2 results

The table shows the average values of TH, RTL, RTJ, and PL% with increasing hop length obtained from MPv2 results; and the R^2 values for power and exponential regression for the average values. The higher R^2 values are highlighted.

Metric	Hop length			R^2 coefficient	
	1-hop	2-hop	3-hop	Exponential	Power
TH (Mbps)	16.32	6.84	3.58	0.9928	**0.9958**
RTL (ms)	11.75	28.07	53.26	0.9923	**0.9961**
RTJ (ms)	0.85	3.48	4.11	0.8288	**0.9255**
PL%	0.05	0.74	0.96	0.8158	**0.9163**

The next section presents the formation of empirical equations for each performance metric, using the R^2 coefficient of the best-fit regression trend that will assist in predicting the cut-off hop length.

4.1.1.2 Performance metric quantification

This section presents details of the equation formation process for TH, RTL, RTJ, and PL%, respectively, using the average values from Table 13 that exhibit MPv2 testbed network performance trends with increasing hop length. As presented in Section 3.2.6, exponential and power regression analyses, and the R^2 coefficient of determination of each of the regression techniques, were used for data analysis. Equation to represent the performance trend of a given KPM was evaluated for the regression technique with the higher R^2.

1. Formulation process of throughput results

In case of TH, as shown in Table 13, the evaluated R^2 coefficient for power regression (R^2 = 0.9958) was more than exponential regression (R^2 = 0.9928). Thus, the power regression equation, Equation 4.1, was evaluated to represent the TH trend. In Equation 4.1, T_m is throughout and N is the hop length and subscript m is used to represent MPv2 unit.

$$T_m = 16.66/N^{1.37} \quad 4.1$$

Equation 4.1 establishes that T_m for $N = 2, 3, 4 \ldots x$ is dependent on the measurement T_m for $N = 1$. Therefore, in order to estimate T_m for $N = x$ hop length between source and destination, the value T_m for $N = 1$ must be known (or measured). The average TH for $N = 1$ obtained for MPv2 experiments was 16.32Mbps. However, for $N = 1$, Equation 4.1 yields T_m to be 16.66Mbps. The value of 16.66 in power regression Equation 4.1 is a constant obtained from the regression equation evaluation using the regression analysis function. Thus, the value of 16.66 in Equation 4.1 is

substituted by constant variable T_1 which represents the average TH measured over $N = 1$. The result of doing such a substitution yields Equation 4.2 to represent the TH capacity trend with increasing hop length between source and destination mesh nodes. Such a treatment to TH capacity equations can also be observed in Gupta et al. (2001), Li et al. (2002), and Johnson et al. (2007a). Therefore, in Equation 4.2, T_1 is the average of TH for all the first hop pairs ($N = 1$) in an experimental testbed or a live network WMN.

$$T_m = T_1 / N_m{}^{1.37} \quad 4.2$$

The average results of RTL, RTJ, and PL%, as shown in Table 13, were also treated with a similar method adopted for TH to obtain respective performance trend equations. The results showed an inclining trend with increase in hop length for RTL, RTJ, and PL%, respectively.

2. Formulation process of round-trip latency results

In the case of RTL, as shown in Table 13, the R^2 coefficient for power regression ($R^2 = 0.9961$) was higher than exponential regression ($R^2 = 0.9923$). Thus, the power regression Equation 4.3 was evaluated to represent trend for RTL, L_m, with increasing hop-length, N.

$$L_m = 11.52 \cdot N^{1.36} \quad 4.3$$

However, Equation 4.3 yields L_m for $N = 1$ as 11.52ms, in contrast to the average L_m obtained for $N = 1$ from MPv2 experiments that was 11.75ms (see Table 13). The value of 11.52 in Equation 4.3 is a constant obtained from the formation of the equation using regression analysis of average RTL results. Thus, adopting a similar approach to the formation of Equation 4.2, the fixed constant value of 11.52 in Equation 4.3 is substituted by variable L_1 to represent the RTL for $N = 1$. The result of doing such a substitution yields Equation 4.4 to represent the RTL trend with increasing hop length, N, between source and destination mesh nodes. In Equation 4.4, L_1 is the average of RTL over the first hop pairs in an experimental testbed or a live network WMN; and N is the hop length between mesh nodes.

$$L_m = L_1 \cdot N^{1.36} \quad 4.4$$

3. Formulation process of jitter results

In case of RTJ, as shown in Table 13, the calculated R^2 coefficient for power regression ($R^2 = 0.9255$) was higher than exponential regression ($R^2 = 0.8288$). Thus, the power regression Equation 4.5 was evaluated to represent trend for RTL, J_m, with increasing hop length, N.

$$J_m = 0.94 \cdot N^{1.5} \quad 4.5$$

For $N = 1$, Equation 4.5 yields J_m = 0.94ms. However, the average RTJ obtained from experimental results shows J_m = 0.85ms for $N = 1$. The value of 0.94 in Equation 4.5 is a constant obtained from the formulation of the power regression trend for RTJ. Thus, the constant 0.94 is substituted for variable J_1 to represent the RTJ for N = 1 in Equation 4.5. The resulting output of the substitution is Equation 4.6 in which J_1 is the average of RTJ over first hop pairs in a WMN testbed or a live network; and N is the hop length between mesh nodes.

$$J_m = J_1 \cdot N^{1.5} \quad 4.6$$

4. Formulation process of packet loss percentage results

In the case of PL% results, as shown in Table 13, the evaluated R^2 coefficient for power regression (R^2 = 0.9163) was higher than the exponential regression (R^2 = 0.8158). Thus, the power regression Equation 4.7 was evaluated for power regression to represent the PL% trend with increasing hop length. In Equation 4.7, P_m is PL% and N is hop length.

$$P_m = 0.06 \cdot N^{2.82} \quad 4.7$$

For $N = 1$, Equation 4.7 yields 0.06% whereas the PL% obtained from experiments is 0.05%. The value 0.06 in Equation 4.7 is a constant obtained from the formulation of the power regression analysis trend. The constant 0.06 in Equation 4.7 is substituted with constant variable P_1 where P_1 is PL% for $N = 1$. The substitution yields Equation 4.8 where P_1 is the average of PL% over the first hop pairs in a WMN testbed or a live network; and N is the hop count.

$$P_m = P_1 \cdot N^{2.82} \quad 4.8$$

This section presented the modelling of results of TH, RTL, RTJ, and PL% shown in Table 13. The results of TH showed a declining trend; and RTL, RTJ, and PL% showed inclining trends with an increase in hop length between source and destination nodes. Such trends for these performance metrics is also observed in the related work presented in Section 2.2.2. The next section presents the scalability quantification of the UniFi testbed experimental results.

4.1.2 UniFi testbed scalability quantification

The UniFi testbed setup and experimentation were completed between the fourth quarter of 2018 and end of the second quarter of 2019. The experimentation testbed migrated from MPv2 to UniFi devices to stay in line with the hardware requirements presented in Section 3.2.3.1 that emphasized the preferred usage of OTS intermediary devices available in the local market or operational in a

real-world WMN deployment. At the start of [the] MPv2 testbed set up and experimentation, the mesh units were available from vendors and also functional in Zenzeleni. However, expansion of experiments using obsolete MPv2 devices was considered unrealistic. Therefore, the experiments migrated to UniFi devices. The UniFi testbed setup was described in Section 3.2.4.2 and the data collection method was presented in Section 3.2.5.2. The UniFi experiments tested inter-cluster network performance between two clusters connected via a base station. The data collected for TH, RTL, RTJ, and PL% were for inter-cluster hop lengths of 2 up to 6. The number of links for each hop length in UniFi testbed was presented in Table 9 in Section 3.2.5.2. Similar to the presentation of results for the MPv2 testbed, this section is also divided in two subsections. Subsection 4.1.2.1 presents the average results of the four performance metrics, TH, RTL, RTJ, and PL%, and the R^2 coefficients of exponential and power regressions of the average results. Subsection 4.1.2.2 presents the equations formed for the best-fit regression for each performance metric.

4.1.2.1 Performance metric results

The experiments in the UniFi testbed collected similar data for the same number of iterations as in MPv2 testbed with some differences. For TH, TCP traffic was transmitted across inter-cluster mesh links, meaning the sender was in one cluster and the receiver was in a second cluster. Since 40 iterations of 1 minute *iPerf* tests were performed for each inter-cluster mesh link (20 iterations in each direction of a link), the results volume consisted of: 40 iterations for 2 and 6 hops, respectively; 160 iterations for 3 and 5 hops, respectively; and 240 iterations of 4 hops. The iteration averages were evaluated for each hop length; and exponential and power regression analyses were conducted for the trend in average TH values with increasing hop length to obtain the R^2 coefficients. Table 14 shows the average TH values for each hop length and the R^2 coefficients obtained from the exponential and power regression analyses. A plot showing the declining trend of TH with increasing hop length along with exponential and regression trend lines for the trend is presented in Appendix A4, Figure A4.5.

Table 14: Average throughput and R^2 values obtained from UniFi results analysis
The table presents the average values for TH with increasing inter-cluster hop length; and the R^2 values for power and exponential regression of the trend in average TH values versus increasing hop length.

	Inter-cluster hop lengths					**R^2**	
	2-hops	**3-hops**	**4-hops**	**5-hops**	**6-hops**	**Exponential**	**Power**
TH average (Mbps)	48.26	38.83	29.11	24.94	20.63	**0.9899**	0.9862

In the case of RTL, RTJ, and PL%, VoIP traffic was sent for multiple flows, incrementing in prime numbers from 2 to 41, across the inter-cluster mesh links. It was mentioned in Section 3.2.5.2 that the choice of such sampling for VoIP flows was selective; and under the assumption that the network performance of one or all metrics will likely degrade past a certain number of flows and hop lengths. Since 20 iterations of 5 minute D-ITG tests were performed for each inter-cluster mesh link, the overall RTL, RTJ, and PL% results volume consisted of: 20 iterations for 2 and 6 hops, respectively; 80 iterations of 3 and 5 hops, respectively; and 120 iterations of 4 hops. Similar to TH, the average of number of iterations was evaluated for each hop length; and the exponential and power regression analyses were conducted for the trend in average RTL, RTJ, and PL% values with increasing hop length for each flow. The average RTL values for each flow over increasing hop length, and the R^2 coefficients obtained for exponential and power regression analyses of the RTL trends are presented in Table 15. The RTL values in Table 15 show an inclining trend representative of an increase in latency with an increase in hop length for each flow. Plots for each flow from 2 up to 41 showing the inclining trend of RTL with increasing hop length along with exponential and regression trend lines for RTL are presented in Appendix A4, Section A4.6.

Table 15: Average round-trip latency results from UniFi testbed

The table presents the average RTL values with increasing hop length for all prime numbered flows from 2 up to 41; and the R^2 values for power and exponential regression for the average values for each flow.

	Average RTL between each inter-cluster hop length (ms)					**R^2**	
Flows	**2-hop**	**3-hop**	**4-hop**	**5-hop**	**6-hop**	**Exponential**	**Power**
2	24.07	31.42	35.71	40.42	50.12	**0.9797**	0.9651
3	30.68	31.59	31.51	35.09	48.32	**0.7188**	0.5299
5	21.66	26.06	31.15	33.85	49.69	**0.9503**	0.8605
7	24.65	29.59	33.47	33.77	47.06	**0.9082**	08413
11	24.42	26.07	33.40	36.70	44.46	**0.9739**	0.8911
13	23.65	26.25	31.86	37.88	44.49	**0.993**	0.9129
17	20.83	25.33	31.31	37.90	50.31	**0.9945**	0.9195
19	21.42	24.61	33.79	37.86	47.69	**0.9823**	0.9281
23	28.45	29.01	37.74	39.12	48.24	**0.9338**	0.8368
29	21.07	29.29	44.40	48.22	60.78	0.9554	**0.9769**
31	24.69	29.80	51.06	51.74	67.94	**0.9309**	0.921
37	25.95	38.24	81.78	86.36	111.99	0.9177	**0.9491**
41	21.12	59.18	90.00	152.21	241.40	0.9665	**0.9908**

The average RTJ values for each flow over increasing hop length, and the R^2 coefficients obtained for exponential and power regression analyses are presented in Table 16. The RTJ values in Table 16 show an inclining trend representative of an increase in jitter with an increase in hop length for each flow. Plots for each flow from 2 up to 41 showing the inclining trend of RTJ with increasing hop length, along with exponential and regression trend lines, are presented in Appendix A4, Section A4.7.

Table 16: Average round-trip jitter results UniFi testbed

The table presents the average RTJ values with increasing hop length for all prime numbered flows from 2 up to 41; and the R^2 values for power and exponential regression for the average values for each flow.

	Average RTJ between each inter-cluster hop length (ms)					R^2	
Flows	**2-hop**	**3-hop**	**4-hop**	**5-hop**	**6-hop**	**Exponential**	**Power**
2	23.01	34.36	39.15	39.81	44.65	0.8212	**0.9486**
3	26.72	36.65	38.74	39.35	45.34	0.8319	**0.9297**
5	22.04	40.08	39.41	43.48	44.76	06583	**0.8354**
7	25.65	40.77	40.37	43.57	45.17	0.6797	**0.847**
11	25.63	33.45	41.65	44.05	45.20	0.8669	**0.9722**
13	23.25	34.42	41.40	44.09	44.89	0.8114	**0.9531**
17	17.60	30.72	40.90	44.40	45.06	0.8045	**0.9488**
19	20.02	30.37	41.42	44.49	45.53	0.8418	**0.9629**
23	20.55	31.77	42.58	44.90	45.94	0.8203	**0.9538**
29	19.11	34.58	44.06	45.64	47.17	0.759	**0.922**
31	20.27	35.65	44.39	45.53	47.02	0.7476	**0.9145**
37	19.34	38.10	46.02	47.12	47.80	06913	**0.8759**
41	18.72	39.57	46.45	50.20	53.56	0.7466	**0.9102**

The average PL% values for each flow over increasing hop length, and the R^2 coefficients obtained from exponential and power regression analyses are presented in Table 17. The PL% values in Table 17 do not show a consistent trend with increase in hop length for any flow. In addition, the average PL% for each flow does not even cross the recommended <1% requirement for one-way PL% for conversation voice (again, refer to Table 4). The low PL% is an indication that the UniFi devices manage to deliver data packets to the destination even though RTL and RTJ rise with increasing hop length and number of flows. Variable trends in PL%, latency and jitter can also be observed in Chissungo et al. (2012), who have stated that these kinds of variations are due to the nature of the medium, which is often unpredictable and even unstable. In Table 17, such an unpredictable spike in PL% can be observed for flows 37 and 41 at 5 hops and then drops to

<1% for 6 hops. Packet loss is a critical performance metric in VoIP communication because high packet loss will cause a call to break up, and too much of this will inevitably result in an incomprehensible conversation (Radman et al., 2010). It is noteworthy to mention that VoIP communication via IM applications such as Messenger, WhatsApp, Skype, and IMO have superseded traditional voice calling due to their cheaper cost (Farooq & Raju, 2019; Stork et al., 2017; Sujata et al., 2015). Therefore, for a WMN that aims to deliver VoIP services within the recommended QoS requirements, a packet loss scalability quantification is a necessity. Using the results of PL% presented in Table 17, the overall average PL% value for each hop length inclusive of all the flows was calculated. The total average PL% showed an inclining trend from hop length 2 to 5 as highlighted in Table 17. Therefore, exponential and power regression analyses were done for the total average PL% against an increasing number of inter-cluster hop lengths from 2 up to 5. A plot showing the inclining trend of total average PL% with increasing hop length, along with exponential and regression trend lines, is presented in Appendix A4, Section A4.8.

Table 17: Average packet loss percentage results for the UniFi testbed

The table shows the average PL% values for a number of flows with increasing number of hop lengths. It can be observed that the PL% varied and stayed <1% for almost all flows over increasing number of hops. In fact, the results are shown up to three decimal place to show the PL%. However, the 6 hop numbers appear as outliers.

	Average PL% between each inter-cluster hop length (%)					R^2	
Flows	**2-hop**	**3-hop**	**4-hop**	**5-hop**	**6-hop**	**Exponential**	**Power**
2	0.386	0.390	0.075	0.262	0.000		
3	0.660	0.354	0.114	0.170	0.000		
5	0.070	0.312	0.225	0.308	0.000		
7	0.094	0.047	0.100	0.135	0.140		
11	0.000	0.051	0.018	0.511	0.000		
13	0.004	0.061	0.048	0.209	0.000		
17	0.018	0.042	0.021	0.148	0.000		
19	0.000	0.055	0.052	0.100	0.000		
23	0.358	0.083	0.187	0.102	0.000		
29	0.060	0.171	0.144	0.336	0.47		
31	0.296	0.191	0.514	0.208	0.06		
37	0.412	0.282	0.604	1.733	0.21		
41	0.066	0.592	0.901	7.949	0.365		
	0.186	0.202	0.231	0.936	0.096	**0.7092**	0.5415
	Total average PL%						

The next section presents the formation of empirical equations for each performance metric using the higher of the two R^2 coefficients.

4.1.2.2 Performance metric quantification

This section presents the details of equation formation for TH, RTL, RTJ, and PL%, respectively; using the actual values obtained from UniFi testbed experiments. As mentioned in Section 3.2.6, exponential and power regression analysis techniques were used for data analysis. Equations to represent performance trends were evaluated for each KPM using the regression technique with the higher R^2 coefficient. In the case of TH, the R^2 coefficient of determination was evaluated for the exponential and power regression of the average TH with increasing hop lengths from 2 up to 6, as shown in Table 14. In the case of RTL and RTJ, the R^2 coefficients of determination were evaluated for exponential and power regression of the average values for each flow from 2 up to 41 with increasing hop lengths from 2 up to 6, as shown in Table 15 and Table 16, respectively. In the case of PL%, the R^2 coefficient was evaluated for exponential and power regression of the total average PL% against increasing inter-cluster hop length from 2 up to 5, as shown in Table 17. The performance trend equations for each network metric were formed for the regression technique with higher R^2 coefficient.

1. Formulation process of throughput results

In the case of TH, the R^2 value of exponential regression (R^2 = 0.9889) was higher than the value of power regression (R^2 = 0.9668), as shown in Table 14. Thus, based on the higher R^2 value, the exponential regression Equation 4.9 was evaluated to represent the throughput trend with increasing hop length between source and destination in two separate mesh clusters. In Equation 4.9, T_u is throughout, N is the hop length and subscript u is used to represent the UniFi unit.

$$T_u = 58.72 \cdot e^{-0.21N} \quad 4.9$$

It is noteworthy to mention that Equation 4.9 is formed by the regression analysis function of TH values from $N = 2$ in the UniFi results shown in Table 14. The value of 58.72 in Equation 4.9 is a constant obtained from the regression analysis of the overall results of UniFi testbed experiments and will be different for TH results with increasing number of hop lengths for results from different WMNs. For example, if the value of 58.72 is replaced by value of TH for $N = 1$ called T_1, then for T_u to be equal to T_1 for $N = 1$, $e^{-0.21N}$ will have to equal 1. However, this is not possible because e, also known as Euler's number, is a constant with the approximate value of 2.7183. Therefore,

$e^{-0.21N} \neq 1$ for $N = 1$, and hence, $T_1 \cdot e^{-0.21N} \neq T_u$ for $N = 1$. This is unlike the power trend equation where the TH value (or any other performance metric) of the first-hop from any WMN could be used with the power slope to predict the performance with increasing hop length. Thus, Equation 4.9 implies that TH values for $N = 2, 3, 4, \ldots, x,$ cannot be predicted using the TH value of $N = 1$ for all WMNs. In order for Equation 4.9 to be able to predict the exponential TH performance trend with increasing hop-length, Equation 4.9 is converted into Equation 4.10, where T_1 is the measured TH value over first hop and N is the hop length. In in Equation 4.10, a constant value of 1 is subtracted from hop length, N, to yield the TH value, T_u, of a particular hop length, N, between source and destination; because by doing such makes the prediction of T_u dependent on the value of T_1.

$$T_u = T_1 \cdot e^{-0.21(N-1)} \qquad 4.10$$

A comparison of predicted TH using Equation 4.10 against the actual values obtained from the UniFi testbed was conducted to show the closeness of the predicted trend to actual results. The reference T_1 value used in Equation 4.10 to predict the trend was 59.53Mbps. The T_1 value for $N = 1$ was calculated using the TH value for $N = 2$ from the UniFi results in Table 14; and using the substitution method with Equation 4.10 as shown in Section A5.2, Appendix A5. The comparison of predicted TH using Equation 4.10 with T_1 = 59.53Mbps, and the average of results from UniFi TH experiments presented in Table 14 is presented in Figure 20.

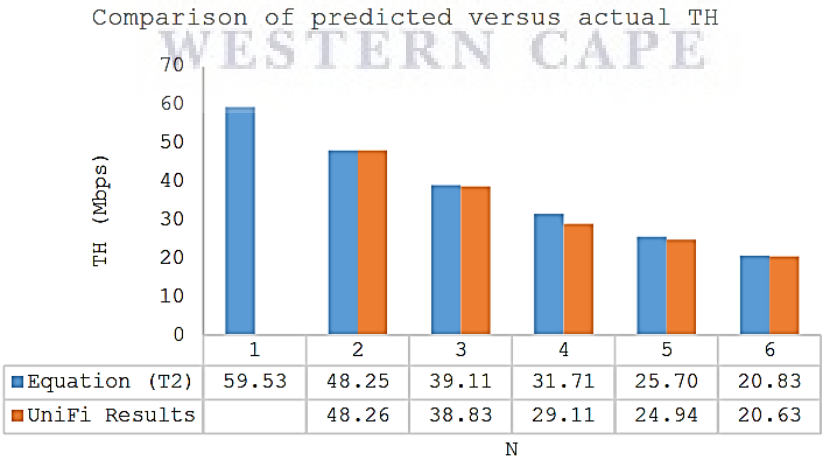

Figure 20: Actual versus predicted throughput values in the UniFi testbed

The figure shows the comparison between TH values predicted using Equation 4.10 and actual TH values obtained from the UniFi results in Table 14.

The closeness between the predicted TH values and actual TH results shown in Figure 20 provides proof for further usage of Equation 4.10 to predict capacity with increasing hop length.

It is noteworthy to mention that the literature review could not find related work investigating TH capacity modelling using different types of regression analysis trends. The TH capacity modelling related work of Gupta et al. (2001), Li et al. (2002) and Johnson (2007a) have stuck to power trend models; and did not consider other types of trend models that could better fit the TH results obtained. Regression analysis of the TH results obtained from UniFi testbed experiments with increasing hop length indicate that there are best-fit regression trends other than power trend that can represent the performance trend more accurately. The approach to formulation of Equation 4.10 provided a framework for RTL, RTJ, and PL% results formulation, in case an exponential trend was observed.

The next section presents a technique to unify the RTL results for flows 2 up to 41 with increasing inter-cluster hop length from 2 up to 6.

2. Formulation process of round-trip latency results

In the case of formulation of RTL results, as shown in Table 15, equations were formulated for each flow from 2 up to 41. Between exponential and power regression analyses of the RTL results, equations were formulated for the regression trend with the higher R^2 coefficient which were shown in Table 15. The equation for each prime number of flows is presented in Table 18.

Table 18: Round-trip latency equations of the Unifi testbed

The table shows the RTL equations for each flow to represent RTL trends with increasing number of hop lengths. In case of flows 2 to 31, exponential regression yielded a higher R^2 coefficient. In case of flows 29, 37, and 41, power regression yielded higher a R^2 coefficient (see Table 15).

Exponential equation			Power equations	
Flow	**Equation**		**Flow**	**Equation**
2	$L_u = 21.07 \cdot e^{0.17N}$		29	$L_u = 20.28 \cdot N^{0.66}$
3	$L_u = 25.75 \cdot e^{0.1N}$		37	$L_u = 24.29 \cdot N^{0.95}$
5	$L_u = 17.53 \cdot e^{0.19N}$		41	$L_u = 20.6 \cdot N^{1.47}$
7	$L_u = 21.48 \cdot e^{0.14N}$			
11	$L_u = 20.30 \cdot e^{0.15N}$			
13	$L_u = 19.6 \cdot e^{0.16N}$			
17	$L_u = 16.5 \cdot e^{0.22N}$			
19	$L_u = 17.25 \cdot e^{0.2N}$			
23	$L_u = 23.84 \cdot e^{0.14N}$			
31	$L_u = 19.43 \cdot e^{0.26N}$			

The equations in Table 18 show that (a) the best-fit trend for RTL results of flows 2 to 31 are of exponential type; and (b) the best-fit trend for RTL results of flows 29 to 41 are of power type. In the equations in Table 18, L_u is the RTL, and N is the inter-cluster hop length. In order to yield single RTL equations, to represent overall RTL performance with increase in hop length for any number of flows, the equations presented in Table 18 were combined in two ways.

2.1.Unification process of exponential latency equations

With reference to Table 18, in order to make L_u in the exponential equations for flows 2 up to 31, dependent on the value of $N = 1$, a similar approach to the formation of Equation 4.10 was adopted. Therefore, 1 was subtracted from N in the power of the exponent of equations for flows 2 up to 31; and the new equations are presented in Table 19.

Table 19: Exponential equations for round-trip latency for each numbers of flows
The table shows the transformed exponential equation for flows 2 to 31 such that the trend equations become dependent on L_1.

Exponential equations	
Flow	**Equation**
2	$L_u = L_1 \cdot e^{0.17(N-1)}$
3	$L_u = L_1 \cdot e^{0.1(N-1)}$
5	$L_u = L_1 \cdot e^{0.19(N-1)}$
7	$L_u = L_1 \cdot e^{0.14(N-1)}$
11	$L_u = L_1 \cdot e^{0.15(N-1)}$
13	$L_u = L_1 \cdot e^{0.16(N-1)}$
17	$L_u = L_1 \cdot e^{0.22(N-1)}$
19	$L_u = L_1 \cdot e^{0.2(N-1)}$
23	$L_u = L_1 \cdot e^{0.14(N-1)}$
31	$L_u = L_1 \cdot e^{0.26(N-1)}$

Before combining the modified exponential equations in Table 19 to yield a singular exponential RTL equation, a comparison of the predicted RTL trends using the equations in Table 19 against the average RTL values of the UniFi testbed, for the respective flows presented in Table 15, was conducted to examine the closeness between results. A reference L_1 for $N = 1$ was calculated using the RTL value for $N = 2$ of each flow using the RTL results in Table 15; using the substitution method presented in Section A5.2, Appendix A5. The substitution method was applied to each exponential equation shown in Table 19 to calculate the L_1 for each flow. The L_1

value for each flow is listed in Table 20. The comparison of the actual average RTL results obtained from UniFi experiments, as presented in Table 15, against the predicted RTL exponential trend, for each flow count is presented in Table 20.

Table 20: Actual versus predicted round-trip latency values for the UniFi testbed (exponential)
The table shows the comparison between predicted and actual values of RTL. The L_1 used by the equations was calculated using the RTL value for N = 2 obtained from the UniFi results.

		RTL (ms) with increasing hop length									
	L_1	2-hop		3-hop		4-hop		5-hop		6-hop	
Flows ↓		Act.*	Pred.**	Act.	Pred.	Act.	Pred.	Act.	Pred.	Act.	Pred.
2	20.31	24.07	24.07	31.42	28.53	35.71	33.82	40.42	40.09	50.12	47.52
3	27.76	30.68	30.68	31.59	33.91	31.51	37.47	35.09	41.41	48.32	45.77
5	17.91	21.66	21.66	26.06	26.19	31.15	31.67	33.85	38.30	49.69	46.31
7	21.43	24.65	24.65	29.59	28.35	33.47	32.62	33.77	37.52	47.06	43.15
11	21.02	24.42	24.42	26.07	28.37	33.40	32.97	36.70	38.30	44.46	44.50
13	20.16	23.65	23.66	26.25	27.76	31.86	32.58	37.88	38.23	44.49	44.87
17	16.72	20.83	20.83	25.33	25.96	31.31	32.35	37.90	40.31	50.31	50.23
19	17.53	21.42	21.41	24.61	26.15	33.79	31.94	37.86	39.01	47.69	47.65
23	24.73	28.45	28.45	29.01	32.72	37.74	37.64	39.12	43.29	48.24	49.80
31	19.04	24.69	24.69	29.80	32.03	51.06	41.54	51.74	53.87	67.94	69.86
Pred.* = Predicted; Act.** = Actual					Actual				Predicted over		
									Predicted under		

The comparison in Table 20 shows that predicted and actual RTL values for 2 hops are same for all flows because the actual value of 2 hops was used to calculate the L_1 for each flow. The differences between predicted and actual RTL values from 3 hops onwards can be noticed in Table 20. The differences between predicted and actual RTL values for each flow from hop length 3 up to 6 are presented in Table A4.3, Section 0, Appendix A4. The differences between actual and predicted RTL values is logical because an equation predicts network performance based on the equation parameters and the results will be estimates in between actual values. If the volume of overall results from 3 to 6 hops, as shown in Table 20, is considered for each flow, then out of 40 predicted RTL values, 62.5% are over (between 0-6ms), and 37.5% are under (between 0-9ms) the actual RTL values. In fact, there was only one case of 31 flows over 4 hops (see Table 20) where the predicted RTL value was under the actual value by 9.52ms. Otherwise, the prediction of RTL values below the actual values ranged approximately between 0-4ms. Since a research gap highlighted the lack of quantification of RTL results with increasing hop length, the network

scalability quantification process progressed with the unification of exponential equations for flows 2 up to 31, as shown in Table 19, based on (a) the exhibited closeness between predicted and actual RTL results, respectively; and (b) the majority of predictions being over the actual RTL. In order to unify the equations, firstly, the average of values of constant *x* in $e^{x(N-1)}$ in the equations shown in Table 19 was evaluated. The average of *x* was calculated to be *0.17*. Secondly, the singular Equation 4.11 is formulated to represent the exponential RTL trend where ε_u is the RTL for exponential regression; L_1 is the average RTL measured over the first hop pairs in a WMN; and *N* is the hop length between mesh nodes.

$$\varepsilon_u = L_1 \cdot e^{0.17(N-1)} \quad 4.11$$

The next subsection presents the unification process of power equation of flows 29, 37, and 41.

2.2.Unification process of power latency equations

With reference to Table 18, the power equations of flows 29, 37, and 41 exhibited inclining trends in powers of *N* with an increase in number of flows. Firstly, the power trend Equation 4.12 is assumed where ϕ_u is the RTL behavior exhibiting a power regression type trend with increasing hop length *N* between mesh nodes; *X* is the power trend; and L_1 is the average RTL measured over first hop pairs.

$$\phi_u = L_1 \cdot N^X \quad 4.12$$

Secondly, two techniques were devised to yield an equation to represent the trend for flows 29, 37, and 41.The techniques used to determine X in N^X is presented as follows:

Technique 1: In this technique, the value *X* was evaluated using equations of flows 29, 37, and 41 as follows:

$$If\ N^X = \frac{(N^{0.66} + N^{0.95} + N^{1.47})}{3}; then$$

$$X = (\frac{\log(N^{0.66} + N^{0.95} + N^{1.47})}{3})/\log N \quad 4.13$$

Using this technique, there will be a different value *X* for each $N > 1$. The relationship between *N* and *X* was plotted for $N = 2$ to 1000 to find an equation to represent the relationship between *N* and *X*. Such an unrealistic range for *N* was chosen for the plot to flatline the inclining values of *X*. The trend for *X* with increasing *N* is shown in Figure 21.

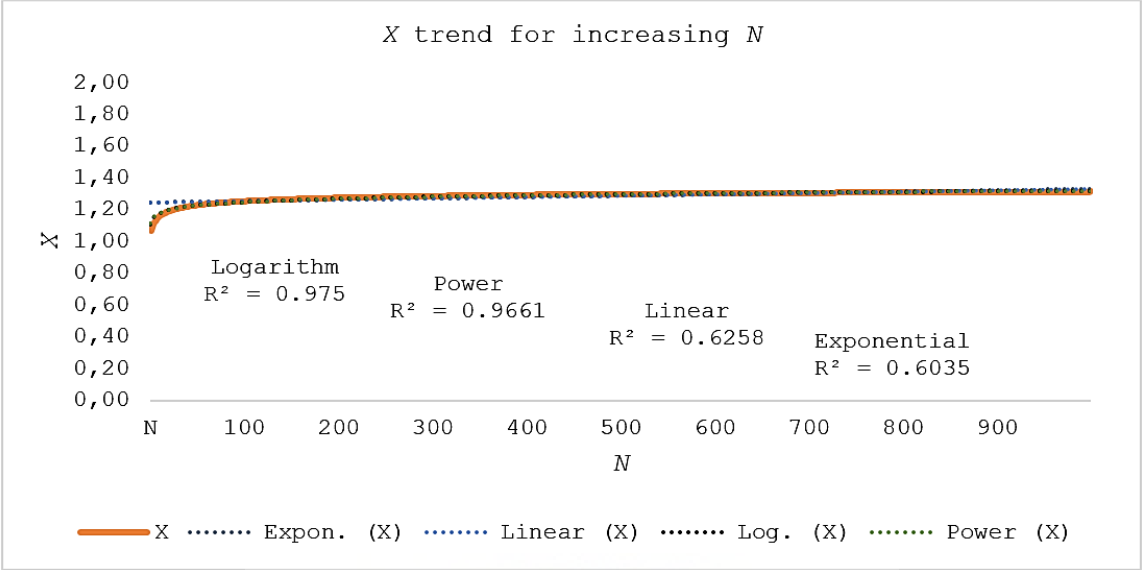

Figure 21: Relationship between X and N for technique 1 of latency unification for UniFi testbed
The figure shows a plot for N = 2 to 1000 versus values of X evaluated from Equation 4.13. The different R^2 values for each regression technique are shown in the figure.

Even though Equation 4.13 is logarithmic, the trend of *X* was further evaluated for best-fit against linear, exponential, logarithmic, and power regression techniques. The results showed that the logarithm relation between *N* and *X* had the highest R^2 value, and yielded Equation 4.14 for the relationship.

$$X = 0.031 \cdot \ln(N) + 1.11 \qquad 4.14$$

Technique 2: In this technique, the average of *X* in the power equations of flows 29, 37, and 41 in Table 15 was evaluated to give N^X as follows:

$$N^X = N^{(0.66+0.95+1.47)/3}$$

$$Thus, N^X = N^{1.03}, and\ X = 1.03$$

Therefore, the final value of power *X* in N^X could either be the one obtained from Technique 1 Equation 4.14, or from Technique 2 (*X = 1.03)*. Therefore, the performance of Equation 4.12 representing ϕ_u was calculated against increasing *N* for *X* obtained from techniques 1 and 2, respectively, to narrow the choice of *X*. To calculate predicted values using Equation 4.12, the reference L_1 value was calculated using the substitution method (shown in Section A5.2, Appendix A5) for flows 29, 37, and 41 using their respective average RTL values for *N = 2* for 2 flows as presented in Table 15. In Table 21, the actual average RTL values for flows 29, 37, and 41, as shown in Table 15, are shown against the predicted RTL values using Equation 4.12 for *X*

evaluated from techniques 1 and 2, respectively. Since, RTL of $N = 2$ for flows 29, 27, and 41 was used to obtain L_1 value for each respective flow, the predicted values for $N = 2$ by technique 1 and technique 2 was the same. However, the difference between actual and predicted values from techniques 1 and 2, respectively, for flows 29, 37, and 41 was quite significant for hop lengths 3 up to 6. The difference between actual and predicted values presented in Table 21 is evidence of the fact that analytical prediction using models yields ideal results, and does not consider the unpredictable and unstable nature of a mesh environment.

Table 21: Actual versus predicted round-trip latency values of UniFi for techniques 1 and 2
The table shows the comparison between actual and predicted values of RTL for flows 23, 37, and 41 with increasing hop length using techniques 1 and 2, respectively. The table shows the values of technique 1 being closer to actual RTL values than technique 2. However, the results show that high number of flows really test the hardware and link quality past 2 hops.

	Flows ↓	**ϕ_u with increasing hop length, *N***					
		L_1	2	3	4	5	6
Actual	29		21.07	29.29	44.40	48.22	60.78
	37		25.95	38.24	81.78	86.36	111.99
	41		21.12	59.18	90.00	152.21	241.40
Technique 1	29	9.62	21.07	33.80	47.56	62.20	77.63
	37	11.84	25.95	41.63	58.57	76.60	95.61
	41	9.64	21.12	33.89	47.68	62.36	77.83
Technique 2	29	10.32	21.07	31.99	43.03	54.14	65.33
	37	12.71	25.95	39.40	52.99	66.68	80.46
	41	10.34	21.12	32.07	43.14	54.28	65.50

Considering the case of real world deployment of WMNs, where the network conditions cannot be controlled, power of X obtained from technique 1, shown as Equation 4.14, was selected. By using X obtained from technique 1, Equation 4.12 predicted values closer to the actual values than with X obtained from technique 2. Therefore, for WMNs using UniFi or UniFi-like network setup, Equations 4.11 and 4.12 are amalgamated to give a unified Equation 4.15 where L_u is the RTL with increasing hop length N. During usage of L_u, the value L_1 will be the average of RTL measured over first hop pairs in a WMN.

$$L_u = (\varepsilon_u + \phi_u)/2 \qquad 4.15$$

The next section presents the process adopted to unify the RTJ results for flows 2 up to 41 with increasing inter-cluster hop length from 2 up to 6.

3. Formulation process of jitter results

In the case of RTJ, equations were also formulated for each flow from 2 up to 41. Between exponential and power regression, equations were formulated for regression analysis with the higher R^2 coefficient. As observed in Table 16, the R^2 coefficient obtained for power regression was higher than exponential regression for all flows. Therefore, equations were formulated for power regression to represent the RTJ trend for each number of flows with increasing hop length. The equations are presented in Table 22 where J_u is the RTJ, and N is the hop length between source and destination mesh devices.

Table 22: Jitter equations of regression trends

The table shows the actual and converted power trend equations for each flow to represent RTJ trend with increasing number of hop lengths. In addition, an equation number column is as added for further reference to the text below.

	Power Regression Equations		
Flows	**Actual**	**Converted**	**Equation number**
2	$J_u = 24.23 \cdot N^{0.39}$	$J_u = J_1 \cdot N^{0.39}$	1
3	$J_u = 27.71 \cdot N^{0.3}$	$J_u = J_1 \cdot N^{0.3}$	2
5	$J_u = 24.65 \cdot N^{0.42}$	$J_u = J_1 \cdot N^{0.42}$	3
7	$J_u = 27.9 \cdot N^{0.33}$	$J_u = J_1 \cdot N^{0.33}$	4
11	$J_u = 26.06 \cdot N^{0.33}$	$J_u = J_1 \cdot N^{0.33}$	5
13	$J_u = 24.43 \cdot N^{0.42}$	$J_u = J_1 \cdot N^{0.42}$	6
17	$J_u = 18.91 \cdot N^{0.61}$	$J_u = J_1 \cdot N^{0.61}$	7
19	$J_u = 20.77 \cdot N^{0.54}$	$J_u = J_1 \cdot N^{0.54}$	8
23	$J_u = 21.56 \cdot N^{0.52}$	$J_u = J_1 \cdot N^{0.52}$	9
29	$J_u = 20.98 \cdot N^{0.57}$	$J_u = J_1 \cdot N^{0.57}$	10
31	$J_u = 22.23 \cdot N^{0.53}$	$J_u = J_1 \cdot N^{0.53}$	11
37	$J_u = 21.93 \cdot N^{0.56}$	$J_u = J_1 \cdot N^{0.56}$	12
41	$J_u = 21.18 \cdot N^{0.64}$	$J_u = J_1 \cdot N^{0.64}$	13

The formulation of power trend equations yielded constants that are multiplied by slope N^x to predict the performance trend with increasing N. Since the formulation by the software tool had input value of $N = 2$ as $N = 1$, if the value of N in equations in Table 22 is substituted to 1, then it should give the RTJ value for $N = 2$ obtained for the RTJ UniFi results in Table 16, but such is not

the case. This is because the constant value in each equation for each flow in Table 22 is an output of the regression equation evaluation using the regression analysis of overall results. In addition, the equations should use the value of RTJ measured for $N = 1$ to predict the performance trend for $N > 1$. Therefore the constants in equations in Table 22 are substituted with variable J_1 to represent the RTJ measured over the first hop length under the assumption that RTJ for $N > 1$ depends on J_1; and the trend slope (the power) remains the same. The converted equations for each flow and equation number for further evaluations are also presented in Table 22 under the heading 'Converted'.

In order to unify the converted power equations for RTJ presented in Table 22, the power of N in each equation of each flow was taken into consideration. In order to decide the unified power for N, the equation of each flow was treated using techniques 1 and 2 that were devised for RTL directly above. The unified power trend Equation 4.16 is offered where J_u is the RTJ behaviour exhibiting a power regression type trend with increasing hop length N between mesh nodes; X is the power trend; and J_1 is the average RTJ measured over first-hop pairs.

$$J_u = J_1 \cdot N^X \tag{4.16}$$

The usage of the two techniques is described as follows:

Technique 1: In this technique, the value X in N^X was evaluated using the equations of each flow in Table 23. Since there are 13 RTJ equations in Table 22, one for each number of flows, let the powers of N in the converted equations in Table 22 be represented by variable Y_n where Y is the power and n is equation number (1, 2, 3, 4, …., 13). Therefore, Y_1 represents the power of N for equation number 1, Y_2 represents the power of N for equation number 2, and so on. The equation numbers (starting with one) are shown in Table 22. Therefore:

$$If\ N^X = \frac{\sum_{i=Y_1}^{Y_{13}} (N^i)}{3}\ ; then$$

$$then, X = \left(\frac{\log\left(\sum_{i=Y_1}^{Y_{13}} (N^i)\right)}{3}\right)/\log N \tag{4.17}$$

Using technique 1, there will be a different value X for each $N > 1$. The relationship between N and X was plotted for $N = 2$ up to 1000 to find an equation to represent the relationship between N and X. Such an unrealistic range for N was chosen for the plot to flatline the inclining values of X. The trend for X with increasing N is shown in Figure 22.

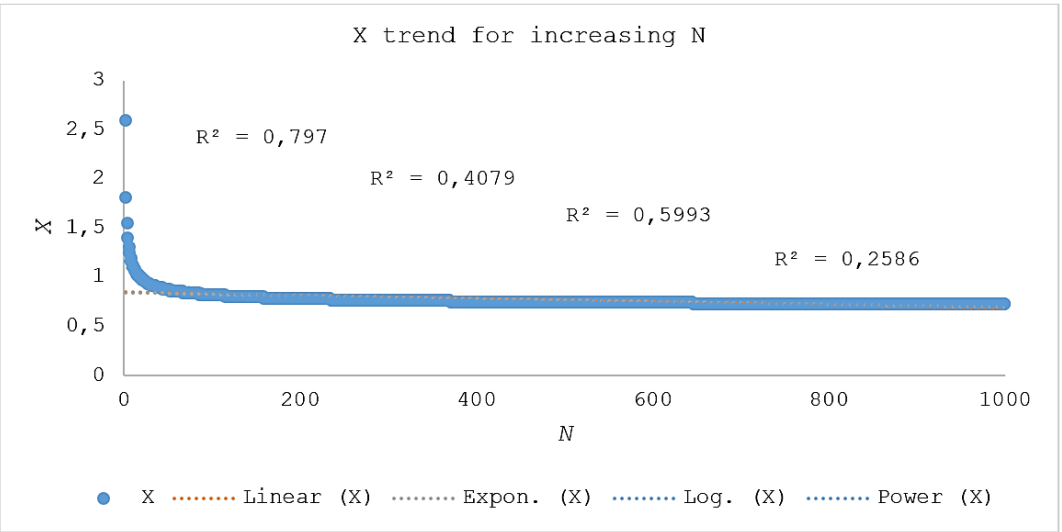

Figure 22: Relationship between X and N for technique 1 of jitter unification for UniFi testbed
The figure shows a plot for N = 2 to 1000 versus values of X evaluated from technique 1. The different R^2 values for each regression technique is shown on the figure.

The trend of *X* was further evaluated for best-fit against linear, exponential, logarithmic, and power regression techniques. The results showed that the power regression between *N* and *X* had the highest R^2 value, and therefore Equation 4.18 was evaluated to represent *X*.

$$X = 1.23 \cdot N^{-0.081} \quad 4.18$$

Therefore, the result of *X* in Equation 4.18 was substituted in Equation 4.16, which yielded Equation 4.19.

$$J_u = L_1 \cdot N^{1.23 \cdot N^{-0.081}} \quad 4.19$$

A comparison was conducted between the average RTJ results from the UniFi testbed experiments in Table 16 with the predicted values using Equation 4.19 from technique 1, to analyse the closeness between actual and predicted values. Firstly, using the converted power equations in Table 22, a reference value for J_1 for $N = 1$ was calculated in order to predict the RTJ trend for each flow count with increasing hop length. Secondly, the reference J_1 value for $N = 1$ for each flow was calculated using the RTJ value for $N = 2$ of each flow from the RTJ results in Table 16; and using the substitution method with each converted equation in Table 22. The calculated J_1 for each flow and the comparison between actual and predicted RTJ values are presented in Table 23.

Table 23: Comparison of actual with predicted values of round-trip jitter from technique 1

The table shows the comparison between actual and predicted values of RTJ for all flows with increasing hop length using X obtained from technique 1.

	RTJ (ms) with increasing hop length										
	J_1	2		3		4		5		6	
Flows ↓		**Act.****	**Pred.***	**Act.**	**Pred.**	**Act.**	**Pred.**	**Act.**	**Pred.**	**Act.**	**Pred.**
2	10.28	23.01	23.01	34.36	35.38	39.15	47.18	39.81	58.41	44.65	69.13
3	11.94	26.72	26.72	36.65	41.09	38.74	54.79	39.35	67.84	45.34	80.29
5	9.84	22.04	22.04	40.08	33.88	39.41	45.18	43.48	55.94	44.76	66.21
7	11.46	25.65	25.65	40.77	39.44	40.37	52.59	43.57	65.12	45.17	77.06
11	11.45	25.63	25.63	33.45	39.42	41.65	52.56	44.05	65.09	45.20	77.02
13	10.38	23.25	23.25	34.42	35.74	41.40	47.66	44.09	59.01	44.89	69.84
17	7.86	17.60	17.60	30.72	27.06	40.90	36.09	44.40	44.68	45.06	52.88
19	8.94	20.02	20.02	30.37	30.77	41.42	41.04	44.49	50.81	45.53	60.14
23	9.18	20.55	20.55	31.77	31.60	42.58	42.13	44.90	52.17	45.94	61.74
29	8.54	19.11	19.11	34.58	29.38	44.06	39.18	45.64	48.52	47.17	57.42
31	9.06	20.27	20.27	35.65	31.17	44.39	41.57	45.53	51.47	47.02	60.92
37	8.64	19.34	19.34	38.10	29.73	46.02	39.65	47.12	49.09	47.80	58.10
41	8.36	18.72	18.72	39.57	28.78	46.45	38.38	50.20	47.52	53.56	56.25
Pred.* = Predicted. Act.** = Actual.				Actual ≈ Predicted				Predicted over actual value			
								Predicted under actual			

Technique 2: In this technique, the average of X in N^X of the power equations of each flow count presented in Table 22 was evaluated as follows. Since there are 13 equations of RTJ, one for each number of flows, let the powers of N in the converted equations in Table 22 be represented by variable Y_n where Y is the power and n is a number (1, 2, 3, 4, …., 13) for each equation shown in Table 22. Therefore, Y_1 represents the power of N for equation number 1, Y_2 represents the power of N for equation number 2, and so on. Therefore, the average of powers of N from Y_1 to Y_{13} was calculated as shown in Equation 4.20.

$$N^X = N^{(\sum_{i=Y_1}^{Y_{13}}(Y_i))/3} \qquad 4.20$$

$$thus, N^X = N^{0.48}, and\ X = 0.48$$

Therefore, the result of X = 0.48 was substituted in Equation 4.16 to yield Equation 4.21.

$$J_u = L_1 \cdot N^{0.47} \qquad 4.21$$

A comparison was conducted between the average RTJ results of the UniFi testbed, presented in Table 16, with RTJ values predicted using Equation 4.21 from technique 2 to analyse the closeness

between actual and predicted values. Similarly to technique 1, firstly, using the converted power equations in Table 22, a reference value for J_1 for $N = 1$ was calculated in order to predict RTJ trends for each flow count with increasing hop length. The reference J_1 value for $N = 1$ was calculated using the RTJ value for $N = 2$ of each flow from the RTJ results in Table 16; using the substitution method with each converted equation in Table 22. The calculated J_1 for each flow and the comparison between actual and predicted RTJ values is presented in Table 24.

Table 24: Comparison of actual with predicted values of round-trip jitter using technique 2
The table shows the comparison between actual and predicted values of RTJ for all flows with increasing hop length using X obtained from Technique 2.

	RTJ (ms) with increasing hop length										
	J_1	2		3		4		5		6	
Flows ↓		Act.**	Pred.*	Act.	Pred.	Act.	Pred.	Act.	Pred.	Act.	Pred.
2	16.61	23.01	23.01	34.36	27.84	39.15	31.87	39.81	35.40	44.65	38.56
3	19.29	26.72	26.72	36.65	32.33	38.74	37.02	39.35	41.11	45.34	44.79
5	15.91	22.04	22.04	40.08	26.66	39.41	30.52	43.48	33.90	44.76	36.93
7	18.52	25.65	25.65	40.77	31.03	40.37	35.53	43.57	39.46	45.17	42.99
11	18.51	25.63	25.63	33.45	31.02	41.65	35.51	44.05	39.43	45.20	42.96
13	16.78	23.25	23.25	34.42	28.13	41.40	32.20	44.09	35.76	44.89	38.96
17	12.71	17.60	17.60	30.72	21.30	40.90	24.38	44.40	27.08	45.06	29.50
19	14.45	20.02	20.02	30.37	24.22	41.42	27.72	44.49	30.79	45.53	33.54
23	14.84	20.55	20.55	31.77	24.86	42.58	28.46	44.90	31.61	45.94	34.44
29	13.80	19.11	19.11	34.58	23.12	44.06	26.47	45.64	29.40	47.17	32.03
31	14.64	20.27	20.27	35.65	24.53	44.39	28.08	45.53	31.19	47.02	33.98
37	13.96	19.34	19.34	38.10	23.40	46.02	26.78	47.12	29.75	47.80	32.41
41	13.52	18.72	18.72	39.57	22.65	46.45	25.93	50.20	28.80	53.56	31.37

Pred.* = Predicted.
Act.** = Actual.

Predicted over actual value

Predicted under actual value

The comparisons in Table 23 and Table 24 showed that while using X obtained from technique 1, Equation 4.16 predicted results closer to the actual RTJ values than with X obtained from technique 2. In fact, it can be observed in Table 24 that the predicted results with increase in traffic flow and number of hops are consistently lower than the actual results, with the difference getting larger with increasing number of flows and hop length. In contrast, in Table 23, the predicted RTJ values are (a) mostly over the actual RTL values, and (b) approximately equal to the actual values for some flows (highlighted in Table 23). Therefore, the X obtained from technique 1 was selected to represent the power of N in the unified RTJ power equation under the

assumption that given the unpredictable nature of the wireless medium as mentioned by Chissungo et al. (2012); and the declining trend in jitter with an increase in hop length as observed in UniFi results and related work of Chissungo et al. (2012) and Castro et al. (2007), it is logical to predict WMN jitter performance over the actual results. Using this for deployment design can aid in preventing performance issues during and after the initial deployment of the WMN; and post-deployment, the WMN can be redesigned based on the actual measured results. The unified RTJ equation is presented via Equation 4.22 where J_1 is the RTJ measured over first-hop, N is hop length between source and destination, and J_u is RTJ for the respective N.

$$J_u = J_1 \cdot N^X; \; where \; X = 1.23 \cdot N^{-0.081} \quad 4.22$$

4. Formulation process of packet loss

In the case of PL%, as highlighted in Table 17, the values did not show a consistent trend with increase in hop length for any number of flows. However, total average PL% for each flow count showed an inclining trend from hop length 2 to 5. Therefore, exponential and power regression analyses were done for the total average PL% against the increasing number of inter-cluster hop lengths from 2 up to 5. The regression analysis showed that the R^2 of exponential regression (R^2 = 0.7092) was higher than power regression (R^2 = 0.5415), as shown in Table 17. Thus, based on the higher R^2 value, the exponential regression Equation 4.23 was evaluated to represent the PL% trend.

$$P_u = 0.087 \cdot e^{0.5N} \quad 4.23$$

Applying the similar technique adopted during formation of Equation 4.10 for TH, Equation 4.23 was converted to Equation 4.24 where P_1 is the average of PL% over the first hop pairs in a WMN testbed or a live network; and N is the hop count.

$$P_u = P_1 \cdot e^{0.5(N-1)} \quad 4.24$$

In Equation 4.24, a constant value of 1 is subtracted from hop length, N, to predict the PL% value, P_u, over a particular hop length between source and destination using the value of P_1. A comparison of predicted P_u using Equation 4.24 against the actual average PL% values obtained from UniFi testbed results was conducted to analyse the difference between the predicted and the actual trends. The reference P_1 values used for Equation 4.24 to predict the trend was calculated using the average PL% value for $N = 2$ from UniFi results in Table 17, and using the substitution method

presented in Section A5.2, Appendix A5. The comparison of predicted PL% using Equation 4.24, and the average PL% results of actual results shown in Table 17 is presented in Figure 23. The comparison in Figure 23 shows that Equation 4.24 mostly predicted values over the actual average PL% values with increasing hop length.

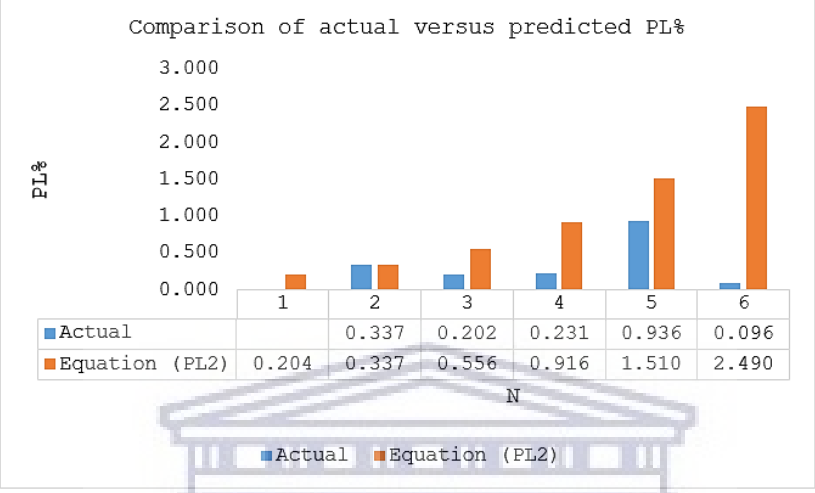

Figure 23: Actual versus predicted packet loss values obtained from UniFi testbed experiments
The figure shows the comparison between predicted PL% values using Equation 4.24 and actual average PL% values obtained from the UniFi results.

It is of significance to mention that the results of PL% were obtained from network emulation experiments that used actual hardware used in the field. The experimental results from network emulation are considered close to reality, and the observations are directly applicable to real situations (Beuran, 2012). Therefore, due to the inconsistent PL% results obtained from experiments over UniFi testbed, this study chose Equation 4.24 for prediction of PL% with increasing hop lengths for designing WMNs. Using this equation to design a WMN can aid in preventing performance issues during and after the initial deployment of the WMN, and it can be redesigned based on the actual measured results post-deployment.

Therefore, the scalability quantification process resulted into two sets of equations for each of the TH, RTL, RTJ and PL% metrics. Equations 4.2, 4.4, 4.6 and 4.8 were formed using average results of TH, RTL, RTJ, and PL%, respectively, of the MPv2 testbed. Equations 4.10, 4.15, 4.22 and 4.24 were formed using the average results of TH, RTL, RTJ, and PL%, respectively, of the UniFi testbed. In Section 5.1.3, discussion of network scalability quantification results is presented. The next section presents the smartphone battery consumption results.

4.2 Smartphone battery consumption

This section reports the results from the battery consumption experiments conducted using LeSs. The smartphone battery consumption experiments firstly investigated the efficiency of using Wi-Fi in LeSs to maximize charge life. Given the presence of CWMN in a low-income rural community, LeS adoption and usage can be promoted via efficient battery management by using Wi-Fi as the primary mode of communication. Secondly, CWMN users can achieve even more efficient battery management by using the least battery consuming social communication applications. Section 2.3.2 showed that Wi-Fi consumes less battery in smartphones as compared to 2G, 3G and BT. In light of that related work, the first phase of smartphone battery consumption experiments, referred to as wireless technology evaluation in Section 4.2.1, investigated the most efficient way to use Wi-Fi in combination with different cellular modes such as 2G and 3G that are always active in the background. The second phase of smartphone battery consumption experiments, referred to as mobile application evaluation in Section 4.2.2, evaluated the battery and data consumption by commonly used IM and SIP communication applications. The experiments were conducted to find the optimal communication application in terms of battery and data consumption. Results of preliminary tests conducted prior to commencement of the wireless technology evaluation which revealed the out-of-box behaviour of the LeSs are presented in Section A4.11, Appendix A4.

4.2.1 Wireless technology evaluation

The first type of tests evaluated battery consumption during VoIP calls over Wi-Fi with LeSs in different cellular network mode combinations; and also 3G with different network mode combinations of Wi-Fi. The data collection method for the wireless technology evaluation was presented in Section 3.3.5.1, and the different network mode combinations were presented there in Table 12. Each brand of LeS had a sample size of 20. Therefore, the overall results collected for each brand of LeS comprised (a) 20 screen ON results for every network combination mode, and (b) 20 screen OFF results for every network combination mode; both for CSIP and Viber, respectively. In order to compare the battery consumption performance of the three LeSs, the results were examined using one-way ANOVA and Tukey post-hoc statistical methods. The details of the data analysis process using one-way ANOVA and Tukey post were described in Section 3.3.6.1.

In Figure 24, an example result of W-2G (see Table 12 for description of acronym) mode VoIP calls using CSIP in screen ON state obtained from one-way ANOVA shows that there is statistical difference between means, and Tukey pot-hoc analysis shows the significance of results. It can be seen in Figure 24 under column 'brand comparison' that the Tukey pot-hoc analysis conducted a pairwise comparison between results of each brand of LeS represented by number 1 for Brand 1, 2 for Brand 2, and 3 for Brand 3, respectively. The interpretation of brand comparison results later will be presented using the example from Figure 24. In Figure 24, the comparison '2-1' under 'brand comparison' column means that the mean of battery consumption result of Brand 2 is greater than that of Brand 1 for the particular network mode combination with a Difference Between Means (DBM) of 6.25% (because results were collected in battery percentage) and 95% of the time the DBM would be between 4.7792% and 7.7208%.

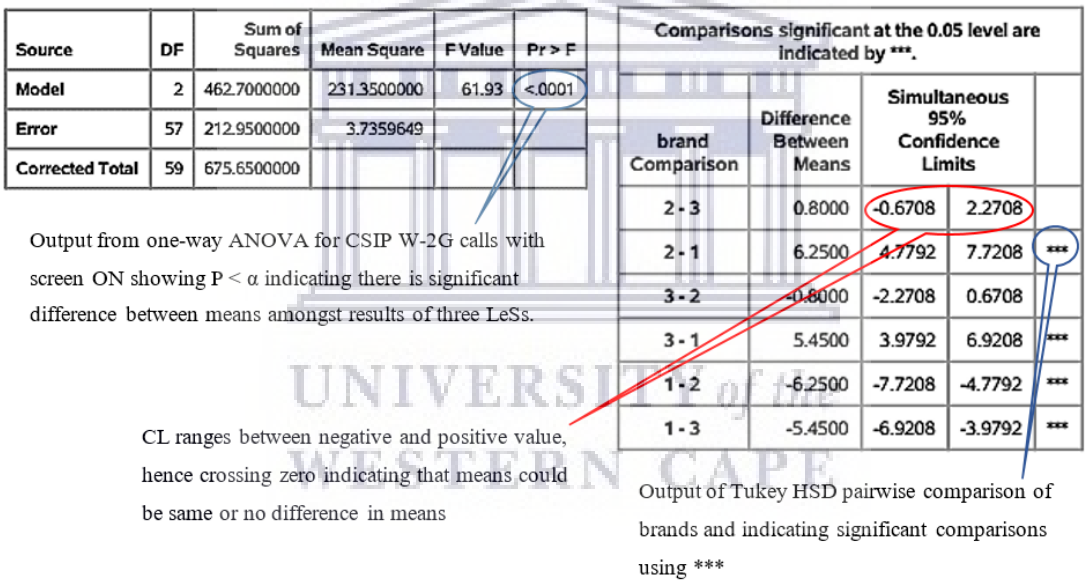

Source	DF	Sum of Squares	Mean Square	F Value	Pr > F
Model	2	462.7000000	231.3500000	61.93	<.0001
Error	57	212.9500000	3.7359649		
Corrected Total	59	675.6500000			

Output from one-way ANOVA for CSIP W-2G calls with screen ON showing P < α indicating there is significant difference between means amongst results of three LeSs.

Comparisons significant at the 0.05 level are indicated by ***.

brand Comparison	Difference Between Means	Simultaneous 95% Confidence Limits		
2 - 3	0.8000	-0.6708	2.2708	
2 - 1	6.2500	4.7792	7.7208	***
3 - 2	-0.8000	-2.2708	0.6708	
3 - 1	5.4500	3.9792	6.9208	***
1 - 2	-6.2500	-7.7208	-4.7792	***
1 - 3	-5.4500	-6.9208	-3.9792	***

CL ranges between negative and positive value, hence crossing zero indicating that means could be same or no difference in means

Output of Tukey HSD pairwise comparison of brands and indicating significant comparisons using ***

Figure 24: Sample result of one-way ANOVA and Tukey analysis of battery consumption results
The figure shows sample results from one-way ANOVA and Tukey post-hoc analyses of battery consumption results of W-2G calls with screen ON; each in its own table. In the ANOVA results, the P value is less than 0.05. This indicated that there is a significant difference in means amongst results of the LeSs. The results of Tukey post-hoc analysis shows which comparison differences are significant. Any difference between means with confidence limits ranging between negative and positive values is considered insignificant.

The significant results of pairwise comparison obtained from Tukey post-hoc analysis are presented next. The significant results for CSIP and Viber screen ON voice call tests are presented in Table 25 and Table 26, respectively. The significant results for CSIP and Viber screen OFF voice call tests are presented in Table 27 and Table 28, respectively. The insignificant results are not presented because they were not used for further analysis. The headings of Table 25, Table 26,

Table 27 and Table 28 are as follows: (a) 'Call type' refers to the particular network mode combination (see Table 12); (b) 'Brand match' represents the two brands of devices being compared; (c) 'DBM' is the difference between the means of battery percentage of the two brands of LeSs used for comparison; and (d) '95% CL' shows the 95% confidence limits of the DBM.

Table 25: Results for CSIP Wi-Fi voice calls with screen ON

Significant results were obtained for all possible Wi-Fi and cellular mode combinations; and only the significant results are shown here. The results of brand match; 2 against 3 for W-2G and W-AUTO; 1 against 3 and 2 against 3 for W-3G; and 1 against 2 and 2 against 3 were considered insignificant; and are therefore not included.

Call type	Brand match	DBM	95% CL	
			Lower	Upper
W-2G	2 – 1	6.25	4.78	7.72
	3 – 1	5.45	3.98	6.92
W-AUTO	1 – 2	1.40	0.34	2.46
	1 – 3	1.55	0.49	2.61
W-3G	2 – 1	2.30	0.25	4.35
W-PLAIN	3 – 1	2.15	1.19	3.11

The significant results of CSIP voice call tests with screen ON in Table 25 are interpreted as follows: (a) in W-2G mode, Brand 1 consumed less battery than Brands 2 and 3; (b) in W-AUTO mode, Brand 1 consumed more battery than Brands 2 Brand 3; (c) in W-3G mode, Brand 1 consumed less battery than Brand 2; and (d) in W-PLAIN mode, Brand 1 consumed less battery than Brand 3.

Table 26: Results for Viber voice calls with screen ON

Significant results are shown by brand match. Brand 1 against 2 for W-AUTO and W-PLAIN; 2 against 3 for W-AUTO and W-PLAIN; and 1 against 3 for 3G-X and 3G were considered insignificant for comparison. Insignificant results were obtained for W-2G and W-3G network mode combinations, and hence not included in the table.

Call type	Brand match	DBM	95% CI	
			Lower	Upper
W-AUTO	2 – 3	2.25	0.64	3.86
	1 – 3	2.20	0.59	3.81
W-PLAIN	3 – 1	1.25	0.17	2.33
3G-X	2 – 1	2.05	0.61	3.49
	2 – 3	2.10	0.66	3.54
3G	2 – 3	1.55	0.17	2.93
	2 – 1	2.60	1.22	3.98

The significant results of Viber voice call tests with screen ON in Table 26 are interpreted as follows: (a) in W-AUTO mode, Brand 3 consumed less battery than Brands 1 and 2; (b) in W-

PLAIN mode, Brand 1 consumed less battery than Brand 3; (c) in 3G-X and 3G modes, Brands 1 and 3 consumed less battery than Brand 2.

The significant results of CSIP voice call tests with screen OFF in Table 27 are interpreted as follows: (a) in W-2G mode, Brands 2 and 3 consumed less battery than Brand 1, and Brand 3 consumed less battery than Brand 2; (b) in W-AUTO mode, Brand 2 consumed less battery than Brand 1, and Brand 3 consumed less battery than Brands 1 and 2; (c) in W-3G mode, Brands 2 and 3 consumed less battery than Brand 1; and (d) in W-PLAIN mode Brand 3 consumed less battery that Brand 1.

Table 27: Results for CSIP Wi-Fi voice calls with screen OFF

Significant results were obtained for all the Wi-Fi and cellular mode combinations. The results of brand 2 against 3 for W-3G and W-PLAIN; and 1 against 2 for W-PLAIN were considered insignificant for comparison, and not included.

Call type	Brand match	DBM	95% CI	
			Lower	Upper
W-2G	1 – 2	1.40	0.79	2.01
	1 – 3	4.15	3.54	4.76
	2 – 3	2.75	2.14	3.36
W-AUTO	1 – 2	2.25	0.91	3.59
	1 – 3	5.15	3.81	6.49
	2 – 3	2.90	1.56	4.24
W-3G	1 – 2	3.95	3.15	4.75
	1 – 3	4.15	3.35	4.95
W-PLAIN	1 – 3	4.80	4.26	5.34

The significant results of Viber voice call tests with screen OFF in Table 28 are interpreted as follows: (a) in W-2G mode, Brands 2 and 3 consumed less battery than Brand 1; (b) in W-AUTO and W-3G modes, respectively, Brand 2 consumed less battery than Brand 1, and Brand 3 consumed less battery than Brands 1 and 2; (c) in W-PLAIN mode Brand 3 consumed less battery that Brand 1; (d) in 3G-X mode, Brands 2 and 3 consumed less battery than Brand 1; and (e) in 3G mode, Brand 2 consumed less battery than Brand 1, and Brand 3 consumed less battery than Brands 1 and 2.

Table 28: Results for Viber voice calls with screen OFF

Significant results were obtained for all the Wi-Fi and cellular mode combinations. The results of brand 2 against 3 for W-2G and W-PLAIN; and 1 against 2 for W-PLAIN; and 2 against 3 for 3G-X were considered insignificant for comparison, and excluded.

Call type	Brand match	DBM	95% CI	
			Lower	Upper
W-2G	1 – 2	3.55	2.69	4.41
	1 – 3	4.15	3.29	5.01
W-AUTO	1 – 2	3.20	2.34	4.06
	1 – 3	5.15	4.29	6.01
	2 – 3	1.95	1.09	2.81
W-3G	1 – 2	2.10	1.14	3.06
	1 – 3	3.75	2.79	4.71
	2 – 3	1.65	0.69	2.61
W-PLAIN	1 – 3	4.10	3.71	4.49
3G-X	1 – 2	1.85	0.15	3.55
	1 – 3	5.00	3.73	6.27
3G	1 – 2	3.15	1.88	4.42
	1 – 3	5.00	3.73	6.27
	2 - 3	1.85	0.58	3.12

The DBM of screen ON and OFF voice calls using CSIP and Viber for 95% CL are presented in Table 29 and

Table 30, respectively. It is very clear from these results that screen OFF should be the preferred screen state for voice call using LeSs.

Table 29: Difference between means of screen ON and OFF for CSIP voice calls

For every Wi-Fi and cellular network mode combination, a screen ON and OFF experiment was carried out. The brightness setting was same for all the smartphones in screen ON state. The experiments highlight the impact of the screen state while using CSIP on the battery consumption.

	Brand 1			Brand 2			Brand 3		
	DBM	95% CL		DBM	95% CL		DBM	95% CL	
		Lower	Upper		Lower	Upper		Lower	Upper
W-AUTO	8.40	8.04	9.25	9.25	8.08	10.42	12.00	10.74	13.26
W-2G	2.85	1.78	10.50	10.50	9.76	11.24	12.45	11.37	13.53
W-3G	7.00	5.57	13.25	13.25	12.43	14.07	12.90	11.34	14.46
W-PLAIN	5.80	5.40	6.20	Not Possible			12.75	11.72	13.77

Table 30: Difference between means of screen ON and OFF for Viber voice calls

For every Wi-Fi and cellular network mode combination, a screen ON and OFF state experiment was carried out. The brightness setting was same for all the smartphones for screen ON. The experiments highlight the impact of screen state on the battery consumption.

	Brand 1			Brand 2			Brand 3		
	DBM	95% CL		DBM	95% CL		DBM	95% CL	
		Lower	Upper		Lower	Upper		Lower	Upper
W-AUTO	8.20	7.00	9.40	11.45	10.51	12.39	11.15	10.05	12.25
W-2G	6.95	5.80	8.10	11.10	10.45	11.75	10.50	9.22	11.78
W-3G	7.25	6.30	8.20	9.60	8.87	10.33	11.35	9.80	12.90
W-PLAIN	5.15	4.13	6.17	Not possible			10.50	9.98	11.02
3G-X	5.65	4.16	7.14	9.55	8.48	10.62	10.60	9.15	12.05
3G	7.70	6.32	9.08	13.45	12.64	14.26	10.80	9.82	11.78

Table 31, Table 32, and Table 33 show the average battery consumption during the more efficient screen OFF for VoIP calls using Brand 1, 2, and 3 LeSs, respectively. The average battery consumption is shown for all the network mode combinations presented in Table 12, in order to identify the least battery draining network mode combination in each of the LeS.

Table 31: Average battery drop for Wi-Fi and 3G VoIP calls for screen OFF state – Brand 1

The table shows the battery percentage drop for Wi-Fi VoIP calls with different cellular mode combination; and 3G VoIP call with different Wi-Fi states for Brand 1 type LeS. The least battery consuming network mode combination is highlighted.

CSIP Wi-Fi SCREEN OFF		**Viber SCREEN OFF**	
Mode	**Battery percentage drop (%)**	**Mode**	**Battery percentage drop (%)**
W-2G	13.4	W-2G	14.15
W-3G	13.60	W-3G	14.20
W-AUTO	13.70	**W-AUTO**	**13.55**
W-PLAIN	**13.35**	W-PLAIN	14
		3G-X	18.75
		3G	18.55

Table 32: Average battery drop for Wi-Fi and 3G VoIP calls for screen OFF state – Brand 2

The table shows the battery percentage drop for Wi-Fi VoIP calls with different cellular mode combination; and 3G VoIP call with different Wi-Fi states for Brand 2 type LeS.

CSIP Wi-Fi - SCREEN OFF		**Viber SCREEN OFF**	
Mode	**Battery percentage drop (%)**	**Mode**	**Battery percentage drop (%)**
W-2G	12	W-2G	10.6
W-3G	**9.65**	W-3G	12.10
W-AUTO	11.45	**W-AUTO**	**10.35**
		3G-X	16.9
		3G	15.40

Table 33: Average battery drop for Wi-Fi and 3G VoIP calls for screen OFF state
The table shows the battery percentage drop for Wi-Fi VoIP calls with different cellular mode combination; and 3G VoIP call with different Wi-Fi states for Brand 3 LeSs.

CSIP Wi-Fi - SCREEN OFF		Viber SCREEN OFF	
Mode	**Battery percentage drop (%)**	**Mode**	**Battery percentage drop (%)**
W-2G	9.25	W-2G	10
W-3G	9.45	W-3G	10.45
W-AUTO	**8.55**	**W-AUTO**	**8.4**
W-PLAIN	8.55	W-PLAIN	9.9
		3G-X	16.7
		3G	13.55

The results for Brand 1 in Table 31 shows that the least battery draining Wi-Fi and cellular radio combination for VoIP calls is W-PLAIN if using CSIP; and W-AUTO if using Viber. The results for Brand 2, presented in Table 32 shows that the least battery draining Wi-Fi and cellular radio combination for VoIP calls is W-3G if using CSIP; and W-AUTO if using Viber. The results for Brand 3 in Table 33 shows that the battery percentage drop is least during VoIP calls over; Wi-Fi with cellular radio in AUTO mode for both CSIP and Viber; and 3G for Viber.

Discussion of the results presented in Table 25, Table 26, Table 27, and Table 28 in order to identify the least battery draining LeS from the 3 brands under comparison; and recommendations on the least battery draining Wi-Fi and cellular radio combinations for each LeS brand based on the results of Table 31, Table 32, and Table 33, are presented in Section 5.2.3. The next section presents the results of mobile applications evaluation.

4.2.2 Mobile applications evaluation

The mobile applications evaluations were conducted to evaluate the battery and data consumption by IMs and SIP clients during VoIP calls. The experiments were carried out after completion of the wireless technology evaluations. The IM applications selected for evaluation were WhatsApp, Messenger, Viber, and IMO; and the SIP applications selected for evaluation were Zoiper, CSIP, and Mizudroid. The selection process of the IM and SIP applications was described in Section 3.3.3.2. The experiments were carried out using the least draining LeS and network mode combination obtained from the data analysis from wireless technology evaluations; and the experiments were conducted in the more efficient screen OFF mode. The details of the method adopted for data collection was presented in Section 3.3.5.2; and data analysis was presented in Section 3.3.6.2. For data analysis of battery consumption, the ABC_x values were evaluated using

Equation 3.2 to compare battery consumption of the IM and SIP applications, and to identify the least battery draining IM and SIP applications. The comparison graph along with ABC_x values of each IM and SIP application are shown in Figure 25. The overall ABC_x results presented in Figure 25 show that IM applications consumed more battery than SIP applications.

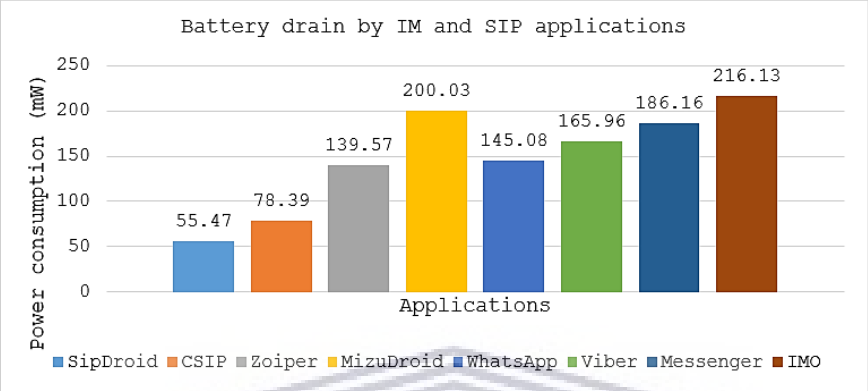

Figure 25: Battery drain comparison of IM and SIP applications

The figure shows the variation in battery consumption by the four SIP clients; and the four IM clients that were chosen for experimentation. IM applications tend to consume more battery than SIP applications.

For data analysis of data consumption, average data consumption results were evaluated for each IM and SIP application using Equation 3.3 that was presented in Section 3.3.6.2. The D_{X30} values were used to compare data consumption amongst each IM and SIP application, and identify the least battery draining IM and SIP application. The comparison graph along with the D_{X30} values of each IM and SIP application are shown in Figure 26. The overall data consumption results show that IM applications consumed less data than SIP applications.

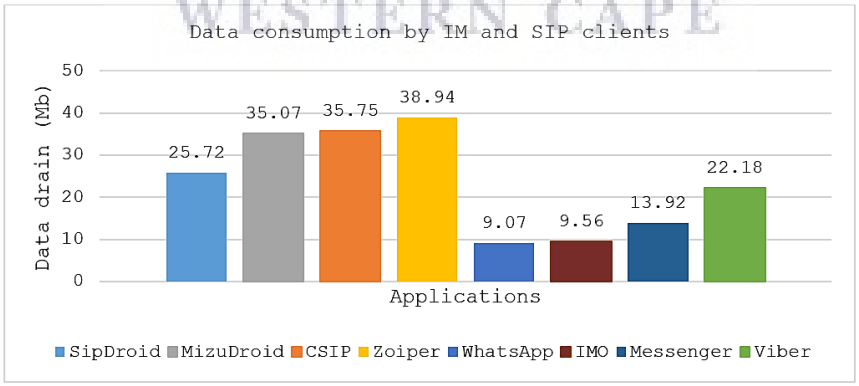

Figure 26: Data consumption comparison of IM and SIP clients

The figure shows the variation in data consumption by the four SIP clients; and the four IM clients that were chosen for experimentation. Results indicate that SIP clients consume much more data than IM applications.

Further, the ABC_x and D_{X30} values are also presented in Table A4.1 and Table A4.2, respectively, of Section A4.9 in Appendix A4. The results presented in Figure 25 and Figure 26 are discussed in detail under Section 5.2.3

4.3 Chapter summary

This chapter firstly, presented the results of scalability quantification in Section 4.1 and secondly, the battery consumption in Section 4.2. The presentation of scalability quantification results began with the average performance results of TH, RTL, RTJ, and PL% with increasing hop length, for MPv2 testbed experiments in Section 4.1.1.1. As expected, the average results of TH showed a declining trend with increase in hop length; and the average results of RTL, RTJ, and PL% showed an inclining trend for each performance metric with increasing hop length. The presentation of the UniFi testbed began with a similar presentation in Section 4.1.2.1. As expected, the results of TH obtained from experiments over inter-cluster hop length 2 to 6 showed a declining trend with an increase in distance. Also as expected, the average results of RTL and RTJ for each prime number flow from 2 up to 41 showed an inclining trend with increase in hop length. However, in the case of PL%, the results for each flow were sporadic. The trend in results of TH, RTL, RTJ, PL% with increasing hop length for both MPv2 and UniFi testbeds were also formulated into equations. This process was shown in Sections 4.1.1.2 and 4.1.2.2, respectively.

Then the chapter relayed the experimental results of smartphone battery consumption in Section 4.2. Section 4.2.1 which showed (a) the significant pairwise comparison results of battery consumption by the three LeS brands in order to identify the least battery draining LeS; (b) the DBM of battery consumption results in screen ON and OFF modes for each LeS and emphasized the importance of keeping screens OFF in LeSs during voice calls to maximize charge life; (c) average battery drop during screen OFF state VoIP calls over Wi-Fi with different cellular radio combinations, in order to identify the least battery draining wireless technology combination for each of the LeSs. Then Section 4.2.2 portrayed the average results of battery and data consumption experiments using VoIP calls over Wi-Fi by four IM and four SIP applications, respectively. Discussion of the results of Sections 4.1 and 4.2, respectively, are presented in Chapter 5.

5 Discussion

The scalability for WMN research consisted of network scalability quantification of WMNs and smartphone battery consumption using voice traffic; these drew inspiration from the Zenzeleni community network in Mankosi. A timeline to show the progress of the scalability quantification and smartphone battery consumption investigations along with the progress of Zenzeleni is presented in Figure 27 with a detailed description in Appendix A6.

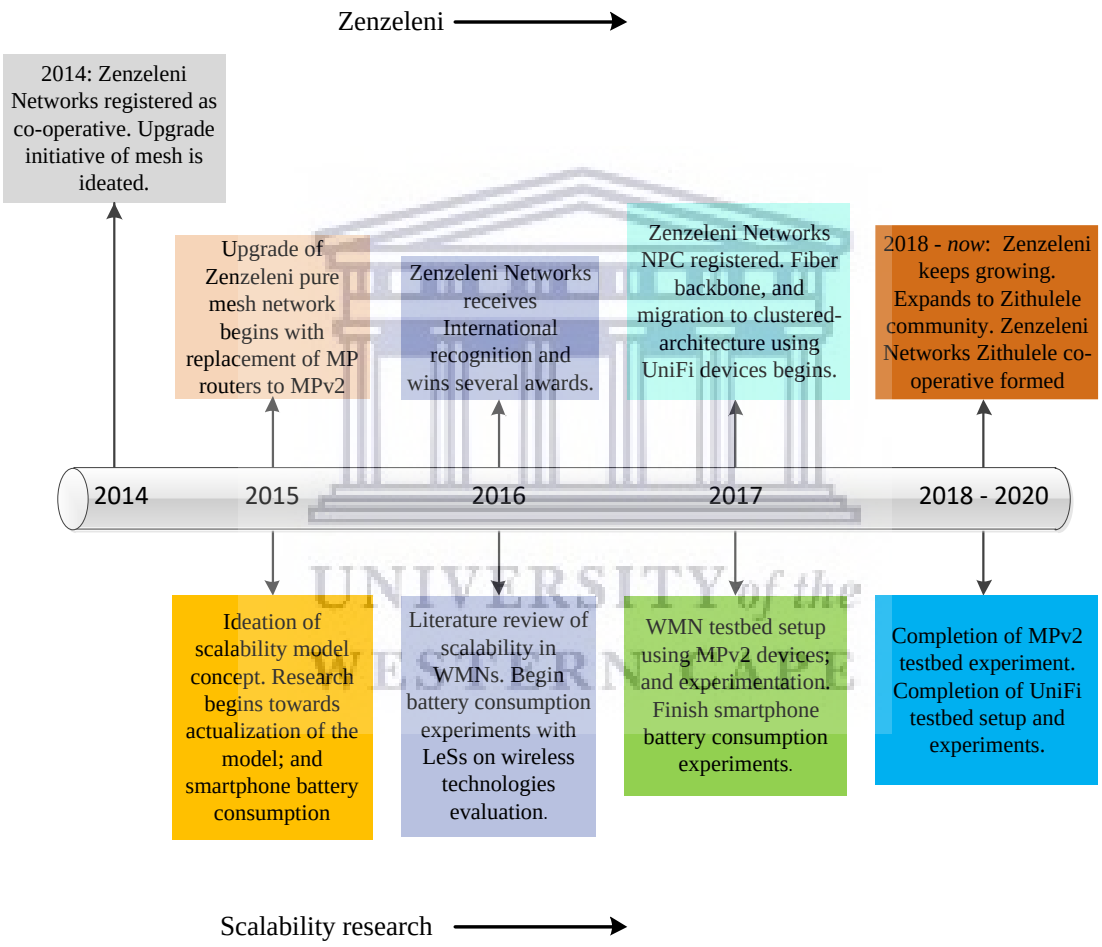

Figure 27: Research progress timeline in comparison to progress of Zenzeleni networks.
The figure shows the research timeline which begins in 2015 in parallel with the Zenzeleni progress timeline. The timeline shows the migrations of Zenzeleni and its impact on the research progress, especially when network topology changed from pure-mesh to clustered topology; and devices were changed from MPv2 to UniFi.

This chapter presents a discussion, in light of related work, of the motivation, methods and results of (a) the investigations on scalability quantification in Section 5.1, and (b) the investigations on smartphone battery consumption in Section 5.2. It is intended that the discussion

of the two main efforts leads to a unique contribution, by combining the results, which is then relayed in the subsequent Conclusion chapter.

5.1 Scalability quantification

The scalability quantification investigations were led by the research question: *Given the baseline (first hop) throughput, latency, jitter, and packet loss, what is the maximum hop length limit between mesh nodes and the gateway in a given wireless mesh network, while maintaining acceptable quality of service limits?* This section begins with a discussion of the motivation in Section 5.1.1 that led to the research question, followed by discussion of the experimental methods used to answer the research question in Section 5.1.2. The scalability quantification investigations ended with scalability prediction equations for TH, RTL, RTJ and PL% for WMNs. These results are discussed in Section 5.1.3 along with a demonstration of how to use the network scalability quantification equations.

5.1.1 Discussion of motivation

The idea to study scalability quantification was motivated by the possibilities of CWMNs towards closing digital gaps in rural and low-income areas. Zenzeleni and its subsidized network service costs for its community members played a large catalyst role to the motivation. In the introduction of Section 2.1, Bahia (2018) and the United Nations reports (2018, 2019) provided evidence that a major percentage of the global population that is not connected to the Internet is borne by sub-Saharan Africa and developing Asia for reasons such as poor infrastructure (to setup any network), affordability, consumer readiness, and availability of relevant network services. A review of CWMN deployments in low-income and rural areas of sub-Saharan Africa, presented in Section 2.1.1; and developing Asia presented in Section 2.1.2, showed that community networks can be a viable means of providing cheap communication options for areas where cellular infrastructure is missing and/or Internet tariffs are unaffordable. However, community networks must still fulfil recommended QoS requirements for reliable delivery of multimedia services to end-users. As shown in Table 4, the performance of throughput, latency, jitter, and packet loss are critical towards meeting recommended multimedia QoS requirements. However, WMNs have often shown declining QoS when increasing the number of hops between source and destination, and when traffic grows; hence exhibiting poor network scalability. In order to contextualize network scalability issues with WMNs, a review of investigations evaluating the network performance of

WMNs with increase in network traffic, client node mobility, and increase in hop length was presented Section 2.2.2. The work of Bicket et al. (2005), Dilmaghani et al. (2005), and Johnson (2007b) evaluated performance of throughput and RTL with increase in hop length; Abolhasan et al. (2007, 2009) evaluated performance of throughput, RTL, and PL% with increase in hop length and traffic load; Nassereddine et al. (2009) observed performance of TH, OWL and PL with increase in hop length and traffic load; Hamidian et al. (2009) measured performance of packet reception rate and download time in experiments with increase in hop count and traffic load; and Chissungo et al. (2012) measured performance of TH, OWL, OWJ, and PL% with increasing hop lengths. Notably, all of the investigations showed degradation in QoS performance metrics.

Other related work looked at protocols, and protocol modification. Pirzada et al. (2006), Abolhasan et al. (2009), Pei et al. (2009), Kulla et al. (2012), and Oe et al. (2015) compared network performance of WMNs under multiple routing protocols in order to find an optimal routing protocol. Draves et al. (2004) and Ahmeda et al. (2014) evaluated network performance of WMNs by changing and comparing routing metrics of mesh routing protocols to find an optimal routing metric. Niculescu et al. (2006) and Castro et al. (2007) proposed packet aggregation as a technique to improve the network performance of WMNs with increasing hop length and traffic load. Tao et al. (2005) proposed a traffic load balancing algorithm to improve packet delivery performance of WMNs with increasing traffic load.

Even though the proposed techniques aimed at improving network performance of WMNs showed improved network performance over the default network setup, performance still exhibited declining trends with increase in congestion, mobility of nodes and hop length. The overall decline in network performance of WMNs motivated the possibility of determining a scalability limit beyond which the network cannot deliver the recommended QoS to end-users. Considering the case of CWMNs, failure to provide QoS will be detrimental to their deployment and growth because end-users will not use a network with poor QoS. Therefore Section 2.2.3 reviewed scalability models developed to predict scalability limits of WMNs with increasing hop length. Gupta et al. (2001), Johnson et al. (2007b) and Li et al. (2002) proposed throughput capacity models to predict throughput capacity limit in WMNs with increasing hop length. It is noteworthy to mention that the throughput scalability models of Gupta et al. (2001), Johnson (2007b) and Li et al. (2002) were formed from throughput (only) performance data obtained from experiments. The importance of using empirical data rather than using theoretical analysis to develop scalability

models is emphasized by Gupta et al (2000) and Gupta et al. (2001). The throughput scalability model developed using experimental data by Gupta et al. (2001) showed that performance declined at a much worse rate than the throughput model obtained from theoretical analysis by Gupta and Kumar (2000). However, the literature review was unable to find latency, jitter and packet loss as quantification models. The lack of latency, jitter, and packet loss scalability models was considered a major research gap for scalability predictions of WMNs since the overall QoS depends on the performance of all KPMs. Hence, the WMN scalability quantification work presented herein was motivated by the belief that KPM-based quantification models can aid in the deployment of new CWMN infrastructures and/or the redesign of existing ones, such that the networks can offer recommended QoS requirements. With more success in this respect, it may be possible to promote the deployment of CWMNs as cheaper communication alternatives.

5.1.2 Discussion of methods

The scalability quantification pursuit utilised an empirical and quantitative approach since numerical data of throughput, latency, jitter and packet loss were to be used to build the scalability models. In Section 3.1, a detailed discussion on the selection of the research approach was presented along with the steps of the experimental design. The overall experimental design adopted to develop the scalability quantification model consisted of (1) deciding on an experimental physical topology; (2) deciding on the type of tests to be used for the experiments; (3) the selection of an experimental technique; (4) the testbed setup, (5) choosing the approach to data collection; and finally, (6) choosing the approach to data analysis. It is noteworthy to mention that steps (1), (2) and (3) were performed once at the beginning of the scalability quantification investigations (between 2015 and 2016) to develop the MPv2 testbed; and were later adopted (and adapted) for the UniFi testbed setup.

The experimental physical topology process presented in Section 3.2.1 determined a simple and optimal WMN topology for experimentation. The process was informed by the multi-hop clustered-hierarchical WMN approach of Zhao and Raychaudhuri (2009), as this approach was shown to have better throughput capacity scaling and performance in comparison to flat WMN topology approaches. Hence, the selection of a clustered-hierarchical WMN topology can be regarded as a recommendation for deploying a scalable CWMN.

The process for selection of type of tests was presented Section 3.2.2. For the scalability quantification investigation, throughput, latency, jitter and packet loss data were needed. In order to measure maximum achievable throughput, TCP tests were selected. Throughput under usage of TCP is representative of reliable traffic transmission because TCP integrates an acknowledgment and re-transmit mechanism to ensure that all packets are correctly delivered. Therefore, the delay before acknowledgment packets are received (latency) has an impact on the TH between the links. Usage of TCP traffic to measure throughput in WMNs was also observed in the related work of Bicket et al. (2005), Johnson (2007b), Draves et al. (2004) and Dilmaghani et al. (2005). To measure latency, jitter, and packet loss, VoIP tests were employed because of VoIP has strict end-user multimedia QoS requirements (conversational voice), as shown in Table 4, as compared to data (best-effort, bulk, and transactional/interactive) QoS requirements. The per second rate at which VoIP packets are sent burdens a network, and, therefore the network scalability quantification study assumed that a WMN ready to support VoIP traffic while maintaining its recommended QoS requirements can be considered ready to support other types of traffic as well. Besides, the prioritization of voice, and later data, was also emphasized by Zenzeleni activity and growth.

The selection process of experimental technique was presented in Section 3.2.3. The related work presented in Section 2.2.2 employed experimental techniques such as analytical (theoretical) modelling, simulation, network emulation, and real-world testing. The scalability quantification study chose network emulation to obtain empirical experimental data for throughput, latency, jitter, and packet loss; and analytical modelling of the network performance data to devise scalability quantification models for each metric. A similar approach was adopted by Gupta et al. (2001), Johnson (2007b) and Li et al. (2002) to obtain throughput scaling models. Pure analytical models fall short of the practicality of real networks or systems because assumptions are made by mathematical network models that consist of limited real-world (or real-hardware) physical layer models; therefore, such models can be considered best-case models. The throughput scalability model built using analytical modelling of experimental data in Gupta et al. (2001) showed the predicted throughput decline to be higher than the predicted throughput decline by the pure analytical throughput scalability model obtained by Gupta and Kumar (2000). Therefore, scalability models devised using the best-case pure analytical investigations were not considered a feasible option for the scalability quantification study. Further, the related work of Niculescu et

al. (2006) evaluated the effectiveness of a packet aggregation mechanism in increasing VoIP capacity in simulated and emulated experimental environments; and the results yielded better VoIP performance in simulation than in network emulation. The results of Niculescu et al. (2006) challenged the practicality of simulation techniques for making decisions about real-world network or systems.

Real-world testing was not considered for the scalability quantification investigations because deploying a real-world experimentation network involved complexities such as the ethics underlying usage of human beings to use a real-world network to capture traffic results for further analysis; in other words, more experimental control complexities. Network emulation involves usage of real equipment, and therefore yields results with higher realism than simulation techniques especially for experiments in which performance of real equipment and/or applications/protocols must be evaluated; and from this point of view it is only slightly inferior to real-world testing. In order to emulate networks, hardware resources in the form of intermediary and end-user devices; and software resources in form of network traffic generators (to generate synthetic traffic) are common requirements. Usage of real hardware to set up the network, and synthetic network traffic generation can be observed in the network emulation related work of Draves et al. (2004), Dilmaghani et al. (2005), Niculescu et al. (2006), Abolhasan et al. (2009, 2007), Hamidian et al. (2009), Kulla et al. (2012), and Chissungo et al. (2012).

Section 3.2.3.1 presented the hardware selection process for the experiments. The selection of intermediary devices, which in the case of the scalability quantification study were the mesh routers, was driven by their operation in a real-world WMN deployment or their availability in the local market. Since the scalability quantification study drew motivation from Zenzeleni, the mesh equipment operational in Zenzeleni between 2015 and 2019 (end of research timeline) was considered for network emulation. In order to emulate end-user devices, and avoid generating traffic from within the mesh routers, RPi2 devices were used for their functional scalability, especially the support these devices can provide for numerous traffic generators available in Linux. Usage of an end-user device tested the processing complexity of the mesh routers at handling traffic forwarding between the 2.4GHz and the 5GHz within the mesh radios. Usage of desktops as end-user devices can be observed in the work of Johnson (2007b) and Chissungo et al. (2012).

Section 3.2.3.2 presented the software requirement process; identifying network traffic generators capable of synthesizing TCP and VoIP traffic. The selection of *iPerf* as the TCP traffic generator was informed by the related work of Kolahi et al. (2011) and Mishra et al. (2015) that compared TCP throughput obtained by multiple traffic generators, and showed a higher TCP throughput achieved by *iPerf*. Since, *iPerf* was not capable of generating particular types of application layer traffic profiles, especially VoIP, D-ITG was chosen to generate specific VoIP traffic profiles as done by Avallone et al., 2005; Botta et al., 2012, 2013). Usage of D-ITG to send VoIP traffic over WMNs was also observed in related work of Tiemeni (2015).

The experimental testbed setup was presented in Section 3.2.4 and consisted of the MPv2 testbed setup in Section 3.2.4.1 and the UniFi testbed setup in Section 3.2.4.2. For the MPv2 testbed, an unplanned positioning of MPv2 nodes, often adopted with CWMNs reviewed in Section 2.1.1, Section 2.1.2, and Roofnet (2005), was adopted for the MPv2 testbed. The schematic of MPv2 testbed is presented in Figure 8. The unplanned positioning of MPv2 nodes was adopted because of the complexity encountered in forming multi-hop clustered topology in the small experimental space of 9.5m by 4.24m due to strong 5GHz Tx of MPv2 mesh backbone regardless of reduction in Tx power to 1dBm; placing MPv2 units at different angles, heights and distances; and disabling MIMO. The unplanned positioning accompanied by DIY Faraday cages on the MPv2 nodes achieved a multi-hop clustered MPv2 testbed topology. Examples of unplanned positioning of mesh nodes in experimental testbeds can be found in the related work of Niculescu et al. (2006) and Chissungo et al. (2012). Usage of OTS shielding and attenuators as observed in the related work of Sanghani et al. (2003), Clancy and Walker (2007), Johnson and Lysko (2007), ElRakabawy et al. (2008), and Rethfeldt et al. (2018) was avoided to achieve a more cost-effective shielding technique. Since the scalability quantification study based its selection of devices on the types operational in Zenzeleni, the experiments were migrated (in 2018) to a testbed using UniFi devices. It is noteworthy to observe that by 2018, MPv2 units had gone out of production; and the researchers were unable to find any other reported CWMN deployments using MPv2 units. The wireless uplinks between UniFi AP units could be manually configured, a feature that was unavailable in MPv2 units, allowing the UniFi testbed setup to adopt a planned layout in a grid form, as done in the mesh experimental testbeds of Clancy and Walker (2007), Johnson and Lysko (2007), and Rethfeldt et al. (2018). The grid pattern adopted for the UniFi testbed is shown in Figure 9 and the UniFi testbed schematics are shown in Figure 10. The manual control over

wireless uplink configuration in UniFi units offers scalability when more nodes need to be added to the testbed in small space. In contrast Mesh routers, that are strictly auto-configuration devices, such as MPv2, require extra expenditure on attenuators and shielding to achieve a grid layout in a small experimental space, thus adding to the experiment cost.

The data collection process was presented in Section 3.2.5. The process fine-tuned the choice of TCP window to evaluate TH performance; and the codec profile for VoIP to evaluate RTL, RTJ and PL% performances. Usage of the default windows size for TCP with *iPerf* was informed by the related work of Johnson (2007a, 2007b) and Kolahi et al. (2011). However, the default TCP window size in the MPv2 and UniFi testbed TH experiments was 85.3KB whereas that used in Johnson (2007a, 2007b) and Kolahi et al. (2011) was 8KB.

In order to yield overall TH (round-trip throughput) between two mesh nodes, TCP tests were conducted from a source to destination and then repeated in the backward direction. A TCP test had to be repeated in the backward direction, because throughput is dependent on latency and the varying Rx strengths received at each mesh node for single hop links in the MPv2 testbed (as shown in Table A3.3) and the UniFi testbed (as shown in Table A3.4) indicated that the OWL between two nodes differed for different directions of traffic. In addition, *iPerf*, the network traffic generator used to inject TCP traffic in the MPv2 testbed, is based on a client-server model meaning that throughput measured reflects one-way performance. Therefore, measurement of round-trip TH was deemed a step forward over experiments that measured end-to-end TCP throughput using *iPerf* such as Johnson (2007a, 2007b), ElRakwaby et al. (2008), Campista et al. (2008), Kolahi et al. (2011), Seither et al. (2011), and Rethfeldt et al. (2018).

The choice of G.711 codec for the VoIP profile was motivated by the G.711 VoIP codec installed on the MPv2 units. Since the network scalability quantification experiments began with an MPv2 testbed, it was deemed necessary to emulate the real-world SIP call functionality offered by the MPv2 routers. Single-flow of G.711 VoIP stream was injected using D-ITG in the MPv2 testbed to measure performance of RTL, RTJ, and PL%. Usage of D-ITG to transmit G.711 traffic was informed by Hamidian et al. (2009) and Tiemeni (2015); and the choice of single-flow transmission to measure performance of network metrics during VoIP call was informed by Chissungo et al (2012). However, Hamidian et al. (2009), Chissungo et al (2012), and Tiemeni

(2015) measured performance of OWL, OWJ, and packet loss performance during one-way traffic to measure performance of VoIP.

The TH, RTL, RTJ, and PL% experiments over the MPv2 testbed provided a framework for experiments over the UniFi testbed. The choice of VoIP codec, was maintained during the UniFi testbed experimentation. The UniFi testbed experiments tested the performance of TH, RTL, RTJ, and PL% performance between the two mesh clusters to emulate the transmission of network traffic between two mesh networks. The scalability quantification research was unable to find related work that evaluated performance of TH, RTL, RTJ, and PL% between multiple mesh networks. Adoption of such an experimental process was motivated by the migration of Zenzeleni in 2017 to clustered architecture consisting of pockets of mesh network using UniFi units connected to each other via a gateway. In addition, to measure performance of RTL, RTJ, and PL% during VoIP tests in the UniFi testbed, VoIP flows to a single UniFi unit were scaled intermittently. For quick scaling of VoIP flows to a point where there will likely be a network metric that has crossed the recommended QoS requirements for VoIP calls, increments of prime numbers from 2 up to 41 was adopted. Performance evaluation of VoIP in a WMN using multiple flows can be observed in related work of Niculescu et al. (2006), Castro et al. (2007), Hamidian et al. (2009), and Tiemeni (2015). Niculescu et al. (2006) scaled VoIP calls uniformly from one call in increments of 1; and the scaling was based on the threshold VoIP call number per-hop**.** Castro et al. (2007) also scaled VoIP flows uniformly but did not disclose the starting flow count and the increment size. Hamidian et al. (2009) scaled VoIP flows uniformly from 1 up to 10 and Tiemeni (2015) evaluated performance of a fixed flow count of 5 VoIP flows. Thus, the related work of Niculescu et al. (2006), Castro et al. (2007), Hamidian et al. (2009), and Tiemeni (2015) present examples of independent choices for VoIP flows much like the selection of VoIP flow count and increment in the UniFi testbed. An intermittent growth trend in the number for VoIP flows was also an attempt to match sporadic Wi-Fi client connections often observed in the real-world world.

The data analysis methods were presented in Section 3.2.6. Usage of regression to obtain a throughput capacity model has been shown in the related work of Johnson (2007a). It is noteworthy to mention that the related work of Gupta and Kumar (2001), Johnson (2007a), and Li et al. (2002) formed power capacity scaling models and did not explore other models that could best fit the capacity performance trend. Nor did these authors, Gupta and Kumar (2001), Johnson (2007a), and Li et al. (2002) discuss why other types of capacity models were not considered to

represent the throughput trends. Therefore, a power model as informed by Gupta and Kumar (2001), Johnson (2007a), and Li et al. (2002); and a regression technique as informed by Johnson (2007a) were adopted to analyse the results of TH, RTL, RTJ, and PL% of the MPv2 and UniFi testbeds, respectively. However, the regression analysis was extended by inclusion of exponential regression in order to investigate possibility of producing a curve to closely represent the actual results in addition to the power curve. The regression technique yielding the higher R^2 coefficient of determination was selected to represent the performance behaviour trend of TH, RTL, RTJ, and PL%, with increasing number of hop length because the larger the R^2 value the better the predicted match of the regression model to the actual results (ASK, 2018). An equation was formulated for the best fit regression technique. The equations obtained from regression analysis of each performance metric of MPv2, and TH and PL% from UniFi testbed were generalized. In the case of equations for each flow for RTL and RTJ obtained in UniFi testbed, the equation for each flow was firstly generalized and then combined to yield a single equation for each metric. The generalization of the performance trend equations was informed by modelling work of Gupta and Kumar (2001), Johnson (2007a), and Li et al. (2002). However, the network scalability quantification was unable to find related work that combined multiple network performance trend equations of different numbers of flows to yield a singular equation to represent the trend of a given network metric. The results of regression analysis; generalization and combination processes were presented in Section 4.1 and are discussed in the next section.

5.1.3 Discussion of results

This section discusses the network scalability quantification equations devised in Section 4.1 for the prediction of maximum hop length between source and destination in a WMN. The work of Gupta and Kumar (2001) and Johnson (2007a) on the formation of throughput scalability models informed the approach of this research to realise scalability quantification equations. The scalability quantification equations for the MPv2 and UniFi testbeds, respectively, were presented in a universal form such that the scalability of the network metric is dependent on the first-hop value of that particular metric. Two sets of equations were obtained for each MPv2 and UniFi testbed, respectively, as a result of regression analysis, combination, and generalization methods. The equations of the MPv2 and UniFi testbeds were not combined because even though the network topologies of both the testbeds were clustered, the testbeds represented different WMN topologies consisting of different brand of devices with different hardware specifications.

Therefore, the subsequent section will demonstrate how to apply the results of this research to other WMNs.

As shown in Table 13, the analysis of the average TH, RTL, RTJ, and PL% results yielded high values of R^2 for power over exponential regression for all metrics. The MPv2 testbed scalability quantification process yielded Equations 4.2, 4.4, 4.6 and 4.8 to represent the trends of TH, RTL, RTJ, and PL%, respectively, with increasing hop length between source and destination. It is noteworthy to mention that the TH scalability equations in the related work of (a) Gupta and Kumar (2001) were obtained from performance results of TH in an emulated MANET testbed; (b) Johnson (2007a) were obtained from performance results of throughput in an outdoor flat-mesh CWMN; and (c) Li et al (2002) were obtained from performance results of TH in a simulated MANET testbed.

The TH scalability equations of linear and grid topologies with RTS/CTS OFF in the related work of Li et al (2002) are similar to those in use here because even though the MPv2 testbed topology was of a clustered type, experimental TCP and VoIP traffic flows were linear; and the RTS/CTS was left in default OFF mode in the MPv2 units. The power slope, -1.37 in the TH Equation 4.2 can be contrasted with the power slope in the equations of Gupta and Kumar (2001), Johnson (2007a), and Li et al (2002). The power slope of TH scalability equations in Gupta and Kumar (2001) is -1.68; in Johnson (2007a) is -1.62; and in Li et al (2002) is -1.744 and -4.98 for grid for linear topology, respectively. It can observed that the power slope of the TH scalability equation obtained from the MPv2 testbed is the lowest when compared with the related work of Gupta and Kumar (2001), Johnson (2007a), and Li et al (2002). Based on observed slopes, it can be inferred that TH in a clustered WMN declines at a slower rate than in both a MANET and flat-mesh WMN, with increasing hop length between source and destination. The scalability quantification literature review, however, was unable to discover published related work that presented scalability models for latency, jitter, and packet loss (hence the research gap). Therefore, the RTL, RTJ, and PL% scalability quantification equations obtained from the MPv2 testbed experimentation and analysis are considered a novel contribution to the research field of network scalability quantification of WMNs.

The UniFi testbed scalability quantification process, presented in Section 4.1.2 yielded Equations 4.10, 4.15, 4.22 and 4.24 to represent performance trends of TH, RTL, RTJ, and PL%,

respectively. Equations 4.10 and 4.24 for TH and PL%, respectively, were of the exponential type; Equation 4.15 for RTL was a combination of exponential and power type; and Equation 4.22 for RTJ was of the power type. The scalability quantification related work in Section 2.2.3 mostly focused on devising power equations for throughput capacity scaling. However, the regression analysis approach adopted herein and the results of Equations 4.10, 4.15, and 4.24 showed that there could be other types of equations that can better represent the performance trends of the metrics.

A demonstration of how to use the scalability equations from MPv2 and UniFi testbeds for prediction of a maximum hop length limit between source and destination nodes in a WMN is presented in Section 6.3.1.

5.2 Smartphone battery consumption

The smartphone battery consumption investigations addressed the research question: *What is the most efficient Wi-Fi and network mode combination; and social communication application, in terms of battery and data consumption, for low-income off-grid users residing in rural areas given the presence of community wireless mesh networks?* This section begins with a discussion of the motivation to answer this question in Section 5.2.1, followed by discussion of the experimental methods used to answer the research question in Section 5.2.2. The results from the smartphone battery consumption experimentation that were presented in Section 4.2 are discussed in Section 5.2.3. It is noteworthy to mention that smartphone battery consumption experiments were carried out separately from the MPv2 and UniFi testbed experiments, with the objective to produce a framework to evaluate battery consumption in smartphones.

5.2.1 Discussion of motivation

The CWMN deployments in sub-Saharan Africa and developing Asia that were presented in Section 2.1 showed that CWMNs offer viable alternatives to traditional network infrastructure. A review of mobile affordability and electricity accessibility, presented in Section 2.3.1, indicated that the key factors affecting Internet penetration were high mobile tariffs, handset prices, and poor access to electricity in sub-Saharan Africa; and high handset prices and poor electricity supply in developing Asia. A report from the GSM Alliance (2015) recommended low-cost LeSs in the range of 25-50USD as a viable solution to Internet-ready device/handset affordability for low-income rural communities. Therefore, CWMNs and LeSs offer a potent combination for more affordable

and accessible communication for low-income rural communities. However, recharging LeSs, that have small battery capacities, on a regular basis, can hinder their successful usage in rural and low-income communities of sub-Saharan Africa and developing Asia, due to poor to no electricity supply in these regions. The smartphone battery consumption research drew inspiration from Zenzeleni, and the challenges faced by the residents of Mankosi in recharging smartphones, that hindered access to low-cost network services offered by Zenzeleni. Rey-Moreno et al. (2016) reported that 84% of the population in rural Mankosi did not have electrical lighting infrastructure and therefore incurred a third type of mobile affordability cost in the form of recharge costs.

Given the plethora of LeSs availability in the market, (in 2015) the smartphone battery consumption study commenced with the objective to devise a framework to compare the properties of LeSs to identify the least battery consuming LeS. The framework considered comparison of LeSs based on battery consumption during communication. Section 2.3.2 showed that Wi-Fi was the best wireless technology for communication in terms of battery consumption when compared to the 2G, 3G, and BT wireless technologies that are commonly found in mobile phones, regardless of the brand of the phone. Therefore, in order to keep the LeSs charged for a longer duration of time, usage of Wi-Fi, as a primary means of communication, was identified as a suitable option by the smartphone battery consumption study. However, it is commonly noticed that cellular technologies such as 2G and 3G are continuously active in the background in smartphones during Wi-Fi usage and add to the battery consumption. The researcher was unable to find published related work that investigated the most efficient way to use Wi-Fi in combination with different cellular technologies idling in the background to further reduce battery consumption in LeSs. Therefore, the smartphone battery consumption research commenced with the development of a wireless technology evaluation framework to compare battery consumption in LeSs during Wi-Fi usage in different network mode combinations; in order to identify the least battery consuming LeS.

In addition, social communication using smartphones and IM applications, e.g. Messenger, WhatsApp, Skype, and IMO have dethroned traditional voice calling and texting methods due to their attractive features and presumably cheaper cost of data (Farooq & Raju, 2019; Stork et al., 2017; Sujata et al., 2015). Thus, it is important to look at how popular communication applications consume data and drain batteries. In order to get the maximum charge life from an LeS in addition to usage of least battery draining Wi-Fi and cellular mode combination, this smartphone battery

consumption study devised a framework to evaluate not only phones, but also applications on those phones. The smartphone battery consumption study deemed it necessary that the selection of the social communication application must be based on the knowledge of the battery consumption in smartphones, so that the least battery draining application as well as the least data consuming application could be selected, to further lower the cost of communication. Therefore, the smartphone battery consumption study commenced with mobile applications evaluation towards the end of 2016 to identify the least battery and data consuming social communication application for usage with LeSs. Alcatel-Lucent (2014) reported application cost rankings based on battery and data consumption but did not disclose their evaluation framework. In addition, the Alcatel-Lucent (2014) report was considered outdated by the mobile applications evaluation for selection of communication applications due to the 2 year gap (approximately) between the Alcatel-Lucent (2014) rankings report and the commencement of the mobile application evaluation study. It is often observed that applications in smartphones receive constant updates and can change battery and data consumption behaviour of communication applications. However, the mobile applications evaluation research was unable to yield any recent evaluations of rankings of communication applications based on mobile application battery and data consumption in smartphones. Therefore, the smartphone battery consumption study commenced with the development of a mobile application evaluation framework to build rankings of communication applications based on their battery and data consumption.

5.2.2 Discussion of methods

The smartphone battery consumption study also took an empirical and quantitative approach, and is consistent with the scalability quantification research approach. This section discusses the overall experimental methods adopted for wireless technology and mobile applications evaluations, respectively. The experimental methods were designed such that the steps could be replicated by technical personnel in other rural community networks, and with any selection of smartphones, to yield results that could assist actual end users in making informed choices about the selection of LeSs and the management of their battery life.

The overall experimental method for smartphone battery consumption investigation consisted of (1) deciding on the experimental physical topology; (2) the type of tests to be used for the experiments; (3) the selection of experiment techniques; (4) the testbed setup; (5) the data

collection approach; and (6) the data analysis approach. The steps were similar to the scalability quantification experiments.

The physical topology selection process was presented in Section 3.3.1. Xiao et al. (2008), Balasubramanian et al. (2009) , Carroll and Heiser (2010), Perrucci et al. (2011), and Friedman et al/ (2011) all showed that a fixed network topology was not a requirement for battery consumption evaluation of smartphones. For further clarification, the MPv2 and UniFi testbeds can be considered examples of fixed topologies because a change in their network topology will also change the outcome of the network performance results. However, battery consumption is a characteristic of the end-user device that uses the network service and is not dependent on the topology of a network. Therefore, for physical topology, the smartphone battery consumption study chose an unplanned network topology for experiments.

The selection process for the type of tests was presented in Section 3.3.2. The smartphone battery consumption experiments prioritized tests that exhibited the primary usage of mobile airtime by the end-users in a low-income rural community. Since the research drew inspiration from Zenzeleni, the mobile airtime expenditure of Mankosi community members reported in Rey-Moreno et al. (2016) was used to select the type of tests. Rey-Moreno et al. (2016) revealed that Mankosi community members spent approximately 21.97% of their individual monthly income on mobile communications split between approximately 18 cellular voice calls, 7 text messages, and 25-30MB data bundles. Therefore, the smartphone battery consumption experiments prioritized voice calls.

The selection of experimental technique was presented in Section 3.3.3. The type of experiment narrowed down to a choice between network emulation and real-world testing, since battery consumption of actual devices had to be measured. Network emulation technique was chosen over real-world testing so that experimental controls could be applied consistently in the collected data. In real world testing, the behaviour of participants (potentially human) cannot be completely controlled (Beuran, 2012). The choice of network emulation to evaluate smartphone battery consumption was further assisted by related work presented in Section 2.3.2 that also used network emulation. In order to emulate the smartphone battery consumption tests, hardware resources were procured in form of LeSs, and software resources in form of voice applications and battery and data profilers. The hardware process was presented in Section 3.3.3.1. Three different

brands of LeSs were procured costing between 37-52USD that fitted closely to the sub-50USD cost range considered affordable by the GSM Alliance (2015). Usage of multiple smartphones can also be observed in Nurminen, and Noyranen (2008), Balasubramanian et al. (2009), Friedman et al (2011), however, their experiments evaluated performance of wireless technologies present in each smartphone individually and did not compare the smartphones against each other. Experiments with multiple LeSs was deemed a must because LeSs with different hardware specifications within a similar price range are commonly available in the market; and comparison of multiple LeSs was going to reveal the impact of different hardware specifications of LeSs on battery consumption. The energy consumption results of Friedman et al (2011) informed the researcher that smartphones with similar wireless radio specifications can consume different amounts of energy for similar amount of data transfer.

Whereas the end-user cannot be forced into using a particular brand, knowledge of the most efficient LeS, in terms of battery consumption, available in the market can assist in making an informed choice. In this way, selection and comparison of multiple LeSs can be seen as a framework for future smartphone battery consumption experiments. Therefore, wireless technology evaluation identified the least battery draining LeS brand between the three chosen for experiments; and the least battery draining Wi-Fi and cellular mode combination in each brand of LeS.

The selection process of software to make VoIP call; and measure the battery and data consumption, was presented in Section 3.3.3.2. In the case of the selection of VoIP software to make voice calls, SIP and IM applications were considered. For wireless technology evaluation, the choice of SIP clients drew inspiration from the MP router operational in Zenzeleni at the time of the experiments that was capable of allowing free inter-network SIP voice calls. At the time, CSIP was recommended by the manufacturers of the MP routers Village Telco (Gillet, 2017). To emulate breakout VoIP calls, Viber IM was chosen based on the Mobile Application Rankings Report by Alcatel-Lucent (2014), that showed Viber had the least overall cost ranking, based on overall battery drain and data consumption, as compared to other widely used IM applications, such as WhatsApp, Facebook Messenger, Blackberry Messenger, and Skype. The mobile application evaluations commenced after completion of the wireless technology evaluation (late 2016 – early 2017) and given the age of the Mobile Applications Cost ranking report by Alactel-Lucent (published in April 2014) that was used for wireless technology evaluation, an updated

report was considered to inform the selection of IM and SIP applications. Therefore, the 2017 first quarter report on the top most-installed applications for Android devices published by Avast Software (2017) was used. The sampling approach, applied to the top 30 ranking list, as shown in Figure 12, yielded WhatsApp Messenger, Messenger, Viber, and IMO applications. The Avast Software (2017) informed ranking for the top 10 (all types of) battery and data drainer applications at their initial start-up in the smartphones, and not during their usage. The only IM application in the list was WhatsApp. Since the mobile application evaluation study was unable to find ranking reports of SIP applications, 4 SIP clients were selected from the Google Play store via a search process that was shown in Figure 13. The selected SIP clients were Zoiper, CSIP, MizuDroid, and SipDroid.

The selection of battery profiling software for wireless technology evaluation was based on the related work of Balasubramanian et al. (2009), Perrucci et al. (2011) and Kalic et al. (2012) that used the default battery profiling application installed on a given smartphone. The selection for battery profiling application for mobile application evaluation was led by the motivation to measure the impact of the usage of IM and SIP applications on battery consumption of the LeSs specifically, excluding other processes in the background. Relying on the conclusions from related work of Bakker (2014), a PTut power estimation tool developed by Zhang et al (2010), was selected to measure average power consumption by the IM and SIP applications. The data consumption by IM and SIP applications was measured by the default data profiler provided with the Android OS. The mobile application evaluation literature review was unable to find related works that spoke of methods of collecting information on the data consumption of applications, specifically social communication applications, using a third-party data profiler.

The wireless technologies evaluation testbed setup was presented in Section 3.3.4.1 and the mobile applications evaluation testbed setup was presented in Section 3.3.4.2. Each of the related work in Section 2.3.2 had a different testbed network topology to measure battery consumption. Such an approach informed us that fixed network topologies were not a requirement for experiment, however, the network topology should remain consistent throughout a set of evaluations for consistency in data collection. Hence, independent approaches to the design of the testbed network topology were adopted for wireless technology evaluation and then the mobile applications were evaluated. At the time of smartphone battery consumption experiments (end of 2015 to 2017), the MPv2 testbed was still in a fine-tuning stage and the UniFi testbed setup had

not even commenced. Therefore, the testbeds for wireless technology evaluation and mobile applications evaluation were setup separately from the scalability quantification testbeds.

The data collection process of wireless technology evaluation was presented in Section 3.3.5.1, and the data collection process for mobile applications evaluation was presented in Section 3.3.5.2. In wireless technology evaluation, to collect battery consumption data, the difference between battery percentage before and after a VoIP call, shown on the notification bar of the LeS in Figure 16, was calculated. Usage of battery percentage as a unit to represent battery drain in smartphones can be observed in Kalic et al. (2012). In order to ensure consistent data collection, experiment controls mentioned in Table 11 were applied in advance of the wireless technology evaluation. The data collection consisted of recording the battery percentage changes during 1 hour VoIP calls using CSIP and Viber applications. In addition, based on related of work of Perrucci et al. (2009), which showed how 3G offers higher data rates with lower battery consumption than 2G, VoIP calls over 3G were also considered for cases when there is an unavailability of a CWMN in the region. The different network mode combinations possible with every LeS brand type used for the experiments; were evaluated and the results were presented in Table 12. The wireless technology evaluation was conducted for both ON and OFF screen states to reveal the impact of screen state on battery consumption during VoIP calls in different network mode combinations. Related work of Carroll et al. (2010) and Perrucci et al. (2011) had already highlighted the impact of screen brightness on battery consumption in smartphones. However, preliminary wireless technology evaluation in screen ON state showed that the screens of the LeSs did not turn off automatically when faced upwards (and away from caller/receiver) and had to be manually turned off. Therefore, it became very vital to carry out screen ON experiments to emphasise the battery charge saved by turning the screen OFF, so that end-users could be informed about the amount of battery charge that can be saved by keeping screens in an OFF state during VoIP communication. Usage of the brightness slider to set the desired brightness can be seen in the related work of Carroll et al. (2010); and the usage of different phone backlight light levels can be observed in the related work of Perrucci et al. (2011). However, the steps to achieve the desired settings in these studies were not presented. Therefore the wireless technology evaluation used a common brightness setting across all the LeSs, using the brightness bar slider, as shown in Figure 17. Similarly, a consistent voice call volume setting was configured across the LeSs, PC speakers, PC internal hardware audio, and YouTube which was used to stream the 1 plus hour media for voice calls. The

related work of Xiao et al. (2008), Carroll et al. (2010), and Perrucci et al (2011, 2009) exhibited experiments that required a specific volume setting. However, the precise methods for setting the volume were not reported. Therefore this wireless technology evaluation used consistent volume settings during the experiment, the details of which are presented in Section 3.3.5.1.

A method to turn OFF LeSs screens completely was devised during wireless technology evaluation since the screens would not turn OFF automatically, because of the absence of proximity sensing to judge the closeness of phone to the ear (Nield, 2017) in the experiments. Each LeS screen was manually turned OFF by pressing their respective power buttons within 5 seconds of a VoIP call. Carroll et al. (2010) conducted tests with different backlight settings including the OFF mode. However, the method to turn the backlight OFF was not revealed.

The mobile application evaluations followed the wireless technologies evaluations; and evaluated battery and data consumption by IM and SIP applications. The reports of Alcatel-Lucent (2014) and Avast (2017) presented mobile application rankings based on battery and data consumption on smartphones, however, the reports did not disclose the methods of data collection. Therefore, the mobile application evaluation study had to devise methods to measure and record battery and data consumption by IM and SIP applications.

The least battery draining LeS and the corresponding Wi-Fi and cellular radio combination obtained as a result of the wireless technology evaluation fulfilled the hardware requirement for mobile application evaluation; and the evaluations were conducted in the battery efficient screen OFF mode. Unlike the wireless technologies evaluation, the VoIP call procedure was refined to 30 minute bi-directional voice traffic transmission; using two audio chunks that were prepared using the method presented in Section 3.3.5.2; and played via two PC speakers, as shown in Figure 15. The impact of 2G and 3G voice calls on power consumption in smartphones can be observed in Perrucci et al. (2011, 2009). However, whether voice data (sample or real human talking) was used in those voice call experiments was not revealed. The data collected from the current wireless technology and mobile applications evaluations, were taken through data analysis processes for conclusions.

The data analysis technique for wireless technology evaluation was presented in Section 3.3.6.1. Data was collected from the 60 LeSs for the different types of network mode combinations. The statistical methods, ANOVA and Tukey post-hoc analysis were selected to make comparisons.

The smartphone battery consumption related work presented in Section 2.3.2 revealed usage as average results, which compare the collected data. Nurminen, and Noyranen (2008), Balasubramanian et al. (2009), Friedman et al (2011) compared the performance of wireless technologies present in multiple smartphones to identify least battery consuming wireless technology in each smartphone; but they did not compare the smartphones against each other. The ANOVA method compared the battery consumption during VoIP calls in each network mode combination. These results are shown in Table 12 for each VoIP application between the three LeSs under experiment in a pairwise manner (Brand 1 with Brand 2, Brand 2 with Brand 3, and Brand 1 with Brand 3) to show whether or not there were significant differences between the mean of battery consumption results between the LeSs. The Tukey's HSD method followed the ANOVA analysis to determine which means were significantly different, in order to identify the least battery draining LeS overall.

The mobile application evaluation data analysis was presented in Section 3.3.6.2. The average battery consumption by an IM or an SIP application was calculated using Equation 3.2. Section 2.3.2 revealed usage using average results, to compare battery consumption data. The data drain figures of IM and SIP applications were normalized for 30 minutes, using Equation 3.3. The results obtained from Equations 3.2 and 3.3 were compared for conclusions.

The next section discusses the empirical results of the wireless technology and mobile applications evaluations, respectively, which were presented in Section 4.2.

5.2.3 Discussion of results

The wireless technology evaluation presented a framework to compare a group of LeSs based on battery consumption to identify the least battery consuming LeS. The empirical results of the wireless technology evaluation were presented in Section 4.2.1. The wireless technology evaluation results consisted of: (a) battery consumption comparison for 3 LeS brands; (b) DBM of screen ON and OFF results for VoIP calls for each LeS for each network mode combination; and (c) average battery consumption during voice calls in the screen OFF mode over Wi-Fi in different network mode combinations and 3G with Wi-Fi active or inactive, for each particular LeS. The results of (a) were presented in Table 25, Table 26, Table 27, and Table 28, and those of (b) were presented in Table 29 and

Table 30. The overall analysis of LeS comparison results of (a) and (b) produced a hierarchy of LeSs for VoIP calls using Wi-Fi or 3G in the more efficient screen OFF mode, with Brand 3 as the least battery draining, Brand 2 in second place and Brand 1 performing inferior to all. Results of (c) for each brand were presented in Table 31, Table 32, and Table 33 for each brand respectively. The results of (c) showed that 3G voice calls consumed more battery than Wi-Fi voice calls in all the LeSs. Such results where 3G consumed more battery than Wi-Fi were also confirmed in Xiao et al. (2008), Balasubramanian et al. (2009), Perrucci et al. (2011), and Kalic et al. (2012). In addition, the results of 3G in (c) showed that with Wi-Fi radio on and idling in the background every LeS consumes more battery than with usage of 3G only. Further, the results of least battery consumption during voice calls over Wi-Fi in different cellular network mode combinations in (c) showed W-PLAIN mode for usage with SIP and IM voice calls in Brand 1; W-3G mode for SIP and W-AUTO for IM voice calls, respectively, with Brand 2; and W-AUTO mode for usage with IM and SIP voice calls in Brand 3. The difference in battery consumption during Wi-Fi communication amongst different brand smartphones but with similar Wi-Fi specifications can also be observed in Nurminen, and Noyranen (2008) and Friedman et al (2011). Therefore the wireless technology evaluation culminated in identifying Wi-Fi as the preferred mode of voice calls regardless of the brand of LeSs; a hierarchy of LeSs from least to most battery consuming LeS for Wi-Fi (or 3G in case Wi-Fi is absent) voice calls in the more efficient screen OFF mode; and different least battery consuming Wi-Fi and cellular radio combinations for different LeSs.

The mobile applications evaluation presented a framework to measure battery and data drain by common IM and SIP applications to further minimize battery consumption in LeSs; and data consumption for network users. Therefore, the mobile application evaluations investigated battery and data drain using the least battery consuming LeS (Brand 3) informed by wireless technology evaluation and its least battery draining Wi-Fi and cellular radio combination for VoIP calls in the battery friendly screen OFF state. The IM applications evaluated were WhatsApp, Messenger, IMO and Viber; and the SIP clients evaluated were SipDroid, CSIP, Zoiper, and MizuDroid.

The empirical results of the mobile application evaluation were presented in Section 4.2.2. The high-level interpretation of overall battery consumption results using Figure 25 revealed that SIP applications consumed less battery than IM applications. Of the eight applications under scrutiny, the SIP client, SipDroid, consumed the least battery, and the IM application IMO

consumed the most. Within their specific groups, as shown in Figure 25, a hierarchy was established for SIP and IM applications, respectively, based on the empirical results of battery consumption. For the SIP clients, the hierarchy of least to most battery consuming was SipDroid, CSIP, Zoiper and MizuDroid. For the IM applications, the hierarchy of least to most battery consuming was WhatsApp, Viber, Messenger, and IMO. The high level interpretation of data consumption results using Figure 26 showed that IM applications had lower data consumption than SIP applications. Of the 8 social communication applications, WhatsApp consumed the least data overall and SipDroid consumed the least data of all SIP application tested. As shown in Figure 26, a hierarchy was established for the particular groups of SIP and IM clients, respectively, based on their data consumption empirical results. In the case of SIP applications, the hierarchy of least to most data consuming application was SipDroid, MizuDroid, CSIP, and Zoiper. It is noteworthy to mention that the mobile application evaluation study was unable to produce related work that evaluated battery and data consumption of SIP clients. In the case of IM applications the hierarchy of least to most data consuming application was WhatsApp, IMO, Messenger, and Viber. Therefore the mobile application evaluation study identified SipDroid as the most suitable SIP application and WhatsApp as the as the most suitable IM application for Wi-Fi VoIP calls for the LeSs.

The Alcatel-Lucent (2014) report had reported IM application usage-cost rankings based on battery and data consumption rankings, respectively, for WhatsApp, Viber, and Messenger (did not evaluate IMO). The battery consumption ranking reported by Alcatel-Lucent (2014) showed WhatsApp to be the least battery consuming followed by Viber and then Messenger. These results are similar to the rankings obtained from this current mobile application evaluation. However, the data consumption ranking reported by Alcatel-Lucent (2014) showed Viber to be least data consuming followed by Messenger and then WhatsApp and were exactly the opposite of the data consumption rankings obtained by this current mobile application evaluation. The difference in IM application rankings of data consumption obtained from mobile applications evaluation and those presented in Alcatel-Lucent (2014) report is evidence that recent application updates play a key role in their data consumption behaviour. The same can be said for the battery consumption behaviour of IM applications, even though the IM application rankings using the current mobile application evaluation and Alcatel-Lucent (2014) were same in terms of battery consumption.

Therefore, constant re-evaluations of IM and SIP applications, to keep end-users informed on the latest rankings in terms of battery and data consumption are necessary.

5.3 Chapter Summary

This chapter discussed the motivation, methods, and results of the scalability quantification and smartphone battery consumption frameworks. The development of the frameworks was motivated by elements such as; CWMNs and LeSs as cheap network access alternatives for low-income rural regions of sub-Saharan African and developing Asia; scalability issues of WMN with increases in size and traffic; lack of a holistic network scalability quantification model built around recommended QoS requirements for end-user multimedia traffic; scarcity of electricity in the abovementioned regions; Wi-Fi as a least battery draining wireless technology compared with 2G and 3G; lack of work on fine-tuned usage of Wi-Fi and cellular radio combination; and lack of work on least battery and data consuming social communication application for usage with the battery capacity restricted LeSs. The discussion of methods adopted to develop the two frameworks showed testbed emulation experiments as a common critical element in both frameworks. Usage of an emulation testbed was informed by related work. Elements selected for testbed experiment design showed, in light of related work (where possible), usage of hardware and software elements accessible to end-users in experiments; data collection methods that used TCP using *iPerf* to measure throughput and voice traffic using D-ITG to measure latency, jitter, and packet loss in case of scalability quantification experiments; data collection methods to measure battery and data consumption using battery and data profilers, respectively, during voice calls in the case of smartphone battery consumption experiments; usage of regression as a data analysis technique for scalability quantification data; and ANOVA, Tukey, and mean as data analysis techniques for smartphone battery consumption. The discussion of results analysed the efficiency of the frameworks in answering the research questions. The scalability quantification experimental results analysis yielded equations for the MPv2 testbed and the UniFi testbed that could be used to predict maximum hop limit in WMN. The smartphone battery consumption experiments yielded the least battery consuming LeS from a group; the least battery consuming Wi-Fi and cellular radio combination in each of the LeSs; that each LeS has its own specific least battery consuming Wi-Fi and cellular radio combination; the least battery and data draining IM and SIP application for Wi-Fi VoIP calls from the group.

6 Conclusion

This chapter presents the overview of research goals in Section 6.1 followed by contributions and recommendation made by the study in Section 6.2 and Section 6.3, respectively, limitations of the study in Section 6.4 and direction for future work in Section 6.5.

6.1 Overview of research goals

The research study investigated the scalability of WMNs to help rural community network designers build more optimal topologies to maintain rigorous QoS requirements. The WMN scalability investigations adopted network traffic emulation using indoor testbeds setup using OTS mesh hardware to measure performances of TH, RTL, RTJ, and PL% with increasing hop length; and to convert performance results into network scalability quantification equations that could be used to find the maximum hop length between source and destination mesh nodes while maintaining recommended QoS performance targets. However, in the process of doing so, it was recognized that the scalability of actual mesh nodes was only one part of the challenge. The second challenge was to help the users of rural community mesh network choose and use LeSs with a view towards conserving battery life. Therefore, in parallel to the network scalability quantification study, smartphone battery consumption investigations were carried out using emulation over testbeds, with a group of OTS LeSs to measure, compare and identify the least battery consuming LeS and wireless radio for communication; and the least battery and data consuming social communication application from a group of top-ranked IM and SIP applications for usage with the LeS units.

6.2 Contribution

The central contribution of the research is a two-pronged framework to help design CWMNs; and offer network administrators the means to help end users choose LeSs and applications to conserve battery life and data. This section presents a summary of the two frameworks.

6.2.1 Scalability quantification framework

The scalability quantification framework is a stepwise approach that considers key performance metrics of wireless mesh networks: throughput, latency, jitter and packet loss; which all contribute towards the scalability of WMNs. The network scalability quantification framework emerged as a result of the investigations that aimed to answer the research question: *Given the baseline (first*

hop) throughput, latency, jitter, and packet loss, what is the maximum hop length limit between mesh nodes and the gateway in a given wireless mesh network, while maintaining acceptable quality of service limits?

Wired and wireless network infrastructure must deliver specific performance targets that are based on the type of network traffic. The performance targets for key network metrics throughput, latency, jitter, and packet loss, for every type of network traffic, are set by ITU-T to deliver QoS to end-users. Researchers over the years have criticized WMNs for their deteriorating network performance as the hop length increases between source and destination nodes; and also with increasing traffic. This claim is based on related work that focused on the performance in WMNs presented in Section 2.2.2. In addition, the related work in Section 2.2.2 showed that the decline in network performance in WMN with increases in hop length and traffic was a characteristic of the network itself, because performance declined regardless of optimizations to improve performance. Therefore, the network scalability quantification study sought to identify the maximum threshold hop limit beyond which a WMN cannot deliver recommended performance targets for throughput, latency, jitter, and packet loss.

Notable related work on scalability quantification, presented in Section 2.2.3, tackled the challenge with proposed throughput quantification models. The scalability quantification study, then followed in these footsteps to develop an experimental model to collect and analyse results of throughput, latency, jitter, and packet loss in order to predict the cut-off hop length limit between mesh router and gateway. The experimental design to arrive at this model, presented in Section 3.2, comprised six steps to determine: 1) physical topology; 2) type of tests; 3) experiment technique; 4) testbed setup; 5) data collection; and 6) data analysis. Together, these steps yielded a scalability quantification model informed by all four KPMs. The physical topology chosen was clustered-type. The types of tests were: a TCP test to yield results for throughput; and voice call tests to yield results for latency, jitter, and packet loss. The experimental technique chosen was network emulation, and entailed a choice of mesh routers (MPv2 and UniFi) and end-user devices (RPi2s); and TCP (iPerf) and voice traffic (D-ITG) generators as key software resources.

There were two indoor multi-hop WMN testbeds used during the course of the network scalability quantification. With Zenzeleni network serving as the main background the first experimental testbed setup commenced towards the end of 2015 with ‘mesh potatoes’, MPv2,

deployed in Zenzeleni. While the MPv2 testbed experiments were still in progress, Zenzeleni migrated to(wards) UniFi devices by the end of 2017. Furthermore, MPv2 devices had gone out of production by then. Thus, in 2018, in order to use mesh routers available in the market and/or functional in CWMNs, a second UniFi testbed was built, using devices similar to those in the new Zenzeleni networks. The detailed process of constructing MPv2 and UniFi testbeds was presented in Sections 3.2.4.1 and 3.2.4.2, respectively.

The data collection process, described in Section 3.2.5, included the performance of throughput, latency, jitter, and packet loss during emulated round-trip traffic transmissions. To measure round-trip throughout performance, TCP traffic was sent in both directions of a link using *iPerf* because the software measured TCP throughput from client-to-server at the server. Measurement of round-trip latency, jitter, and packet loss performance data, was centered on a voice traffic profile. The G.711 encoding scheme was selected for the voice traffic because it has the largest voice payload size (not counting the overhead) amongst commonly used codecs. In addition, this encoding scheme was also in-line with the G.711-encoded SIP voice calls supported by the MPv2 units. The MPv2 testbed experiments collected network performance data of bi-directional throughput; and single-flow round-trip latency, jitter, and packet loss, for each hop link pair in the testbed. The data collection method for the MPv2 testbed was later expanded during experimentation over the UniFi testbed. However, the choice of traffic profiles remained the same. The UniFi testbed experiments measured performance of round-trip throughput over inter-cluster hop lengths; and multiple voice flows in the specific case of latency jitter and packet loss. The details of data collection methods chosen for MPv2 and UniFi testbeds were presented in Sections 3.2.5.1 and 3.2.5.2, respectively.

The data analysis produced scalability quantification equations as a result of the application of mathematical modelling techniques to the data collected from experiments over the MPv2 and UniFi testbeds. The modelling of results was conducted using power and exponential regression analysis techniques; and equations were formed for the regression technique with the higher R^2 value. The latency, jitter, and packet loss results required further mathematical modelling to combine the results of multiple-flows into a singular equation for each network metric. The details of the mathematical modelling techniques adopted for MPv2 and UniFi testbeds were presented in Sections 4.1.1.2 and 4.1.2.2, respectively.

The end result of the mathematical modelling led to performance trend equations for each network performance metric. The different network metric equations revealed that (a) performance metrics in WMNs have different scaling trends, as shown by the power equations obtained from the MPv2 testbed experimentation, and exponential equations obtained from UniFi testbed experimentation; (b) it is imperative to know the first-hop length value of each network metric in order to predict scalability of the given network metric; and (c) the scalability of a WMN depends on the network topology. A demonstration to predict the maximum cut-off hop limit using the scalability equations obtained for MPv2 and UniFi testbeds was presented in Section 6.3.1.

The overall research considered the network scalability quantification framework, adopted to answer the research question presented earlier in this section, as a unique contribution that can be used by the WMN research community and CWMN engineers to predict hop-length scalability that can offer voice traffic QoS in WMNs.

6.2.2 Smartphone battery consumption framework

The smartphone battery consumption framework is the outcome of investigations that aimed to answer the research question: *What is the most efficient Wi-Fi and network mode combination; and social communication application, in terms of battery and data consumption, for low-income off-grid users residing in rural areas given the presence of community wireless mesh networks?*

The literature review showed that high tariffs, handset prices, and low electricity access in sub-Saharan Africa (in Section 2.3.1.1), and high handset prices and poor electricity supply in developing Asia (in Section 0) were key factors contributing to low Internet penetration rates in these regions. In addition, the solar-power setup that powered Zenzeleni networks between 2012 and 2017, due to absence of electricity in the community, presented an alternative electrification model for deployment of CWMNs in areas with scarce electricity. Another factor to be taken into consideration is that the relatively small battery capacity of LeSs have presented recharging challenges for regions with scarce or no electricity supply. Due to the LeS recharging issue, end-users in such regions struggle to use CWMNs effectively.

Related work presented in Section 2.3.2 compared multiple wireless technologies in a smartphone and indicated that Wi-Fi consumes less battery than any other wireless radio. However, it emerged that managing elements such as the cellular radio active in the background during usage of Wi-Fi; and usage of certain social communication applications can further

decrease battery drain in LeS. The literature review was unable to reveal published related work tackling the abovementioned elements. Therefore, the smartphone battery consumption study utilised an experimental design to compare and analyse results of battery consumption during (a) communication over Wi-Fi in different cellular radio combination modes; and (b) usage of different social communication applications. The experimental design, presented in Section 3.3, kept to steps similar to the scalability quantification experiment design.

The physical topology in Section 3.3.1 reveals that having a specific type of network setup is not a requirement when measuring end-user devices; unlike the performance of a network. The types of tests, described in Section 3.3.2, were based on network traffic tests for experiments, and prioritized voice calling. This choice was made by drawing on conclusions from a survey from Rey-Moreno et al. (2016) on a Zenzeleni community's mobile airtime usage. Emulation was again chosen as the experimental technique, and is described in Section 3.3.3. Again, emulation required both hardware and software resources. The wireless technology evaluation was conducted using three different LeSs (20 for each type) selected from the local market at the time of experiments. Their selection process was presented in Section 3.3.3.1. The objective behind using multiple LeSs in the wireless technology evaluation was to show potential end-users how to compare battery consumption results along with revealing least battery draining Wi-Fi and cellular technology combination for voice calls. The key software requirement for wireless technology evaluation was the battery measurement tool supplied with the LeSs; and SIP and VoIP applications for voice calls. The selection process for software resource for wireless technology evaluation was presented in Section 3.3.3.2.

Following the finalization of hardware and software resources, an experimental testbed was set up; and data collection and data analysis techniques ensued. The stepwise details of the testbed setup and data collection for wireless technology evaluation were presented in Sections 3.3.4.1 and 3.3.5.1, respectively. The collected data were: drop in battery percentage during firstly voice calls in screen ON and OFF states over Wi-Fi with different cellular radio combinations, and secondly 3G voice calling with Wi-Fi radio in active/idle and off modes. The data analysis in Section 3.3.6.1 described the ANOVA and Tukey post-hoc statistical methods that were used to compare the results from the three different LeSs.

The mobile applications evaluation extended the wireless technology evaluation and used the most battery efficient LeS, obtained from the previous results, to compare VoIP (social communication) applications. The key software decisions involved selection of VoIP applications, and battery and data measurement tools. The VoIP applications chosen were commonly used IM and highly ranked SIP applications at the time of evaluation. The battery profiler consisted of a third-party tool that recorded power draw by the applications during their usage as a result of CPU load; and a default data measuring application provided with the LeSs. The stepwise details of the experimental testbed setup; data collection and data analysis techniques adopted for mobile applications evaluation were presented in Section 3.3.4.2, Section 3.3.5.2, and Section 3.3.6.2, respectively.

The end result of the wireless technology evaluation led to the identification of the least battery draining LeSs amongst the 3 brands used in experiments; and the least battery draining Wi-Fi and cellular radio combination in each of the LeSs for voice calls in least battery draining screen OFF state. The wireless technology evaluation revealed that there is no common least battery draining Wi-Fi and cellular radio combination that can be applied to all LeSs; and each LeS has its own specific least battery draining Wi-Fi and cellular radio. The results of mobile application evaluation led to the identification of the least battery and data draining IM and SIP application for Wi-Fi VoIP calls. The results showed IM applications consumed less data than SIP applications; but SIP applications consumed less battery than IM applications. However, the results of the mobile application evaluation revealed that the application version plays a major role in battery and data consumption, and figures can change for updated versions of applications.

In the light of constant advancement of LeS hardware and software; and social communication applications, the overall research considers the smartphone battery consumption framework, consisting of wireless technology and mobile application evaluation, which is adopted to answer the research question presented earlier in this section. This is a significant contribution for similar future experiments, which should be used to promote low-cost smartphone adoption in rural low-income areas with irregular or no electricity supply.

A demonstration of usage of the smartphone battery consumption framework to compare LeS; to identify the least battery draining Wi-Fi and cellular radio combination in each of the LeSs

compared; and to compare IM and SIP application examples (social communication applications) in terms of battery and data consumption is presented in Section 6.3.2.

6.3 Recommendations

The overall research framework consisting of mesh network scalability quantification and smartphone battery consumption frameworks is a recommendation in itself for researchers and network engineers involved in research aiming at scalability in WMNs and/or promoting community WMNs. Based on the overall findings from the abovementioned framework, the research recommends that investigations involving any performance related aspect of WMNs or battery and data consumption in smartphones should use network emulation technique (or real-world testing if possible). Within the scope of network emulation, further recommendation entails the usage of hardware and software in the network emulation. It is recommended that the hardware used in experiments should be recent and readily available in the market or functional in a CWMN in case of mesh routers. In the case of software resources; network traffic generation tools should be able to measure performance results of all the network metrics using end-user traffic profiles; and social communication applications should be of the most recent version.

Based on the experimental findings of the network scalability quantification evaluation, the network metric equations are recommended for prediction of throughput, latency, jitter, and packet loss network metrics with increasing hop-length using the first-hop length value of each metric; and the baseline first-hop length values for each metric should be measured using the network emulation technique. The network scalability quantification equations are also recommended for existing WMN infrastructures aiming to offer voice services within the QoS recommendations. For cases of existing WMNs, there will likely be cases where the mesh devices are not similar to the ones used in this research, however, the fist-hop values of the existing WMNs can be used with the equations to estimate baseline hop length limits. For more detailed network scalability quantification investigations, the recommendation is to adopt the network scalability quantification framework; and modify it to suit the QoS objectives of the particular WMN. To decide a baseline deployment strategy, demonstration of usage of the network scalability quantifications to decide maximum hop limit is presented in Section 6.3.2.

Based on the smartphone battery consumption investigation findings, the research recommends usage of Wi-Fi as the primary wireless technology with LeSs for voice

communication for end-users in rural and low-income regions with scarce electricity, given the presence of CWMN. It is recommend for researchers, especially with interest in promoting low-cost Internet penetration methods in rural low-income regions, to participate in an experimental study of battery and data consumption, like the wireless technology and mobile applications evaluations. Given the presence of multiple LeSs in the market, the wireless technology evaluation framework is recommended for constant comparison of LeSs based on their battery consumption and the results need to be communicated via a medium easily accessible to end-users. It is recommended that in addition to communication of comparison results of LeSs in terms of battery consumption, the wireless technology evaluation must also be communicated and the least battery consuming wireless radio combination in each LeS needs to be compared. Similarly, the constant updates of social communication applications by their developers can fluctuate their battery and data consumption figures, and the rankings obtained as a result of a mobile applications evaluation, such as those of IM and SIP applications in this research, may change. Therefore, the mobile applications framework is recommended for constant comparison of social communication applications based on their battery and data consumption and then communicate the results via a medium easily accessible to end-users to assist them in selecting the least battery and data consuming applications.

However, it is important to close this section by mentioning that the selection of an LeS or a social communication applications is ultimately a personal decision and factors such as per-capita or per-household income and applications trends can affect the selection of brands.

6.3.1 Demonstration of how to use the scalability equations

This section presents a demonstration to predict the maximum cut-off hop limit using the scalability Equations 4.2, 4.4, 4.6, and 4.8 obtained from the MPv2 testbeds; and Equations 4.10, 4.15, 4.22 and 4.24 obtained from the UniFi testbeds. In order to demonstrate the application of the equations towards predicting the maximum cut-off hop limit of WMNs, take note of the following: (a) the threshold values using the recommended multimedia QoS requirements for conversation voice presented in Table 4, which were modified for round-trip traffic; (b) the cut-off hop length limit of the worst scaling network metric, this was used to decide the maximum hop length limit between source and destination; and (c) the average 2 hop values for each performance metric obtained from the UniFi testbed experiments, as reference first-hop values. The threshold

values for TH, RTL, RTJ, and PL% used for predicting the maximum hop-length limit of WMNs are presented in Table 34.

Table 34: Network metric threshold values for prediction of scalability limit
The table shows the threshold values selected to predict scalability limit. The values are adapted from the VoIP requirements for QoS presented in Table 4.

QoS metric	Threshold
TH	640Kbps
RTL	< 300ms
RTJ	< 30ms
PL%	< 2%

The TH threshold between a mesh link, regardless of the hop length, that is considered reliable for VoIP calls was selected as 640Kbps, which is twice the recommended data rate for conversational voice, inclusive of 320Kbps upload and 320Kbps download rates. The RTL threshold value chosen for prediction was <300ms, which is also twice the preferred requirement of one-way latency for VoIP. The RTL threshold value assumed that the latency values from caller to receiver, and vice-versa, are the same. The RTJ threshold value chosen for prediction was < 30ms which is the same as the preferred requirement for one-way jitter for VoIP. The RTJ value was kept the same as the recommended average one-way jitter for VoIP, because jitter represents variation in latency. Therefore, the demonstration assumes that since jitter in the direction of caller to receiver is representative of variation in one-way latency, then the jitter in the opposite direction (from receiver to caller) is also representative of one-way latency. Hence, RTJ representative of RTL, which is total latency from caller to receiver and back, is the average of jitter of both directions. The PL% threshold value chosen is <2%, which is cumulative of all the packets lost on the round-trip path. The selected PL% threshold value is twice the recommended one-way PL% percentage for conversational voice in Table 4.

It is noteworthy to mention that the study was unable to find reported literature with such a KPM-based approach to scaling models for WMNs. Niculescu et al. (2006) have used R-score to determine VoIP quality in their experiments with increasing number of hop lengths. However, the R-score is built upon one-way latency, jitter, and packet loss rate metrics rather than round trip.

6.3.1.1 Throughput hop length limit

The cut-off TH value used for predicting hop length performance was 640Kbps as shown in Table 34. The VoIP calls using the G.711 codec, as used in the MPv2 and UniFi testbed experiments,

require 174.2Kbps bandwidth per call in a real world scenario (see Section A1.3, Appendix A1 for bandwidth requirements for different VoIP codecs). Therefore, given the threshold TH of 640Kbps and the bandwidth requirement of 174.2Kbps by one G.711 encoded VoIP call, it can be stated that a mesh link with a maximum achievable TH of 640Kbps can support up to three G.711 encoded VoIP calls. Therefore, TH scalability predictions for optimal (or threshold) hop length to support 3 G.711 encoded VoIP calls were carried out using Equation 4.2 of the MPv2 testbed and Equation 4.10 of the UniFi testbed; and both are shown in Figure 28. A reference TH value of 48.26Mbps, which is the average TH value for 2 hops from the UniFi testbed data presented in Table 14, was used for T_1 in the TH equations.

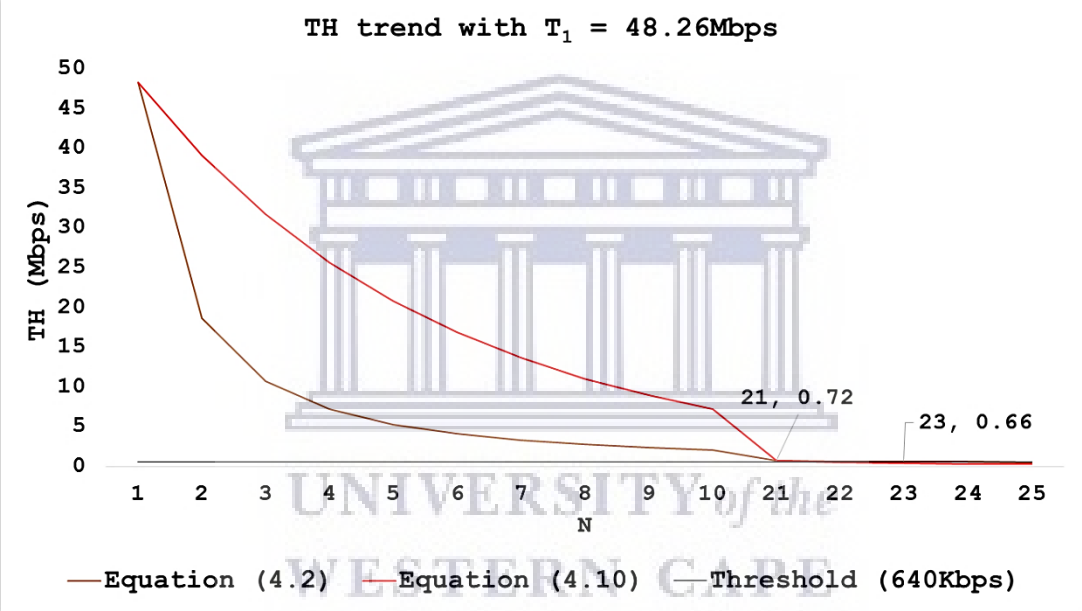

Figure 28: Hop length limit predictions using throughput quantification equations
The figure shows trends for throughput using the value of 48.26Mbps used as the average value for 1-hop length between source and destination mesh nodes, and was obtained from UniFi experiments for 2 hop lengths between two mesh clusters.

It can be observed in Figure 28 that if a WMN were scaled according to either Equation 4.2 or 4.10, then the particular WMN is capable of offering 3 G.711 encoded VoIP calls for N > 10. The TH scalability under Equations 4.2 and 4.10 shows that a WMN is capable of offering three G.711 encoded VoIP calls for up to 23 hops if it is scaled according to Equation 4.2; and 21 hops if it is scaled according to Equation 4.10.

6.3.1.2 Round-trip latency hop length limit

The cut-off value used for predicting the RTL scalability with increasing hop length was 300ms as shown in Table 34. It is important to highlight that the RTL Equation 4.4 of the MPv2 testbed and Equation 4.15 of the UniFi testbed represent RTL trend for transmission 172B of G.711

encoded VoIP packets sent at the rate of 50pps evaluating to a total of 8600B of data sent per second. For prediction, a reference RTL value of 24.05ms that is the average of RTL values for each prime numbered flow for 2-hops shown in Table 14, was used for L_1 in the RTL equations. Figure 29 shows the RTL scalability predictions using Equations 4.4 and 4.15 to find the RTL threshold hop length limit beyond which a given WMN cannot offer RTL of 300ms. The RTL scalability predictions show that: (a) if RTL in a WMN is scaled according to Equation (4.4), then the threshold hop limit would be approximately 6 hops for that WMN; and (b) if RTL in a WMN is scaled according to Equation 4.15, then the threshold hop limit of that WMN would be 11 hops.

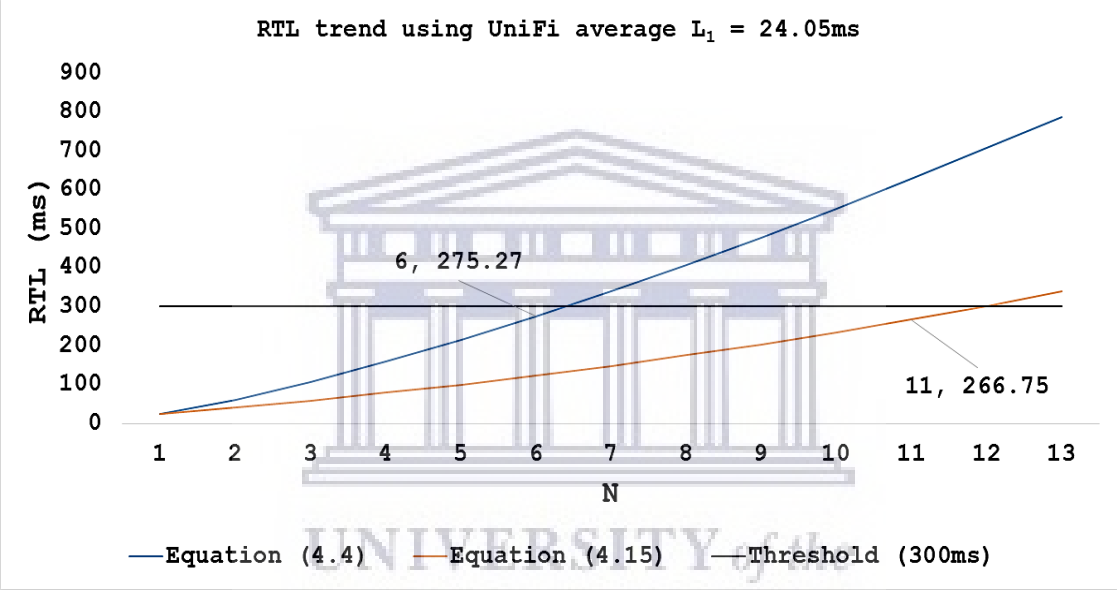

Figure 29: Hop length limit predictions using round-trip latency quantification equations
The figure shows predicted scalability trends for RTL using Equation 4.4 (MPv2) and Equation 4.15 (UniFi); and using the value of 24.05ms as the average first hop RTL between source and destination mesh nodes. Cut-off predition using Equation 4.4 is approximately 6 hops; and Equation 4.15 is approximately 11 hops.

6.3.1.3 Round-trip jitter

The cut-off RTJ value used for predicting the RTJ scalability with increasing hop length was 30ms (threshold) as shown in Table 34. The RTJ scalability Equation 4.6 for the MPv2 testbed and Equation 4.22 for the UniFi testbed represent the variance in RTL during transmission G.711 encoded VoIP packets over the testbed networks. To evaluate the RTJ trend using Equations 4.6 and 4.22, and to predict the maximum cut-off hop length, a reference RTJ value of 21.69ms, which is the average of RTJ values for each prime numbered flow for 2 hops shown in Table 16, was used for J_1 in the RTJ scalability equations. The RTJ scalability trend is presented in Figure 30 and shows that if the RTJ in a WMN is scaled according to either Equation 4.6 or 4.22, then the threshold hop limit for that WMN would be approximately 1 hop. It is noteworthy to mention that

this cut-off hop length limit of 1 may seem unrealistic, however, the results are predicted using a reference first-hop jitter value that can differ amongst WMNs.

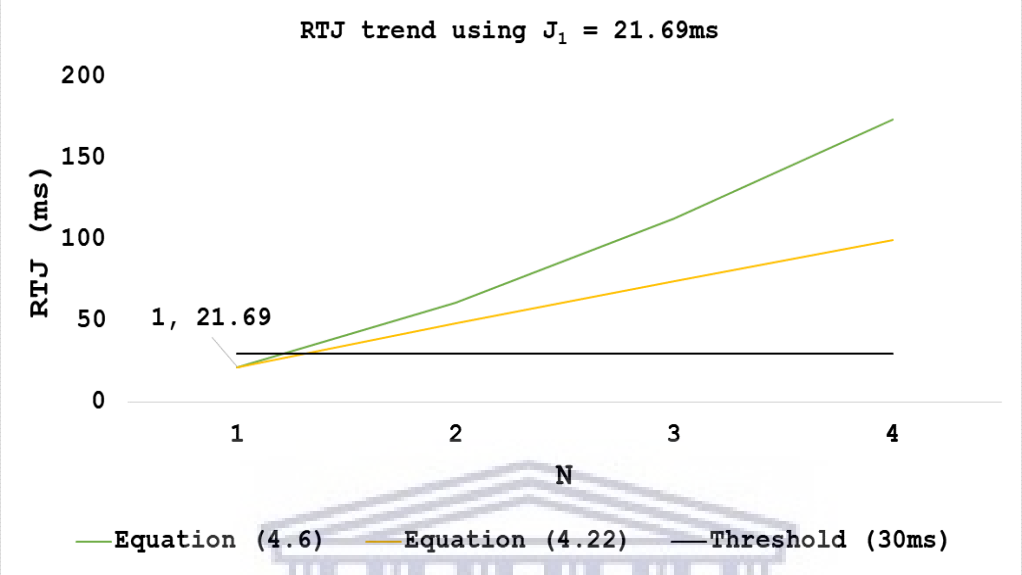

Figure 30: Hop length limit predictions using round-trip jitter quantification equations
The figure shows predicted scalability trends for RTJ using Equation 4.6 for MPv2 and Equation 4.22 for UniFi); and using the value of 21.69ms as the average first hop RTL between source and destination mesh nodes. Cut-off prediction using Equation 4.6 or Equation 4.22 is approximately 1 hop.

6.3.1.4 Packet loss percentage

The cut-off value used for predicting PL% with increasing hop length was <2% (threshold) as shown in Table 34, twice the recommended <1% one-way PL% recommended for interactive voice as presented in Table 4. The PL% scalability Equation 4.8 for the MPv2 testbed and Equation 4.24 for the UniFi testbed represent the PL% trend for round-trip G.711 encoded VoIP traffic transmission. To evaluate the PL% trend using Equations 4.8 and 4.24, and to predict a maximum cut-off hop length, a reference PL% value of 0.186% was used for P_1 which is the average of PL% values for each prime numbered flow for 2 hops presented in Table 17. The evaluated PL% trend presented in Figure 31 shows that (a) if a WMN is scaled according to Equation 4.8, then the threshold hop limit for that WMN would be approximately 2 hops; and (b) if a WMN is scaled according to Equation 4.24, then the threshold hop limit for that WMN would be 5 hops.

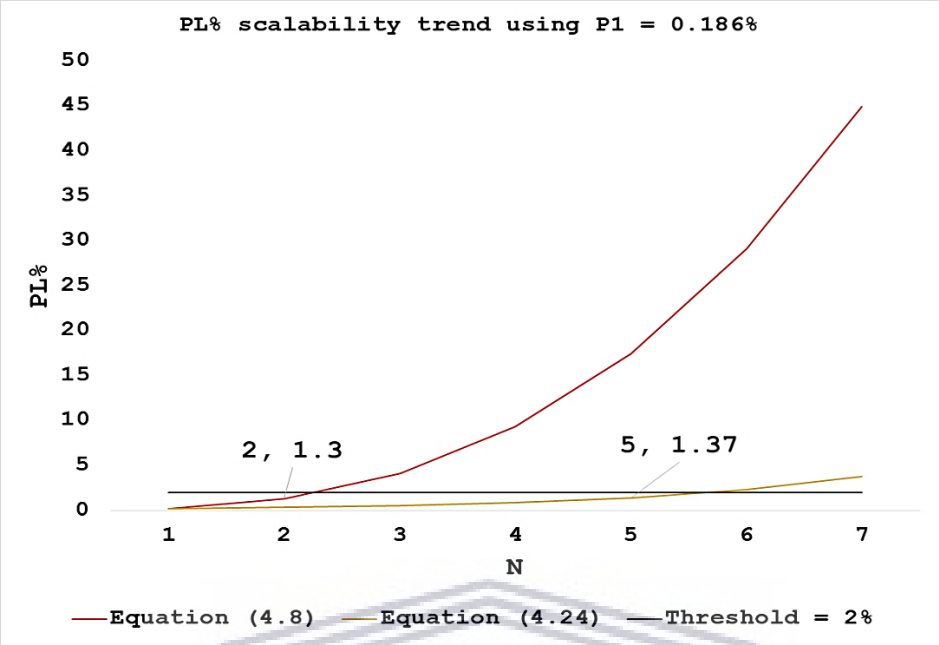

Figure 31: Hop length limit prediction using packet loss quantification equations

The figure shows the scalability trends for PL% using Equation 4.8 (MPv2) and Equation 4.24 (UniFi); and using the value of 0.186% as the average first hop PL%. Cut-off prediction using Equation 4.8 is approximately 2 hops; and Equation 4.24 is approximately 5 hops.

6.3.1.5 Putting the four KPMs together

As mentioned earlier, the maximum cut-off hop length of the worst scaling network metric ultimately decides the optimal hop length limit between source and destination mesh nodes. After prediction of scalability trends for TH, RTL, RTJ, and PL% using equations of MPv2 and UniFi testbeds, respectively, RTJ showed the worst scaling behaviour with a cut-off hop limit of only 1 hop. RTJ is significantly important for networks that are supporting (or intend to support) VoIP because high jitter causes fluctuations in the call quality leading to choppy and dropped calls. Therefore, according the demonstration of the hop-limit predictions using RTJ Equations 4.6 and 4.22 where J_1 = 21.69ms, the hop distance between a mesh device and base station should not cross 1 hop. Correlating the maximum cut-off hop length obtained from scalability prediction to the results of RTJ obtained from UniFi testbed experiments in Table 16, it can be observed that the average RTJ values of each prime numbered flow crossed the 30ms threshold after 2 hops. However, the 2 hop distance in the UniFi testbed, as shown in Figure 10, is the inter-cluster hop length between two UniFi units which was 1 hop from the base station in line with the hop-length scalability predictions. With further reference to RTJ results in Table 16, it can be observed that the UniFi experimental network was able to maintain the threshold RTJ of 30ms for all the 41 VoIP flows for an inter-cluster hop length of 2. Therefore, based on the RTJ results from the UniFi

testbed in Table 16 and the scalability prediction results of RTJ, it can be stated that a WMN that scales under Equation 4.6 or Equation 4.22 with measured first hop RTJ value equal to 21.69ms can offer at least 41 G.711 encoded VoIP calls over an inter-cluster hop length distance of 2 hops where a mesh device in each cluster is 1 hop from the base station.

It is very important to mention that the first-hop values for network metrics can be different for different WMNs (experimental or testbed) and therefore the cut-off hop length limit will differ if the MPv2 or UniFi testbed equations are used for predictions. However, the equations can still be used to predict baseline cut-off hop length limit WMNs; and the selection of the specific set of equations can be based upon the similarity of mesh router hardware specification similarity. Therefore, this scalability quantification framework is recommended to the research community and CWMN engineers for experimentation and further development.

6.3.2 Demonstration of how to use the smartphone comparison framework

This section presents a demonstration on the usage of the smartphone battery consumption framework to identify: (a) the least battery consuming LeS from a group; (b) the least battery consuming Wi-Fi and cellular radio combination for an LeS; and (c) the least battery consuming social communication application for an LeS. Within the framework, (a) and (b) formed the wireless technology evaluation sub-framework and (c) formed the mobile applications evaluation sub-framework. The demonstration shows how the wireless technology evaluation results assisted in identifying (a) and (b); and how the mobile applications evaluation results assist in identifying (c).

6.3.2.1 Wireless technology evaluation

The wireless technology evaluation compared 3 LeSs available in the market at the time of the experiments (see Section 3.3.3.1). CSIP SIP client and Viber IM applications were used to make voice calls (see Section 3.3.3.2). The testbed setup was presented in Section 3.3.4.1; and the data collection method was presented in Section 3.3.5.1. For each brand, data for battery percentage drop during voice calls over Wi-Fi with different cellular radio combinations (the combinations are shown in Table 12) was collected using the default battery profiler on the LeSs. Data was collected for voice calls in screen ON and OFF modes for the network mode combinations shown in Table 12. The data analysis technique was presented in Section 3.3.6.1. The analysis techniques selected were: ANOVA and Tukey post-hoc methods to compare the brands; DBM of screen ON

and OFF results to emphasize importance of keeping phone screens OFF during voice calls; and average battery drop percentage results during voice calls for each network mode combination to identify the least battery draining Wi-Fi and cellular radio combination in each LeS. The empirical results output from data analysis were presented in Section 4.2.1. This section shows how the analysed empirical results can be used to identify the least battery consuming LeS from Brand 1, Brand 2, and Brand 3; and the least battery consuming wireless radio combination in each brand. The demonstration is presented in a brand-wise manner where results of Brand 1 are discussed against results of Brand 2 and Brand 3; results of Brand 2 are discussed against results of Brand 1 and Brand 3; and results of Brand 3 are discussed against results of Brand 1 and Brand 2.

1. Brand 1

Beginning with the results of CSIP Wi-Fi voice calls with screen ON, which was presented in Table 25, Brand 1 displayed lower battery consumption than (a) both Brand 2 and 3 for W-2G; (b) Brand 2 for W-3G; and (c) Brand 3 for W-PLAIN mode voice calls, respectively. However, for W-AUTO mode calls, Brand 1 showed higher drains than Brand 2 and 3. In the case of Viber voice calls with screen ON that was presented in Table 26, Brand 1 displayed lower battery consumption than (a) Brand 2 for 3G and 3G-X calls; and (b) Brand 3 for PLAIN mode calls. The results for CSIP and Viber Wi-Fi voice calls with screen OFF that were presented in Table 27 and Table 28, respectively, showed that Brand 1 consumed more battery than Brand 2 and Brand 3 for all network combination modes. Therefore the brand comparison results show that the Brand 1 is more energy efficient than its rival Brand 2 and Brand 3 LeSs when VoIP calls are conducted in screen ON state in W-2G cellular mode. However, Brand 1 could not outperform Brand 2 or Brand 3 in any of the Wi-Fi and cellular radio combinations during the more efficient screen OFF mode VoIP calls.

The battery consumption results to identify the least battery draining network mode combination in Brand 1 that were presented in Table 31 showed that the least battery draining Wi-Fi and cellular radio combination for VoIP calls is W-PLAIN if using CSIP; and W-AUTO if using Viber. Therefore, the wireless technology evaluation identified that the least battery draining Wi-Fi and cellular radio combination for voice call by end-users with Brand 1 is W-PLAIN, that is, usage of just Wi-Fi for communication and keeping cellular radios off. In the case where the Wi-Fi is absent, and given the presence of 3G coverage in the community, VoIP calls can be conducted over 3G mode with the Wi-Fi radio turned off.

2. Brand 2

In the case of Brand 2 LeSs, it is important to mention that the Wi-Fi radio in Brand 2 could not be turned active after setting the phone to 'Airplane' mode and therefore the W-PLAIN mode tests could not be conducted. However, such a feature drawback was not mentioned in the online specifications[54] of the Brand 2 LeS, and was only discovered during identification of the possible Wi-Fi and cellular radio combinations after purchase.

The results of CSIP Wi-Fi voice calls with screen ON, which were presented in Table 25, showed that Brand 2 drained less battery than Brand 1 during voice calls in W-AUTO mode. Results for Wi-Fi voice calls with screen OFF when using CSIP, which were presented in Table 27, showed that Brand 2 consumed less battery than Brand 1 during voice calls in W-2G, W-AUTO, and W-3G mode combinations (all the network mode combinations possible with Brand 2), respectively. Results for Viber voice calls with screen ON, presented in Table 26, showed that Brand 2 consumed more battery than; (a) Brand 3 for W-AUTO; and (b) Brand 1 and Brand 3 for 3G-X and 3G calls, respectively. Viber results for Brand 2 with screen OFF, presented in Table 45, showed that; (a) Brand 2 consumed less battery that Brand 1 in all the network mode combinations (except W-PLAIN because the network mode was not possible in Brand 2); and (b) Brand 2 consumed more battery than Brand 3 in significant results of W-AUTO, W-3G, and 3G mode combinations. In summation, the comparison results with screen OFF state voice calls using Viber and CSIP showed that Brand 2 consumed less battery than Brand 1 in all the network mode combinations. Therefore, the wireless technology evaluation result patterns showed Brand 2 to be a better option than Brand 1 but an inferior option to Brand 3 for voice calls in the less battery draining screen OFF mode.

It is important to mention that the lower cost of Brand 2 as compared to its competitors, Brand 1 and Brand 3 in this case, is an attractive feature which can draw the attention of low-income rural end-users prioritizing handset cost for purchasing a smartphone. Therefore, information on the battery drain figures of the Brand 2 LeS for all the possible network mode combinations in the more battery efficient screen OFF state becomes a must. The battery

[54] Vodacom SmartKicka specification link: https://techcentral.co.za/vodacom-smart-kicka-review/50181/

consumption results to identify the least battery draining network mode combination for voice call in the least battery draining screen OFF state in Brand 2 were presented in Table 32.

The results in Table 32 showed that the least battery draining Wi-Fi and cellular radio combination for VoIP calls is W-3G with CSIP; and W-AUTO with Viber. Therefore, given the presence of a CWMN, the least battery draining Wi-Fi and cellular radio combination for voice calls by end-users with Brand 2 is W-3G, that is, usage of just Wi-Fi for communication with cellular radio in 3G mode. In the case where Wi-Fi is absent, and there is 3G coverage in the community, VoIP calls can be conducted over 3G mode with Wi-Fi radio turned off.

3. Brand 3

The Brand 3 smartphones were the most expensive of the 3 LeSs costing 51.32USD per-unit. With the higher price tag, Brand 3 came with faster processor and bigger screen than Brands 1 and 2, and yet the same battery capacity as Brand 2.

The results for Wi-Fi voice calls with screen ON using CSIP, which were presented in Table 25, revealed that Brand 3 consumed less battery than Brand 1 in W-AUTO combination. In fact this was the only screen ON state CSIP voice call test where Brand 3 consumed less battery than other brands. For CSIP voice calls with screen OFF, that were shown in Table 27, Brand 3 showed lower battery consumption than; (a) Brand 1 for W-3G, and W-PLAIN mode voice calls; and (b) both Brand 1 and Brand 2 for W-2G, and W-AUTO mode voice calls. Results for Viber voice calls with screen ON, which were presented in Table 26, showed that, Brand 3 consumed less battery than both Brand 1 and Brand 2 for W-AUTO mode. In addition, in screen ON mode, Brand 3 outperformed Brand 2 in 3G-X and 3G type VoIP calls. Results for voice call tests with screen OFF while using Viber, which were presented in Table 28, showed that Brand 3 consumed less battery than; Brand 1 during voice calls in W-2G and W-PLAIN modes; Brand 2 during 3G-X mode voice calls; and both Brand 1 and Brand 2 during W-AUTO, W-3G and 3G voice calls. Analysis of brand comparison results of Brand 3 against its rivals Brand 1 and Brand 2 revealed Brand 3 to be the least battery draining LeS for VoIP calls using Wi-Fi or 3G in the more efficient screen OFF mode.

The battery consumption results to identify the least battery draining network mode combination in Brand 3 in Table 33 showed that that the least battery draining Wi-Fi and cellular radio combination for VoIP calls was W-AUTO with CSIP and Viber. Therefore, for Brand 3, the

wireless technology evaluation study identified W-AUTO mode, that is, usage of just Wi-Fi for communication and keeping cellular radio in 3G/2G mode, as the least battery draining cellular radio mode for VoIP calls over Wi-Fi. In the case where Wi-Fi is absent, and given the presence of 3G coverage in the community, VoIP calls can be conducted over 3G mode and Wi-Fi radio turned off.

It is very important to mention that the study promotes deployment and usage of CWMNs in low-income rural regions as a cheap network infrastructure alternative that end-users can access via Wi-Fi on their smartphones. In the case where Wi-Fi is absent in the low-income rural region, the wireless technology evaluation presented 3G as the next best option for the VoIP calls using the LeS. It is noteworthy to mention that the LeS used for experiments only had up to 3G cellular radio as can be seen from the LeS specifications in Table 10; and therefore the wireless technology evaluations were limited to the evaluation of network mode combinations of 2G and 3G. The next section discusses the results of the mobile applications evaluation.

6.3.2.2 Mobile applications evaluation

The mobile applications evaluation selected 8 social communication application in the form of 4 trending IM applications and 4 highly ranked (by Google Play) SIP applications for comparison, based on battery and data consumption during voice calls (see Section 3.3.3.2). The testbed setup was presented in Section 3.3.4.2; and the data collection method was presented in Section 3.3.5.2. The mobile applications evaluation considered 30 minute voice call experiments using the least battery consuming LeS, informed by wireless technology evaluation. The PTut energy profiler was used to measure power consumption and the default data profiler on the LeS was selected to measure data consumption during the voice calls. Power consumption reflects the battery consumption because the higher the power draw, the higher the battery consumption. The adopted data analysis techniques were presented in Section 3.3.6.2. Equation 3.2 was devised to analyse battery consumption (using energy consumption) results; and Equation 3.3 was formed to analyse data consumption results.

The analysed results of battery consumption were shown in Figure 25. The battery consumption results showed that 3 of the 4 SIP applications showed lower battery consumption than every single IM application. Comparisons between battery consumption results of SIP and IM applications showed that: (a) SipDroid consumed approximately 4 times less battery than IMO,

3.4 times less than Messenger, 3 times less than Viber, and 2.6 times less battery than WhatsApp; (b) CSIP showed battery consumption approximately 2.8 times less than IMO, 2.4 times less than Messenger, 2.1 times less than Viber, and 1.9 times less than WhatsApp; (c) Zoiper showed battery consumption 1.5 times less than IMO, 1.3 times less than Messenger, and 1.2 times less than Viber; (d) Zoiper and WhatsApp exhibited almost similar battery consumption; and (e) MizuDroid exhibited battery consumption 1.37 times more than WhatsApp, 1.2 times more than Viber, 1.07 times more Messenger, and 1.08 times less than IMO. Comparisons between battery consumption results of SIP clients showed that SipDroid consumed the least battery followed by CSIP, Zoiper, and MizuDroid (in that order). Comparisons of battery consumption results of IM applications showed that WhatsApp consumed the least battery followed by Viber, Messenger, and IMO (in that order). Therefore, SipDroid consumed the least battery overall and WhatsApp consumed the least battery amongst the IM applications.

The data consumption results were presented in Figure 26. The data consumption results showed that all IM applications consumed less data than every single SIP application. Comparison between data consumption results of IM and SIP applications showed that: (a) WhatsApp consumed approximately 3 times less data than SipDroid, and approximately 4 times less data than CSIP, Zoiper and MizuDroid, respectively; (b) IMO exhibited data consumption approximately 2.7 times less than SipDroid, 3.7 times less than CSIP and MizuDroid, and 4 times less than Zoiper; (c) Messenger exhibited data consumption; approximately 1.8 times less than SipDroid, 2.5 times less than CSIP and MizuDroid, and 2.8 times less than Zoiper; (d) Viber exhibited data consumption; approximately similar to SipDroid; 1.6 times less than CSIP and MizuDroid; and 1.8 times less than Zoiper. Comparison between data consumption results of SIP clients showed that SipDroid consumed least data followed by MizuDroid, CSIP, and Zoiper (in that order). Comparison between data consumption of IM applications showed that WhatsApp consumed least data followed by IMO, Messenger, and Viber (in that order). Therefore WhatsApp consumed the least data of all the IM and SIP applications.

6.3.2.3 Putting the battery and data consumption results together

The end result of wireless technology identified: (a) Brand 3 as the least battery consuming LeS from a group of 3 LeSs (Brand 2 and Brand 1 finished in second and third place respectively); (b) W-AUTO, W-3G and W-PLAIN as the least battery consuming Wi-Fi and cellular radio

combination modes for Brand 3, Brand 2, and Brand 1, respectively; and (c) CSIP as the least battery consuming and WhatsApp as least data consuming voice calling social communication application for an LeS.

It is noteworthy to mention that the choice of LeSs can depend on the smartphone market; social communication application and type of traffic can depend on usage trends. Therefore, the smartphone battery consumption framework is recommended to the research community and network engineers aiming to promote LeSs in rural regions for further experimentation and development.

6.4 Limitations

In the case of the network scalability quantification study, the voice packets were sent at a constant rate. The voice traffic transmission over the MPv2 and UniFi testbeds was representative of a best-case scenario which assumed that there is no other traffic flowing on the mesh network, except for auto-generated routing control packets, during a call. The network scalability quantification study assumed that end-users linked to a mesh AP during a voice call were static. The quantification was based on network performance of voice calls encoded by one-type (G.711) of voice codec with the highest bandwidth per-call requirement and the largest voice payload size. The statistical analysis of performance trends was conducted using power and exponential regression techniques only. Only R^2 was used as a goodness-of-fit measure to decide between power and exponential regression techniques. The UniFi testbed setup experienced configuration restrictions, due to the commercial nature of the Ubiquity devices such as: (a) the antenna gain in each LB being pre-set to 23dBi by the manufacturer which could not be changed; (b) the Tx power in the LB units could not be reduced below 4dBm; (c) the MIMO feature could not be disabled in the UniFi units (to match the MPv2 testbed), and the Tx and antenna gain levels could only be minimized below 4dBm and 4dBi, respectively; and (d) the UniFi units required a DHCP server to function and could only be controlled from a central UniFi controller. In the case of smartphone battery consumption study, similarly to scalability quantification study, investigations were limited to voice calls only. At the end of the network scalability quantification and smartphone battery consumption experiments, either the hardware had been phased out (MPv2 and LeSs) or there were new versions of software (router firmware and IM and SIP applications).

6.5 Future work

Performance of WMN under bursty traffic will be considered in future experiments. In addition, future network performance studies will consider different types of data traffic with network saturation, thus burdening the mesh network to a much greater extent. Mobility of end-users and its impact on network performance will be explored in future work along with the possibility of a testbed setup in an outdoor environment to introduce real-world aspects to the testing. Network access to everyday end-users will be considered so that data from real traffic flow can be collected and even more realistic predictions can be made. Future quantification experiments will study network performance of WMNs under multiple voice codecs and performance trend fitting using other regression analysis techniques. In addition to R^2, other types of goodness-of-fit measures will be used to decide the regression technique that best fits a network metric performance trend. Future related investigations will consider battery consumption during usage of IM chatting, video streaming, web browsing, audio/video playback, and radio. One the chief limitations of LeS study is the age of the LeSs and the IM and SIP applications that were considered in the study. Considering the progress that has been made over time in the architecture of LeSs and IM and SIP applications, the future work will seek to update the experiments with more recent devices and social communication applications to stay with the trend.

This thesis closes by stating that these research methods continue to be expanded and refined to deepen the understanding of scalability in WMNs and of smartphone battery consumption, in order to promote their effective deployment in rural and low-income communities with little, intermittent or no electricity supplies.

Bibliography

Abolhasan, M., Hagelstein, B., & Wang, J. C. P. (2009). Real-world Performance of Current Proactive Multi-hop Mesh Protocols. *Proceeding of the 15th Asia-Pacific Conference on Communications (APCC 2009), October*, 44–47. https://doi.org/10.1109/APCC.2009.5375690

Abolhasan, M., Wang, J. C. P., & Franklin, D. R. (2007). On Indoor Multi-hopping capacity of Wireless Ad-Hoc Mesh Networks. *Proceedings of the 4th IEEE Internatonal Conference on Mobile Adhoc and Sensor Systems (MASS 2007)*, 1–6. https://doi.org/10.1109/MOBHOC.2007.4428720

Agbenonwossi, E. E. (2018). Triumphing Over Distance and Time: The Case of Wireless Ghana. In Alan Finlay (Ed.), *Global Information Society Watch 2018 Community Networks* (pp. 133–136). Association for Progressive Communications (APC), ISBN: 9789295113060.

Ahmeda, S. S., & Farhan, R. K. (2014). Routing Protocols for Wireless Mesh Networks : Performance Study. *Proceedings of the 1st International Congress on Computer, Electronics, Electrical, and Communication Engineering (ICCEECE 2014)*, *59*, 142–148. https://doi.org/10.7763/IPCSIT.2014.V59.26

AirJaldi. (2018). Company Overview. In *Rural Broadband Privately Limited*. https://airjaldi.com/

Akyildiz, I. F., & Wang, X. (2009). Introduction. In *Wireless Mesh Networks* (1st ed., pp. 1–13). John Wiley & Sons, Ltd, ISBN: 9780470059616. https://doi.org/10.1002/9780470059616

Akyildiz, I. F., Wang, X., & Wang, W. (2005). Wireless Mesh Networks: A Survey. *Computer Networks*, *47*(4), 445–487. https://doi.org/10.1016/j.comnet.2004.12.001

Alcatel-Lucent. (2014). *Mobile Application Rankings Report by Alcatel-Lucent*. https://tweakimg.net/files/upload/alcatallucent.pdf

ASK. (2018). Coefficient of Determination, R-squared. In *Academic Skills Set - Newcastle University*. Newcastle University. https://internal.ncl.ac.uk/ask/numeracy-maths-statistics/statistics/regression-and-correlation/coefficient-of-determination-r-squared.html

Avallone, S., Emma, D., Pescapé, A., & Ventre, G. (2005). Performance Evaluation of an Open Distributed Platform for Realistic Traffic Generation. *Performance Evaluation*, *60*(1–4), 359–392. https://doi.org/10.1016/j.peva.2004.10.012

Avast. (2017). *Avast Android App Performance and Trend Report by Avast Software*. Avast Software. http://files.avast.com/files/marketing/pr/avast/reports/%0A2017/2017-q1-avast-android-app-preformanceand-trend-report.pdf

Backens, J., Mweemba, G., & van Stam, G. (2010). A Rural Implementation of a 52 Node Mixed Wireless Mesh Network in Macha, Zambia. In A. Villafiorita, R. Saint-Paul, & A. Zorer (Eds.), *E-Infrastructures and E-Services on Developing Countries. AFRICOMM 2009* (Vol. 38, pp. 32–39). Springer, Berlin, Heidelberg. https://doi.org/10.1007/978-3-642-12701-4_4

Bahia, K. (2018). Connected Society: State of Mobile Internet Connectivity 2018. In *GSM Association*.

https://www.gsma.com/mobilefordevelopment/ connected-society/

Bai, R., & Singhal, M. (2006). DOA: DSR over AODV Routing for Mobile Ad Hoc Networks. *IEEE Transactions on Mobile Computing*, *5*(10), 1403–1416. https://doi.org/10.1109/TMC.2006.150

Bakker, A. (2014). Comparing Energy Profilers for Android. *Proceedings of the 21st Twente Student Conference on IT (TScIT 2014)*. http://fmt.cs.utwente.nl/files/sprojects/217.pdf

Balasubramanian, N., Balasubramanian, A., & Venkataramani, A. (2009). Energy Consumption in Mobile Phones: A Measurement Study and Implications for Network Applications. *Proceedings of the 9th ACM SIGCOMM Conference on Internet Measurement Conference (IMC 2009)*. https://doi.org/10.1145/1644893.1644927

Belur, S. B. (2018). Addressing Sustainability in Rural Connectivity: A Case Study of Gram Marg Community-led Networks. In Alan Finlay (Ed.), *Global Information Society Watch 2018 Community Networks* (pp. 150–156). Association for Progressive Communications (APC), ISBN: 9789295113060.

Beuran, R. (2012). *Introduction to Network Emulation* (1st ed.). Jenny Stanford Publishing, ISBN: 9789814310918.

Bicket, J., Aguayo, D., Biswas, S., & Morris, R. (2005). Architecture and Evaluation of an Unplanned 802.11b Mesh Network. *Proceedings of the 11th Annual International Conference on Mobile Computing and Networking (MobiCom 2005)*. https://doi.org/10.1145/1080829.1080833

Bidwell, N. J., & Jensen, M. (2019a). Section 1: Summary. In L. Nordstrom (Ed.), *Bottom-up Connective Strategies: Community-led Small-scale Telecommunication Infrastructure Networks in the Global South* (1st ed., pp. 8–28). Association of Progressive Communications (APC), ISBN: 9789295113091.

Bidwell, N. J., & Jensen, M. (2019b). Section 2: Community Networks - Operational and Technical Research. In L. Nordstrom (Ed.), *Bottom-up Connective Strategies: Community-led Small-scale Telecommunication Infrastructure Networks in the Global South* (1st ed., pp. 90–93). Association of Progressive Communications (APC), ISBN: 9789295113091.

Botta, A., Dainotti, A., & Pescape, A. (2010). Do You Trust Your Software-based Traffic Generator? *IEEE Communications Magazine*, *48*(9), 158–165. https://doi.org/10.1109/MCOM.2010.5560600

Botta, A., Dainotti, A., & Pescape, A. (2012). A Tool for the Generation of Realistic Network Workload for Emerging Networking Scenarios. *Computer Networks*, *56*(15), 3531–3547. https://doi.org/10.1016/j.comnet.2012.02.019

Botta, A., Donato, W. De, Dainotti, A., Avallone, S., & Pescape, A. (2013). *D-ITG 2.8.1 Manual*. http://www.grid.unina.it/software/ITG/

Buttrich, S. (2006). *ItrainOnline Mesh Networks* (Issue May). ItrainOnline Multimedia Training Kit (MMTK). http://www.itrainonline.org/itrainonline/mmtk/wireless_en/17_Mesh_Networking/17_en_mmtk_wireless_mesh-networking_handout.pdf

Campista, M. E. M., Esposito, P. M., Moraes, I. M., Costa, L. H. M., Duarte, O. C. M., Passos, D. G., de Albuquerque, C. V. N., Saade, D. C. M., & Rubinstein, M. G. (2008). Routing Metrics and Protocols for Wireless Mesh Networks. *IEEE Network*, *22*(1), 6–12. https://doi.org/10.1109/MNET.2008.4435897

Carroll, A., & Heiser, G. (2010). An Analysis of Power Consumption in a Smartphone. *Proceedings of the USENIX Annual Technical Conference (USENIXATC '010)*. https://www.usenix.org/event/usenix10/tech/full_papers/Carroll.pdf

Castro, M. C., Dely, P., Karlsson, J., & Kassler, A. (2007). Capacity Increase for Voice over IP Traffic through Packet Aggregation in Wireless Multihop Mesh Networks. *Proceedings of the Future Generation Communication and Networking (FGCN 2007)*, *2*, 350–355. https://doi.org/10.1109/FGCN.2007.81

Chaudhry, A. U. (2015). *Spectrum Requirements for Interference-Free Wireless Mesh Networks* [PhD Thesis, Department of Systems and Computer Engineering, Carleton University, Ottawa,]. https://curve.carleton.ca/system/files/etd/f77eb997-1a7e-4fda-93a5-441eef94d7e6/etd_pdf/fe64c74081ab9d67eed87e2a12bcf5d3/chaudhry-spectrumrequirementsforinterferencefreewireless.pdf

Chiang, C.-C., WU, H.-K., Liu, W., & Gerla, M. (1997). Routing in Clustered Multihop Mobile Wireless Networks with Fading Channel. In H. K. P. Pung, J. Biswas, & L. H. Ngoh (Eds.), *Networks: The Next Millennium - Proceedings of the IEEE Singapore International Conference on Networks (SICON 1997)* (1st ed., Vol. 1, pp. 197–211). World Scientific Publishing. http://nrlweb.cs.ucla.edu/nrlweb/publication/show/289

Chissungo, E., Blake, E., & Le, H. (2012). Investigation into Batmand-0.3.2 Protocol Performance in an Indoor Mesh Potato Testbed. *Proceedings of the 26th International Conference on Advanced Information Networking and Applications Workshops (AINA Workshops 2012)*, 526–532. https://doi.org/10.1109/WAINA.2012.285

Chmielewski, D. (2014). *Messaging, Video Among Top Battery-Draining Apps*. Recode. https://www.recode.net/2014/4/29/11626206/its-not-necessarily-the-phone-these-apps-are-draining- your-battery

Cisco. (2016). *Voice Over IP - Per Call Bandwidth Consumption*. https://www.cisco.com/c/en/us/support/docs/voice/voice-quality/7934-bwidth-consume.html

Clancy, T. C., & Walker, B. D. (2007). MeshTest: Laboratory-Based Wireless Testbed for Large Topologies. *Proceedings of the 3rd International ICST Conference on Testbeds and Research Infrastructure for the Development of Networks and Communities (TridentCom 2007)*, 1–6. https://doi.org/10.1109/TRIDENTCOM.2007.4444659

Cole, R. G., & Rosenbluth, J. H. (2001). Voice over IP performance monitoring. *ACM SIGCOMM Computer Communication Review*, *31*(2), 9–24. https://doi.org/10.1145/505666.505669

Collings, S. (2011). *Phone Charging Micro-businesses in Tanzania and Uganda* (Issue September). Global Vollage Energy Partnership (GVEP) International. www.gvepinternational.org

Creswell, J. W. (2014). *Research Design: Qualitative, Quantitative, and Mixed Methods Approaches* (4th ed.). SAGE Publications Inc., ISBN: 9781452226095.

De Couto, D. S. J., Aguayo, D., Bicket, J., & Morris, R. (2003). A high-throughput path metric for multi-hop wireless routing. *Proceedings of the 9th Annual International Conference on Mobile Computing and*

Networking - MobiCom '03, *11*(4), 134. https://doi.org/10.1145/938985.939000

Dilmaghani, R. B., Manoj, B. S., Jafarian, B., & Rao, R. R. (2005). Performance evaluation of RescueMesh: A Metro-scale Hybrid Wireless Network. *Proceeding of the 1st IEEE Workshop on Wireless Mesh Networks Held in Conjunction with 2nd Annual IEEE Communications Society Conference on Sensor and Ad Hoc Communications and Networks (WiMesh - SECON 2005)*. http://citeseerx.ist.psu.edu/viewdoc/summary?doi=10.1.1.531.718

Draves, R., Padhye, J., & Zill, B. (2004). Routing in Multi-radio, Multi-hop Wireless Mesh Networks. *Proceedings of the 10th Annual International Conference on Mobile Computing and Networking (MobiCom 2004)*. https://doi.org/10.1145/1023720.1023732

Dugan, J., Estabrook, J., Ferbuson, J., Gallatin, A., Gates, M., Gibbs, K., Hemminger, S., Jones, N., Qin, F., Renker, G., Tirumala, A., & Warshavsky, A. (2016). *iPerf - The Ultimate Speed Test Tool for TCP, UDP and SCTP*. ESnet. https://iperf.fr/

Ebenezer, B., Amoah, G., & Atkinson, J. (2006). *Wireless Ghana A Case Study prepared by Community Based Libraries and Information Technology (CBLit)*. The OPLAN Foundation. http://109.69.9.58/wp-content/uploads/2011/10/Wireless-Ghana-A-Case-Study.pdf

Egyedi, T., Vrancken, J. L. M., & Ubacht, J. (2007). Inverse infrastructures: Coordination in Self-organizing Systems. *Proceedings of the 5th International Conference on Standardization and Innovation in Information Technology (SIIT - 2007)*, 23–36. https://doi.org/10.1109/SIIT.2007.4629314

ElRakabawy, S. M., Frohn, S., & Lindemann, C. (2008, June). ScaleMesh: A Scalable Dual-Radio Wireless Mesh Testbed. *Proceedings of the 5th IEEE Annual Communications Society Conference on Sensor, Mesh and Ad Hoc Communications and Networks Workshops (SECON Workshops - 2008)*. https://doi.org/10.1109/SAHCNW.2008.21

Farooq, M., & Raju, V. (2019). Impact of Over-the-Top (OTT) Services on the Telecom Companies in the Era of Transformative Marketing. *Global Journal of Flexible Systems Management*, *20*(2), 177–188. https://doi.org/10.1007/s40171-019-00209-6

FGV Direito Rio. (2016). *Community Connectivity: Building the Internet from Scratch* (L. Belli (ed.); 1st ed., Issue 1). https://internet-governance.fgv.br/sites/internet-governance.fgv.br/files/publicacoes/community_connectivity_-_building_the_internet_from_scratch_0.pdf

Friedman, R., Kogan, A., & Krivolapov, Y. (2011). On Power and Throughput Tradeoffs of WiFi and Bluetooth in Smartphones. *Proceedinggs of the 30th IEEE International Conference on Computer Communications (INFOCOM - 2011)*, *12*(7), 900–908. https://doi.org/10.1109/INFCOM.2011.5935315

Gillet, T. (2017). *SECN-3.0 User Guide*. VillageTelco. http://download.villagetelco.org/userdocs/secn/secn-3.0/

Goldsmith, A., Effros, M., Koetter, R., Medard, M., Ozdaglar, A., & Zheng, L. (2011). Beyond Shannon: The Quest for Fundamental Performance Limits of Wireless Ad Hoc Networks. *IEEE Communications Magazine*, *49*(5), 195–205. https://doi.org/10.1109/MCOM.2011.5762818

GSM Alliance. (2016). *Connected Society: Mobile Connectivity Index Launch Report*. GSM Association. http://www.mobileconnectivityindex.com/widgets/connectivityIndex/pdf/ConnectivityIndex_V01.pdf

GSMA Intelligence. (2015). *The Mobile Economy 2015*. GSM Association. www.gsmaintelligence.com

Gupta, P., Gray, R., & Kumar, P. R. (2001). *An Experimental Scaling Law for Ad hoc network*. http://citeseerx.ist.psu.edu/viewdoc/summary?doi=10.1.1.13.1422

Gupta, P., & Kumar, P. R. (2000). The Capacity of Wireless Networks. *IEEE Transactions on Information Theory*, *46*(2), 388–404. https://doi.org/10.1109/18.825799

Hamidian, A., Palazzi, C. E., Chong, T. Y., Navarro, J. M., Korner, U., & Gerla, M. (2009). Deployment and Evaluation of a Wireless Mesh Network. *Proceedings of the 2nd International Conference on Advances in Mesh Networks (MESH - 2009)*, 66–72. https://doi.org/10.1109/MESH.2009.19

Hardes, T. (2015). *Performance Analysis and Simulation of a Freifunk Mesh Network in Paderborn using B.A.T.M.A.N Advanced* (Issue October) [Master's Thesis, Department of Computer Science, University of Paderborn]. http://thardes.de/wp-content/uploads/2016/03/thesis.pdf

Hatti, S., & Kamakshi, M. B. (2013). Performance Analysis of ETX and ETT Routing Metrics Over AODV Routing Protocol in WMNs. In N. Chaki, N. Meghanathan, & D. Nagamalai (Eds.), *Lecture Notes in Electrical Engineering* (Vol. 131, pp. 817–826). Springer New York. https://doi.org/10.1007/978-1-4614-6154-8_79

Heimerl, K., Menon, A., Hasan, S., Ali, K., Brewer, E., & Parikh, T. (2015). Analysis of Smartphone Adoption and Usage in a Rural Community Cellular Network. *Proceedings of the 7th International Conference on Information and Communication Technologies and Development (ICTD - 2015)*. https://doi.org/10.1145/2737856.2737880

HimVani. (2006). *Dharamsala gets a Silicon Valley Connection*. HimVani. http://www.himvani.com/378/dharamsala-gets-a-silicon-valley-connection/

IEA. (2017). Energy Access Outlook 2017: From Poverty to Prosperity. In *IEA Publications*. International Energy Agency. https://www.iea.org/reports/energy-access-outlook-2017

ITU-T. (1998). ITU-T Recommendation G.107, The E-model: A Computational Model for Use in Transmission Planning. In *International Telecommunication Union Telecommunication Standardization Sector (ITU-T)*. International Telecommunication Union. http://www.itu.int/rec/T-REC-G.107-199812-S/en

ITU-T. (2001a). ITU-T Recommendation G.1000, Communications Quality of Service: A Framework and Definitions. In *International Telecommunication Union Telecommunication Standardization Sector (ITU-T)*. International Telecommunication Union. https://www.itu.int/rec/T-REC-G.1000/en

ITU-T. (2001b). ITU-T Recommendation G.1010, End-user Multimedia QoS Categories. In *International Telecommunication Union Telecommunication Standardization Sector (ITU-T)*. International Telecommunication Union. https://www.itu.int/rec/T-REC-G.1010-200111-I

ITU-T. (2003). ITU-T Recommendation G.114, One-way Transmission Time. In *International Telecommunication Union Telecommunication Standardization Sector (ITU-T)*. International Telecommunication Union.

https://www.itu.int/rec/T-REC-G.114-200305-I/en

ITU-T. (2008). Recommendation ITU-T E.800, Definitions of Terms Related to Quality of Service. In *International Telecommunication Union Telecommunication Standardization Sector (ITU-T)*. International Telecommunication Union. https://www.itu.int/rec/T-REC-E.800-200809-I

ITU. (2019). Measuring Digital Development Facts and figures 2019. In *ITUPublications*. International Telecommunications Union. https://www.itu.int/en/mediacentre/Documents/MediaRelations/ITU Facts and Figures 2019 - Embargoed 5 November 1200 CET.pdf

Janevski, D. T., Jankovic, D. M., & Markus, M. S. (2017). Quality of Service Regulation Manual. In *International Telecommunication Union Telecommunication Development Sector*. International Telecommunication Union. http://www.itu.int/pub/D-PREF-BB.QOS_REG01-2017

Jiandong Li, Haas, Z. J., & Min Sheng. (2002). Capacity Evaluation of Multi-channel Multi-hop Ad hoc Networks. *Proceeding of the IEEE International Conference on Personal Wireless Communications (ICPWC - 2002)*, 211–214. https://doi.org/10.1109/ICPWC.2002.1177279

Johnson, D. (2007a). *Performance Analysis of Mesh Networks in Indoor and Outdoor Wireless Testbeds* [Masters, Electrical, Electronic and Computer Engineering, University of Pretoria]. https://repository.up.ac.za/handle/2263/24634

Johnson, D. (2013). *Re-architecting Internet Access and Wireless Networks for Rural Developing Regions* (Issue March) [PhD, Department of Computer Science, University of California at Santa Barbara]. https://people.cs.uct.ac.za/~djohnson/Files/david_phd_2013.pdf

Johnson, D. (2007b). Evaluation of a Single Radio Rural Mesh Network in South Africa. *Proceedings of the 2nd International Conference on Information and Communication Technologies and Development (ICTD - 2007)*, 285–293. https://doi.org/10.1109/ICTD.2007.4937415

Johnson, D., & Lysko, A. (2007). Overview of the Meraka Wireless Grid Testbed for Evaluation of Ad-hoc Routing Protocols. *Proceedings of the Southern Africa Telecommunication Networks and Applications Conference (SATNAC - 2007)*. http://hdl.handle.net/10204/1574

Kalic, G., Bojic, I., & Kusek, M. (2012). Energy Consumption in Android Phones When Using Wireless Communication Technologies. *Proceedings of the 35th International Convention on Information, Communication, and Electronic Technology (MIPRO - 2012)*, 754–759. http://ieeexplore.ieee.org/xpl/articleDetails.jsp?arnumber=6240745

Kanchanasut, K., Lertsinsubtavee, A., Tunpan, A., Tansakul, N., Mekbungwan, P., Weshsuwannarugs, N., & Tripatana, P. (2018). Building Last-metre Community Networks in Thailand. In Alan Finlay (Ed.), *Global Information Society Watch 2018 Community Networks* (pp. 232–234). Association for Progressive Communications (APC), ISBN: 9789295113060.

Koehncke, C. (2017). *WebRTC Impacts on Battery Life*. Chris Kranky. https://www.chriskranky.com/webrtc-impacts-on-battery-life/

Kohler, E., Morris, R., Chen, B., Jannotti, J., & Kaashoek, M. F. (2000). The Click Modular Router. *ACM Transactions on Computer Systems*, *18*(3), 263–297. https://doi.org/10.1145/354871.354874

Kolahi, S. S., Narayan, S., Nguyen, D. D. T., & Sunarto, Y. (2011). Performance Monitoring of Various Network Traffic Generators. *Proceedings of the 13th International Conference on Computer Modelling and Simulation (UKSim - 2011)*, 501–506. https://doi.org/10.1109/UKSIM.2011.102

Konrad, A. (2015). Free Apps With Ads May Be Killing Your Phone's Battery and Data Plan. In *Forbes*. Forbes. https://www.forbes.com/sites/alexkonrad/2015/04/01/free-app-ads-kill-phone-battery-and-data/#7380259f23cc

Kosky, P., Balmer, R., Keat, W., & Wise, G. (2013). Computer Engineering. In *Exploring Engineering: An Introduction to Engineering and Design* (3rd ed., pp. 161–183). Elsevier, ISBN 9780124158917. https://doi.org/10.1016/B978-0-12-415891-7.00008-X

Kulla, E., Hiyama, M., Ikeda, M., & Barolli, L. (2012). Performance Comparison of OLSR and BATMAN Routing Protocols by a MANET Testbed in Stairs Environment. *Computers & Mathematics with Applications*, *63*(2), 339–349. https://doi.org/10.1016/j.camwa.2011.07.035

Laerd Statistics. (2018). *One-way ANOVA*. Laerd Statistics. https://statistics.laerd.com/statistical-guides/one-way-anova-statistical-guide.php

Lee, H. (2010). *Wireless Mesh Networks: Protocol, Design, and Performance Evaluation* (Issue March) [PhD, Department of Electrical Engineering, Stanford University]. http://purl.stanford.edu/kx780hc2331

Leedy, P. D., & Ormrod, J. E. (2015). Analyzing Quantitative Data. In *Practical Research: Planning and Design* (11th ed., pp. 229–268). Pearson Education Limited. https://www.pearson.com/us/higher-education/product/Leedy-Practical-Research-Planning-and-Design-11th-Edition/9780133741322.html

Li, P., Pan, M., & Fang, Y. (2012). Capacity Bounds of Three-Dimensional Wireless Ad Hoc Networks. *IEEE/ACM Transactions on Networking*, *20*(4), 1304–1315. https://doi.org/10.1109/TNET.2011.2178123

Lu, N., & Shen, X. S. (2014). Scaling Laws for Throughput Capacity and Delay in Wireless Networks — A Survey. *IEEE Communications Surveys & Tutorials*, *16*(2), 642–657. https://doi.org/10.1109/SURV.2013.081313.00039

Luca de Tena, L. de S., & Rey-Moreno, C. (2018). Challenging Inequality in Post-apartheid South Africa: A Bottom-up, Community-led Business Model for Connectivity. In Alan Finlay (Ed.), *Global Information Society Watch 2018 Community Networks* (pp. 222–226). Association for Progressive Communications (APC), ISBN: 9789295113060.

Marina, M. K., & Das, S. R. (2006). Ad hoc On-demand Multipath Distance Vector Routing. *Wireless Communications and Mobile Computing*, *6*(7), 969–988. https://doi.org/10.1002/wcm.432

Marina, M. K., & Das, S. R. (2001). On-demand multipath distance vector routing in ad hoc networks. *Proceedings Ninth International Conference on Network Protocols. ICNP 2001*, 14–23. https://doi.org/10.1109/ICNP.2001.992756

Martin, H., & Ledet-Pedersen, J. (2011). *Inter-Flow Network Coding for Wireless Mesh Networks* [Masters,

Department of Electronic Systems, Aalborg University]. https://downloads.open-mesh.org/batman/papers/batman-adv_network_coding.pdf

Master of Code Global. (2017). *App Store vs Google play: Stores in numbers*. Medium.Com. https://medium.com/master-of-code-global/app-store-vs-google-play-stores-in-numbers-fd5ba020c195

Mertler, C. A. (2018). Quantitative Research Methods. In *Introduction to Educational Research* (2nd ed., p. 344). SAGE Publications, Inc. https://us.sagepub.com/sites/default/files/upm-assets/89874_book_item_89874.pdf

Metageek. (2019). *Understanding WiFi Signal Strength*. Metageek. https://www.metageek.com/training/resources/wifi-signal-strength-basics.html

Minitab. (2016). *What is Tukey's Method for Multiple Comparisons ?* Minitab. https://support.minitab.com/en-us/minitab/18/help-and-how-to/modeling-statistics/anova/supporting-topics/multiple-comparisons/what-is-tukey-s-method/

Mishra, S., Sonavane, S., & Gupta, A. (2015). Study of Traffic Generation Tools. *International Journal of Advanced Research in Computer and Communication Engineering*, *4*(6), 4–7. https://doi.org/10.17148/IJARCCE.2015.4635

Mweetwa, F., & van Stam, G. (2018). Community Engagement in Community Networks in Rural Zambia: The Case of Macha Works. In Alan Finlay (Ed.), *Global Information Society Watch 2018 Community Networks* (pp. 256–259). Association for Progressive Communications (APC), ISBN: 9789295113060.

Nasipuri, A., & Das, S. R. (1999). On-demand Multipath Routing for Mobile Ad Hoc Networks. *Proceedings of the 8th International Conference on Computer Communications and Networks (ICCCN - 1999, Cat. No.99EX370)*, 64–70. https://doi.org/10.1109/ICCCN.1999.805497

Nassereddine, B., Maach, A., & Bennani, S. (2009, November). The Scalability of the Hybrid Protocol in Wireless Mesh Network 802.11s. *Proceedings of the 9th IEEE Mediterrannean Microwave Symposium (MMS - 2009)*. https://doi.org/10.1109/MMS.2009.5409759

Niculescu, D., Ganguly, S., Kim, K., & Izmailov, R. (2006). Performance of VoIP in a 802.11 Wireless Mesh Network. *Proceedings of the 25th IEEE International Conference on Computer Communications (INFOCOM - 2006)*. https://doi.org/10.1109/INFOCOM.2006.243

Nield, D. (2017). All the Sensors in Your Smartphone, and How They Work. In *Gizmodo.com*. Gizmodo. https://gizmodo.com/all-the-sensors-in-your-smartphone-and-how-they-work-1797121002

Noll, R. G. (1999). Telecommunications Reform in Developing Countries. In A. O. Kruger (Ed.), *Economic Policy Reform: The Second Wave, University of Chicago Press, Spring, 2000*. University of Chicago Press, Spring, 2000. http://www.ssrn.com/abstract=181030

Nurminen, J. K., & Noyranen, J. (2008). Energy-Consumption in Mobile Peer-to-Peer - Quantitative Results from File Sharing. *Proceedings of the 5th IEEE Consumer Communications and Networking Conference (CCNC - 2008)*, 729–733. https://doi.org/10.1109/ccnc08.2007.167

Oe, K., Koyama, A., & Barolli, L. (2015). Proposal and Performance Evaluation of a Multicast Routing Protocol for

Wireless Mesh Networks Based on Network Load. *Mobile Information Systems*, *2015*, 1–10. https://doi.org/10.1155/2015/523294

Om, S., Rey-Moreno, C., & Tucker, W. (2017, May). Investigating battery consumption in low-end smartphones: Preliminary results. *Proceedings of the 2017 IST-Africa Week Conference (IST-Africa - 2017)*. https://doi.org/10.23919/ISTAFRICA.2017.8102309

Om, S., & Tucker, W. D. (2018a). Battery and Data Drain of Over-The-Top Applications on Low-end Smartphones. *Proceedings of the 2018 IST-Africa Week Conference (IST-Africa - 2018)*. https://ieeexplore.ieee.org/document/8417297

Om, S., & Tucker, W. D. (2018b). Investigation of a Dual-band Dual-radio Indoor Mesh Testbed. *Proceedings of the 2018 Southern Africa Telecommunication Networks and Applications Conference (SATNAC - 2018)*, 330–335. http://hdl.handle.net/10566/5251

Palit, R. (2011). *Modeling and Evaluating Energy Performance of Smartphones* [University of Waterloo]. https://uwspace.uwaterloo.ca/handle/10012/6534

Pawlikowski, K., Jeong, H.-D. J., & Lee, J.-S. R. (2002). On Credibility of Simulation Studies of Telecommunication Networks. *IEEE Communications Magazine*, *40*(1), 132–139. https://doi.org/10.1109/35.978060

Pei, T., Zeng, W., Zhang, Z., & Peng, T. (2009). An Improved Hierarchical AODV Routing Protocol for Hybrid Wireless Mesh Network. *Proceedings of the 1st International Conference on Networks Security, Wireless Communications and Trusted Computing (NSWCTC - 2009)*, *1*, 588–593. https://doi.org/10.1109/NSWCTC.2009.112

Perkins, R. (2015). 'Free' apps may not be so free after all: They take a big toll on your phone. In *news.usc.edu*. news.usc.edu. https://news.usc.edu/79081/beware-of-an-ads-hidden-costs-in-free-mobile-apps/

Perrucci, G. P., Fitzek, F. H. P., Sasso, G., Kellerer, W., & Widmer, J. (2009). On the Impact of 2G and 3G Network Usage for Mobile Phones' Battery Life. *Proceedings of the 15th European Wireless Conference (EW - 2009)*, 255–259. https://doi.org/10.1109/EW.2009.5357972

Perrucci, G. P., Fitzek, F. H. P., & Widmer, J. (2011, May). Survey on Energy Consumption Entities on the Smartphone Platform. *Proceedings of the 73rd Vehicular Technology Conference (VTC - 2011)*. https://doi.org/10.1109/VETECS.2011.5956528

Pirzada, A., Portmann, M., & Indulska, J. (2006). Performance Comparison of Multi-Path AODV and DSR Protocols in Hybrid Mesh Networks. *Proceedings of the 14th IEEE International Conference on Networks (ICON - 2006)*, *2*. https://doi.org/10.1109/ICON.2006.302624

Radman, P., Singh, J., Domingo, M., Arnedo, J., & Talevski, A. (2010). VoIP: Making Secure Calls and Maintaining High Call Quality. *Proceedings of the 8th International Conference on Advances in Mobile Computing and Multimedia (MoMM - 2010)*. https://doi.org/10.1145/1971519.1971532

Raluca, M.-E. (2010). *Practical Wireless Mesh Networks and their Applications* [John Hopkins University].

http://www.dsn.jhu.edu/~yairamir/Raluca_thesis.pdf

Rao, S. S. N., Krishna, Y. K. S., & Rao, K. N. (2013). Performance Evaluation of Routing Protocols in Wireless Mesh Networks. *International Journal of Computer Applications*, *68*(7), 20–25. https://doi.org/10.5120/11592-6933

Rethfeldt, M., Beichler, B., Raddatz, H., Uster, F., Danielis, P., Haubelt, C., & Timmermann, D. (2018, April). Mini-Mesh: Practical assessment of a miniaturized IEEE 802.11n/s mesh testbed. *Proceedings of the 19th IEEE Wireless Communications and Networking Conference (WCNC - 2018)*. https://doi.org/10.1109/WCNC.2018.8377247

Rey-Moreno, C., Tucker, W. D., Cull, D., & Blom, R. (2015). Making a Community Network Legal within the South African Regulatory Framework. *In the Proceedings of the 7th International Conference on Information and Communication Technologies and Development (ICTD - 2015) (p. Article 57)*. https://doi.org/10.1145/2737856.2737867

Rey-Moreno, Carlos. (2017). Supporting the Creation and Scalability of Affordable Access Solutions: Understanding Community Networks in Africa. In *Internet Society*. Internet Society (ISOC). https://www.internetsociety.org/doc/cnafrica

Rey-Moreno, Carlos, Blignaut, R., Tucker, W. D., & May, J. (2016). An In-depth Study of the ICT Ecosystem in a South African Rural Community: Unveiling Expenditure and Communication Patterns. *Information Technology for Development*, *22*(sup1), 101–120. https://doi.org/10.1080/02681102.2016.1155145

Rey-Moreno, Carlos, Roro, Z., Tucker, W. D., Siya, M. J., Bidwell, N. J., & Simo-Reigadas, J. (2013). Experiences, Challenges and Lessons from Rolling Out a Rural WiFi Mesh Network. *Proceedings of the 3rd ACM Symposium on Computing for Development (ACM DEV - 2013)*, Article 11. https://doi.org/10.1145/2442882.2442897

Rey-Moreno, Carlos, Ufitamahoro, M. J., Venter, I., & Tucker, W. (2014). Co-designing a Billing System for Voice Services in Rural South Africa. *Proceedings of the 5th ACM Symposium on Computing for Development - (ACM DEV - 2014)*, *5*, 83–92. https://doi.org/10.1145/2674377.2674389

Sampaio, S., & Vasques, F. (2014a). Exploiting DHT's Properties to Improve the Scalability of Mesh Networks. In M. Khosrow-Pour (Ed.), *Encyclopedia of Information Science and Technology, Third Edition* (3rd ed., Issue July, pp. 6177–6185). IGI Global. https://doi.org/10.4018/978-1-4666-5888-2.ch609

Sampaio, S., & Vasques, F. (2014b). Routing Protocols for IEEE 802.11-Based Mesh Networks. In M. Khosrow-Pour (Ed.), *Encyclopedia of Information Science and Technology, Third Edition* (3rd ed., Issue February 2015, pp. 6295–6306). IGI Global. https://doi.org/10.4018/978-1-4666-5888-2.ch619

Sanghani, S., Brown, T. X., Bhandare, S., & Doshi, S. (2003). EWANT: The Emulated Wireless Ad Hoc Network Testbed. *Proceedings of the 4th IEEE Wireless Communications and Networking Conference (WCNC - 2003)*, *3*, 1844–1849. https://doi.org/10.1109/WCNC.2003.1200667

SAS. (2013). The ANOVA Procedure. In *SAS/STAT 13.1 User's Guide* (13.1). SAS Institute Inc.

https://support.sas.com/documentation/cdl/en/statug/66859/PDF/default/statug.pdf

Sathiaseelan, A. (2017). *TakNet – Community networking in Thailand - APNIC Blog*. Asia-Pacific Network Information Centre (APNIC). https://blog.apnic.net/2017/02/17/taknet-community-networking-thailand/

Seither, D., Konig, A., & Hollick, M. (2011). Routing performance of Wireless Mesh Networks: A practical evaluation of BATMAN advanced. *Proceedings of the 36th IEEE Conference on Local Computer Networks (LCN - 2011)*, 897–904. https://doi.org/10.1109/LCN.2011.6115569

Song, S., Rey-Moreno, C., Esterhuysen, A., Jensen, M. J., & Navarro, L. (2018). Introduction: The Rise and Fall and Rise of Community Networks. In A. Finlay (Ed.), *Global Information Society Watch 2018 Community Networks* (pp. 7–10). Association for Progressive Communications (APC), ISBN: 9789295113060.

Sonicwall. (2019). *Wireless: SNR and RSSI and Noise, Basics of Wireless Troubleshooting*. https://www.sonicwall.com/support/knowledge-base/wireless-snr-and-rssi-and-noise-basics-of-wireless-troubleshooting/180314090744170/

Stork, C., Esselaar, S., Chair, C., & Kahn, S. (2017). OTT - Threat or Opportunity for African Telcos? *Telecommunications Policy*, *41*(7–8), 600–616. https://doi.org/https://doi.org/10.1016/j.telpol.2017.05.007

Suantak, M. (2018). The Community Network as a Connectivity Strategy for Rual and Remote Myanmar. In Alan Finlay (Ed.), *Global Information Society Watch 2018 Community Networks* (pp. 184–186). Association for Progressive Communications (APC), ISBN: 9789295113060.

Subramanian, L., Surana, S., Patra, R., Nedevschi, S., Ho, M., Brewer, E., & Sheth, A. (2006). Rethinking Wireless in the Developing World. *Hot Topics in Networks*, 43–48. http://tier.cs.berkeley.edu/docs/wireless/large_wild.pdf

Sujata, J., Sohag, S., Tanu, D., Chintan, D., & Shubham, P. (2015). Impact of Over the Top (OTT) Services on Telecom Service Providers. *Indian Journal of Science and Technology*, *8*(4), 145–160. https://doi.org/10.17485/ijst/2015/v8iS4/62238

Sullivan, L. (2016). The ANOVA Approach. In *Hypothesis Testing - Analysis of Variance (ANOVA)*. Bostom University School of Public Health. http://sphweb.bumc.bu.edu/otlt/MPH-Modules/BS/BS704_HypothesisTesting-ANOVA/

Surana, S., Patra, R., & Nedevschi, S. (2008). Beyond Pilots: Keeping Rural Wireless Networks Alive. *Proceedings of the 5th USENIX Symposium on Networked Systems Design and Implementation (NSDI - 2008)*, 119–132. https://doi.org/10.1.1.141.4754

Szigeti, T., & Hattingh, C. (2004). *End-to-End QoS Network Design: Quality of Service in LANs, WANs, and VPNs* (1st ed.). Cisco Press, ISBN:9781587051760.

Tao, X., Kunz, T., & Falconer, D. (2005). Traffic Balancing in Wireless MESH Networks. *Proceedings of the International Conference on Wireless Networks, Communications and Mobile Computing*, *1*, 169–174. https://doi.org/10.1109/WIRLES.2005.1549404

Tiemeni, G. L. N. (2015). *Performance Estimation of Wireless Networks using Traffic Generation and Monitoring*

on a Mobile Device [University of the Western Cape]. http://hdl.handle.net/11394/4809

Tucker, W. D. (2018). How a rural community built South Africa's first ISP owned and run by a cooperative. In *The Conversation*. https://theconversation.com/how-a-rural-community-built-south-africas-first-isp-owned-and-run-by-a-cooperative-87448

Ubiquiti. (2019). *UniFi - Configuring wireless uplink* (pp. 1–15). Ubiquiti Networks. https://help.ui.com/hc/en-us/articles/115002262328-UniFi-Configuring-Wireless-Uplink

Ubiquiti Networks. (2019a). *Datasheet - LiteBeam AC Gen2*. Ubiquiti Networks. https://www.ui.com/airmax/litebeam-ac-gen2/

Ubiquiti Networks. (2019b). *Datasheet - UniFi AC Mesh*. https://dl.ubnt.com/datasheets/unifi/UniFi_AC_Mesh_DS.pdf

Ubiquiti Networks. (2019c). *UniFi Enterprise System Controller - User guide*. Ubiquiti Networks. https://dl.ubnt.com/guides/UniFi/UniFi_Controller_V5_UG.pdf

UN. (2018). *World Urbanization Prospects: The 2018 Revision*. United Nations. https://population.un.org/wup/Publications/

UN. (2019). *World Economic Situation and Prospects*. United Nations. https://www.un.org/development/desa/dpad/

VillageTelco. (2011). *Mesh Potato Specifications*. VillageTelco. https://villagetelco.org/mesh-potato/

VillageTelco. (2015). *Mesh Potato 2.0 - Basic Edition*. https://store.villagetelco.com/mesh-potatoes/mesh-potato-2-basic.html

VillageTelco. (2016). *Mesh Potato - "All Wheel Drive Edition."* VillageTelco. https://store.villagetelco.com/mesh-potatoes/mp2-awd.html

Wallsten, S. J. (2003). Regulation and Internet Use in Developing Countries. *SSRN Electronic Journal - World Bank Policy Research Working Paper No. 2979, December*. https://doi.org/10.2139/ssrn.366100

Xiao, Y., Kalyanaraman, R. S., & Yla-Jaaski, A. (2008). Energy Consumption of Mobile YouTube: Quantitative Measurement and Analysis. *Proceedings of the 2nd International Conference on Next Generation Mobile Applications, Services, and Technologies (NGMAST - 2008), October*, 61–69. https://doi.org/10.1109/NGMAST.2008.26

Zhang, L., Tiwana, B., Qian, Z., Wang, Z., Dick, R. P., Mao, Z. M., & Yang, L. (2010). Accurate Online Power Estimation and Automatic Battery Behavior Based Power Model Generation for Smartphones. *Proceedings of the 8th IEEE/ACM/IFIP International Conference on Hardware/Software Codesign and System Synthesis - (CODES/ISSS - 2010)*, 105–114. https://doi.org/10.1145/1878961.1878982

Zhao, S., & Raychaudhuri, D. (2009). Scalability and Performance Evaluation of Hierarchical Hybrid Wireless Networks. *IEEE/ACM Transactions on Networking*, *17*(5), 1536–1549. https://doi.org/10.1109/TNET.2008.2011987

Zikomangane, P. (2018). A Free Wireless Network in the DRC: An Answer to Internet Shutdowns and Exorbitant Access Costs. In Alan Finlay (Ed.), *Global Information Society Watch 2018 Community Networks* (pp. 111–

114). Association for Progressive Communications (APC), ISBN: 9789295113060.

Appendix

A1. Supporting data for related works

A1.1. Summary of community wireless mesh network deployments

Table A1.1: Synopsis of examples of community wireless mesh network deployments
The table shows a summary of issues and advantages of the CWMN examples of sub-Saharan Africa and developing Asia extracted from the their description presented in earlier sections

CWMN	Deployment reason	Services provided	Revenue	Challenges	Active
Mesh Bukavu	High cost of Internet prices.	Intranet. Cached content sharing and local chat.	None	Mountainous region and frequent electricity cuts is a hurdle in expansion. Continued funding.	Yes
Wireless Ghana / ACWN	Requested by community to close gap on digital isolation of the area.	Digital libraries with Internet access.	Undisclosed amount.	Regular funding. Absence of power grid in areas.	Yes
Macha	Unreliability of GSM, expensive data rates.	ICT training to locals. Internet.	Unknown	Expansion due to lack of interest from commercial ISP.	?
Peebles Valley	Explore least cost 802.11 network for AIDS clinic, schools, homes, farms and other clinic infrastructure.	Internet	Unknown	Project shut due to high cost of VSAT, and lack of continued support	No
CN Palghar Project / Gram Marg	Absence of mobile coverage, no Internet	Internet	Internet coupons.	CAPEX to sustain, expand, and implement new projects	Yes
DCWMN / AirJaldi	Mountainous region, little to no electricity, no Internet.	Internet. Cached content sharing. VoIP	Wi-Fi data packages	Mostly installation challenges due tough terrains	Yes
TakNet	Lack of cheap broadband. Low literacy level. Bank on entrepreneurial opportunities in the rural area,	Internet, VoD, and VoIP.	Monthly subscription.	Expensive cost of backhaul.	Yes
ASORCOM	Absence of mobile network coverage	Internet. Cached content sharing.	Undisclosed donations from village members.	Project shut due to competition from introduction of mobile telecommunication services, and lack of funding for expansion	No

A1.2. Mobile connectivity index structure

Table A1.2: Mobile connectivity index structure.
Breakdown of the four key enablers of mobile Internet penetration, along with their dimensions comprising of the individual indicators (GSM Alliance, 2016).

Enabler	Dimension	Indicator	Source
Infrastructure (25%)	Mobile infrastructure (30%)	2G network coverage (20%)	ITU
		3G network coverage (30%)	GSMA Intelligence
		4G network coverage (25%)	
		Years since 3G network launch (25%)	
	Network performance (30%)	Mobile download speeds (50%)	OpenSignal
		Mobile latencies (50%)	
	Other enabling infrastructure (20%)	Access to electricity (25%)	World Bank
		Number of servers per 1 million people (20%)	
		International bandwidth per user (20%)	ITU
		Fixed broadband subscriptions (15%)	
		Fixed download speeds (10%)	Measurement Lab
		Fixed latencies (10%)	
	Spectrum (20%)	Spectrum assigned to mobile operators <1 GHz12 (65%)	GSMA Intelligence
		Spectrum assigned to mobile operators >1 GHz (35%)	
Affordability (25%)	Mobile tariffs (20%)	Cost of postpaid 500 MB data plan (40%)	ITU/World Bank
		Cost of prepaid 500 MB data plan (40%)	
		Cost of voice call bundle (20%)	
	Handset price (20%)	Cost of entry-level handset (100%)	GSMA/World Bank
	Income (20%)	GNI per capita (100%)	World Bank
	Inequality (20%)	Gini co-efficient (100%)	World Bank/CIA, World Factbook
	Taxation (20%)	Tax as a % of TCMO[55] (100%)	GSMA
Consumer (25%)	Basic skills (50%)	Adult literacy rate (25%)	UNESCO/CIA, World Factbook
		Mean years of schooling[56] (25%)	UN
		School life expectancy[57] (25%)	UNESCO
		Tertiary enrolment rate (25%)	
	Gender equality (50%)	Gender literacy ratio (30%)	UNESCO
		Gender labour participation ratio (10%)	World Bank Global / Findex
		Gender bank account ratio (20%)	ILO
		Gender years of schooling ratio (30%)	UN
		Gender GNI per capita ratio (10%)	

[55] TCMO = Total cost of mobile ownership
[56] This measures the average number of years of education received by people aged 25 and older, based on current attainment levels. It is different from school life expectancy because the latter is calculated using enrolment rates.
[57] This is the total number of years of schooling (primary to tertiary) that a child can expect to receive given current enrolment rates. It is therefore a forward-looking indicator.

Content (25%)	Local relevance (50%)	Number of gTLDs[58] per capita (25%)	TLDLogic, ZookNIC
		Number of ccTLDs[59] per capita (25%)	
		Quality of e-government services23 (25%)	UN
		Facebook penetration rate (15%)	Facebook
		Wikipedia edits per user (10%)	Wikipedia Statistics
	Availability (50%)	Accessible Wikipedia articles for the average person (10%)	Wikipedia Statistics, Ethnologue
		Accessible website content for the average person (10%)	
		Average accessibility of the top 100 mobile apps to the average person (80%)	App Annie, Ethnologue

A1.3. Voice codec bandwidth requirements

The total bandwidth consumed by VoIP streams (in bps) is collective of the VoIP sample payload (in Bytes, B) and the different Layer 2 (L2) overhead. The amount of overhead per VoIP call depends on the Layer 2 technology used:

- Total of 40-B consisting of 20-B IP + 8-B UDP + 12-B Real-Time Transport Protocol (RTP) headers.
- Compressed Real-Time Protocol (cRTP) reduces the IP/UDP/RTP headers to 2 or 4 Bytes (cRTP is not available over Ethernet).
- 6-B for Multilink Point-to-Point Protocol (MP) or Frame Relay Forum (FRF) version 12, FRF.12 Layer 2 (L2) header.
- 1-B for the end-of-frame flag on MP and Frame Relay frames.
- 18-B for Ethernet L2 headers, which include 4-B of Frame Check Sequence (FCS) or Cyclic Redundancy Check (CRC)

Per call bandwidth is calculated as follows:

- Total packet size = (L2 header: MP or FRF.12 or Ethernet) + (IP/UDP/RTP header) + (voice payload size)
- PPS = (codec bit rate) / (voice payload size)
- Bandwidth = total packet size * PPS

[58] gTLD = Generic top-level domain
[59] ccTLD = Country code top-level domain

The total bandwidth requirement by VoIP calls using some common codecs is presented in Table A1.3.

Table A1. 3: Bandwidth requirement for VoIP calls by common codecs

Table presents the bandwidth requirement during VoIP call by common voice codecs. The bandwidth requirement is for call in one direction and therefore, the overall bandwidth requirement per call is double the bandwidth values shown. The table is adapted from Cisco (2016).

Codec information			Bandwidth calculation					
Codec & Bit Rate (Kbps)	Codec Sample Size (Bytes)	Codec Sample Interval (ms)	Voice Payload Size (Bytes)	Voice Payload Size (ms)	Packets Per Second (PPS)	Bandwidth MP or FRF.12 (Kbps)	Bandwidth w/cRTP MP or FRF.12 (Kbps)	Bandwidth Ethernet (Kbps)
G.711 (64)	80	10	160	20	50	82.8	67.6	87.2
G.729 (8)	10	10	20	20	50	26.8	11.6	31.2
G.723.1 (6.3)	24	30	24	30	33.3	18.9	8.8	21.9
G.723.1 (5.3)	20	30	20	30	33.3	17.9	7.7	20.8
G.726 (32)	20	5	80	20	50	50.8	35.6	55.2
G.726 (24)	15	5		20	50	42.8	27.6	47.2
G.728 (16)	10	5	60	30	33.3	28.5	18.4	31.5
G722_64k (64)	80	10	160	20	50	82.8	67.6	87.2
ilbc_mode_20 (15.2)	38	20	38	20	50	34.0	18.8	38.4
ilbc_mode_30 (13.33)	50	30	50	30	33.3	25.867	15.73	28.8

An example show how to calculate the required bandwidth for a G.711 call (64 Kbps codec bit rate) with cRTP, MP, and the default 160 bytes of voice payload is as follows:

- Total packet size (B) = (MP header of 6By) + (compressed IP/UDP/RTP header of 2B) + (voice payload of 160B) = 168B
- Total packet size (bits) = (168B) * 8bits per byte = 1344 bits
- PPS = (64Kbps codec bit rate) / (160 * 8 bits) = 50pps
- Bandwidth per call = voice packet size (1344 bits) * 50pps = 67.2Kbps

Explanation of terms in Table A1.3 are as follows (Cisco, 2016):

1. Codec Bit Rate (Kbps): Based on the codec, this is the number of bits per second that need to be transmitted in order to deliver a voice call. (codec bit rate = codec sample size / codec sample interval).
2. Codec Sample Size (Bytes): Based on the codec, this is the number of bytes captured by the Digital Signal Processor (DSP) at each codec sample interval. For example, the G.729 coder

operates on sample intervals of 10ms, which corresponds to 10B (80 bits) per sample at a bit rate of 8Kbps. (codec bit rate = codec sample size / codec sample interval).

3. Codec Sample Interval (ms): This is the sample interval at which the codec operates. For example, the G.729 coder operates on sample intervals of 10ms, which corresponds to 10B (80 bits) per sample at a bit rate of 8Kbps. (codec bit rate = codec sample size / codec sample interval).
4. Voice Payload Size (Bytes): The voice payload size represents the number of Bytes (or bits) that are filled into a packet. The voice payload size must be a multiple of the codec sample size. For example, G.729 packets can use 10, 20, 30, 40, 50, or 60 Bytes of voice payload size.
5. Voice Payload Size (ms): The voice payload size can also be represented in terms of the codec samples. For example, a G.729 voice payload size of 20ms (two 10ms codec samples) represents a voice payload of 20-B [(20B * 8) / (20ms) = 8 Kbps].
6. PPS: Represents the number of packets that need to be transmitted every second in order to deliver the codec bit rate. For example, for a G.729 call with voice payload size per packet of 20-B (160 bits), 50 packets need to be transmitted every second [50pps = (8Kbps) / (160 bits per packet)].

A2. Hardware specifications

A2.1. Mesh Potato version 1 specifications

The MP had the following specifications (VillageTelco, 2011) :

- Atheros AR2317 SoC
- 8/16 MB Flash/electrically erasable programmable read-only memory (EEPRAM).
- Silicon labs FXS port chipset - 1 x RJ-11
- 1 x RJ-4510/100Mbit LAN port
- IEEE 802.11b/g; Frequency Band - 2.4 to 2.462GHz
    - Antenna Type : Internal Omnidirectional PCB Antenna
    - Transmit EIRP power: 1-24 Mbit 20dBm or 36-54 Mbit 17dBm
- Firmware: Linux kernel 2.26.3; OpenWRT Kamikaze (customized version); BATMAN mesh routing daemon Version 0.3; and Asterisk 1.4.11

- Power Options: AC adaptor (supplied) PoE or PoTL (Power over Telephone Line) which carry Voice/Data/Power via a single Cat5/6 cable to the MP. Similar to a passive PoE connector but also carries voice telephone line connection allowing phone to be plugged in remotely from the device.

A2.2. Mesh Potato version 2 specifications

The Mesh Potato-2.0 (MP2) had the following specifications (VillageTelco, 2015):

- Atheros AR9331 which SoC with 2.4Ghz 802.11n 1×1 router in a single chip.
- MIPS 24K processor operating at 400MHz. 16/64MB flash/ram configuration
- Two 100-BaseT Ethernet ports
- FXS port based on Silicon Labs Si3217x chipset
- USB 2.0 host/device mode support
- Standard power supply 7.5-12VDC

A2.3. Mesh Potato All-wheel-drive specifications

The Mesh Potato – all wheel drive (MPv2) - had the following specifications (VillageTelco, 2016):

- Atheros AR9331 SoC with a 2.4GHz 802.11n 1×1 router in a single chip
    - Internal antenna for 2.4GHz operation
- FXS port based on Silicon Labs Si3217x chipset
- 16/64MB flash/RAM memory configuration
- Two 100Base-T Ethernet ports
- High-speed UART for console support
- A second radio module based on the MediaTek/Ralink RT5572 chipset which supports IEEE 802.11b/g/n 2T2R (2×2 MIMO) operation on 2.4 and 5 GHz bands.
    - No external antenna out-of-the-box.
- Internal SD card slot capable of supporting local content serving, data caching, and general data storage applications.
- Internal USB port which can be used for a memory device, GSM 3G/4G dongle or other USB devices.
- Power options: PoE/PoTL adaptor with specifications as MP.

A2.4. UniFi specifications

The UniFi has the following specifications (Ubiquiti Networks, 2019b):

- Power Method: 24V Passive PoE
- Maximum Tx Power
    - 2.4GHz – 30dBm
    - 5GHz – 30dBm
- Firmware: Version 4.0.21.9965
- Antennas: (2) External Dual-Band Omni Antennas
    - 2.4 GHz – 3dBi
    - 5 GHz – 4dBi
- Wi-Fi Standards: 802.11 a/b/g/n/r/k/v/ac
- Networking interface: One 10/100/1000 Ethernet Port

A2.5. Litebeam AC-*Gen2* specifications

The Litebeam has the following specification (Ubiquiti Networks, 2019a)

- Firmware:
- Power Method: 24V, 0.3A Gigabit PoE.
- Gain: 23dBi.
- Networking Interface: (1) 10/100/1000 Ethernet Port.
- Processor Specs MIPS 74Kc.
- Memory 64 MB DDR2.
- Channel Sizes: PtP Mode at 10/20/30/40/50/60/80 MHz; PtMP Mode at 10/20/30/40 MHz
- Operating Frequency (MHz) - 5150 – 5875 (worldwide)

A2.6. Server specifications

A Linux PC was configured locally to fulfil the requirements with the specifications as follows:

- Storage: 500GB
- RAM: 16GB
- Processor: Intel(R) Core(TM) i5-4670k at 3.40GHz, quad-core
- OS: Linux Ubuntu 18.04.2 LTS

A2.7. Raspberry Pi-2 specifications

The specifications are as follows:

- Model: B Version: 1.1
- Processor: 900MHz quad-core ARM Cortex-A7 CPU
- RAM: 1GB
- Storage: Micro SD card slot
- Wi-Fi: Nano-USB IEEE 802.11 b/g/n adapter from Edimax model EW-7811Un with Realtek RTL8188CUS chipset supporting speeds up to 150 Mbps.
- OS: Raspbian 9 (based on Debian Stretch)

A3. MPv2 and UniFi testbeds preparation supporting data

A3.1. Clustered-hierarchical mesh topology

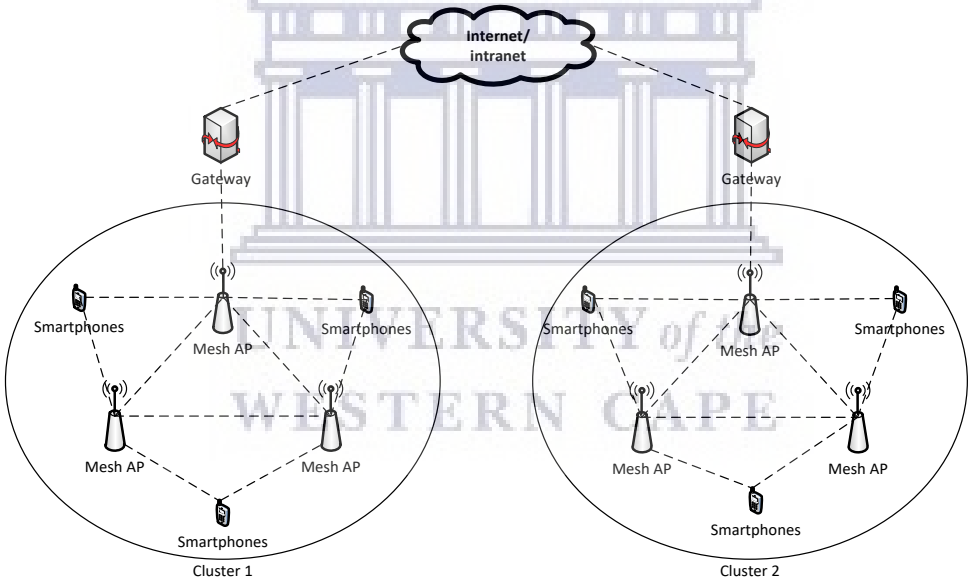

Figure A3.1: An example clustered-hierarchical WMN topology
The figure shows an example of the type of topology to be used for experiments in this study. The dotted line are wireless connections. The cloud can be Internet or intranet.

A3.2. MPv2 testbed pre-setup procedure

The section presents the pre-setup procedure for MPv2 testbed setup.

1. Selection of number of devices

The testbed setup process initiated with selection of number of units. For the testbed, 6 MPv2 units were purchased[60] from manufacturers of the devices, VillageTelco[61]. At the time of purchase (end of 2015), the MPv2 units were considered to be in the final beta phase of production by the manufacturers, and hence, to avoid risk of financial loss, and unknown to the performance and reliability of the devices, only 6 units were purchased. A topology design consisting of 2 clusters of 3 MPv2 units per cluster was adopted for the testbed. The specifications of MPv2 unit used in this research are presented in Appendix A2, Section A2.3 (Mesh Potato – 'All wheel drive'). The clusters linked to each other via 1 MPv2 unit from each cluster sharing a single-hop link. Figure A3.2 shows the adopted topology for the MPv2 testbed. The next step present the route establishment process used by the mesh routing protocol implemented in MPv2 units.

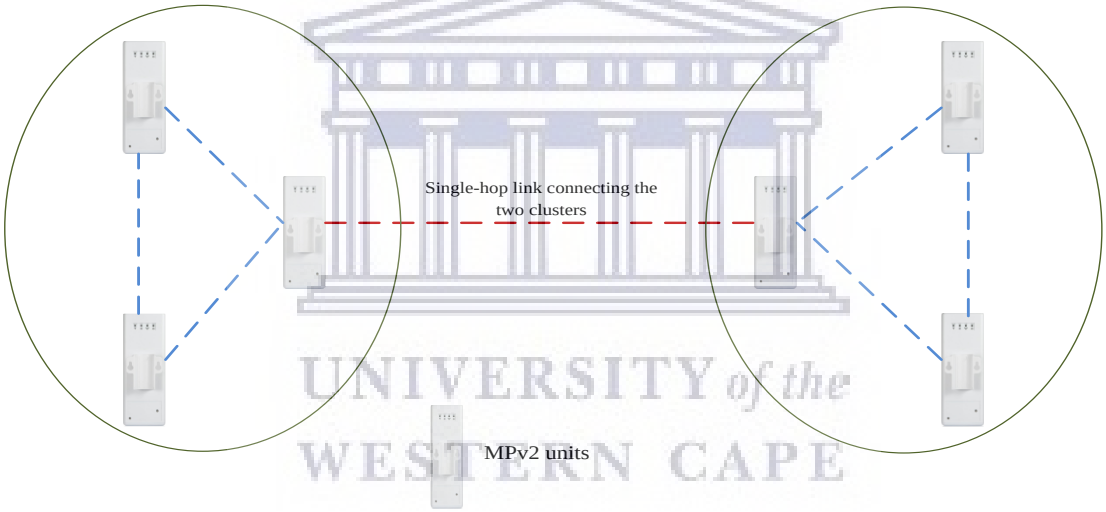

Figure A3.2: Clustered physical topology for MPv2 testbed
The figure shows the network topology to be used for the MPv2 testbed.

2. Understanding the route establishment process

In order to form multi-hop testbed, it was very important to understand the mesh link establishment process of the MPv2 units. The MPv2 firmware called Small Enterprise Campus Network (SECN) implemented BATMAN-adv version IV-2016.1 distance-vector based routing protocol which operates at the layer 2 of open systems interconnect (OSI) protocol stack. Therefore, in a mesh

[60] The funding was provided by Center of Excellence at Department of Computer Science, UWC.
[61] VillageTelco link: www.villagetelco.org

network implementing BATMAN-adv routing protocol, MAC addresses instead of IP addresses are used to identify the participating mesh nodes. During route establishment process, every BATMAN-adv node broadcasts Originator Message (OGM) packets at fixed interval of 1-second (default setting) consisting of new network information and routes to all the neighbouring mesh nodes in order to establish a mesh network (Hardes, 2015; Martin & Ledet-Pedersen, 2011). A BATMAN-adv OGM packet consists of many fields and is shown in Table A3.1 along with their description. The transmitting and reception of OGM packets is done using a virtual mesh interface called *bat0*.

Table A3.1: Header fields in the originator message packet of BATMAN-adv
The table shows the different header fields in the BATMAN-adv OGM packet and their description (Hardes, 2015).

Field	Description
Version	The version of BATMAN-adv protocol. The version installed on the MPv2 was 2016.1 belonging to version IV of BATMAN-adv
Time-to-live (TTL)	Limits the number of times a single OGM can traverse a mesh node to avoid OGM packet flooding. The value is set to 50.The TTL is decremented by 1 every time an OGM traverses a node.
Flags	Specifies whether there is a direct link to the sender or it is chosen as the next best hop
Sequence number	Used to detect duplicate OGMs and calculate link quality
Originator	MAC address of OGM originating node
Previous sender	MAC address of last sender.
Transmission link Quality (TQ)	It describes the link quality for the complete route towards the originator. The TQ is an 8-bit value, between 0 to 255.

An OGM packet is processed by a receiving mesh node only if the TQ value is greater than 0, or the packet is from a sing-hop neighbour. Thus, BATMAN-adv relies on the TQ metric in the OGM packets to determine link quality, and establish low latency and stable routes between participating mesh nodes (Hardes, 2015; Martin & Ledet-Pedersen, 2011). In a BATMAN-adv network, once an OGM packet has been processed by a mesh node, it is either re-broadcast by that node or deleted. Before re-broadcast; (a) the TTL value is decremented by 1 (if the TTL value decrements to 0, then the OGM is deleted); and (b) a hop penalty is reduced from the TQ value. The default hop penalty value is 15 which means that before an OGM packet is re-broadcasted from a mesh node, its TQ value gets reduced by 15 points (Hardes, 2015). Figure A3.2 shows the routing list of an MPv2 after a route establishment process; and the description of the different columns in the routing list is presented in Table A3.2. At this juncture in review of BATMAN-adv, it was evident

that the TQ value had to be manipulated for successful setup of a multi-hop MPv2 testbed in the small area given.

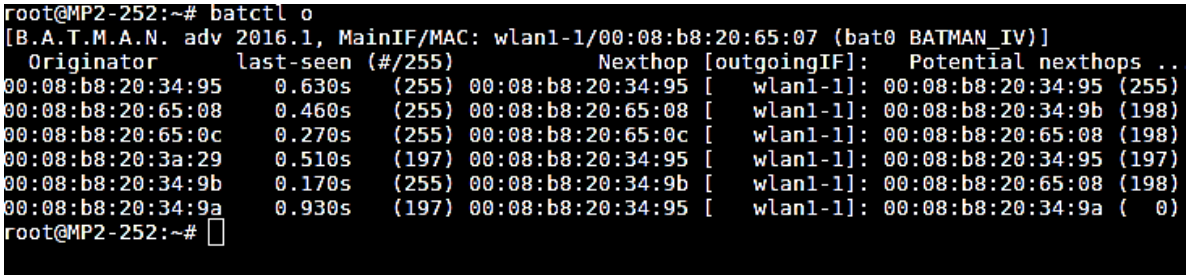

Figure A3.3: Sample originator list at an MPv2 node

The originator list shown is accessed via the command line interface on the mesh nodes. It shows the single-hop neighbours, next-hop links to destinations multi-hop away, and link strength. Figure 9 is a captured screenshot from an MPv2 node. The differences between the MAC address in the 'Originator' column and the 'Nexthop' column is implication of presence of multiple hops between 'Originator' node and the local node.

Table A3.2: Description of different columns in the routing table of MPv2 node

The table shows the description of the different columns of the routing table. The routing table can be accessed using the command line interface or the web interface

Column heading	Description
Originator	Holds the MAC addresses of the nodes generating OGM packets in the network. Since, BATMAN-adv operates on operating systems interconnect (OSI) layer 2, the MAC address is enough to clearly identify a mesh participant
Last-seen	Holds the time stamp to save the time when the last OGM of this originator was received. This value is important in order to purge outdated entries. This could be the case if an originator leaves the network as the route to this device becomes invalid and is not usable any more.
(#/255)	Identifies the Transmission Quality (TQ) value. The metric used by BATMAN-adv in establishing the best next-hop neighbour
Nexthop	Shows the MAC address of the mesh node to which data will be forwarded first.
outgoing IF	Specifies the hardware interface to use if the originator should be reached as BATMAN-adv supports multiple interfaces
Potential nexthops	Specifies the MAC address of the mesh node that will become Nexthop in case the current Nexthop node becomes unavailable.

3. Device shortcomings

The out-of-box MPv2 units did not consist of any antenna for the 5GHz radio. As shown in Figure A3.4, the MPv2 units were only supplied with two Reverse Polarity Subminiature version A (RP-SMA) connectors, attached to the I-PEX connector for the 5GHz radio chipset, to install two external antennas. Therefore two indoor omni-directional 2.4G/5GHz dual-band 4.5dBi high-gain printed circuit board (PCB) antenna were installed in each MPv2 unit.

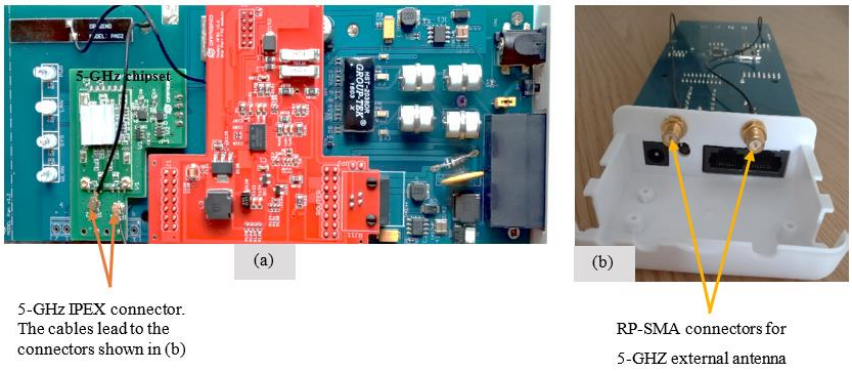

Figure A3.4: Out-of-box MPv2 units with the RP-SMA connectors but no 5GHz antenna.
Figure shows the motherboard of an MPv2 unit in (a) with 5GHz radio chipset and the I-PEX connectors for the 5GHz external antenna. The connecting cables from the I-PEX connector lead to the RP-SMA connectors shown in (b).

A3.3. UniFi testbed pre-setup procedures

1. Selection of number of devices

The testbed setup process began with selection of number of units. For the UniFi testbed, 9 UniFi units and 2 Litebeam AC-*Gen2* (LB) PtMP units were purchased[62] from the manufacturers of the devices, Ubiquiti[63]. The LB units were used to include PtMp link in the testbed to match the usage of PtMp links using similar devices in Zenzeleni-Mankosi and Zenzeleni-Zithulele. The adopted physical topology design to be used for testbed setup consisted of; (a) 2 multi-hop mesh clusters of 4 UniFi units per cluster; (b) 1 base station UniFi unit configured to function as cluster gateway (CG) for the 2 clusters; (c) one LB unit functioning in station mode (LB-S) and sharing wired connection with the base UniFi unit; (d) one LB in AP mode (LB-AP) to form wireless PtP link with the LB-S; and (e) a gateway device with wired connection to the LB-AP mode. The planned physical topology for the UniFi testbed is shown in Figure A3.5. The specifications of the UniFi, and LB devices are presented in Section A2.4, and Section A2.5 respectively. The next step presented the route establishment process used by the UniFi device.

[62] The funding was provided by Centre of Excellence at Department of Computer Science, UWC.
[63] Ubiquiti link: www.ui.com

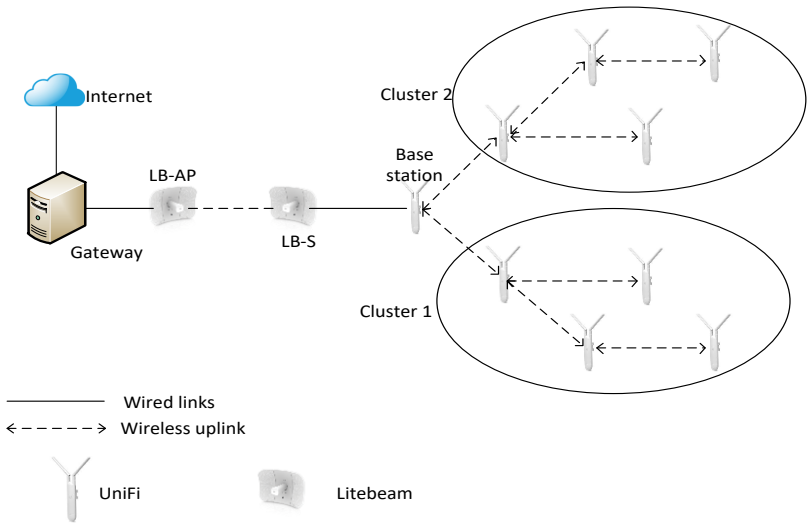

Figure A3.5: Clustered physical topology for UniFi testbed experiments
The figure shows the network topology to be used for the UniFi testbed.

2. *Understanding the route establishment process*

The UniFi units are unlike any other mesh devices because they do not use any underlying layer 2 or 3 mesh routing protocol, but instead use wireless uplink feature to form multi-hop connection.

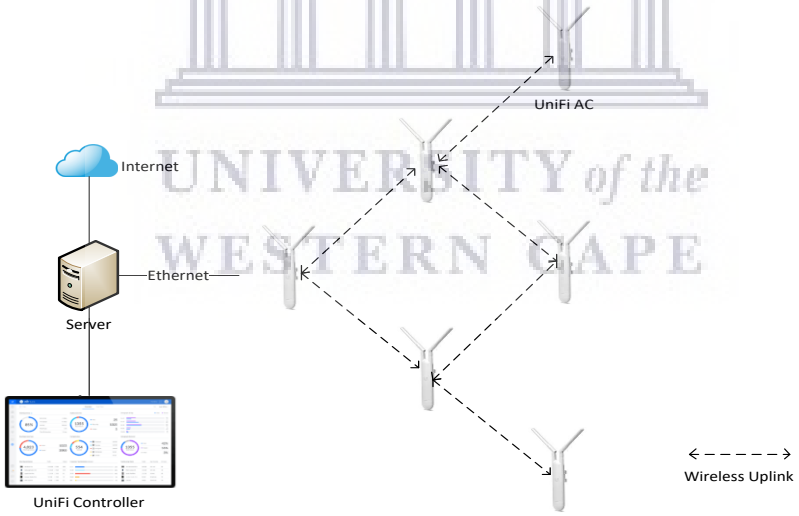

Figure A3.6: Wireless uplink multi-hop connections
The figure shows the wireless uplink connection to form a mesh topology using UniFi devices

As shown in Figure A3.6, in the wireless uplink configuration; (a) one UniFi AP is configured as a base station and linked via Ethernet to a desktop running DHCP server for IP address distribution to the other UniFi APs in the network; and (b) the other APs are linked to the base station AP via either direct wireless uplink (single-hop) or indirectly via other APs (multi-hop) with uplink route to the base station AP (Ubiquiti, 2019). The IP addresses to the UniFi APs

are allocated via the DHCP server, linked to the base station because UniFi devices are only APs and do not consist of in-built DHCP server. The UniFi devices can be configured via a central UniFi network management controller (Ubiquiti Networks, 2019c). The UniFi controller is implemented on the desktop/server with wired connection to the base unit for automatic adoption of the other UniFi units linked wirelessly to the base unit.

3. Device shortcomings

The UniFi devices cannot form connectivity without a DHCP server. A desktop running Linux Ubuntu 18.04.2 LTS was added to the setup to implement the DHCP server and UniFi controller. The specifications of the desktop are presented in Section A2.6. It is noteworthy to mention that if the DHCP server shut down, then the entire network of UniFi units receiving IP addresses from the DHCP server became inactive.

A3.4. Received signal strengths in MPv2 testbed

Table A3.3: Received signal strength for each single-hop link between MPv2 nodes

The table shows the Rx values measured at each MPv2 of the single-hop links formed with other MPv2 units. For example, the average Rx measured at MPv2 node 252 for link with MPv2 number 25 is -68.8-dBm.

MPv2 Rx measured		**Rx values (dBm)**					
at	for	1	2	3	4	5	Average
@ 252	**25**	-72	-64	-70	-72	-66	-68.8
	24	-54	-52	-54	-54	-46	-52
	23	-58	-60	-58	-58	-56	-58
@ 25	**252**	-66	-74	-72	-64	-66	-68.4
	22	-58	-60	-54	-60	-60	58.4
	20	-56	-52	-60	-56	-56	-56
@ 24	**252**	-54	-48	-54	-50	-54	-52
	23	-70	-70	-70	-70	-70	-70
@ 23	**252**	-62	-56	-60	-56	-60	-58.8
	24	-72	-72	-72	-72	-72	-72
@ 22	**25**	-60	-56	-60	-56	-62	-58.8
	20	-68	-66	-68	-66	-66	-66.8
@ 20	**25**	-52	-58	-56	-52	-58	-55.2
	22	-70	-70	-68	-68	-70	-69.2

A3.5. Received signal strengths in UniFi testbed

Table A3.4: Received signal strength for each single-hop link between UniFi nodes

The table shows all the Rx of single-hop links received at UniFi nodes. The last two digits of the MAC addresses are used to number the nodes. Decoding the table, in the 'Links' column of the table, a link 94 – a0 means single-hop link between UniFi node 94 and a0; and the Rx of node a0 recorded at node 94.

	Cluster A - Rx (dBm)			Cluster B - Rx (dBm)			
Links	1	2	Average	**Links**	1	2	Average
94 - a0	-60	-60	-60	94 - 4a	-58	-60	-59
a0 - 94	-60	-60	-60	4a - 94	-60	-58	-59
a0 - 84	-55	-54	-54.5	4a - 10	-48	-51	-73.5
84 - a0	-54	-55	-54.5	10 - 4a	-51	-48	-73.5
a0 - 26	-71	-61	-66	4a - 79	-55	51	-53
26 - a0	-61	-71	-66	79 - 4a	-51	-55	-53
84 - 7a	-63	-58	-60.5	79 - 74	-68	-71	-69.5
7a - 84	-58	-63	-60.5	74 - 79	-71	-68	-69.5

A3.6. D-ITG configuration commands

1. ITGSend command details for VoIP traffic:

   -a <IP Address> -rp <port number> -m <type of metre> -t <duration> VoIP -x <VoIP codec> -h <audio transfer protocol>

   Description:

   -a = destination IP address; *-rp* = port number; *-m* = type of meter which in this case is rttm (round-trip time metre); *-t* = duration in milliseconds; VoIP = type of VoIP traffic; *-x* = type of codec which in this case was G.711; *-h* = audio transfer protocol which in this case was RTP.

   The final ITGSend script file contained the command to generate the VoIP traffic and a looked as follows:

   ```
   -a 192.168.1.124 -rp 10001 -m rttm -t 300000 VoIP -x G.711.2 -h RTP
   ```

2. Description of ITG send command in bash script file:

   ITGSend <name of ITGSend script file> -l <save log on sender file name> -x <save log on receiver file name>

   sleep <interval time>

3. Bash script used to execute 20 iterations of the ITGsend command for VoIP traffic:

   ```
   #!/bin/bash
   ```

```
ITGSend ITGSend_script_file -l 1send -x 1receive
sleep 5
ITGSend ITGSend_script_file -l 2send -x 2receive
.
.
sleep 5
ITGSend ITGSend_script_file -l 20send -x 20receive
sleep5
ITGSend ITGSend_script_file -l 20send -x 20receive
```

4. Description of command in bash script:

```
ITGDec <name of ITGSend log> >> <name of ITGSend log.txt>
```

5. ITGSend file with commands to execute 5-flows:

-a 192.168.1.124 -rp 10001 -m rttm -t 300000 VoIP -x G.711.2 -h RTP
-a 192.168.1.124 -rp 10002 -m rttm -t 300000 VoIP -x G.711.2 -h RTP
-a 192.168.1.124 -rp 10003 -m rttm -t 300000 VoIP -x G.711.2 -h RTP
-a 192.168.1.124 -rp 10004 -m rttm -t 300000 VoIP -x G.711.2 -h RTP
-a 192.168.1.124 -rp 10005 -m rttm -t 300000 VoIP -x G.711.2 -h RTP

A3.7. Final data collected volume

The total number of iterations for TH, RTL, RTJ, and PL% collective of the number of iterations for each mesh link of each hop length for MPv2 testbed data collection is shown in Table A3.5.

Table A3.5: Total number of throughput, latency, jitter and packet loss test iterations from MPv2 testbed experiments
Table shows number of mesh links for each hop length. For each mesh link mesh link for every hop length, there were 20 + 20 iterations for TH; and 20 iterations for RTL, RTJ, and PL%. Therefore, total number of iterations for each mesh link for every hop length is calculated.

		TCP	VoIP
		Throughput	RTL, RTJ, and PL%
Hop length	Mesh links	Total iterations	Total iterations for each mesh link
1	7	(20 + 20) X 7 = 280	20 X 7 = 140
2	4	(20 + 20) X 4 = 160	20 X 4 = 80
3	4	(20 + 20) X 4 = 160	20 X 4 = 80

The total number of test iterations for UniFi testbed data collections for: (a) single flow TH collective of 20 + 20 iterations for each mesh link of each inter-cluster hop length; and (b) for each multiple flow from 2 up to 41 for RTL, RTJ, and PL% collective of 20 iterations for every flow count from 2 up to 41 for each mesh link of each inter-cluster hop length is shown in Table A3.6.

Table A3.6: Total number of throughput, latency, jitter and packet loss test iterations from UniFi testbed experiments
Table shows number of mesh links for each inter-cluster hop length. For each mesh link for every hop length, there were 20 + 20 iterations for TH; and 20 iterations for RTL, RTJ, and PL%. Performance RTL, RTJ, and PL% were evaluated for 2-flows up to 41-flows for each mesh link. Therefore, total number of iterations for each flow for each mesh link for every hop length is calculated.

		TCP	G. 711 - VoIP
		Throughput	RTL, RTJ, and PL%
Hop length	**Mesh links**	**Total iterations**	**Total iterations for each flow from 2 up to 41**
2	1	40	20 per-flow
3	4	(20 + 20) X 4 = 160	20 X 4 = 80 per-flow
4	6	(20 + 20) X 6 = 240	20 X 6 = 120 per-flow
5	4	(20 + 20) X 4 = 160	20 X 4 = 80 per-flow
6	1	40	20 per-flow

A3.8. Description of wireless network mode combinations

Table A3.7: Wireless network mode combinations
Figure shows the different Wi-Fi and cellular radio mode; and 3G and Wi-Fi mode combination possible with the LeSs acquired.

Call Type	Application	Network-mode description
W-AUTO	CSIP and Viber	Wi-Fi calls with cellular radio in 2G/3G network mode
W-2G	CSIP and Viber	Wi-Fi calls with cellular radio in GSM network mode
W-3G	CSIP and Viber	Wi-Fi calls with cellular radio in 3G network mode
W-PLAIN	CSIP and Viber	Wi-Fi calls with cellular radios turned off , hence achieving partial-airplane mode
3G-X	Viber only	Voice calls using 3G data with Wi-Fi radio ON but not connected to any AP
3G	Viber only	Voice calls using 3G data with Wi-Fi radio OFF

A3.9. Script file to extract the power consumption from log file

```
# open the log file to read
file = open('D:/UWC/self/cpuid/imom1.log')

# create the output csv file to write to
outfile = open("D:/UWC/self/cpuid/output.csv", "w")

# start reading the line of log file
line = file.readline()

# while reading a line, look for string with CPUID of the application
# if the line has the CPUID  of the application, write it to the CSV
file
# read the next line of the input file
```

```
while line:
    if 'CPU-10100' in line:
        print(line.strip(), file=outfile)
    line = file.readline()
file.close()
# close log file once done reading all the lines
```

A3.10. Versions of the IM and SIP mobile applications

Table A3.8: Versions of IM and SIP application used in mobile application evaluation.
The table shows the version of the IM and SIP applications used in the experiments. The Android Package Kit (APK) files of the applications were used for installation.

Instant Messengers		SIP Clients	
Type	**Version**	**Type**	**Version**
WhatsApp	2.17.190	Zoiper	1.51
Messenger	121.0.0.15.70	CSipSimple	1.02.03
Viber	6.9.1.16	MizuDroid	2.4.0
IMO	9.8.000000006691	SipDroid	4.0 beta

A4. Plots of network performance trends

A4.1. MPv2 – throughput plot

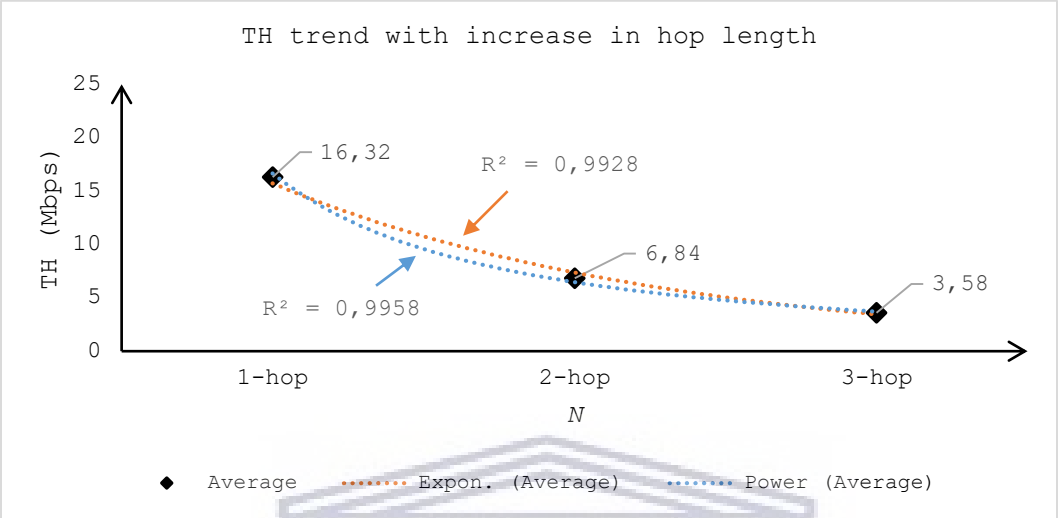

Figure A4.1: Performance of TH with increasing number of hop length

The graph shows the drop in TH with increase in number of hops, N, between MPv2 units. The average values of TH; and the R^2 values for exponential and power regression techniques calculated using the average TH values are displayed on the plot.

A4.2. MPv2 – round-trip latency plot

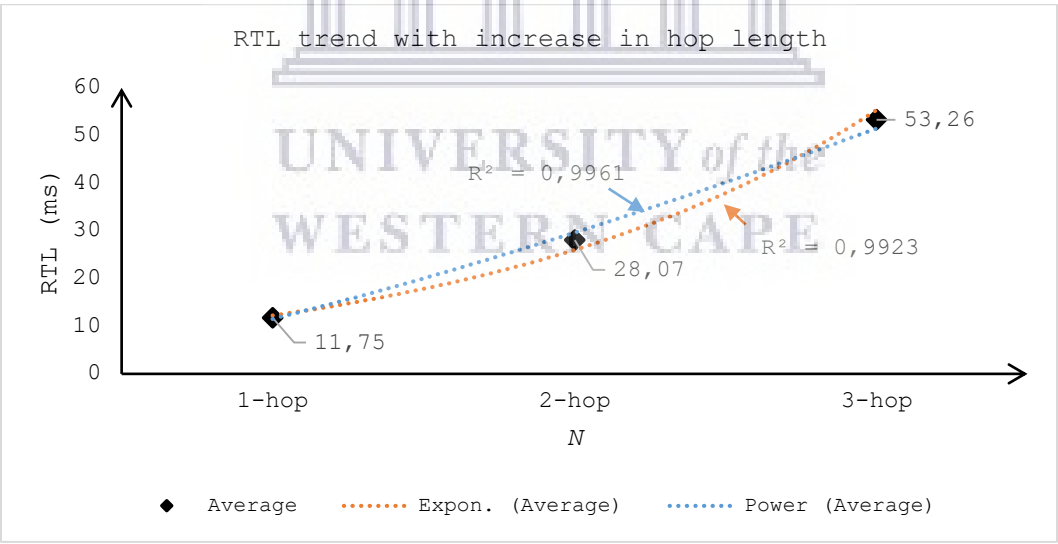

Figure A4.2: Performance of RTL with increasing number of hop length

The graph shows the rise in RTL with increase in number of hops, N, between MPv2 units. The average RTL values; and the R^2 values for exponential and power regression techniques calculated using the average RTL values, are displayed on the plot.

A4.3. MPv2 – round-trip jitter plot

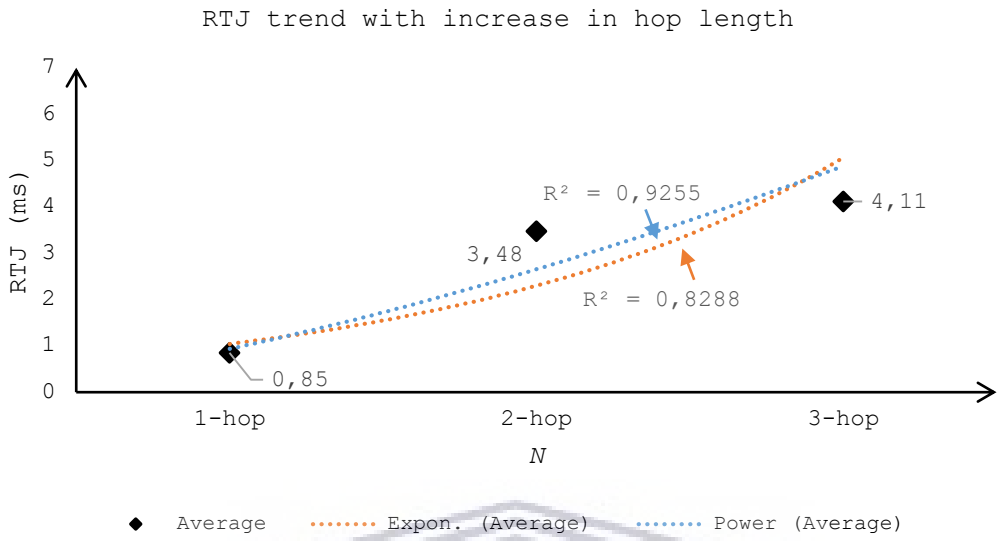

Figure A4.3: Performance of RTJ with increasing number of hop length

The graph shows the rise in RTJ with increase in number of hops, N, between MPv2 units. The average RTJ values; and the R^2 values for exponential and power regression techniques calculated using the average RTJ values, are displayed on the plot.

A4.4. MPv2 – packet loss percentage plot

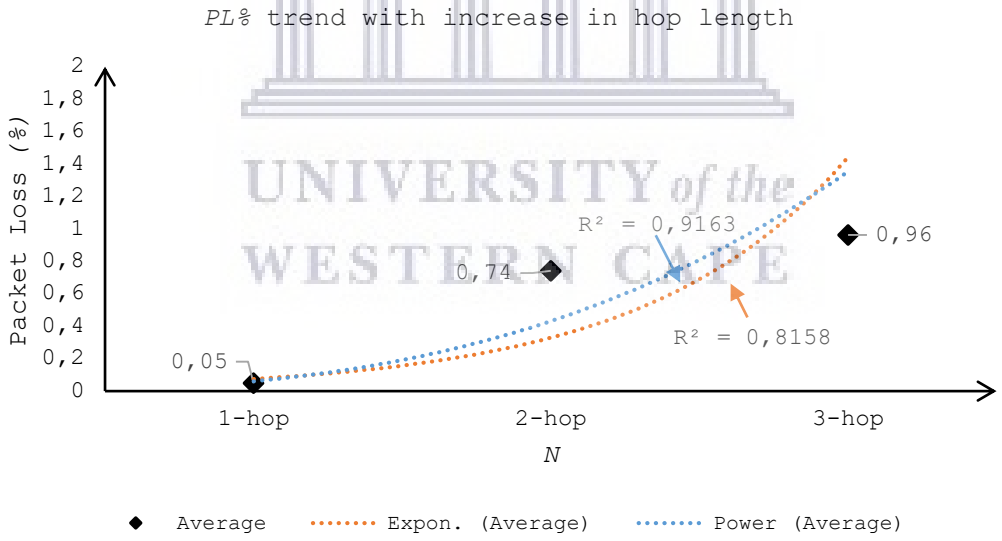

Figure A4.4: Performance of PL% with increasing number of hop lengths

The graph shows the rise in PL% with increase in number of hops, N, between MPv2 units. The average PL% values; and the R^2 values for exponential and power regression techniques calculated using the average PL% values, are displayed on the plot.

A4.5. UniFi – throughput plot

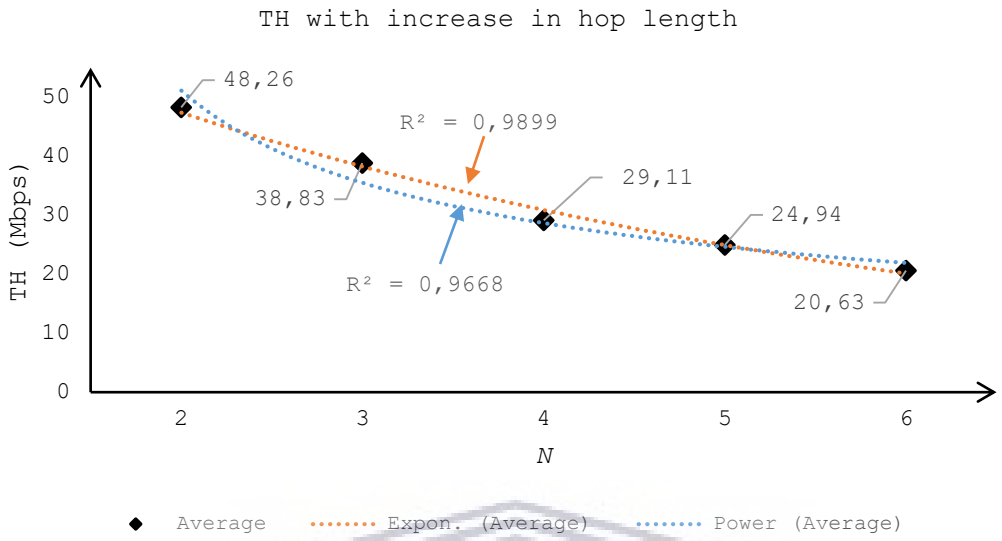

Figure A4.5: Performance of TH with increasing number of hop lengths

The graph shows the decline in average TH values with increase in number of inter-cluster hop lengths, N, between UniFi units. The average TH values; and the R2 coefficient for exponential and power regression analysis calculated using the average TH values are displayed on the plot.

A4.6. UniFi – round-trip latency plots

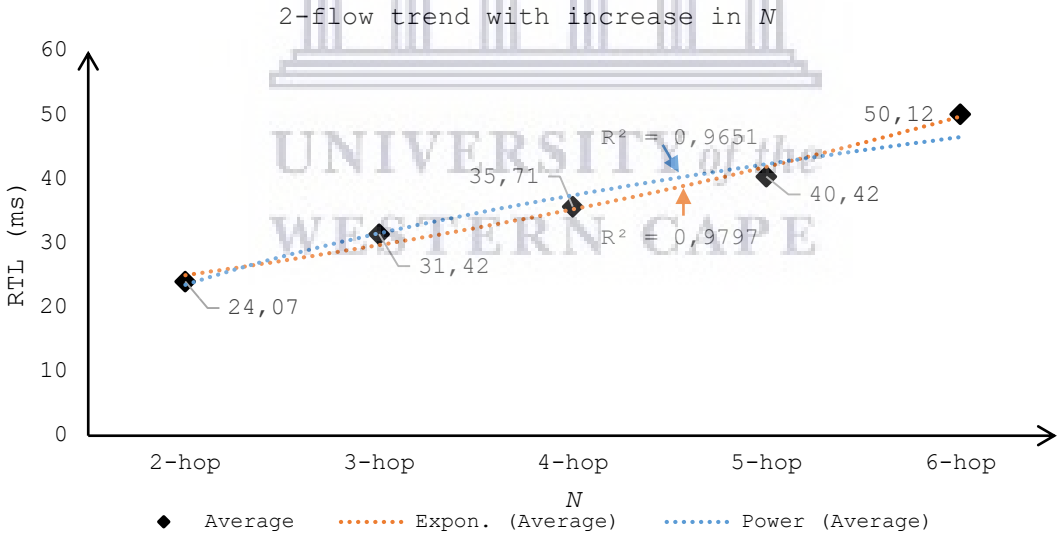

Figure A4.6: Average round-trip latency performance of 2-flows with increasing number of hop lengths, N

The graph shows the trend in average RTL values of 2-flows with increase in number of hop lengths N between UniFi units. The average values of RTL for 2-flows are displayed on the graph. The R^2 values for exponential and power regression techniques calculated using the average RTL values are also displayed on either side of the respective regression trendlines.

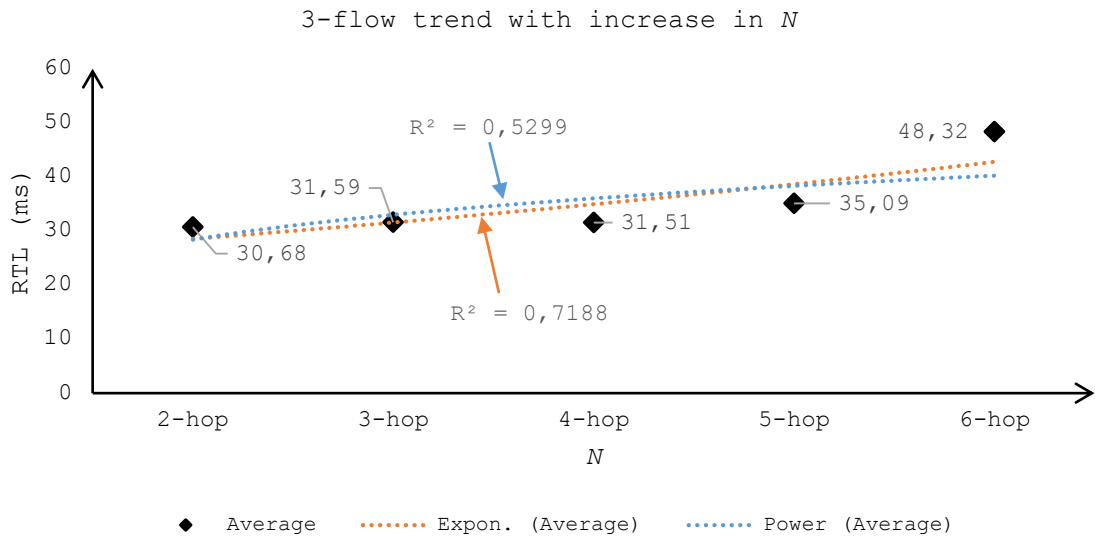

Figure A4.7: Average round-trip latency performance of 3-flows with increasing number of hop lengths, N
The graph shows the trend in average RTL values of 3-flows with increase in number of hop lengths N between UniFi units. The average values of RTL for 3-flows are displayed on the graph. The R^2 values for exponential and power regression techniques calculated using the average RTL values are also displayed on either side of the respective regression trendlines.

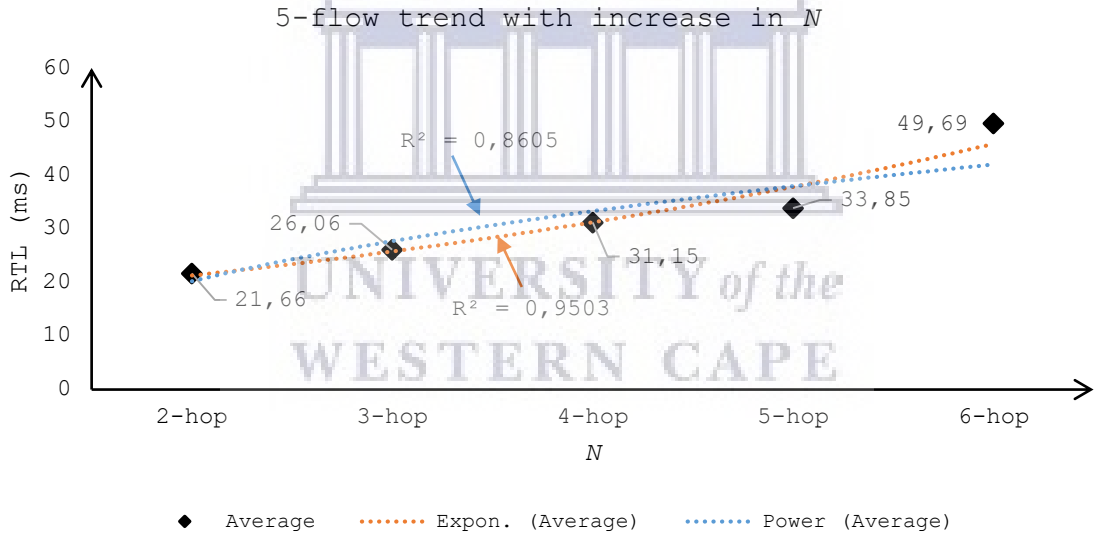

Figure A4.8: Average round-trip latency performance of 5-flows with increasing number of hop lengths, N
The graph shows the trend in average RTL values of 5-flows with increase in number of hop lengths N between UniFi units. The average values of RTL for 5-flows are displayed on the graph. The R^2 values for exponential and power regression techniques calculated using the average RTL values are also displayed on either side of the respective regression trendlines.

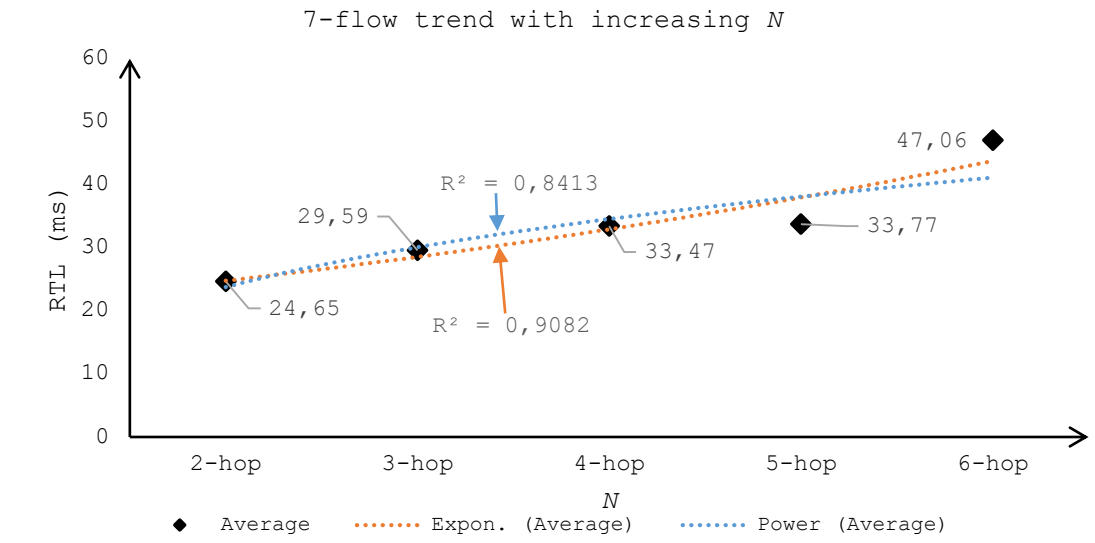

Figure A4.9: Average round-trip latency performance of 7-flows with increasing number of hop lengths, N
The graph shows the trend in average RTL values of 7-flows with increase in number of hop lengths N between UniFi units. The average values of RTL for 7-flows are displayed on the graph. The R^2 values for exponential and power regression techniques calculated using the average RTL values are also displayed on either side of the respective regression trendlines.

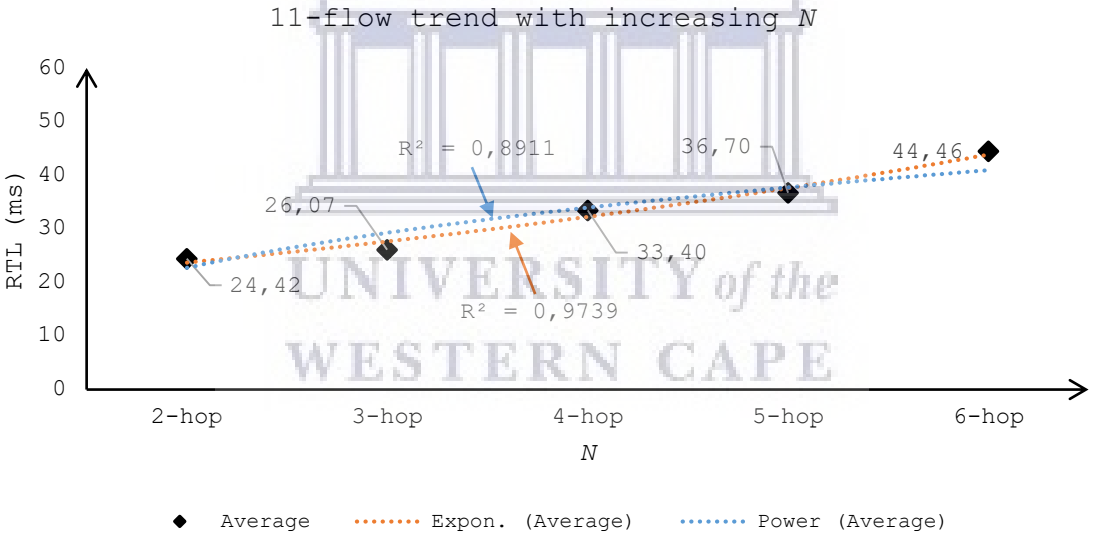

Figure A4.10: Average round-trip latency performance of 11-flows with increasing number of hop lengths, N
The graph shows the trend in average RTL values of 11-flows with increase in number of hop lengths N between UniFi units. The average values of RTL for 11-flows are displayed on the graph. The R^2 values for exponential and power regression techniques calculated using the average RTL values are also displayed on either side of the respective regression trendlines.

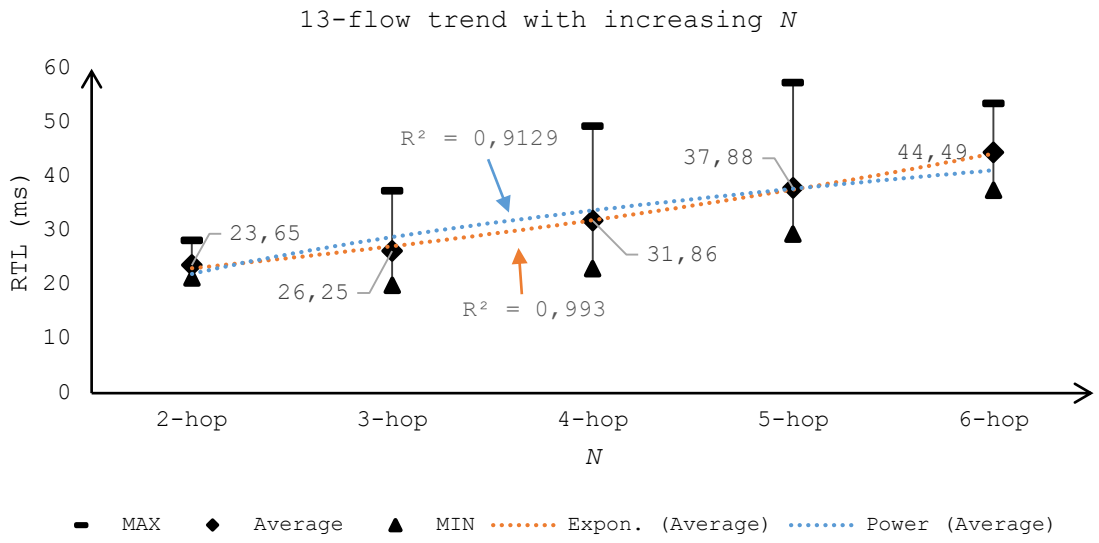

Figure A4.11: Average round-trip latency performance of 13-flows with increasing number of hop lengths, N
The graph shows the trend in average RTL values of 13-flows with increase in number of hop lengths N between UniFi units. The average values of RTL for 13-flows are displayed on the graph. The R^2 values for exponential and power regression techniques calculated using the average RTL values are also displayed on either side of the respective regression trendlines.

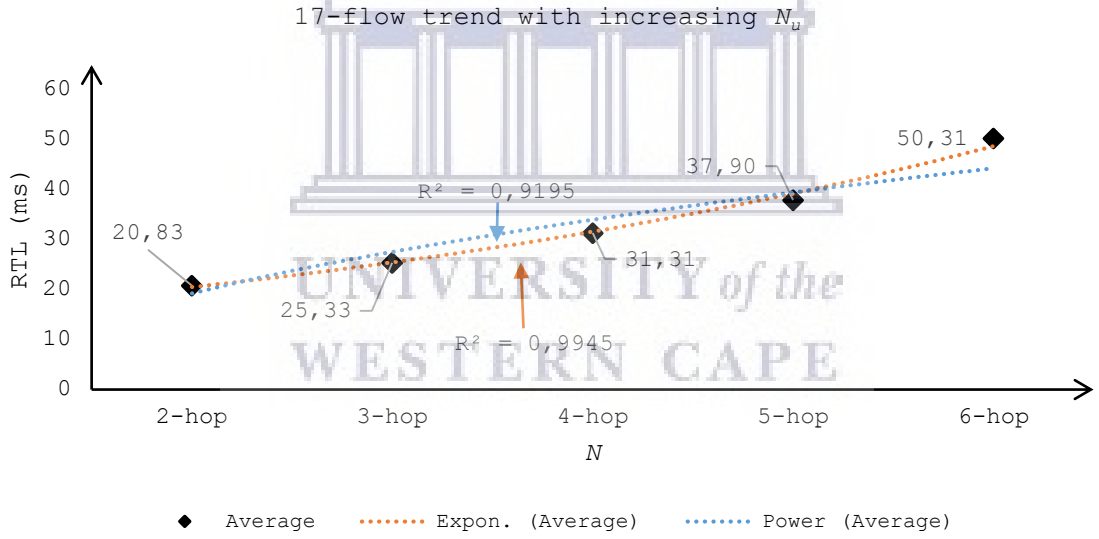

Figure A4.12: Average round-trip latency performance of 17-flows with increasing number of hop lengths, N
The graph shows the trend in average RTL values of 17-flows with increase in number of hop lengths N between UniFi units. The average values of RTL for 17-flows are displayed on the graph. The R^2 values for exponential and power regression techniques calculated using the average RTL values are also displayed on either side of the respective regression trendlines.

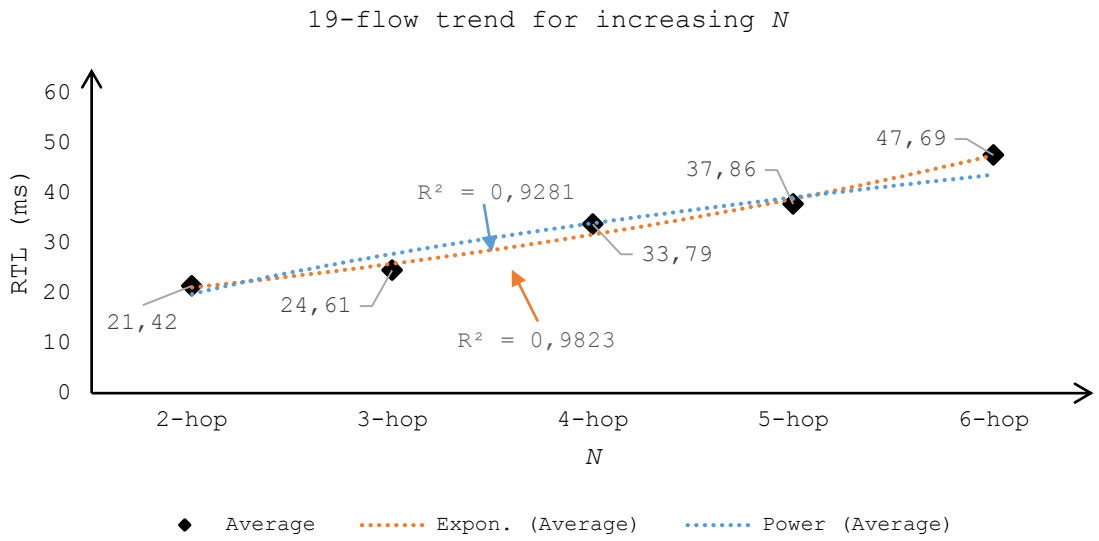

Figure A4.13: Average round-trip latency performance of 19-flows with increasing number of hop lengths, N
The graph shows the trend in average RTL values of 19-flows with increase in number of hop lengths N between UniFi units. The average values of RTL for 19-flows are displayed on the graph. The R^2 values for exponential and power regression techniques calculated using the average RTL values are also displayed on either side of the respective regression trendlines.

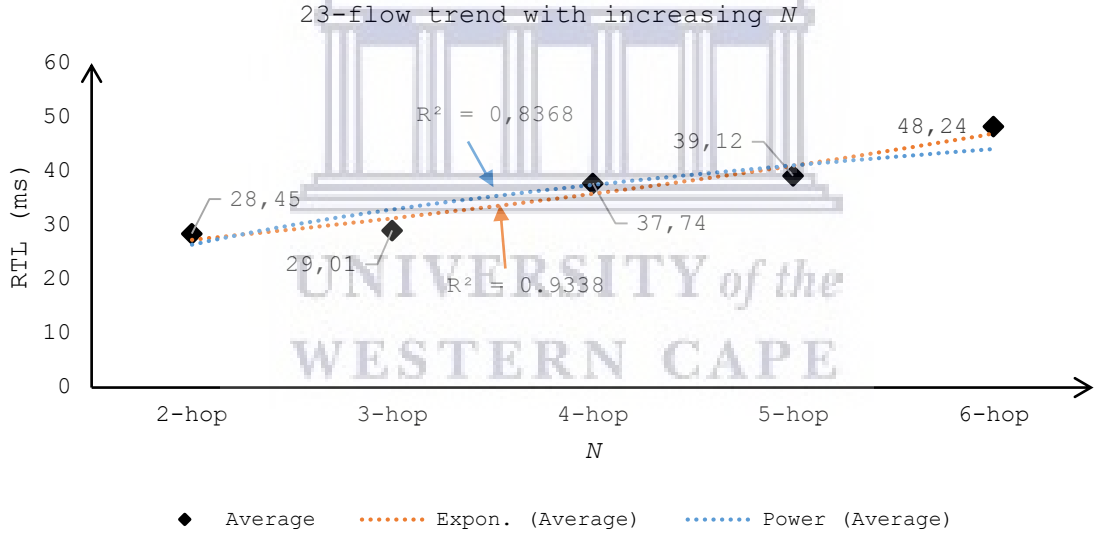

Figure A4.14: Average round-trip latency performance of 23-flows with increasing number of hop lengths, N
The graph shows the trend in average RTL values of 23-flows with increase in number of hop lengths N between UniFi units. The average values of RTL for 23-flows are displayed on the graph. The R^2 values for exponential and power regression techniques calculated using the average RTL values are also displayed on either side of the respective regression trendlines.

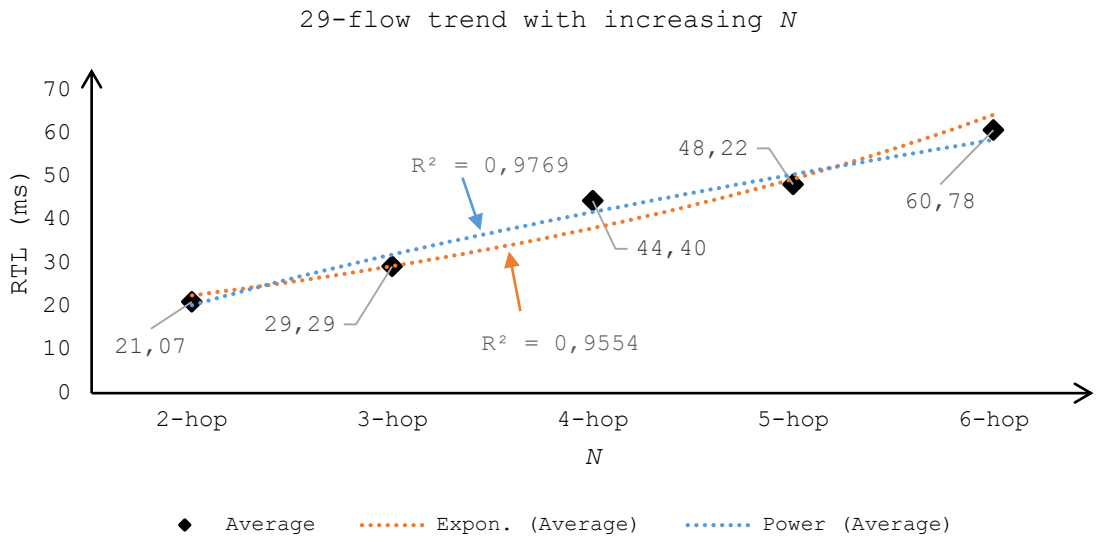

Figure A4.15: Average round-trip latency performance of 29-flows with increasing number of hop lengths, N
The graph shows the trend in average RTL values of 29-flows with increase in number of hop lengths N between UniFi units. The average values of RTL for 29-flows are displayed on the graph. The R^2 values for exponential and power regression techniques calculated using the average RTL values are also displayed on either side of the respective regression trendlines.

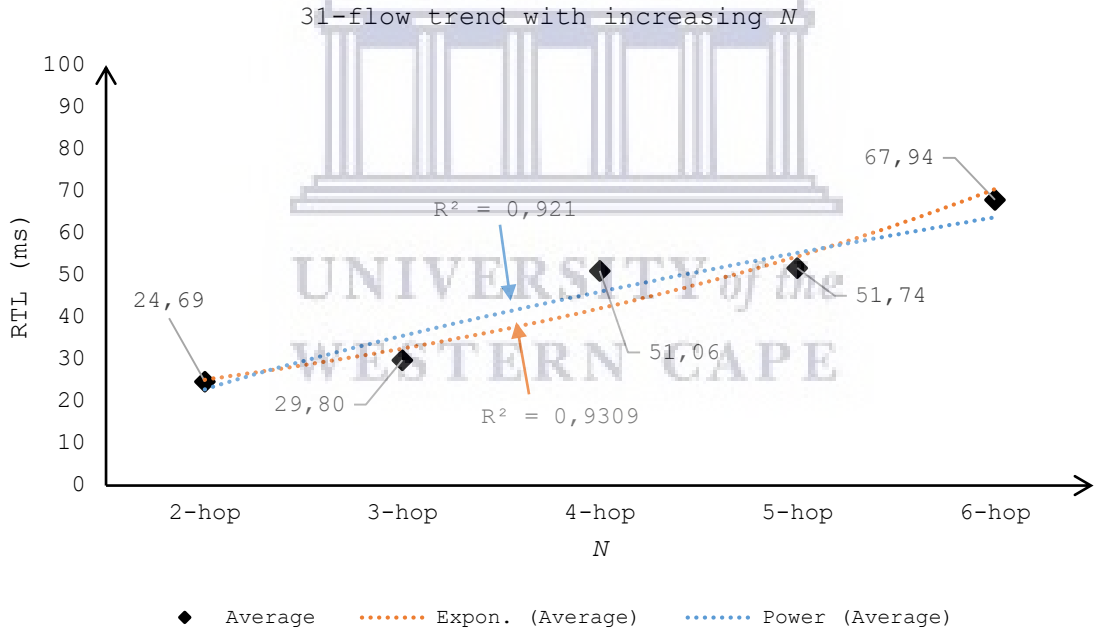

Figure A4.16: Average round-trip latency performance of 31-flows with increasing number of hop lengths, N
The graph shows the trend in average RTL values of 31-flows with increase in number of hop lengths N between UniFi units. The average values of RTL for 31-flows are displayed on the graph. The R^2 values for exponential and power regression techniques calculated using the average RTL values are also displayed on either side of the respective regression trendlines.

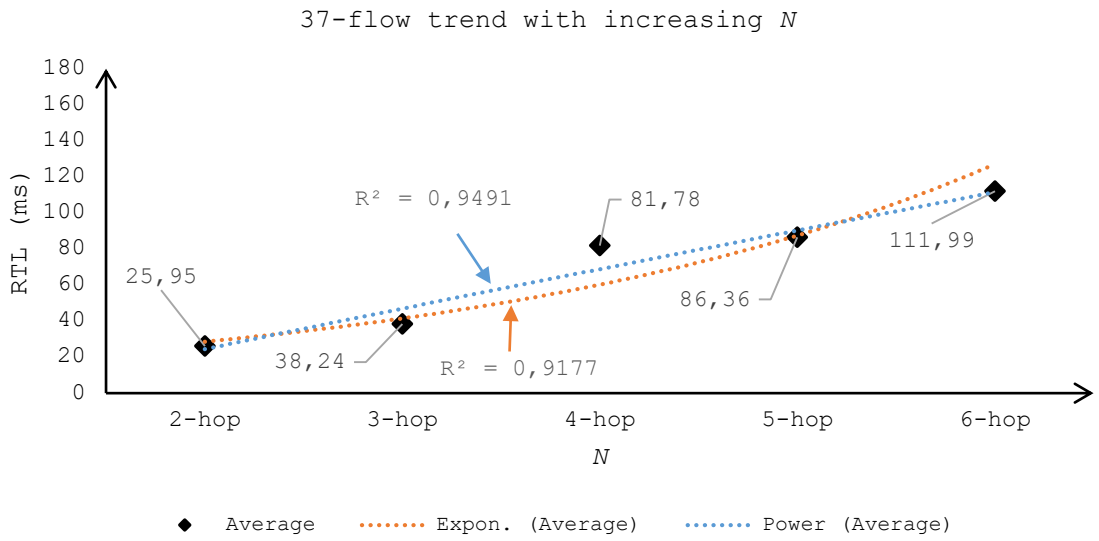

Figure A4.17: Average round-trip latency performance of 37-flows with increasing number of hop lengths, N
The graph shows the trend in average RTL values of 37-flows with increase in number of hop lengths N between UniFi units. The average values of RTL for 37-flows are displayed on the graph. The R^2 values for exponential and power regression techniques calculated using the average RTL values are also displayed on either side of the respective regression trendlines.

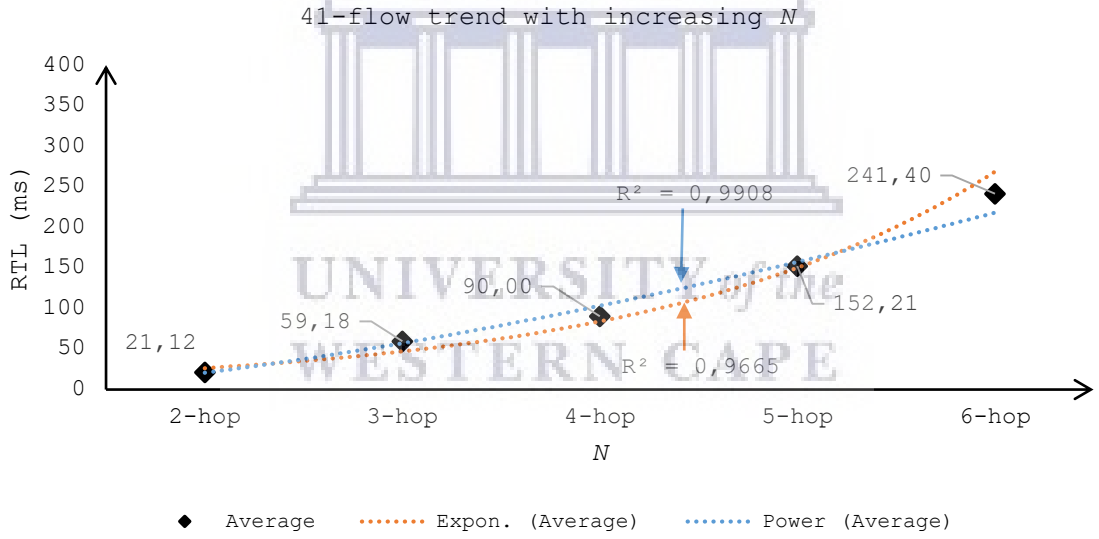

Figure A4.18: Average round-trip latency performance of 41-flows with increasing number of hop lengths, N
The graph shows the trend in average RTL values of 41-flows with increase in number of hop lengths N between UniFi units. The average values of RTL for 41-flows are displayed on the graph. The R^2 values for exponential and power regression techniques calculated using the average RTL values are also displayed on either side of the respective regression trendlines.

A4.7. UniFi – round-trip jitter plots

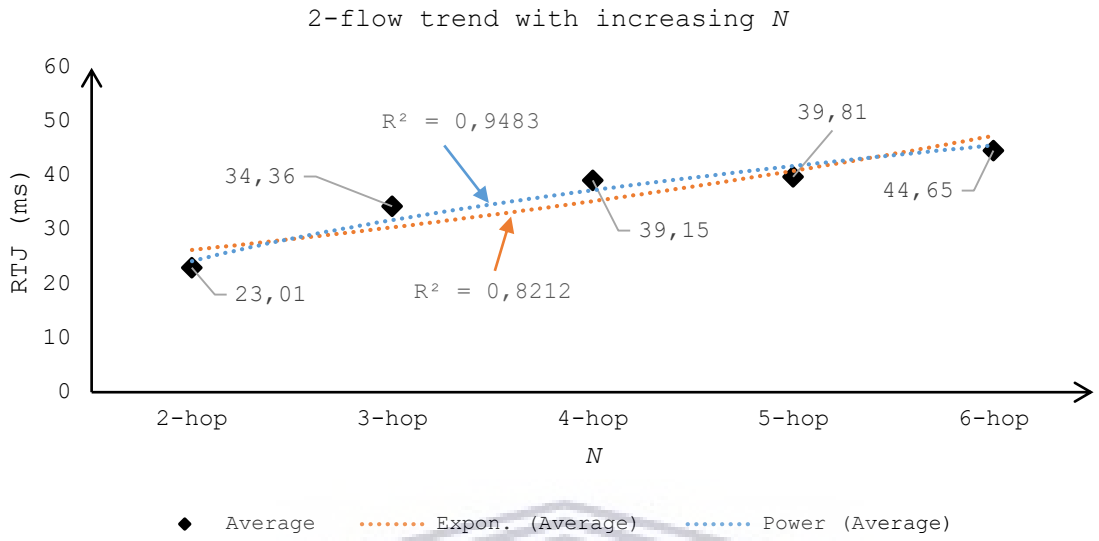

Figure A4.19: Average round-trip jitter performance of 2-flows with increasing number of hop lengths, N
The graph shows the trend of RTJ values for 2-flows with increase in number of hop lengths N between UniFi units. The average values of RTJ for 2-flows are displayed on the graph. The R^2 values for exponential and power regression techniques calculated using the average jitter values are also displayed on either side of the respective regression trendlines.

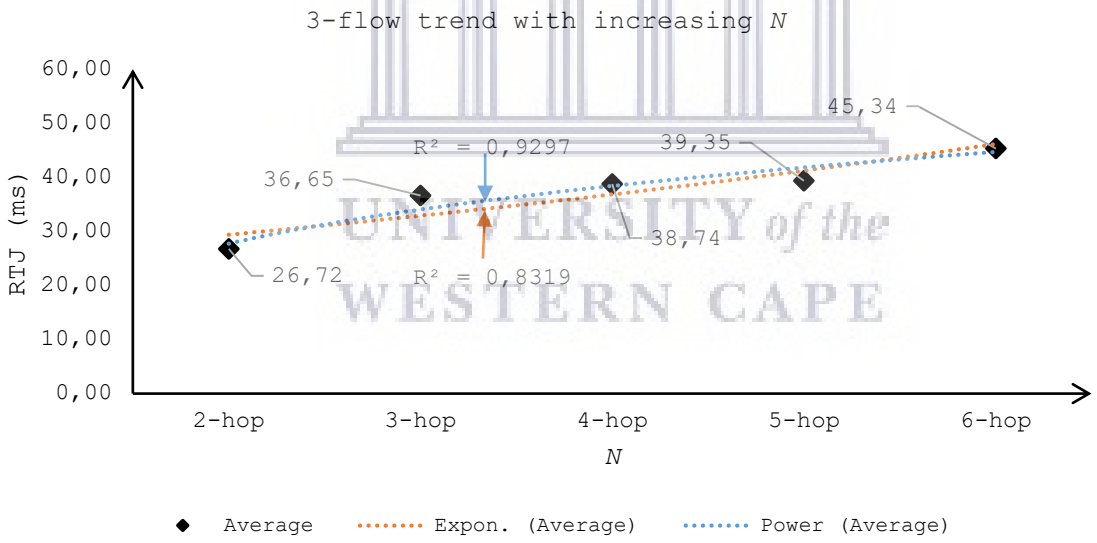

Figure A4.20: Average round-trip jitter performance of 3-flows with increasing number of hop lengths, N
The graph shows the trend of average RTJ values for 3-flows with increase in number of hop lengths N between UniFi units. The average values of RTJ are displayed on the graph. The R^2 values for exponential and power regression techniques calculated using the average RTJ values are also displayed on either side of the respective regression trendlines.

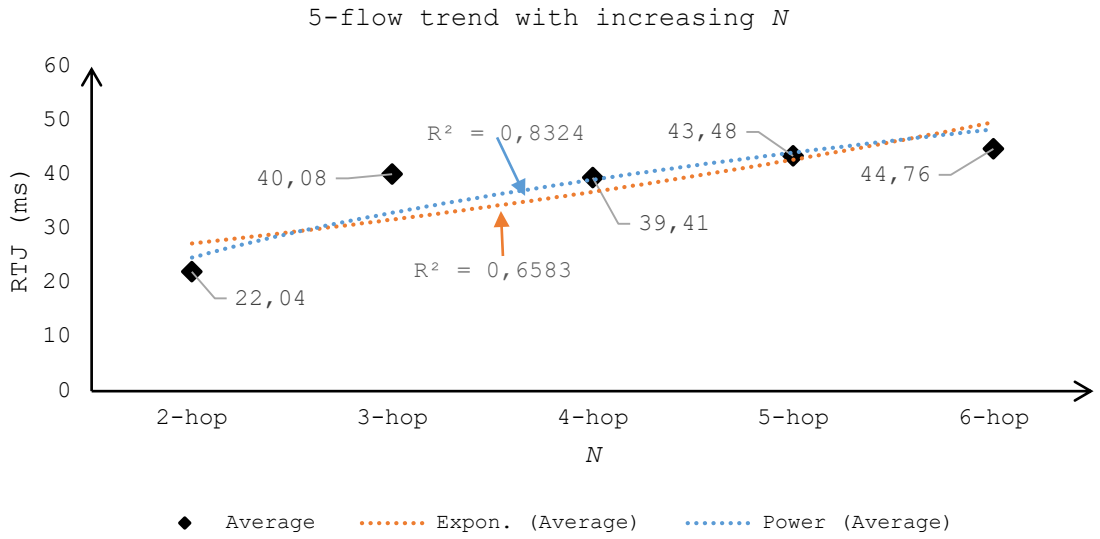

Figure A4.21: Average round-trip jitter performance of 5-flows with increasing number of hop lengths, N
The graph shows the trend of average RTJ values for 5-flows with increase in number of hop lengths N between UniFi units. The average values of RTJ are displayed on the graph. The R^2 values for exponential and power regression techniques calculated using the average RTJ values are also displayed on either side of the respective regression trendlines.

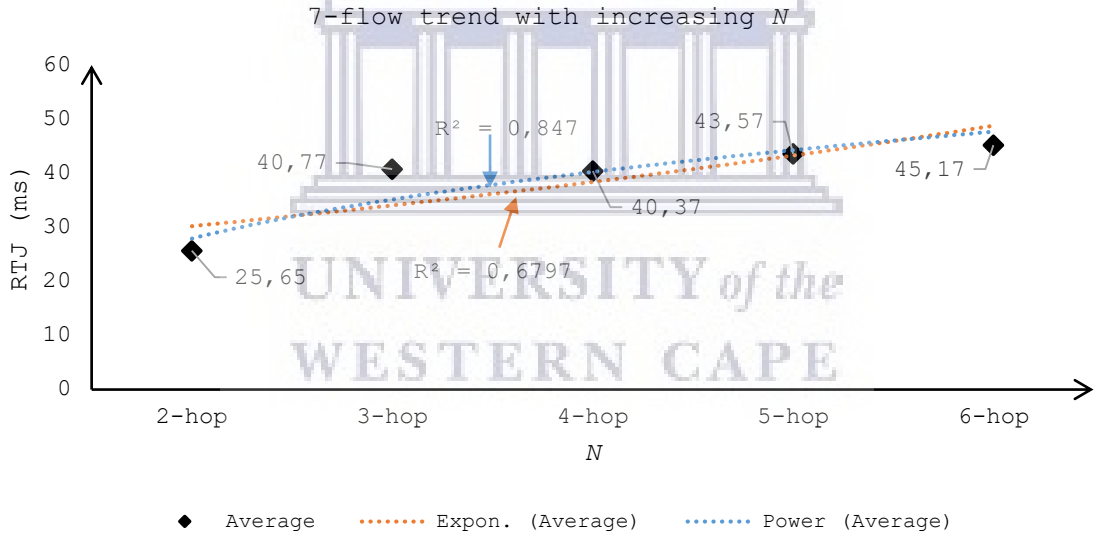

Figure A4.22: Average round-trip jitter performance of 7-flows with increasing number of hop lengths, N
The graph shows the trend of average RTJ values for 7-flows with increase in number of hop lengths N between UniFi units. The average values of RTJ are displayed on the graph. The R^2 values for exponential and power regression techniques calculated using the average RTJ values are also displayed on either side of the respective regression trendlines.

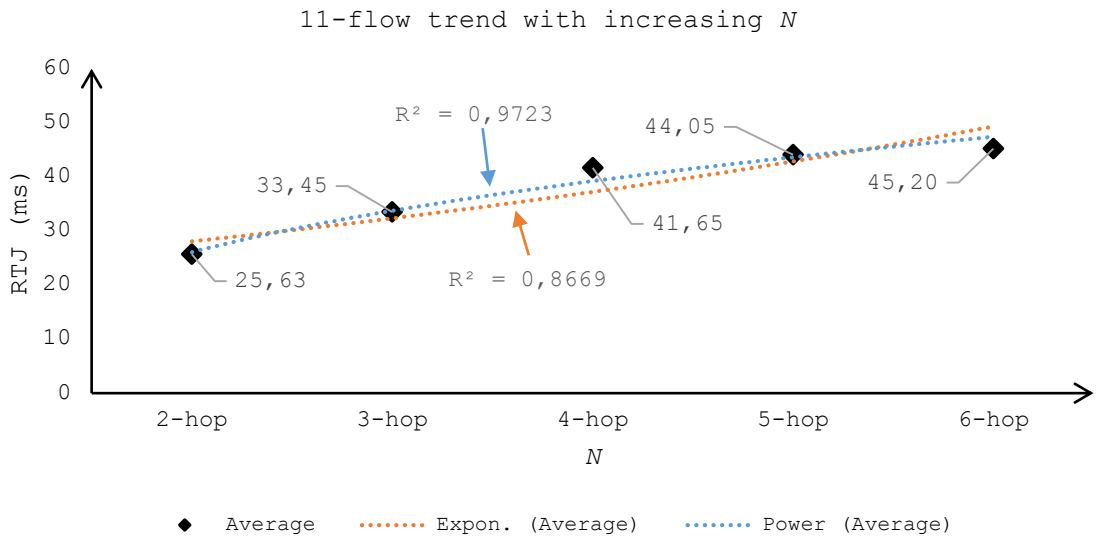

Figure A4.23: Average round-trip jitter performance of 11-flows with increasing number of hop lengths, N
The graph shows the trend of average RTJ values for 11-flows with increase in number of hop lengths N between UniFi units. The average values of RTJ are displayed on the graph. The R^2 values for exponential and power regression techniques calculated using the average RTJ values are also displayed on either side of the respective regression trendlines.

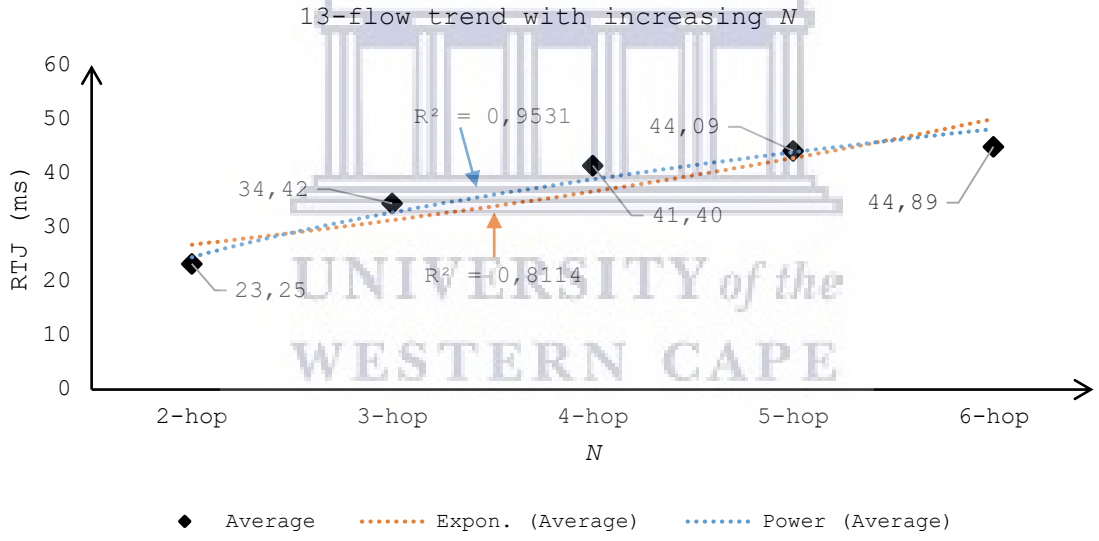

Figure A4.24: Average round-trip jitter performance of 13-flows with increasing number of hop lengths, N
The graph shows the trend of average RTJ values for 13-flows with increase in number of hop lengths N between UniFi units. The average values of RTJ are displayed on the graph. The R^2 values for exponential and power regression techniques calculated using the average RTJ values are also displayed on either side of the respective regression trendlines

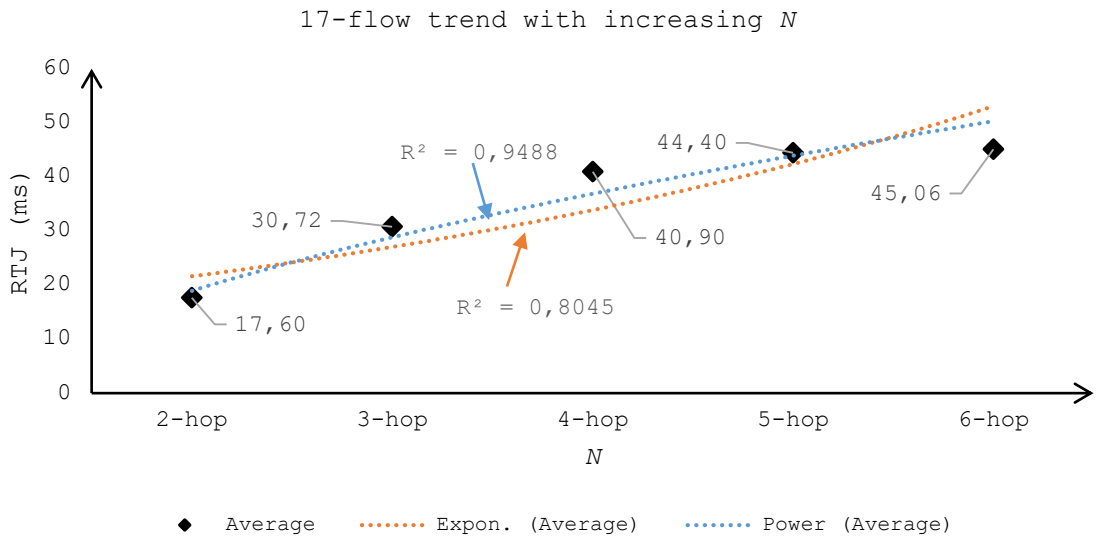

Figure A4.25: Average round-trip jitter performance of 17-flows with increasing number of hop lengths, N
The graph shows the trend of average RTJ values for 17-flows with increase in number of hop lengths N between UniFi units. The average values of RTJ are displayed on the graph. The R^2 values for exponential and power regression techniques calculated using the average RTJ values are also displayed on either side of the respective regression trendlines

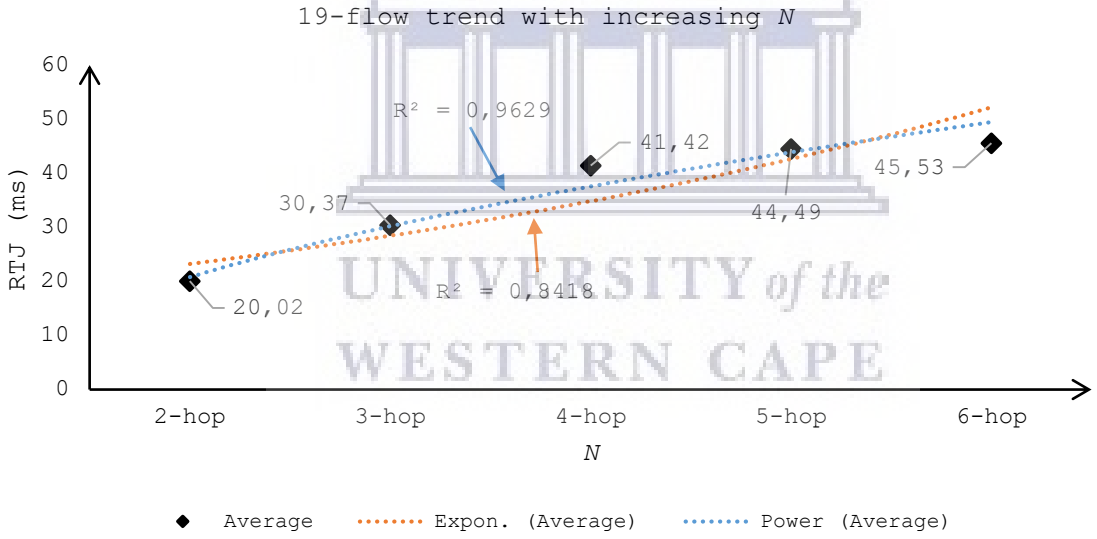

Figure A4.26: Average round-trip jitter performance of 19-flows with increasing number of hop lengths, N
The graph shows the trend of average RTJ values for 19-flows with increase in number of hop lengths N between UniFi units. The average values of RTJ are displayed on the graph. The R^2 values for exponential and power regression techniques calculated using the average RTJ values are also displayed on either side of the respective regression trendlines.

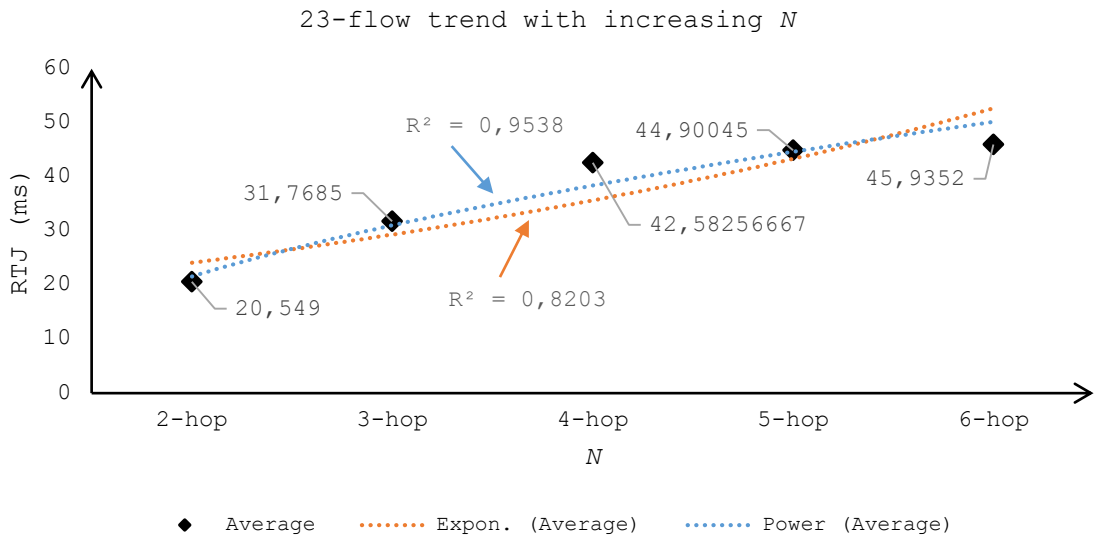

Figure A4.27: Average round-trip jitter performance of 23-flows with increasing number of hop lengths, N
The graph shows the trend of average RTJ values for 23-flows with increase in number of hop lengths N between UniFi units. The average values of RTJ are displayed on the graph. The R^2 values for exponential and power regression techniques calculated using the average RTJ values are also displayed on either side of the respective regression trendlines.

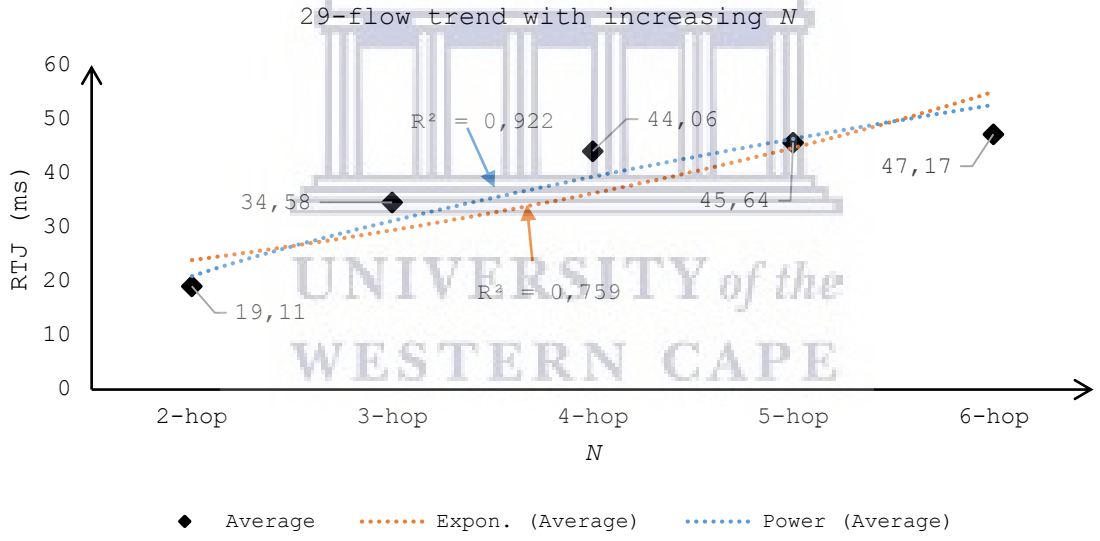

Figure A4.28: Average round-trip jitter performance of 29-flows with increasing number of hop lengths, N
The graph shows the trend of average RTJ values for 29-flows with increase in number of hop lengths N between UniFi units. The average values of RTJ are displayed on the graph. The R^2 values for exponential and power regression techniques calculated using the average RTJ values are also displayed on either side of the respective regression trendlines.

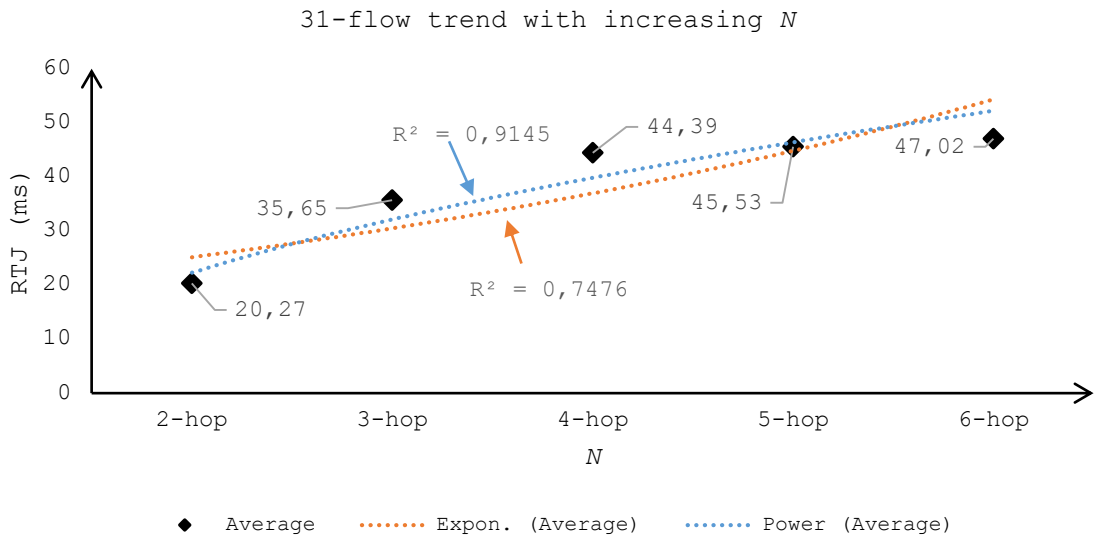

Figure A4.29: Average round-trip jitter performance of 31-flows with increasing number of hop lengths, N
The graph shows the trend of average RTJ values for 31-flows with increase in number of hop lengths N between UniFi units. The average values of RTJ are displayed on the graph. The R^2 values for exponential and power regression techniques calculated using the average RTJ values are also displayed on either side of the respective regression trendlines.

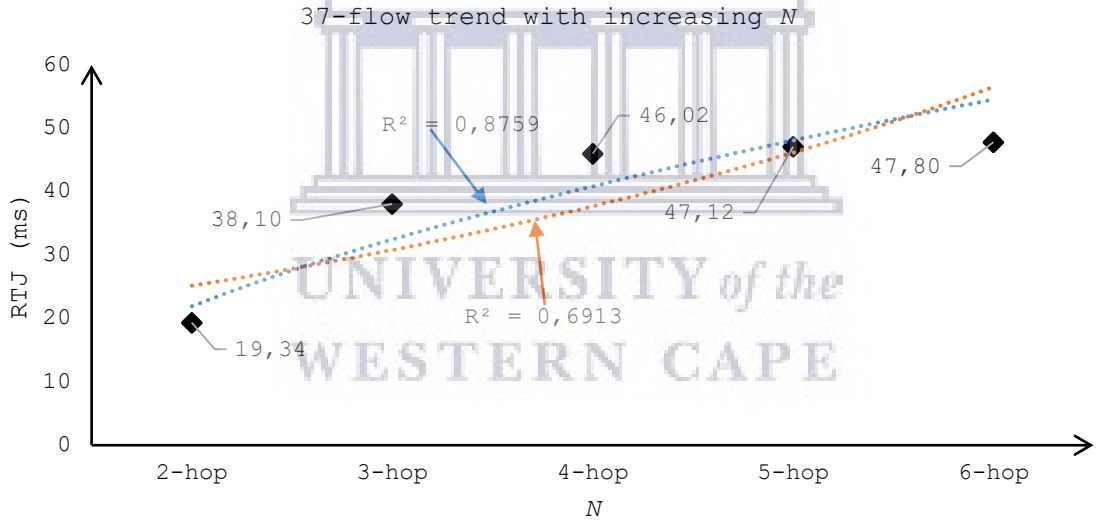

Figure A4.30: Average round-trip jitter performance of 37-flows with increasing number of hop lengths, N
The graph shows the trend of average RTJ values for 37-flows with increase in number of hop lengths N between UniFi units. The average values of RTJ are displayed on the graph. The R^2 values for exponential and power regression techniques calculated using the average RTJ values are also displayed on either side of the respective regression trendlines.

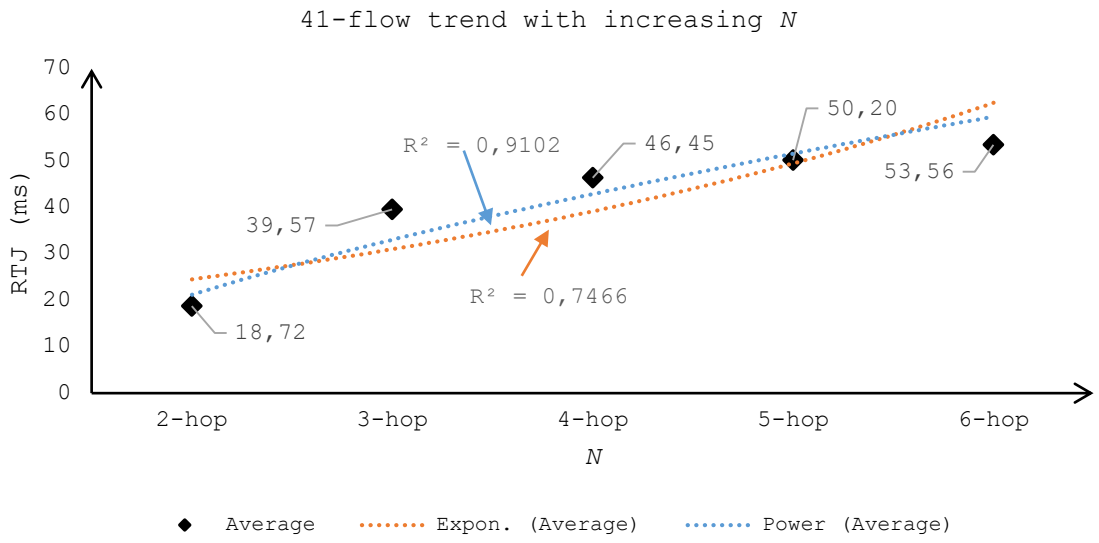

Figure A4.31: Average round-trip jitter performance of 41-flows with increasing number of hop lengths, N
The graph shows the trend of average RTJ values for 41-flows with increase in number of hop lengths N between UniFi units. The average values of RTJ are displayed on the graph. The R^2 values for exponential and power regression techniques calculated using the average RTJ values are also displayed on either side of the respective regression trendlines.

A4.8. UniFi – packet loss percentage plot

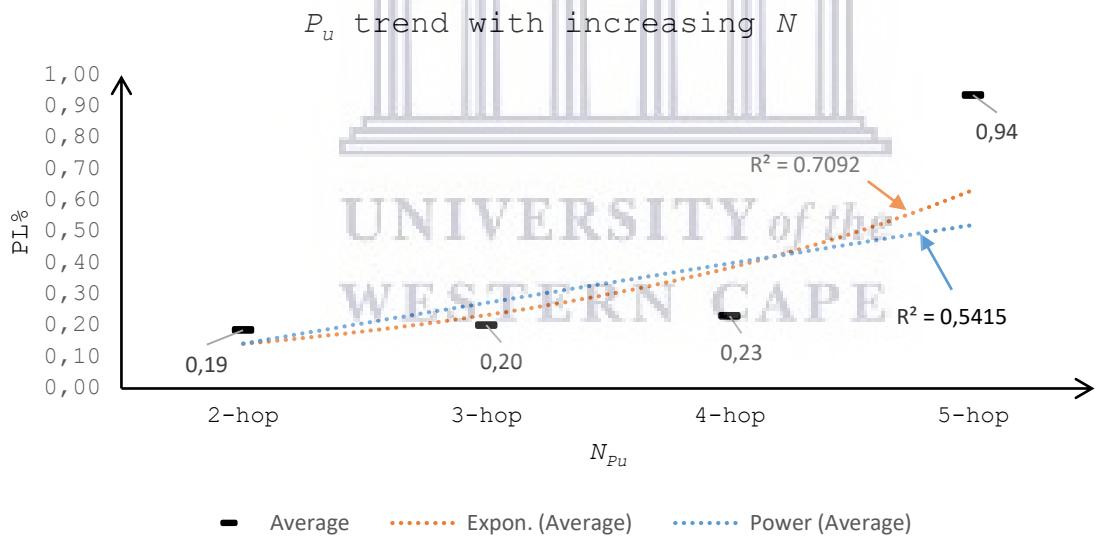

Figure A4.32: Performance of P_u with increasing number of hop lengths, N
The graph shows the trend in P_u with increase in number of hop lengths, N, between UniFi units. The average values of P_u are displayed on the graph. The R^2 values for exponential and power regression techniques calculated using the average P_u values is also displayed on either side of the respective regression trendline.

A4.9. Average battery and data consumption by mobile applications

Table A4.1: Average battery consumption of IM and SIP clients over 30 minute screen OFF voice call
The table shows the average battery consumption numbers by the IM and SIP clients.

Instant messengers	ABC_x (mW)		SIP clients	ABC_x (mW)
WhatsApp	145.08		SipDroid	55.47
Viber	165.96		CSIP	78.39
Messenger	186.16		Zoiper	139.57
IMO	216.13		MizuDroid	200.03

Table A4.2: Average data consumption of IM and SIP clients over 30 minute screen OFF voice call
The table shows the actual average data consumption numbers by the IM and SIP clients.

Instant messengers	D_{X30} (MB)		SIP clients	D_{X30} (MB)
WhatsApp	145.08		SipDroid	55.47
Viber	165.96		CSIP	78.39
Messenger	186.16		Zoiper	139.57
IMO	216.13		MizuDroid	200.03

A4.10. Difference between actual and predicted values of RTL in UniFi results

Table A4.3: Difference between predicted and actual values of RTL.
The table shows the difference between predicted and actual values of RTL obtained by subtracting the actual RTL value from the predicted RTL value.

Flows	2-hops	3-hops	4-hops	5-hops	6-hops
2	0	2.89	1.89	0.33	2.6
3	0	-2.32	-5.96	-6.32	2.55
5	0	-0.13	-0.52	-4.45	3.38
7	0	1.24	0.85	-3.75	3.91
11	0	-2.3	0.43	-1.6	-0.04
13	-0.01	-1.51	-0.72	-0.35	-0.38
17	0	-0.63	-1.04	-2.41	0.08
19	0.01	-1.54	1.85	-1.15	0.04
23	0	-3.71	0.1	-4.17	-1.56
31	0	-2.23	9.52	-2.13	-1.92

A4.11. Smartphone trial tests

The LeS pilot tests involved learning the features, functionalities, and abnormalities in the three types of phones so that experiments could be conducted smoothly. Two discoveries were made

during the pilot run. Firstly, an observational one-week stand-by battery drain consistency test of all the LeSs yielded that three units of Brand 1 type exhibited very high rate of battery drain as compared to the remaining seventeen units. The three abnormal Brand 1 units were returned to the vendor and replaced. Secondly, before commencing experiments for wireless technologies emulation, a few preliminary tests were conducted to investigate the possible network mode combinations possible with the three types of LeSs for which the voice call tests were to be conducted. It was discovered during investigation of different wireless network mode combinations that Brand 2 type phone did not have the functionality of turning on Wi-Fi while phone was in airplane mode. Therefore, plain Wi-Fi experiments could not be conducted for Brand 2 type phones.

A5. Details of nomenclature and substitution method

A5.1. Nomenclature

N	Hop length between MPv2 or UniFi units.
T_1	Throughput measured over first hop length, $N = 1$, in MPv2 or UniFi testbed, respectively.
L_1	Round-trip latency measured over first hop length, $N = 1$, in MPv2 or UniFi testbed.
J_1	Jitter for round-trip latency measured over first hop length, $N = 1$, in MPv2 testbed.
P_1	Packet loss percentage during round-trip traffic measured over first hop length, $N = 1$, in MPv2 testbed or UniFi testbed.
T_m	Throughput with increasing hop length between, N, between MPv2 units.
L_m	Round-trip latency with increasing hop length, N, between MPv2 units.
J_m	Jitter for round-trip latency with increasing hop length, N_m, between MPv2 units.
P_m	Packet loss percentage for round-trip traffic with increasing hop length, N_m, between MPv2 units.
T_u	Throughput with increasing hop length between, N, between UniFi units.
ε_u	Round-trip latency for exponential regression with increasing hop length, N, between UniFi units.
ϕ_u	Round-trip latency for power regression with increasing hop length, N, between UniFi units.
L_u	Round-trip latency with increasing hop length, N, between UniFi units.
J_u	Jitter for round-trip latency with increasing hop length, N, between UniFi units.
P_u	Packet loss percentage for round-trip traffic with increasing hop length, N, between UniFi units.

A5.2. Substitution method

Example: Calculating T_1 using TH value of $N = 2$ from UniFi results in Table 14.

Let's call the TH value for $N = 2$ as T_2.

According to Table 14, T_2 = 48.26-Mbps;

Equation (4.10) is; $T_u = T_1 \cdot e^{-0.21(N-1)}$;

For $N = 2$, $T_u = T_2$;

Therefore, $48.26 = T_1 \cdot e^{-0.21(2-1)}$;

Hence T_1 = 59.53-Mbps

NB: Similar method has been adopted to find L_1, J_1, and P_1 during comparison of actual and predicated values for UniFi scalability quantification.

A6. Scalability research versus Zenzeleni timeline

As shown in Figure 27, the research[64] commenced in the first quarter of 2015, a time during which the Zenzeleni cooperative, the Zenzeleni NPC, and the UWC research team had initiated migration of the Zenzeleni community network from MP routers to MPv2 routers with the objective to explore cost-effective and power-efficient ways to broaden the use of community network so that the residents, in addition to voice calls, could also access Internet services such as Facebook and WhatsApp via personal smartphone handsets. The research identified that the scalability issues with WMNs with increase in traffic, and distance between source and destination could thwart deployment goals of CWMNs such as Zenzeleni to provide affordable network services within the recommended QoS requirements to the low-income rural users. Therefore, a scalability quantification study began in the first quarter of 2015 with an idea of a scalability model for WMNs that could be used to predict their optimal scalability limit within the recommended multimedia QoS requirements presented in Table 4 of Section 2.2.1. During the initial phases of network scalability quantification study, the research identified that the capability of the end-users to be able to regularly access the cheap network services through CWMNs such as Zenzeleni is equally important as deploying a scalable CWMN to offer the cheap network services. It is commonly known that WMNs provide network access via Wi-Fi hotspots; and smartphones, which have become primary mobile device for all types of communication, provide easy mobile solution to Wi-Fi access. In 2015 recharging the smartphones on regular basis was a major challenge in the Mankosi community because of little or no electricity supply in the community. Due to lack of

[64] The word "research" refers to the research of scalability of wireless mesh community networks which comprised of the scalability quantification study and the smartphone battery consumption study.

electricity, community members preferred usage of feature phones due to their long battery life. In addition, the Mankosi community members had to pay to recharge their mobile phones at a Zenzeleni recharge point or private kiosk. In addition, given the low monthly income of the Mankosi community members (Carlos Rey-Moreno et al., 2016, 2014), smartphone handset affordability was also questionable. Therefore, in the second quarter of 2015, the scalability research was extended by addition of smartphone battery consumption investigations to find power-efficient ways to integrate low-cost smartphones in the community and utilize the cheap network services provided by the Zenzeleni community network. In order to bridge the smartphone device ownership gap, low cost LeSs costing between 25-50USD; and recommended by the GSMA in their mobile economy report as a low-cost smartphone alternative for low-income communities (GSMA Intelligence, 2015); were identified as an affordable smartphone option for the low income Mankosi community members. The low-end specifications, especially battery capacity, in the LeSs stressed the importance of the smartphone battery consumption study because unplanned usage of the LeSs could lead to quick depletion their batteries leaving end-users with escalated recharge costs due to frequent visits to the recharge stations. Therefore, the smartphone battery consumption study investigated power-efficient methods to utilize network services using LeSs. The smartphone battery consumption study was divided into wireless technologies, and mobile applications evaluation respectively. The objective of wireless technologies evaluation was to find the least battery draining Wi-Fi and cellular radio combination for usage with the LeSs in light of the related work on battery consumption in smartphones, presented in Section 2.3.2, which showed Wi-Fi as the least battery draining wireless technology amongst 3G, 2G, and BT. The objective of mobile applications evaluation was to find the least battery draining social communication application for the LeSs to counter the battery consumption from usage of multiple communication applications such as WhatsApp and Messenger both.

In the year of 2016, as shown in Figure 27, while Zenzeleni network was receiving recognition and winning awards, the research was conducting: (a) literature review related to scalability in WMNs; and (b) literature review on smartphone penetration in developing regions of the world and wireless technology experimentation to identify the least battery draining Wi-Fi and cellular radio combination for usage with the LeSs. Literature review on scalability of WMNs led to revelation of: (a) several CWMNs in the low income and rural communities of sub-Saharan Africa and developing Asia, presented in Section 2.1 of the thesis, that were also deployed with

the aim to offer cheap network services much like Zenzeleni; (b) recommended multimedia QoS requirements, presented in Section 2.2.1; (c) QoS in WMNs, presented in Section 2.2.2 of this thesis, which showed that network performance of throughput, latency jitter and packet loss, that are considered key network performance metrics, declined in WMNs with increase in hop length source and destination; and network traffic; and (d) existing scalability models for WMNs, presented in Section 2.2.3 of this thesis, which yielded mostly throughput scalability models to predict throughput capacity only with increase in hop lengths. Therefore, as shown in Figure 41, scalability quantification experimentation that considered network performance of all the key network performance metrics commenced in early 2017. Literature review on state of smartphones in developing regions in Section 2.3 led to the revelation that: (a) sub-Saharan Africa is affected by high tariffs, handset prices, and low electricity access similar to Mankosi; and (b) developing Asia is affected by high handset prices and poor electricity supply. Along with the literature review of scalability in WMNs and smartphones in developing regions, the wireless technology experimentation progressed. The wireless technology evaluation compared battery consumption during usage of Wi-Fi for voice calls with different cellular radio combinations amongst three LeSs to narrow the least battery draining LeS and the least battery draining Wi-Fi and cellular radio combination in an LeS. The objective of comparing multiple LeSs was to develop a framework to identify and compare least battery draining Wi-Fi and cellular radio combination in multiple LeSs available in the market. The results of wireless technology evaluation were published in Om et al. (2017). With the completion of wireless technologies evaluation, the smartphone battery consumption study began mobile applications evaluation.

As shown in Figure 27, scalability quantification study that considered the network performance of Zenzeleni under MPv2 in perspective began setup of a WMN testbed using MPv2 routers in first quarter of 2017. While the scalability quantification experiments were being conducted over the MPv2 testbed, Zenzeleni network in Mankosi registered Zenzeleni NPC, subscribed to a fiber backhaul for the Zenzeleni networks and began plans of network overhaul. The plans to overhaul the Zenzeleni networks to a clustered-topology; and replace MPv2 deices with Ubiquiti UniFi AP devices for mesh and Litebeam for long-distance PtP, commenced at the end of 2017. By the end of 2017, the mobile applications evaluation using the least battery draining LeS and Wi-Fi and cellular radio combination identified from the wireless technology evaluation was completed. The mobile application evaluations compared power consumption by common IM

and SIP applications. The mobile application evaluations required usage of IM and SIP applications which consumed data. Therefore, the data consumed by the IM and SIP applications were also collected and compared to identify the least data draining social communication application. The results of mobile applications evaluation which consisted of both battery and data drain by common IM and SIP applications, respectively, was published in Om et al. (2018a).

In the year 2018, as shown in Figure 27, Zenzeleni network saw massive changes consisting of network topology overhaul and expansion to Zithulele community. The MPv2 testbed experiments were completed in end of first quarter of 2018; and the results of preliminary experimentation to show the successful setup of an indoor multi-hop WMN testbed using MPv2 devices was published in Om et al. (Om & Tucker, 2018b). However, at the completion of MPv2 testbed experiments in mid-2018, the objectives of the scalability quantification study were expanded to consider the network performance of Zenzeleni under the new UniFi mesh devices. In the third quarter of 2018, investigations on scalability quantification began with a setup of a WMN testbed using UniFi devices.